

DISSERTATION

PROFILING THE ANTIVIRAL SMALL RNA RESPONSE IN MOSQUITOES TO ARBOVIRUS INFECTION:
INTRA- AND INTERSPECIES COMPARISONS AND RELATIONSHIP TO VECTOR COMPETENCE

Submitted by

Abhishek N. Prasad

Department of Microbiology, Immunology, and Pathology

In partial fulfillment of the requirements

For the Degree of Doctor of Philosophy

Colorado State University

Fort Collins, Colorado

Summer 2014

Doctoral Committee:

Advisor: Gregory D. Ebel

Kenneth E. Olson

Carol D. Blair

Aaron C. Brault

Ann M. Hess

Copyright by Abhishek N. Prasad 2014

All Rights Reserved

ABSTRACT

PROFILING THE ANTIVIRAL SMALL RNA RESPONSE IN MOSQUITOES TO ARBOVIRUS INFECTION: INTRA- AND INTERSPECIES COMPARISONS AND RELATIONSHIP TO VECTOR COMPETENCE

Arthropod-borne viruses (arboviruses) are a taxonomically diverse group of viruses which represent emerging/re-emerging threats to global human and livestock health. By far, the most prevalent vectors of arboviruses are mosquitoes, though ticks and sandflies are also significant vectors for viruses causing human disease. Since the discovery of *Aedes aegypti* as the primary vector for yellow fever virus in the early 1900's, an astounding amount of money and effort has been expended on trying to control arbovirus transmission. For most of this time, efforts have primarily focused on controlling vector mosquito populations, with variable results. With the advancement of molecular biology, much knowledge has been gained on how viruses infect, replicate within, and are eventually transmitted by their arthropod vectors. However, we still lack a detailed understanding of how mosquitoes control arbovirus infection and mitigate pathogenesis.

Unlike vertebrates, mosquitoes and other invertebrates lack adaptive immune systems, as well as many of the important innate immune effectors vertebrates possess to combat viral infection. However, mosquitoes do possess sophisticated mechanisms for dealing with microbial infection. RNA interference (RNAi) is the major innate immune response in mosquitoes to virus infection. Work over the past nearly 20 years has illustrated the importance

of RNAi pathways in controlling arbovirus infection; however, many unanswered questions regarding RNAi and its role in vector/virus ecology remain.

Accordingly, this dissertation focused on investigating the role of two RNAi pathways, the small interfering RNA (siRNA) pathway, and the PIWI-interacting RNA (piRNA) pathway, in controlling West Nile virus (WNV) infection in *Culex* spp. mosquitoes. We first began by performing a comparative analysis of the antiviral small RNA response in field-collected *Culex* spp. mosquitoes to WNV to colonized strains of *Culex* mosquitoes. Utilizing next-generation sequencing technology, we sequenced viral-derived small RNA populations corresponding to products of both the siRNA and piRNA pathways and made both intra- and interspecies comparisons in the targeting of the virus genome by these pathways. Doing so, we were able to find a remarkable amount of conservation in the targeting of the virus genome by the siRNA pathway between several species and populations within species, but also found that *Cx. quinquefasciatus* mosquitoes exhibited a unique targeting profile of the virus genome by this pathway. We also found 24-30 nucleotide RNAs, consistent in size with products of the piRNA pathway, were produced in significantly different proportions amongst different mosquito species/populations.

This led us to further investigate the role of the piRNA pathway during arbovirus infection. We analyzed piRNA populations from *Cx. tarsalis* mosquitoes infected with either flaviviruses (i.e. WNV) or alphaviruses (i.e. Western equine encephalitis virus, Sindbis virus) and looked for characteristic signatures of the “ping-pong” dependent amplification loop, a model proposed for the biogenesis of piRNAs. In congruence with published studies on flavivirus infection in mosquitoes, but in contrast to published studies on alphavirus infection in

mosquitoes, we found no signatures of ping-pong dependent amplification in any of the virus infection models of *Cx. tarsalis*. After further analysis and comparison to a small RNA library sequenced from alphavirus *Ae. aegypti* mosquitoes, we concluded that the differential biogenesis of viral-derived piRNA-like small RNAs in response to arbovirus infection in mosquitoes is dependent upon the vector-virus pairing.

Lastly, we sought to determine the effect of RNAi on either restricting or permitting virus escape from the midgut of mosquitoes. Using multiple biological replicates and sampling over numerous time points, we sequenced small RNA populations from WNV-infected *Cx. quinquefasciatus* mosquitoes. We found that neither the siRNA nor piRNA pathways appear to be functionally active at early points during infection, which are arguably the most important for virus in establishing an infection. Surprisingly, we found no association between the siRNA targeting profiles of the virus genome and the infection phenotype, i.e. midgut restriction or midgut escape.

The studies included in this dissertation show a large degree of intra- and interspecies conservation of viral genome targeting by the exogenous siRNA pathway, with the notable exception of *Cx. quinquefasciatus*, which exhibited a high degree of intraspecies correlation, but differed from the other species studied in this regard. Secondly, we provided evidence suggesting that biogenesis and/or processing of viral-derived piRNA-like small RNAs is differentially modulated depending on the virus-vector pairing. Lastly, we found no evidence for the early induction of the siRNA or piRNA pathways following peroral exposure to WNV, and that once initiated, these pathways collectively fail to restrict the virus from disseminating from

the midgut. Taken together, the studies entailed in this dissertation contribute to the rapidly expanding body of knowledge regarding the antiviral function of RNAi pathways in controlling arbovirus infection in mosquitoes.

ACKNOWLEDGEMENTS

There are far too many people with their respective contributions to my life to name individually (I believe it is an unwritten rule that an “Acknowledgements” section cannot be longer than the dissertation itself), so for brevity’s sake I will list a few of them who have invaluable impacted my life for the better.

My mother, Dr. Sudha K. Murthy; and my father, Dr. Nadipuram R. Prasad and his wife, Ai Khuyen Prasad; for their endless support, guidance, and love; through the hardest of times and the best of them. My brother, Aadarsh Prasad, for support, brotherhood, and friendship. My little sister, Ai Khuyen “FiFi” Prasad, for being adorable. My entire extended family, both living and passed, for all of their support and love. Joseph Fronczek for nearly three decades (!!!) of friendship and brotherhood, and Randi Fronczek for marrying him despite knowing that I came along as part of the package. Beverly Singleman for being like a second mother to me. Sarah Hamilton Spaulding for showing me that time and distance are no obstacle for true friendship. Charlie and Peggy Combs for always treating me like a son and “adopting” me into their family. Josh White for being a true friend through thick and thin. Mario Ortega for never letting me take myself too seriously. Dr. Carl Brown III and Karen Brown for friendship and wonderful times. Tess Sierra Halonen for periodically dragging me away from the lab during the last two years to catch a breath. Nathan Grubaugh, Vicki Parsons Grubaugh, Laura Dickson Goss, Nathan Goss, Ben Krajacich, Shifra Goldenberg, Jacob Meyers and Alyssa Brayshaw...my tenure in Colorado has been immeasurably brightened by the friendships I share with each of you! Mike Swanson for being a great friend and roommate. Heather Elliot at Sliders Bar and

Grill for being the best bartender in the world and providing a great atmosphere for me to unwind after long nights in the lab. Dalton F. Dangler for knowing me better than I know myself. All the musicians and bands whose music has helped me maintain some semblance of sanity throughout the last 32 years. Also, I'd like to thank my four-legged friends: Charly Grubaugh, Chaz Goss, Jake Goss, Murphy Krajacich, and Gunner "Monkey" Swanson.

This work would not have been possible without the guidance, mentorship, and inspiration from the following people:

My graduate committee: Dr. Kenneth Olson, Dr. Carol Blair, Dr. Aaron Brault, and Dr. Ann Hess; all of whom contributed enormously to the successful completion of my dissertation. Their expertise in their respective areas of research have proved immensely valuable in molding me into a better scientist. Dr. Doug E. Brackney (aka "KotD", "PapaPhDug") for all the years of friendship and the intense intellectual conversations (both work-related and not), as well as major contributions to my development as a scientist. You definitely made this journey interesting, to say the least. All current and former members of the Ebel lab for friendship, scientific discussions, technical assistance during various projects, and advice. Drs. Bryan Grieg Fry and Wolfgang Wüster for friendship and the inspiration to pursue a career in science. The entire faculty and staff of the Colorado State University Arthropod and Infectious Disease Laboratory and the Infectious Disease Annex. Most importantly, I'd like to thank my Ph.D advisor, Dr. Gregory D. Ebel, for his mentorship and friendship throughout the last 5 years; for guiding me through both the successes and the failures, and for realizing the potential in me to

become a successful researcher. To state the obvious, none of this work would have been possible without his patient guidance and support.

Lastly, I'd like to thank all of the scientists, philosophers, and thinkers of the past and present, in my field or not, for their contributions to the sum of human knowledge about the Universe we inhabit. Everything we do as scientists today was built on the blood, sweat, and tears (often times literally) of someone else yesterday. To paraphrase Bernard of Chartres, we are but dwarves standing on the shoulders of giants.

TABLE OF CONTENTS

ABSTRACT	ii
ACKNOWLEDGEMENTS	vi
Chapter 1: Literature Review	1
Chapter 2: Small RNA Profiling of the Anti-WNV Response in Field-Collected <i>Culex sp.</i> Mosquitoes: Evidence for Stereotypical Targeting of the Viral Genome and Comparison to Colonized Mosquitoes	42
Chapter 3: Virus-vector pairings determine the molecular signatures of virus-derived piRNA-like small RNAs in mosquitoes.....	70
Chapter 4: Small RNA Response of <i>Culex quinquefasciatus</i> to West Nile Virus Infection: Relationship to Vector Competence.....	114
Chapter 5: Concluding Remarks.....	135
References	141

Chapter 1: Literature Review

Background

Arthropod-borne viruses (arboviruses) represent a taxonomically diverse group of viruses that persist in nature through transmission cycles between hematophagous arthropod vectors and vertebrate hosts [1]. Known arboviruses belong to seven different families: *Flaviviridae*, *Togaviridae*, *Bunyaviridae*, *Rhabdoviridae*, *Reoviridae*, a single genus from *Orthomyxoviridae* (*Thogotovirus*), and the sole genus/species from *Asfarviridae* (*Asfivirus*, African swine fever virus, ASFV) [2]. With the exception of *Asfarviridae*, which possesses a double-stranded DNA (dsDNA) genome [3], all other arboviruses have RNA genomes, though the polarity, single or double-strandedness, presence of one or multiple segments, and organization of the genome differs between families. As of April 2014, there are 637 viruses listed in “The International Catalog of Arboviruses Including Certain Other Viruses of Vertebrates” [4], of which at least 214 are known or probable arboviruses, at least 287 are possible arboviruses, and the remainder are probably or definitely not arboviruses [1] (these numbers have likely increased).

Arbovirus infection is a serious emerging/re-emerging threat globally to both human and livestock health. Several billion people, primarily living in tropical, underdeveloped, and impoverished nations are currently at risk of infection from one or more arboviruses, with perhaps hundreds of millions of infections occurring annually from dengue viruses (*DENV*, *Flaviviridae*) alone [5]. Largely due to globalization, numerous arboviruses, such as West Nile virus (*WNV*, *Flaviviridae*) and chikungunya virus (*CHIKV*, *Togaviridae*) have expanded their

geographic ranges dramatically. Most recently, as of April 2014, local transmission of CHIKV has occurred in several Caribbean nations, starting in Saint Martin in December 2013 and quickly spreading to other countries, marking the first instances of autochthonous transmission of this virus in Western hemisphere [6]. In addition, climate change resulting in the geographic expansion of arthropod vector species is also expected to significantly contribute to the increase of arbovirus prevalence [7, 8]. Increasing global temperatures may also result in increased disease transmission by reducing the extrinsic incubation period (EIP) required by arboviruses to replicate in and be transmitted by their arthropod vectors [9]. Finally, the importation of a large variety of domestic and exotic animals for the agriculture and pet trades may contribute to the transfer of arboviruses to non-endemic regions [10].

Prevention of arbovirus transmission has historically and presently primarily relied upon vector control strategies; in the case of mosquitoes, by far the most prevalent vectors of arbovirus disease, larvacide treatment and adulticide treatments are common preventative measures. However, failure to maintain adequate mosquito control programs, along with other factors such as urbanization, insecticide and drug resistance, and genetic adaptation by pathogens has resulted in the emergence/resurgence of arbovirus diseases [11]. More modern experimental approaches to curbing arbovirus transmission include sterile insect technique [12-14] and the related “Trojan female technique” [15], development of a variety of transgenic mosquitoes incapable of virus transmission [16-22], and the use of *Wolbachia* (Rickettsiales), a maternally-inherited Gram negative insect endosymbiont bacterium, to reduce mosquito lifespans below the threshold of most arbovirus EIPs or to block transmission of arboviruses [23-29]. With regards to generation of transgenic mosquitoes, these efforts have greatly

benefitted from the full genome sequencing of three medically important mosquito species: the yellow fever mosquito (*Aedes aegypti*), the southern house mosquito (*Culex quinquefasciatus*), and the malaria mosquito (*Anopheles gambiae*) [30-32].

Flaviviridae and the genus *Flavivirus*

The *Flaviviridae* are a large family of viruses comprised of four genera: *Flavivirus*, *Pestivirus*, *Hepacivirus*, and the newly accepted *Pegivirus* [33, 34]. All members of *Flaviviridae* possess a lipid-bilayer enveloped nucleocapsid housing a single-stranded, positive sense RNA genome [35], though the genes encoded vary by genus. The RNA genome serves as the viral mRNA, and is thus infectious to cells [36], and is 5'-m⁷GpppAp capped and lacks poly(A) tailing at the 3' terminus [37, 38]. Genomic RNA is translated into a single polyprotein precursor which is co- and post-translationally cleaved into individual proteins by both viral encoded and host proteases. Structural proteins are encoded at the N-terminal region of the polyprotein, while non-structural (NS) proteins make up the remainder. Out of the four genera, only the genus *Flavivirus* is known to contain members transmitted by arthropod vectors.

The genus *Flavivirus* is comprised of over 70 species of viruses [39], most of which are arboviruses or insect-specific viruses. Members of the genus *Flavivirus* include YFV, DENV, West Nile virus (WNV), Japanese encephalitis virus (JEV), St. Louis encephalitis virus (SLEV), and tick-borne encephalitis virus (TBEV), among others. The name of the genus is derived from the Latin word *flavus*, meaning “yellow”, describing the jaundice caused in infected, symptomatic persons by the type species, yellow-fever virus (YFV). YFV itself holds a special place in the

annals of virology, being the first virus, or “filterable agent”, shown to be responsible for a human disease [40].

Flavivirus genomes are ~11 kilobases (kb) in length, and contains three structural proteins in the 5'- portion (Capsid, C; pre-membrane, prM; envelope, E) and seven NS proteins making up the rest of the genome (NS1, NS2a, NS2b, NS3, NS4a, NS4b, NS5). The mature virion is a small, spherical particle of ~50 nanometers (nm) in diameter with a ~30 nm electron dense core surrounded by a lipid bilayer envelope [41]. Flaviviruses enter cells via binding of cellular receptors and entry into clathrin-coated pits resulting in endocytosis (receptors implicated in cellular entry in both mosquitoes and mammals are discussed in greater detail in the “Pathogenesis in Mosquitoes and Mammals” section) [42, 43]. Virions are uncoated via a conformational change in the E glycoprotein from a homodimeric to a trimeric structure in low pH endosomes, resulting in fusion of the viral and cellular membranes and release of the viral nucleocapsid into the cytoplasm [42, 44-46]. Following this, the capsid dissociates with the RNA, which triggers the translation of viral proteins, replication of the viral genome, and packaging of virions [47, 48]. Replication of the viral genomic RNA occurs within virus-induced membrane structures (IMS) at the surface of the endoplasmic reticulum (ER) [49], and is mediated in part by the NS5 protein, which has both RNA-dependent RNA polymerase (RdRP) [50, 51] and methyltransferase [52] activity. The organelle of origin for IMS's varies between flaviviruses; the IMS for WNV appears to be derived from the ER [53, 49], with reorganization of the membrane being mediated by NS2A, NS2B, NS4A, and NS4B [49, 54]. Using the genomic RNA as a template, an antisense strand is synthesized by RdRP activity of NS5, which is then used as the template to produce positive-strand genomic RNAs. Immature virions are formed in

the lumen of the ER [55], and derive their lipid-bilayer envelope by budding through this organelle [56]. Mature virions emerge from the trans-Golgi network, wherein furin-mediated cleavage of prM into the pr peptide and M protein is necessary to produce infectious particles [57, 58]. Mature virions exit the cell via exocytosis [39].

WNV and Flavivirus Evolution

Theories regarding flavivirus evolution must take into account the following considerations: (1) their degree of genetic relatedness, (2) the natural ecology of the viruses (i.e. vectors, if any, and vertebrate hosts), and (3) their geographic distribution [59]. One theory of vector-borne flavivirus evolution is that they arose from non-vectorized ancestors, some of which eventually adapted to arthropod hosts [60]. Flaviviruses can be divided into three main categories, determined both by their phylogenetic relationships to one another as well as their ecological niches: those vectored by mosquitoes, those vectored by ticks, and those with no known vectors [61]. Genetic and antigenic relatedness between flaviviruses strongly correlates with their vector preference (i.e. mosquito or tick-borne) [62, 63]. Some interesting observations can be made when attempting to classify flaviviruses. Mosquito-borne flaviviruses fall into two distinct subgroups: those which have been primarily isolated from *Aedes sp.* mosquitoes, and those that have primarily been isolated from *Culex sp.* mosquitoes, with the *Aedes* subgroup containing two paraphyletic groups (one with YFV and the other with DENV) comprising 16 species, and the *Culex* group comprising 21 species (as of 2007) [59]. Interestingly, none of the viruses isolated primarily from *Aedes* have an avian cycle, and none of the viruses isolated from *Culex* involve a primate cycle [59]; this is likely due to the feeding

preferences inherent to each genus. Additionally, the primary disease manifestation in humans of viruses isolated in the *Aedes* group is hemorrhagic fever, while the diseases caused by viruses in the *Culex* group are primarily encephalitides [64]. Among the tick-borne flaviviruses, two groups exist: those associated with seabirds, and those associated with mammals (the TBEV complex) [65].

WNV belongs to the JEV complex within the genus *Flavivirus* and the family *Flaviviridae*, based on its antigenic similarity to other viruses in this complex [61]. There are five distinct lineages (some sources state as many as eight, including putative lineages [66]) of WNV, with Lineage I and II being the predominant lineages most isolates fall into. Lineage I has the largest geographic distribution, and is divided into several clades: clade 1a includes the pathogenic strain introduced into North America in 1999 (WNV_{NY99}), and is most associated with causing neuroinvasive disease, clade 1b includes Kunjin virus (KUNV), a mildly pathogenic strain endemic to Australia [67-70], and clade 1c includes isolates from India [71]. Lineage II was believed to be isolated to sub-Saharan Africa, but since 2004 has been responsible for outbreaks in Europe, specifically in Hungary, Greece, and Spain [72-74], and now appears to be established in Europe [75]. Lineages III, IV, and V are mostly restricted to Eastern Europe (III and IV), and India (V) [76]. Interestingly, Koutango virus (KOUV), a flavivirus initially classified as a separate species [77], but later shown to be a WNV variant [78, 70], has primarily been isolated from rodents and ticks, peculiar hosts for WNV [66].

Like all RNA viruses, WNV is thought to exist in nature as a quasispecies, or a collection of diverse genotypes diverged from a common ancestral genotype within a single infected host (or cell) [79, 80]. RNA viruses replicate with extremely high mutation rates [81], owing at least

in part to the lack of proof-reading activity of most viral RdRPs, resulting in relatively low-fidelity replication (estimated error rate for many viral RdRPs is a single misincorporated base for every 10^4 - 10^6 nucleotides [82]; for flaviviruses this would translate to ~1 mutation per genome per replication event). High mutation rates may present a problem to viruses as excess mutations could potentially lead to population extinction [81, 83-85], since most mutations negatively impact viral fitness, as seen in a study with vesicular stomatitis virus (VSV, *Rhabdoviridae*) [86]. However, high mutation rates could be expected to benefit a large population, even if they may be detrimental on individuals [87], with the low fidelity of the viral RdRP allowing for rapid mutation and adaptation to new or changing environments. In support of this, studies with a CHIKV mutant expressing a high-fidelity RdRP have shown the mutant virus exhibited lower infection and dissemination rates in *Ae. aegypti* mosquitoes compared to the wild-type virus [88]. Thus, it becomes clear that RNA viruses have to find a balance between mutational robustness and replicative fitness. One mechanism for this may be epistatic interaction, where the combined effect of multiple mutations affects fitness differently than any individual mutation may be expected to on its own [81]. Indeed, this has been shown to be the case in the La Réunion island strain of CHIKV [89].

Global Importance of Flaviviruses

As a group, arboviruses have a global distribution, being found on all continents except Antarctica, but many species are endemic to tropical or subtropical regions which provide for perennial transmission cycles through cold-blooded arthropod vectors [1]. Members of the genus *Flavivirus* are predominantly mosquito-borne, and those which cause human disease are

primarily encephalitic (JEV, WNV, SLEV, TBEV) or hemorrhagic fever viruses (DENV, YFV).

Flaviviruses such as DENV and YFV have probably been afflicting humans since pre-history, but it has only been relatively recently that the variety and severity of the diseases they cause has been appreciated. While vaccines exist for flaviviruses like YFV and JEV, sporadic outbreaks of these viruses still occur, often with significant mortality rates, with YFV-infection killing roughly 30,000 people annually [90-94]. The global burden of DENV alone is estimated to be in the hundreds of millions of infections per year, and recent years have seen the expansion of flaviviruses such as WNV into new territories. Since its introduction into the United States in 1999, WNV has caused more than 16,000 cases of neuroinvasive disease and more than 1,500 deaths, as of 2012 [95].

Tick-borne flaviviruses less commonly cause human disease, however there are several viruses that can cause sporadic outbreaks resulting in severe clinical manifestations. By far the most prevalent agents of human disease in this group are the TBEV serocomplex of viruses. Several thousand infections by TBE viruses are reported each year, with some outbreaks exhibiting case fatality rates as high as 50% [65].

West Nile Virus Epidemiology and Ecology

WNV was first isolated from the blood of a woman exhibiting febrile illness in the West Nile district of northern Uganda in 1937 [96]. During the next thirty years, large outbreaks of febrile illness caused by WNV (though few cases of neuroinvasive disease) were reported in Israel and South Africa [97], along with the first epidemic of WNV neuroinvasive disease in Europe [98]. No significant outbreaks were reported from the years 1975-1993, however from

1994-2000 there were numerous large epidemics resulting in meningoencephalitis (inflammation of the meninges, brain, or both; henceforth collectively referred to as encephalitis) in North Africa, Europe, North America, and the Middle East [97], including an outbreak in Romania in 1996 that resulted in nearly 400 cases of neuroinvasive disease and at least 17 deaths [99]. In 1999, an outbreak of viral encephalitis occurred in New York City, New York, U.S.A., [100] which preliminary analysis determined to be caused by a KUNV/WNV-like flavivirus [101], later shown to be a strain of WNV nearly identical to that of an isolate from a dead goose in Israel in 1998 [68]. WNV_{NY99} rapidly expanded its range in the U.S. over the next several years, but was displaced starting in 2001 by a new genotype (WNV_{WN02}) [102], and was rendered completely extinct in favor of WNV_{WN02} by 2004 [103]. The reason for this displacement of the original genotype was found to be due to the WNV_{WN02} genotype exhibiting a dramatically shorter EIP in native mosquitoes than its rival [104], which resulted in increased transmission and proliferation, though a more recent study found no such difference in EIP between WNV_{NY99} and WNV_{WN02} [105]. WNV_{WN02} differs from WNV_{NY99} by three nucleotide (nt) mutations, only one of which is non-synonymous, resulting in a valine replacing an alanine in position 159 of the E glycoprotein (E-A159V) [102, 106], though the direct effect this mutation has on the virus phenotype is unknown. This situation is mirrored by the 2005 La Réunion island outbreak of CHIKV. The strain of CHIKV responsible for this outbreak, which resulted in >3500 confirmed infections and an additional ~250,000 suspected infections (and unusual for CHIKV infections, several hundred fatalities [107]) and facilitated the spread of the virus to other islands and eventually mainland Europe, was found to have a single nucleotide substitution resulting in an alanine to valine at position 229 of the E1 envelope glycoprotein (E1-A229V)

[108]. Subsequent studies demonstrated that this mutation, as well as others subsequently found in later isolates, conferred a fitness advantage to the virus in the Asian tiger mosquito (*Ae. albopictus*), a species it was not normally vectored by [109, 89, 110, 111], and an invasive species that can occur in the absence of (or compete with or even replace in cases of sympatry [112-118]) *Ae. aegypti*, a previously established vector of CHIKV. This adaptive plasticity of arboviruses to new environments and potentially new vectors/hosts demonstrates that given competent arthropod vectors, a pool of amplifying vertebrate hosts, and a mechanism for overwintering (if necessary), arboviruses can spread with relatively little resistance [119].

In nature, WNV persists in an enzootic cycle between ornithophilic vector mosquitoes and birds, primarily of the order Passeriformes (“perching birds”). At least 65 species of mosquitoes in the U.S. , primarily of the genus *Culex* [120-123], have been found to be infected with the virus [95]. The ability of a species, population, or individual within a population to successfully transmit a given pathogen is known as vector competence, and is influenced by both intrinsic (i.e. genetics) and extrinsic factors (i.e. environment) [124], and can vary dramatically between species [121-123, 125-129]. Besides mosquitoes, both ixodid (hard) and argasid (soft) tick species have been found to be naturally infected with West Nile virus [130-133], sometimes with infection rates as high as 11.7% [131]. Ticks have been proposed to serve as potential reservoirs for the virus during bird migration-mediated transfer of the virus between geographical locations [134], and ticks have experimentally been shown to be capable of transmitting the virus [135, 136]; however, the importance of ticks in the maintenance and transmission of WNV in nature remains unknown.

Susceptibility to WNV infection varies in birds, with at least 326 species of birds being susceptible to infection [95]. Passeriformes, Charadriiformes (shorebirds, gulls and auks), and domestic geese (order Anseriformes) exhibit the highest susceptibility to infection, severe disease, and mortality [137-140], with Psittaciformes (parrots) and Galliformes (fowl) being the least susceptible to infection and disease [138]. Corvids (Corvidae; crows, ravens, etc.) in particular develop high viremia titers and exhibit high mortality rates, often in the absence of marked clinical pathology [141-143], other than behavioral changes such as lethargy a day prior to death [144]. Prior to the 1998 outbreak in Israel, WNV was not associated with avian virulence, and the observed mortality in both wild and captive birds is considered unique to the introduction of the virus to North America [145]. It has been shown that a single mutation in the NS3 helicase, resulting in a threonine to proline substitution at position 249 of the protein (NS3-T249P) is responsible for this dramatic shift in virulence in the WNV_{NY99} strain compared to previous isolates [146]. In addition to aves, at least 30 other species of vertebrates are known to become infected with WNV [147]. Reptiles such as alligators [148-152], crocodiles [153, 154], and snakes [155] may serve as amplification/overwintering hosts for the virus, as with other arboviruses [156-161].

Human and equine infections typically occur as spillover events, whereby they are fed on by infected mosquitoes either due to a lack of suitable avian prey, or simply by opportunity. Mammals such as humans and equines are not thought to be capable of sustaining WNV transmission cycles due to the inability to develop sufficient viremia titer to transmit back to mosquitoes (established as being 10^4 - 10^5 plaque forming units [PFUs]/mL of blood [137]), and are therefore considered to be dead-end hosts for the virus [162].

Mosquito Vectors of WNV in the United States

Mosquitoes known as competent vectors of WNV primarily belong to the genus *Culex*. In particular, the *Cx. pipiens* complex, which includes *Cx. pipiens*, *Cx. quinquefasciatus*, *Cx. australicus*, and *Cx. globocoxitus*, have world-wide distributions and exhibit varying competencies to WNV [124]. In the United States, the predominant vector of WNV differs based on geographical location. In the Northeastern U.S, *Cx. pipiens* and *Cx. restuans* appear to cause the majority of infections [163, 164]. *Cx. tarsalis*, the species thought to be responsible for the westward expansion of the virus, is the predominant vector in the central and Western U.S. [165, 166]; the sister taxon to *Cx. pipiens*, *Cx. quinquefasciatus* is a major vector in the Southern U.S. [167], and *Cx. nigripalpus* is most responsible for WNV transmission in Florida stretching down to Puerto Rico [168, 169]. In addition to *Culex* mosquitoes, mosquitoes in the genera *Aedes* and *Ochlerotatus* are moderately competent in laboratory settings, and may serve as peripheral or bridge vectors in the avian-Culex cycle, though due to their primarily mammalian feeding preferences, their importance in the maintenance and transmission of the virus is in question [127].

WNV Pathogenesis in Mosquitoes and Mammals

In mosquitoes, WNV (and other arboviruses) are generally thought to cause persistent, non-lytic infections [170, 171], though apoptotic cell death has been observed in mosquito midguts and salivary glands after infection with a variety of arboviruses [172-179] (discussed in greater depth in the “Mosquito Innate Immunity to Virus Infection” section). Since they ultimately require to be amplified and transmitted, and that eventual transmission is likelier

through a healthy vector, it would seem beneficial to arboviruses to produce primarily benign infections within their arthropod hosts [180]. This appears to be the case with several arboviruses [181-183]. However, infection by arboviruses is apparently not without cost, as studies have shown infected mosquitoes exhibit decreased fecundity [184, 185] and increased blood-feeding, which ultimately increases the likelihood of transmission, but may also increase the likelihood of injury or death to the mosquito by its prey [124]. Intriguingly, resistance to WNV infection in a highly susceptible colony of *Cx. pipiens* was correlated with decreased survivorship, indicating that mounting a robust immunological response may have deleterious consequences for the insect as well [180]. Taken together, the variety of studies investigating the cost of virus infection in vectors seem to indicate that vector/virus pairing and mode of transmission (horizontal or vertical) appear to strongly affect the virulence of arbovirus infection in mosquitoes [186].

After imbibing a bloodmeal containing WNV, the first site of infection in mosquitoes occurs in the mesenteron (midgut) epithelium, where the virus presumably enters cells through receptor-mediated endocytosis, as with other flaviviruses [187, 188]. Studies with DENV-2 and Venezuelan equine encephalitis virus (VEEV, *Togaviridae*) indicate that only a small number of cells (as low as 10-15) of the midgut epithelium are initially infected [189-191]. A secreted protein, mosquito galactose-specific C-type lectin (mosGCTL-1), has been shown to interact with the E glycoprotein of WNV and facilitates its contact with the cellular surface receptor mosquito protein tyrosine phosphatase-1 (mosPTP-1) [192] in both *Cx. quinquefasciatus* and *Ae. aegypti* mosquitoes, though whether this interaction directly results in endocytosis of the virion or merely functions as attachment scaffolding is unknown [193]. Several mosGCTL-1

paralogs (but not mosGCTL-1 itself) have recently been shown to enhance DENV-2 infection in *Ae. aegypti* as well [194]. In addition to the C-type lectins, heat-shock proteins [195, 196], laminin receptor [197], and prohibitin [198] have also been implicated as cellular receptors for DENV, though the role they may play in WNV infection is unknown. Following replication in the midgut, the virus can disseminate into the hemocoel of the insect, infecting and replicating within a variety of tissues including the muscles surrounding the alimentary tract, fat bodies, hemocytes, and nervous tissue, before finally invading the salivary glands, which may result in transmission [199]. During the course of infection, the virus encounters and must circumvent numerous physical and immunological barriers, i.e. the midgut infection barrier [200], the midgut escape barrier [201], the salivary gland infection barrier [202], and the salivary gland escape barrier [203], with failure to do so at any of these points eliminating the possibility of transmission.

In mammalian systems, numerous cellular receptors have been proposed to participate in viral binding and entry [193]. Receptors implicated to be used by various flaviviruses, including WNV, include the glycosaminoglycan (GAG) heparin sulfate [204-209], heat shock proteins [210-215], the C-type lectins DC-SIGN and L-SIGN [216-221], mannose receptor [222], and CLEC5A [223], laminin receptor [224], phosphatidylserine receptors TIM [225, 226] and TAM [225], Integrin $\alpha\beta 3$ [227, 228], scavenger receptor Class B type I [229], claudin-1 (a component of tight junctions) [230, 231], and the natural killer cell activating receptor NKp44 [232]. Most of these studies were performed using DENV, but it is possible that a dependence on some or all of these receptors is shared by WNV.

Keratinocytes and resident dendritic cells (DCs) are the first cells to become infected after a mammal is infected with WNV from percutaneous exposure through the bite of a mosquito, with the mosquito secreting proteins in its saliva that help facilitate infection [233]. Migration of infected DCs to the draining lymph nodes may aid the virus in spreading to the visceral organs and invasion of the central nervous system (CNS) [95], which can result in the most serious disease manifestations associated with WNV infection; namely aseptic meningitis or encephalitis. Invasion of the CNS may occur through one or more mechanisms, i.e. direct crossing of the blood-brain barrier (BBB), facilitated transport across the BBB by infected macrophages (“Trojan horse”), passage through the BBB endothelium, or retrograde axonal transport to the CNS via olfactory or peripheral neurons [234, 95]. Approximately 80% of people infected with WNV are asymptomatic, and ~20% exhibit a febrile illness. Neuroinvasive disease associated with WNV is rare, occurring in <1% of patients [235]. Risk factors implicated in the development of WNV neuroinvasive disease include advanced age, gender, alcohol abuse, and diabetes, among others [236-240, 95]. Additionally, individuals with the CCR5 Δ 32 mutation, which confers resistance to HIV-1 infection [241, 242], are also at increased risk of symptomatic WNV infection [243].

WNV Vaccine Development

Vaccines for YFV, JEV, and TBEV have been approved for use in humans for some time now [244]. However, at present time, there is not an approved vaccine for use in humans for WNV [245], though several exist for equines [246]. The E glycoprotein is the major target of neutralizing antibodies, and therefore the protein has largely been the focus of vaccine

development [247]. There are numerous candidate human vaccines for WNV in various phases of research and development, utilizing a variety of strategies such as live attenuated viruses/chimeras, plasmid DNA, inactivated virus, E glycoprotein subunits, replicons, or virus-like particles (VLPs) [248]. Most of these vaccines are in the preclinical stage of development, however two are in phase I clinical trials and a single vaccine candidate is currently in stage II clinical trials [248]. The latter vaccine, ChimeriVAX-WN02 (Sanofi Pasteur, France) is a chimeric YFV-17D virus expressing WNV prM/E genes in place of the same genes from YFV [244]. Data from a phase II clinical trial showed that 28 days following inoculation, seroconversion was achieved in >96% of subjects, and that the vaccine was highly immunogenic and safely tolerated by all age groups at all dosage levels [249]. A second phase II study using only subjects ≥50 years old found that among these subjects, seroconversion rates were >92% with a single dose of the ChimeriVAX vaccine [250], indicating that this vaccine shows promise as a safe and efficacious prophylaxis against WNV.

In addition to WNV-specific vaccines, the efficacy of existing flavivirus vaccines, such as for JEV or YFV, has been investigated for cross-protection against WNV [245, 251-253]. There has been some evidence in animal models of cross-protective immunity to WNV following vaccination with heterologous flaviviruses [254, 255]. In mice, only partial protection upon challenge with WNV was seen after vaccination with the mouse brain-derived JE-VAX (BIKEN, Japan) inactivated virus vaccine [256]. However, the cell culture-derived JE-ADVAX (Vaxine, Australia) [257], which is formulated with inactivated JEV antigen and Advax, a polysaccharide, plant inulin-derived adjuvant [258], showed significant protection in mice after challenge with WNV [245, 253]. In human studies, the results of vaccination with heterologous flavivirus

vaccines have been less encouraging [259, 251]. The development of an effective, safe vaccine for WNV has some promising prospects, but given the early stages of development for most potential candidates, it may be a few years before one is approved and available for use in humans [246]. Additionally, factors such as the low cost effectiveness of a vaccine due to the relatively rare incidence of disease [260], and the seasonal and relatively unpredictable nature of WNV infection (making the design of clinical trials problematic) [246], may further delay these efforts.

Mosquito Innate Immune Responses to Virus Infection

Invertebrates lack an adaptive immune system, as well as many of the effector molecules present in mammalian innate immune response (i.e interferon), but they possess sophisticated mechanisms for dealing with microbial pathogens. The following section on insect innate immunity was excerpted from **“The Role of Innate Immunity in Conditioning Mosquito Susceptibility to West Nile Virus” Prasad et al *Viruses* 2013, 5, 3142-3170** [261], which attempts to focus mostly on the mosquito innate immune response to WNV infection, but draws heavily from published data in a variety of other invertebrate host/virus systems, and is included to provide a detailed overview of insect innate immune pathways and their role in controlling arbovirus infection.

Small RNA Regulatory Pathways

Small RNA regulatory pathways (SRRPs) are an integral component of endogenous pre- and post-transcriptional gene regulation. Three primary classes of small RNAs exist within

metazoans: micro-RNAs, (miRNAs), small-interfering RNAs (siRNAs), and PIWI-interacting RNAs (piRNAs), being distinguished by both the size of the small RNA product, and their biogenesis. Invertebrates lack type I and type III interferon (IFN) responses, which are the main innate immune pathways through which vertebrates respond to virus infection. Rather, in invertebrates, there is ample evidence highlighting the role of SRRPs in antiviral innate immunity. Exogenous RNA interference (exo-RNAi) via the siRNA pathway appears to be the primary small RNA response; however, involvement of the piRNA pathway in antiviral defense has recently been described in both mosquitoes and mosquito cell culture. In this section, we will discuss the role of these pathways and their components in the context of antiviral defense to WNV.

Exo-siRNA Pathway

RNA interference (RNAi) was first described in plants as a mechanism for “post-transcriptional gene silencing” [262], and later, “virus-induced gene silencing” [263], two phenomena which, at the time, were seemingly unrelated. Several years after these initial observations, double-stranded RNA (dsRNA) was found to be the trigger for RNAi in *Caenorhabditis elegans* [264] and *Drosophila melanogaster* [265]. In invertebrates and plants, exo-RNAi is induced by cellular recognition of long dsRNAs as pathogen-associated molecular patterns (PAMPs), which naturally occur as viral genome replication intermediates and genomic RNA secondary structures in the case of RNA viruses, and as convergent transcripts in DNA viruses. These dsRNAs are recognized and cleaved by Dicer-2 (DCR2), a cytoplasmic RNase III enzyme, resulting in 19-23 base pair (bp) fragments (predominately 21 bps) termed siRNAs.

siRNA duplexes produced in this manner exhibit 5' monophosphates and 3' hydroxyls, as well as two-nucleotide (nt) overhangs on their 3' termini. These siRNAs are then loaded into the Argonaute-2 (AGO2)-containing RNA-induced silencing complex (RISC) through association with a DCR2/R2D2 heterodimer [266]. After the duplex is unwound a single-stranded RNA known as the guide strand remains associated with the RISC, and is 2'-O methylated by the methyltransferase HEN1 [267, 268], and the complementary strand, known as the passenger strand, is degraded. The RISC then recognizes cognate mRNA (in this case, virus genomic RNA) by sequence complementarity with the guide strand. Cleavage of the target occurs through the Slicer endonuclease activity of AGO2 [269]. Unlike miRNAs, where mismatches between the guide strand and target are tolerated, even a single mismatch in complementarity between an siRNA and its target can result in diminished or abolished silencing [270, 271]. In this way, the siRNA pathway acts as a highly potent antiviral pathway in controlling arbovirus infection.

The role of the siRNA pathway in antiviral defense in arthropods has been the subject of intense investigation in recent years. In *Drosophila*, numerous studies have demonstrated that RNAi inhibits virus replication [272-274]. Notably, *Drosophila* with a null mutant DCR2 enzyme exhibit ~70% mortality and dramatically higher virus titers when inoculated with Sindbis virus (SINV, *Togaviridae*), as compared to wild-type controls [273]. In mosquitoes, evidence of the involvement of the siRNA pathway during arbovirus infection has been observed in several virus/arthropod pairings, including o'nyong-nyong virus (ONNV, *Togaviridae*) in *Anopheles gambiae* [275], Sindbis virus (SINV, *Togaviridae*) in *Aedes aegypti* [276, 277], and DENV in *Ae. aegypti* [278]. viRNAs produced in response to WNV had been detected in *Drosophila* S2 cells, but not *Ae. albopictus* C6/36 cells [279] due to a dysfunctional siRNA pathway [280, 281]

resulting from a single nucleotide deletion introducing a premature stop codon within the open reading frame (ORF) of DCR-2 [282]. One potential pitfall in interpreting the results of these studies is the utilization of non-natural virus/vector pairings and/or infection routes (i.e. intrathoracic inoculation), with the exception of Sanchez-Vargas et al. [278]. Brackney et al. utilized next-generation sequencing (NGS) to profile the antiviral RNAi response to WNV in its natural vector, *Cx. quinquefasciatus* mosquitoes, following peroral infection, and found viRNAs produced in the midgut of mosquitoes at 7 and 14 days post-infection (dpi) [283]. viRNAs produced in this manner were primarily 21 nts in length (indicative of DCR2 processing), and were asymmetrically distributed along the entire length of the virus genome.

Given the requirement for high target sequence complementarity in siRNAs, it comes as no surprise that RNAi can drive viral diversity and evolution through the generation of RNAi-escape mutants that differ sufficiently from the master sequence. Viral escape from one or a few transfected siRNAs has been observed in a variety of different systems, including hepatitis C virus (HCV, *Flaviviridae*) [284], human immunodeficiency virus-1 (HIV-1, *Retroviridae*) [271], turnip mosaic virus (TuMV, *Potyviridae*) [285], and poliovirus (PV, *Picornaviridae*) [286]. Based on the observation that WNV population structure was more complex in mosquitoes than in birds [287], it was hypothesized that the mosquito RNAi pathway may serve as a potent selective pressure on the virus to favor generation and maintenance of rare mutants. Indeed, a correlation between nucleotide targeting and increased likelihood for corresponding point mutations has been observed [283], though it is important to note that this observation was associative, and does not demonstrate causation. Taken together, these studies highlight the role this pathway may play in mosquito innate antiviral immunity, and shed light on how it may

influence virus diversification and evolution. Moreover, the error rate of the virus replicase complex may serve in part as an evolutionary mechanism for circumventing the mosquito siRNA-based antiviral response through the generation of rare mutants which differ sufficiently from the master sequence. This is circumstantially supported by the observation that a chikungunya virus (CHIKV, *Togaviridae*) mutant expressing a high fidelity RdRP exhibited lower infection and dissemination titers in mosquitoes as compared to the wild-type virus [88]. However, it should be noted that the molecular basis for this observation was not investigated, and that immunological factors other than RNAi could potentially influence the fitness of a genetically homogeneous virus population.

Systemic RNAi, first described in plants and worms, is the process by which the siRNA response spreads beyond the site of initiation into surrounding cells and tissues (see [288] for a review). The mechanism of spread differs between plants and animals, with short-distance transport of siRNAs in plants occurring through plasmodesmal junctions connecting cells, and long-distance transport being mediated by the vascular system. In *C. elegans*, spread of the RNAi signal is mediated by members of the SID family of transmembrane transporters [289, 290]. Evidence suggests that this process may occur in dipterans as well, and has broad implications in understanding RNAi-based antiviral immunity in these systems. Studies in flies have revealed a systemic RNAi pathway [291, 292], and cell-to-cell spread of viRNAs produced in response to Semliki Forest virus (SFV, *Togaviridae*) infection has been demonstrated in mosquito cell culture [293]. In *C. elegans*, primary viRNAs are amplified in a target dependent manner by the endogenous RNA-dependent RNA polymerase (RdRP) RRF-1, which contributes to systemic RNAi spread and subsequent maintenance of long-term silencing [294]. Secondary

viRNAs produced in this manner are composed entirely of antisense polarity, and exhibit 5' di- or triphosphates, making them structurally unique, and thus a distinct class of small RNA molecules [295, 296]. While an RdRP capable of amplifying viRNAs has not been conclusively identified in dipterans, a recent publication suggests that viral RNA produced during flock house virus (FHV, *Nodaviridae*) infection in *Drosophila* can be reverse-transcribed into viral cDNAs mediated by the reverse transcriptase activity of endogenous long terminal repeat (LTR)-retrotransposons [297]. Viral cDNA produced in this manner may then be integrated into the host cell genome, or circularized into stable, extrachromosomal DNA which can be efficiently transcribed into dsRNAs that can be fed back into the siRNA pathway, leading to a primed immune response, and allowing for a persistent infection to develop. Additionally, viRNAs produced in response to FHV infection in *C. elegans* have been observed to be transgenerationally inherited from mother to offspring in successive generations [298], raising the intriguing possibility that similar mechanisms of amplification and non-Mendelian, extrachromosomal inheritance of small RNAs may exist in mosquitoes as well, though it should be noted that to date, there is a lack of experimental data supporting this. Given the aforementioned importance of the RNAi pathway in mosquito innate immunity to viral infection, inheritance of viRNAs might be expected to influence mosquito vector competence and arbovirus populations in nature.

Vago

Cross-talk between SRRPs and other innate immune pathways is an emerging feature of mosquito antiviral defense against arboviruses. DCR2 belongs to the same family of DExD/H-

box helicases as the RIG-I-like receptors, which are involved in the induction of the IFN response in mammalian systems. Deddouche et al. reported that the secreted peptide *vago* is induced in *D. melanogaster* in response to *Drosophila C virus* (DCV, *Dicistroviridae*) and SINV infection in the fat bodies of flies, and that induction of *vago* was reliant on the amino terminal DExD/H-box domain of DCR2 [299]. Notably, infection by FHV did not induce *vago* expression, likely due to the FHV encoded viral suppressor of RNAi, B2, which binds dsRNA thereby interfering with downstream signaling by DCR2. While *vago* was shown to control virus infection in this study, the mechanism by which it did so was unclear. Pradakar et al. further explored *vago*'s role in antiviral immunity using cultured mosquito cells and WNV [300]. It was found that *vago* was effective in limiting WNV infection in *Cx. quinquefasciatus*-derived Hsu cells, and that induction of *vago* resulted in activation of Jak/STAT signaling, leading to the induction of the STAT-dependent virus inducible gene *vir-1*, thereby restricting WNV replication. Although the identity of the cellular receptor for *vago* is currently not clear, studies published to date suggest that components of the RNAi pathway can have diverse, multifunctional roles in controlling arbovirus infections in mosquitoes.

PIWI-Interacting RNA Pathway

Recent evidence suggests that a second class of small RNAs with distinct biogenesis may also be induced in arthropods following virus infection. The p-element induced wimpy testes (PIWI) class of Argonaute proteins were first discovered in 1997 by Lin et al. and shown to be potent regulators of spermatogenesis in *Drosophila* [301]. In 2006, several studies were published indicating that PIWI proteins interact with a unique class of small RNAs, named PIWI-

interacting RNAs (piRNAs; the nomenclature at the time was variable, and they were also referred to as repeat-associated small interfering RNAs [rasiRNA], which are now considered a distinct subclass of piRNAs) [302-306]. piRNAs exhibit some unique features that distinguish them from miRNAs and siRNAs. First, piRNAs are considerably larger than most miRNAs or siRNAs, the latter two ranging from 20-23 nts in length, the former 24-30 nts. Secondly, piRNAs are produced from single stranded precursor molecules independently of Dicer processing. Like siRNAs, but not miRNAs, piRNAs are modified by HEN1, which results in 2'-O-methylation at the 3' terminus of the RNA [268, 307]. Additionally, expression of piRNAs shows tissue specificity, with gonadal tissue being highly enriched for this species and associated proteins. Endogenously transcribed and processed piRNAs have been shown to be important repressors of transposable elements (TEs) in these tissues. However, expression of piRNAs has been detected in somatic tissue as well [308, 309].

Biogenesis of piRNAs is proposed to occur through two pathways: the primary pathway and the ping-pong dependent amplification loop. In the primary pathway, piRNAs are processed from single-stranded precursor molecules transcribed from genomic loci (piRNA clusters). In flies, primary piRNAs are associated with PIWI and Aubergine (AUB) [310], and are typically antisense to TEs [305]. Primary piRNAs produced in this manner exhibit a strong bias for a uridine residue at the 5'-terminus of the transcript (U_1). These primary piRNAs are then fed into the ping-pong dependent amplification cycle, whereby after binding to their target transcript, cleavage occurs 10 nts upstream from the 5' terminus of the primary piRNA [311, 312]. Thus, Argonaute 3 (AGO3)-associated secondary piRNAs exhibit an adenine residue in the 10 position (A_{10}). Secondary piRNAs subsequently bind complementary transcripts, resulting in cleavage at

the A₁₀-U basepairing, producing piRNAs corresponding to the sequence of the initial primary piRNA they were derived from, thereby restarting the cycle.

Recently, the piRNA pathway has been implicated in antiviral immunity in invertebrates. A possible hypothesis is that the piRNA pathway can act in a compensatory manner, such as when the siRNA pathway is overburdened or suppressed. Indeed, in *Drosophila*, flies with a null mutant PIWI protein exhibited significantly higher titers of WNV in comparison to wild-type controls [279]. Silencing of AGO3 in *An. gambiae* has been shown to result in increased dissemination of ONNV [275], and dsRNA-knockdown of piRNA-pathway component proteins has been shown to result in increased titers of SFV in *Ae. aegypti*-derived Aag2 cells, with knockdown of PIWI-4 in particular showing considerable effect in this regard [313]. Additionally, sequencing of small RNAs in DENV2-infected *Ae. albopictus* C6/36 cells, which as previously mentioned, have a dysfunctional siRNA pathway [280-282], revealed a shift from the stereotypically predominant distribution of siRNAs (19-23nts, no significant strand bias) to products consistent with the piRNA pathway (24-30 nts, predominately positive strand, A₁₀ bias) [281]. Wu et al. described a population of virus-derived small RNAs in their sequencing of persistently-infected *Drosophila* ovary somatic sheet (OSS) cells that held hallmarks of piRNAs; specifically, being between 24-30 nts in length, exhibiting a strong (95%) strand bias, and a preference for a 5' uracil (though, notably, no bias for an A₁₀ was seen) [314]. Similarly, 24-30 nt small RNAs produced in response to DENV2 in *Ae. aegypti* mosquitoes have been found by deep-sequencing [315]. Interestingly, piRNA-like small RNAs sequenced in the latter study exhibited no preference for a 5' uracil, and only a slight bias for an A₁₀ residue.

Recently, piRNA-like small RNAs exhibiting characteristics of ping-pong dependent amplification have been sequenced in mosquitoes and mosquito cells after virus infection. Morazzani et al. found that piRNA-like small RNAs are produced in the soma (non-ovarial tissue) of both *Ae. aegypti* and *Ae. albopictus* after infection with CHIKV, and that, unlike endogenously transcribed piRNAs, dsRNA was likely the biogenic precursor for virus-derived piRNAs [282]. Likewise, small RNAs from Aag2 and *Ae. albopictus*-derived U4.4 cells infected with SINV shared these same characteristics [316]. In the same study, sequencing data from C6/36 cells infected with La Crosse virus (LACV, *Bunyaviridae*) revealed ping-pong dependent signatures in the piRNA-like viral small RNA population. Similar results from small RNA deep-sequencing of virus infected invertebrate hosts has also been seen in Rift Valley fever virus (RVFV, *Bunyaviridae*) infected mosquito cells [317], as well as Schmallenberg virus (SBV, *Bunyaviridae*)-infected *Culicoides sonorensis*-derived KC cells and Aag2 cells, and blue-tongue virus (BTV, *Reoviridae*)-infected *Culicoides* and mosquito cells [318] (though notably, 24-30 nt small RNAs sequenced from BTV-infected cells did not exhibit signatures of ping-pong dependent amplification). The disparity between different virus/host pairings producing piRNAs either possessing or lacking signatures of ping-pong dependent amplification suggests that the piRNA response may be differentially modulated in response to infection by diverse viruses.

While no studies profiling the piRNA response in a *Culex* mosquito/WNV pairing have been published, the existing data in these numerous other infection models suggest that it too may play a significant role in this system.

WNV sfRNA as a viral suppressor of RNAi (VSR)

Most arboviruses cause persistent infections within their arthropod vectors. This has led to speculation as to how these viruses maintain infection in the face of a robust RNAi response. In addition to the evolutionary mechanisms (i.e. the viral replicase error rate) described above, many plant and insect-specific viruses have developed molecular mechanisms for subverting the host RNAi response. For example, the previously mentioned FHV encodes a protein, B2, which binds to dsRNA and inhibits the function of DCR2, effectively rendering the siRNA pathway inert [319]. Plasmid-expressed LACV NSs protein has been shown to inhibit IFN and RNAi in mammalian cells and mice [320, 321]. However, NSs fails to show any RNAi-suppressive effect in LACV-infected C6/36 cells or in NSs plasmid-transfected U4.4 cells infected with SFV [320]. A recent publication demonstrated that DENV NS4b functions as a VSR in human Huh7 cells via inhibition of dsRNA processing by Dicer [322]. However, whether NS4b behaves similarly in mosquitoes has not been investigated, and to date, no VSR activity has been described for an arbovirus protein during mosquito infection. Thus, it is currently not clear how arboviruses establish and maintain persistent infection of arthropods.

Recently, intriguing evidence has been presented that viral subgenomic RNAs may function as VSRs in some cases. All flaviviruses studied thus far produce a sub-genomic RNA product (sfRNA) from the 3' UTR of the virus genome [323]. In WNV, this RNA comprises the last 525 nts of the virus genome. sfRNA is produced by incomplete degradation of the viral genome by the cellular 5'-to-3' exoribonuclease XRN1, which stalls on the conserved pseudoknot-like structures present at the 5'-terminus of the 3' UTR, resulting in large amounts of sfRNA accumulating within infected cells [324, 325]. Recent evidence using fluorescent

reporter assays suggests that the WNV sfRNA may act as a VSR by interfering with Dicer in a concentration-dependent manner [326], though this type of assay alone may be prone to misinterpretation, and should be corroborated by genetic rescue experiments [327]. The mechanism through which sfRNA exerts this effect is unclear, but it is hypothesized that it acts as a decoy substrate for DCR2. Interestingly, sfRNA has also been shown to act in a negative feedback loop by suppressing XRN1 activity due to the enzyme stalling at the 3'UTR [328], illustrating that multiple antiviral pathways can be manipulated by this decay product.

Immune Signaling Cascades

In addition to RNAi, there are numerous other innate immune pathways responsible for protecting insects from pathogenic organisms. These include the Toll, Immune Deficiency (Imd) and the Janus kinase (Jak)/signal transducer and activator of transcription (STAT) pathways, as well as the phenoloxidase (PO) cascade. Early characterization of these pathways revealed that the Toll pathway was activated upon challenge with gram-positive bacteria and fungi whereas the Imd pathway is responsive to gram-negative bacteria. In each case, signal transduction events initiated upon recognition of PAMPs by pattern recognition receptors (PRRs) results in the transcription of downstream effector molecules, specifically antimicrobial peptides (AMPs). The specific factors responsible for Jak/STAT activation and the downstream effector molecules are not well characterized, but numerous gene products are transcriptionally controlled by this pathway. The PO cascade is integral in wound healing and melanization of pathogenic organisms. Activation of PO results from cuticular damage or PAMP recognition. Traditionally thought to confer protection against bacterial, fungal and parasitic pathogens, recent evidence

suggests that these pathways may also play a role in antiviral immunity. The details of these pathways have been extensively reviewed previously [329, 330].

Toll Pathway

The Toll pathway was originally described in *Drosophila* as an evolutionarily conserved signaling cascade involved in the establishment of the dorso-ventral axis as well as in many other developmental processes [330, 331]. It has since been characterized as having a significant role in innate immunity to gram-positive bacteria and fungi [332, 333]. More recently, some studies suggest that the Toll pathway may serve an important role in antiviral immunity. In 2005, Zambon et al. observed a significant increase in the expression of the Toll regulated AMPs, Drosomycin and Metchnikowin, upon *Drosophila* X virus (DXV; *Birnaviridae*) challenge of *Drosophila* [334]. It was further shown that flies lacking a functional Toll pathway were significantly more susceptible to DXV challenge. Similarly, it was determined that Toll pathway components and AMPs were significantly up-regulated upon DENV infection of *Ae. aegypti* mosquitoes [335]. Further, suppression of Cactus (a negative regulator of Toll signaling) or MyD88 (a Toll signaling adapter protein) resulted in modest but significant reductions and accumulations of infectious DENV particles in the mosquito midguts, respectively [336]. These findings were confirmed by another study in which Toll pathway components were up-regulated upon DENV infection of *Ae. aegypti* salivary glands [337]. In addition, a modest increase in Dif (a Toll inducible NF- κ B transcription factor) was recognized during early stages of SINV infection of *Ae. aegypti* [338]. Together, these data suggest that the Toll pathway plays a

role in antiviral immunity in insects; however, others have observed conflicting results [339-341].

Colpitts et al. observed significant reductions in the expression levels of the *Ae. aegypti* ortholog of *Drosophila* Spätzle 5 (an upstream signaling peptide of the Toll pathway) upon *Ae. aegypti* infection with three flaviviruses; WNV, yellow fever virus (YFV, *Flaviviridae*) and DENV [339]. In addition, transcript levels of the *Ae. aegypti* ortholog to *Drosophila* Toll was reduced upon YFV infection. These findings challenge those previously published by Xi et al. [335]. Many confounding factors may account for this difference, including but not limited to experimental design, mosquito strains, virus strains and/ or environmental conditions. The authors of this study did not directly address these discrepancies, but rather suggested that viral-associated reductions potentially indicate an evolved mechanism by which arboviruses suppress antiviral pathways. However, there is currently no evidence supporting this. Using the SFV – *Aedes* U4.4 cell system, Fragkoudis et al. observed a down-regulation of Toll pathway component transcript levels upon infection by SFV. Furthermore, prior activation of the Toll pathway did not seem to adversely affect SFV replication in U4.4 cells [340]. From these studies it is difficult to determine with confidence the contribution of the Toll pathway to antiviral immunity of insects as a whole. However, these findings may indicate that Toll-mediated antiviral activity is specific to each virus–insect pairing. With regards to WNV, little is known about the role of this pathway during infection of insects except for the apparent down-regulation of the Spätzle5-like cytokine during infection of *Ae. aegypti* mosquitoes and that none of the canonical Toll pathway genes and/or associated AMPs were significantly altered during WNV infection of *Cx. quinquefasciatus* [341]. Further research will be needed to fully elucidate the possible

contributions of Toll pathway mediated antiviral immunity during WNV infection of mosquitoes.

Immune Deficiency (Imd) Pathway

The Imd pathway is another immune signaling cascade of insects and bears striking similarities to the Tumor Necrosis Factor (TNF) pathway of mammals. It was initially described after the identification of a mutant *Drosophila* line that had significantly decreased levels of numerous AMPs, yet maintained normal levels of another AMP, Drosomycin [332, 342, 343]. These findings indicated that the expression of AMPs were controlled by two or more regulatory cascades. It was later determined that *imd* mutant flies were highly susceptible to infection with gram-negative bacteria yet maintain resistance to gram-positive bacteria and fungi [330]. Recently, the Imd pathway has been implicated in antiviral immunity in insects. The first indication of the potential significance of the Imd pathway during viral infections was observed in the *Drosophila* - cricket paralysis virus (CrPV; *Dicistroviridae*) model [344]. Somewhat paradoxically, the authors found that while AMPs were not up-regulated during infection with CrPV, suggesting that neither the Imd or Toll pathways were responsive to CrPV infection, mutant flies lacking components of the Imd pathway were more susceptible to viral infection resulting in shortened lifespan and increased viral replication. Together, these data suggest that Imd activation is uncoupled from AMP induction during infection with CrPV, and implies that induction of the Imd pathway results in transcription of several other genes with presently unknown roles in immunity [345]. The role of the Imd pathway in antiviral immunity is further supported by the observations of Avadhanula et al. and Huang et al. Using a novel SINV

replicon transgenic *Drosophila* line, the authors observed increased AMP expression as well as a modest but significant increase in susceptibility of Imd-deficient lines to SINV challenge [346, 347]. Additionally, Sigma virus (SIGMAV; *Rhabdoviridae*) infection of *Drosophila* induced the expression of numerous Imd controlled AMPs; however, the significance of these observations on SIGMAV replicative fitness or fly survivorship were not assessed [348]. While there have been several studies implicating the role of Imd during antiviral immunity, there have been just as many suggesting otherwise. The induction of almost all AMPs were observed during DXV infection of *Drosophila*, yet mutant flies lacking a functional Rel (an Imd inducible transcription factor) were no more susceptible to DXV challenge than the controls [334]. Further, a lack of AMP induction was observed during DCV infection of *Drosophila* [299, 349]. As with the Toll pathway, it is difficult to discern the significance of the Imd pathway in antiviral immunity based on these studies. This uncertainty is further confounded by the fact that the majority of these viruses do not naturally infect *Drosophila*, with the exception of SIGMAV and DCV.

These ambiguities in the literature also encompass mosquito–virus interactions. Recently, a cecropin-like peptide presumed to be under the control of the Imd signaling cascade was found to be significantly induced upon DENV infection of *Ae. aegypti* salivary glands [337]. Characterization of this peptide revealed that it could potentially inhibit DENV and CHIKV replication in mosquito cell culture. However, the significance of its antiviral effect has not been confirmed with *in vivo* knock-down studies. In addition, other studies have observed either down-regulation or insignificant differences in the expression of Imd-controlled AMPs or pathway components during SFV infection of *Aedes* U4.4 cells or ONNV infection of *An. gambiae* [340, 350], although in the former study, decreased SFV replication in Imd and

Jak/STAT activated U4.4 cells was observed. The biological relevance of these findings is difficult to determine at this time because functional assays assessing their significance during natural infections of adult mosquitoes have not been performed. Studies investigating the role of Imd during WNV infection of mosquitoes are lacking, and it remains to be seen what if any effect this pathway has on shaping antiviral immunity to WNV in relevant mosquito vectors; however, it was demonstrated that Imd gene transcripts and/or associated AMP transcripts were unaltered during WNV infection of *Cx. quinquefasciatus* [341].

Jak/STAT Pathway

The Jak/STAT pathway is an evolutionarily conserved pathway first described for its role in embryonic segmentation in *Drosophila* [351]. Subsequently it was determined that it has an important role in antibacterial defense. It is composed of the three major components, the receptor Domeless, the Janus Kinase (Jak) Hopscotch, and the transcription factor STAT [352, 353, 351]. Unlike the Toll and Imd pathways, a well characterized subset of inducible effector AMPs have not been associated with this pathway; however, a handful of inducible genes containing a STAT binding site in their promoters have been identified, with some of these gene products appearing to have antiviral effects.

The initial findings implicating a role of Jak/STAT in antiviral immunity in insects were observed in the *Drosophila*–DCV model. By performing microarray analysis on bacterial, fungal, and DCV challenged flies, the authors identified a subset of gene products that were up-regulated during DCV infection but not during fungal or bacterial challenge [349]. Upon closer inspection the authors identified a gene, *vir-1*, that contained the STAT binding site within its

promoter and was strongly induced during DCV and FHV challenge. Furthermore, it was demonstrated that Jak/STAT deficient flies were more susceptible to DCV challenge as determined by increased DCV replication and increased mortality. These results were confirmed by studies performed by Kemp et al. who also demonstrated that the Jak/STAT pathway was important in *Drosophila* antiviral immunity to CrPV [354]. Interestingly, when Jak/STAT deficient flies were challenged with five other evolutionarily divergent viruses, including SINV, DXV and FHV, the authors found no effect on the survivorship of the flies. These results indicate that Jak/STAT involvement in antiviral immunity may be specific to each virus–insect pairing and not broadly applicable to all systems.

A role for Jak/STAT involvement in mosquito immunity to arboviruses has been described. Specifically, components of the Jak/STAT pathway as well as Jak/STAT inducible gene products were found to be up-regulated upon DENV infection of *Ae. aegypti* mosquitoes [355, 335]. Included in these findings were two novel Jak/STAT inducible genes termed Dengue Virus Restriction Factors 1 and 2 (DVRF1-2). Further, it was demonstrated that suppression of these two genes resulted in 2.5- and 2.2-fold increases in DENV-2 replication in mosquitoes, respectively [355]. In addition, a recent study demonstrated that WNV induces the expression of *vago* in Hsu cells. Subsequent silencing of *vago* increased WNV titers. The antiviral effect of *vago* expression was determined to arise from downstream *vir-1* activation via *vago*-induced Jak/STAT signaling. Studies in mosquitoes will be needed to validate the *in vivo* role of *vago* in controlling arbovirus infection. As with the Toll and Imd pathways others have observed conflicting data on the role of Jak/STAT pathway in antiviral immunity. In these studies there were no indications of Jak/STAT up-regulation upon infection in four separate virus – vector

models (ONNV/*An. gambiae*, SFV/*Aedes* U4.4 cells, WNV-DENV-YFV/*Ae. aegypti*, WNV/*Cx. quinquefasciatus*) [350, 340, 339, 341]. However, as previously mentioned, activation of the Jak/STAT pathway prior to SFV infection resulted in reduced viral replication in U4.4 cells. From these studies it is difficult to accurately assess the importance of the Jak/STAT pathway in antiviral immunity. Future studies assessing the importance of this pathway on arboviral infection, dissemination and transmission rates within mosquitoes will help clarify its significance. In the context of WNV and mosquitoes, this holds true especially considering the systems utilized; however, it is difficult to determine the relevance considering that one study was limited to cell culture and the other in an ancillary vector. Additional research into the role of Jak/STAT in antiviral immunity in primary mosquito vectors is clearly required in order to fully understand its possible influence on mosquito antiviral responses.

Phenoloxidase (PO) Cascade

Among arthropods, the PO cascade is an evolutionarily conserved extracellular pathway responsible for wound healing and melanization of bacterial and parasitic pathogens [329]. This pathway can be induced by cuticular damage or upon recognition of PAMPs. This in turn activates a serine protease cascade ultimately resulting in the activation of the prophenoloxidase activating enzyme (PPAE). Active PPAE cleaves the prophenoloxidase zymogen to produce PO, which catalyzes the conversion of mono- and diphenolic substrates to quinones, which are then converted to melanin [329]. While direct melanization of viruses has not been observed, there is evidence that by-products of the pathway may have antiviral effects. It was demonstrated that plasma from the tobacco budworm has virucidal effects on

Helicoverpa zea single capsid nucleopolyhedrovirus (HzSNPV; *Baculoviridae*) and chemical inhibition of PO resulted in increased viral titers [356, 357]. It was also determined that 5,6 dihydroxyindole, a byproduct of the PO cascade, could almost completely inactivate *Autographa californica* nucleopolyhedrovirus (AcMNPV; *Baculoviridae*) *in vitro* [358]. Similar antiviral activity has been observed in mosquitoes. Tamang et al. observed increased SINV titers in *Armigeres subalbatus* mosquitoes after suppression of prophenoloxidase I [359]. Such observations were also found during SFV infection of U4.4 cells. Specifically, recombinant SFV over-expressing an inhibitor of the PO cascade was able to replicate to significantly higher titers than the control virus. It was further determined that inhibition of the PO cascade could decrease the survivorship of SFV infected *Ae. aegypti* [360]. The authors went on to demonstrate that the specific effector molecules involved in the antiviral effects were the pathway intermediate quinones. The specific nature of their antiviral effect remains to be determined. Together, these studies highlight the potential role of the PO cascade in insect immunity to arboviruses. These are the first studies to assess the role of the PO cascade in antiviral immunity in mosquitoes and it will be interesting to see if this antiviral effect is conserved among other virus – vector pairings. Future research into the involvement PO cascade during WNV infection of *Culex spp.* mosquitoes is warranted.

Cellular Processes

In addition to RNAi and the PAMP-induced signaling cascades previously discussed, evidence suggests that multi-functional cellular processes can have significant effects on arboviruses in arthropods. Cellular processes, such as apoptosis and autophagy, are important

in maintaining homeostasis in multicellular organisms and integral to their development. Autophagy, in effect, is the recycling center of the cell. It serves an important role in removing damaged organelles and protein aggregates which can put undue stress on the cell, ultimately reducing their constituent macromolecules to basic molecular building blocks and sources of energy. In addition, it appears to function as an innate immune defense against numerous prokaryotic and eukaryotic intracellular pathogens [361, 362]. Interestingly, the role of autophagy during viral infections is not well defined. In some systems, autophagy functions in an antiviral capacity while in others it can be commandeered and utilized in a pro-viral manner [363]. However, to date, little is known about the role of autophagy during arboviral infections of arthropods with the exception of the studies discussed below, which indicate a role in antiviral immunity. Apoptosis is the process of programmed cell death (PCD) which plays an integral role in eliminating old, injured or defective cells from organisms. This process can be differentiated from necrosis by its ability to control the release of cellular components in apoptotic bodies which can be scavenged by phagocytic cells and thereby diminishing any potential immunologic over-reaction [364]. It has been observed that such an approach to stress-induced cell death could predispose viruses and their associated PAMPs to antigen presenting cells. Not coincidentally many viruses have devised mechanisms by which to subvert or avoid apoptosis altogether [365]. In recent years it has become evident that apoptosis may function as an antiviral defense in insects especially with regards to arboviruses.

Autophagy

Autophagy is an evolutionarily conserved pathway that serves an important role in maintaining cellular homeostasis and cell survival [366]. Induction of autophagy results in the formation of double-phospholipid membrane vesicles termed autophagosomes which sequester the targeted organelles and proteins. Subsequently, the autophagosomes fuse with lysosomes forming autolysosomes which mediate degradation of the contents [367]. During normal growth conditions autophagy maintains cellular homeostasis by degrading unwanted or damaged organelles and protein aggregates. In times of cellular stress, autophagy catabolizes these cellular components thereby generating a pool of energy and macromolecules that maintain crucial cellular functions until favorable growth conditions return [366]. In addition, it appears to play a significant role in antiviral immunity in invertebrates. Shelly et al. demonstrated that deletion of autophagy-related genes (*Atg's*) increased vesicular stomatitis virus (VSV; *Rhabdoviridae*) replication and decreased *Drosophila* survivorship [368]. It was later demonstrated that pre-formed PAMPs in the context of UV-inactivated virus appear to interact with Toll-7 at the plasma membrane, which leads to the activation of autophagy independently of the canonical Toll pathway [369]. These studies were the first to examine the antiviral role of autophagy to an arbovirus in the context of an invertebrate host. Additional studies are required in order to clarify whether these findings can be replicated in natural virus–vector pairings.

Apoptosis

Apoptosis is a conserved mechanism of programmed cell death in multicellular organisms [370] that is critical to a variety of biological processes including embryonic development, maintenance of homeostasis, and lysis of virus-infected cells by cytotoxic T-lymphocytes [364]. In vertebrates, apoptosis may be induced through two known pathways: the extrinsic, or death-receptor pathway, and the intrinsic, or mitochondrial pathway [371], though in dipterans only the intrinsic pathway is known to exist [372].

Many viruses from diverse families encode anti-apoptotic genes, such as inhibitors of apoptosis (IAPs), p53-binding proteins, and bcl-2 homologs. This has led to the hypothesis that apoptosis functions as an innate immune pathway in response to viral infection [365]. FHV strongly induces apoptotic events in *Drosophila* DL-1 cells through depletion of the *Drosophila* inhibitor-of-apoptosis-1 (DIAP1) protein, a negative regulator of initiator caspase DRONC and effector caspase DrICE; however, replication of FHV is not negatively impacted by apoptosis [373]. Similar depletion of host cell IAPs were observed in DL-1 cells [374] and *Spodoptera frugiperda* (order Lepidoptera) SF21 cells [374, 375] infected with AcMNPV, which encodes its own viral IAP, p35, with depletion of IAPs in both cell lines being triggered by viral DNA replication [374]. However, p35-deficient mutant viruses demonstrated reduced infectivity of SF21 cells, and reduced infectivity and lethality in *Spodoptera frugiperda* larvae [376]. Furthermore, studies in flies infected with FHV or AcMNPV reveal that rapid induction of apoptosis by the upstream regulator p53 limits viral gene expression and proliferation [377], further highlighting the importance of apoptosis in controlling virus infection in these systems.

Numerous studies have investigated the role apoptosis plays in arbovirus infection models. Apoptosis is a natural consequence of arbovirus infection in mammalian cells, where cytopathic effect (CPE) is frequently seen; conversely, most arboviruses are thought to cause minimal cytopathology in insect cells, instead resulting in non-lytic, persistent infections [170, 171]. However, cell death consistent with apoptosis has been observed in mosquito midgut and salivary gland tissues following infection with a variety of arboviruses [172, 174, 176-179, 175, 173], including WNV. With regards to WNV, apoptosis in the midgut epithelium [177] or salivary glands [174, 173] of *Cx. pipiens* or *Cx. quinquefasciatus* mosquitoes was associated with a resistance to infection or reduced ability to transmit virus, respectively. Thus, an attractive hypothesis is that apoptosis functions in an antiviral capacity to arbovirus infection in mosquitoes, and that it may be more likely to occur in mosquitoes incapable of vectoring a particular virus rather than permissive hosts [378, 379]. Indeed, pro-apoptotic genes in a refractory strain of *Ae. aegypti* mosquitoes were significantly up-regulated between 24 and 48 hours post-infection (hpi) in response to DENV2 infection as compared to a susceptible strain of *Ae. aegypti* or blood-only fed mosquitoes from the same strain [380]. In the same study, dsRNA-knockdown of the caspase inhibitor AelAP1 in two susceptible strains converted the phenotype from susceptible to refractory, and knockdown of initiator-caspase *AeDronc* in the refractory strain resulted in increased permissiveness to DENV2 infection. The same group previously reported up-regulation of pro-apoptotic genes in the DENV2-susceptible strain in comparison to the refractory strain at 48 hpi [381], indicating that apoptotic events controlling virus infection may be induced acutely and rapidly limit the course of infection. However, it is important to note that neither of these studies directly measured apoptotic events in midgut

tissue after DENV2 infection, and that the methods used to measure differential gene expression were different between studies (qPCR and suppressive subtractive hybridization, respectively [380, 381]). Conversely, modulation of apoptosis by RNAi-mediated silencing of either apoptosis inhibitors or initiators in *Ae. aegypti* subsequently infected with SINV produced results contrary to the hypothesis that apoptosis acts in an antiviral manner to arbovirus infection in mosquitoes [382]. Specifically, inhibition of apoptosis led to decreased infection and dissemination rates, and induction of apoptosis led to greater infection and dissemination. The authors speculate that experimental systemic induction or inhibition of apoptosis prior to virus infection, in contrast to apoptosis being stimulated in individual cells in response to virus infection, resulting in widespread destruction of structural barriers to viral infection/dissemination, may account for this apparent discrepancy. In summary, the variety of studies in mosquitoes investigating the role of apoptosis in response to arbovirus infection strongly implicate the pathway as contributing to the acute antiviral response; and that either the presence or lack of an effective apoptotic response has important consequences for vector competence in mosquitoes.

Chapter 2: Small RNA Profiling of the Anti-WNV Response in Field-Collected *Culex sp.*

Mosquitoes: Evidence for Stereotypical Targeting of the Viral Genome and Comparison to

Colonized Mosquitoes

Introduction

Vertebrates and invertebrates differ in their mechanisms for combatting microbial infections. Vertebrates possess both innate and adaptive immune systems; however, invertebrates lack an adaptive immune system entirely, as well as several important innate immunity antiviral effector molecules found in vertebrate systems (i.e. IFN). Most eukaryotic organisms possess pathways for recognizing pathogen-associated molecular markers (PAMPs). PAMPs are recognized by pattern recognition receptors (PRRs), which can be membrane bound, cytoplasmic, or secreted. Double-stranded RNA (dsRNA) is a PAMP which acts as a potent trigger for the RNA interference (RNAi) pathway, the major innate immune response to virus infection in invertebrates, including dipterans such as mosquitoes [383]. Processing through the RNAi pathway involves endonucleolytic digestion of dsRNA into 19-23 bp small-interfering RNA (siRNA) duplexes, of which a single strand, known as the guide strand, is loaded into the RISC and facilitates sequence-specific degradation at complementary regions of target transcripts (such as viral RNA). Numerous studies have investigated the role of RNAi in modulating arbovirus infection in mosquitoes [275, 384, 276, 278, 283, 315, 282, 279, 293, 281, 316, 317]. However, many questions remain to be answered regarding the extent of variation in this response across mosquito species and populations within species.

The historical and current literature clearly demonstrates that mosquito species, populations within species, and individuals within populations vary in their intrinsic ability to become infected with a pathogen, support its replication, and eventually transmit to a vertebrate host (i.e. in their vector competence) [121, 122, 124, 123, 125-127]. The extent to which mosquito innate immunity to virus infection contributes to this well documented variation in vector competence is poorly understood. The importance of RNAi in controlling virus infection in insects is evident given that (1) mosquitoes engineered either by transgenesis [18] or by co-infection with a recombinant heterologous virus [385-387] to express dsRNA against a given virus are resistant to infection, and (2) mosquitoes [388] or flies [389, 273] or their cells [390] that have deficiencies in the RNAi pathway may rapidly succumb to virus infection. On the other hand, competent mosquitoes infected by West Nile virus (WNV, *Flaviviridae*) [283] and other viruses such as dengue virus (DENV, *Flaviviridae*) [315], Sindbis virus (*SINV*, *Togaviridae*) [276], and chikungunya virus (CHIKV, *Togaviridae*) [282] mount robust RNAi-based responses that seem to have minimal impact on virus replication. Importantly, no published studies of mosquito RNAi have examined field-collected populations of vector mosquitoes. This is a critical shortcoming since these are the mosquitoes that are generally responsible for virus transmission in nature.

Accordingly, we sought to investigate the extent of variation in the anti-WNV small RNA response in natural and colonized populations of mosquitoes. We hypothesized that mosquito species and populations within a species may vary quantitatively and/or qualitatively in their RNAi response to viral infection. Specifically, we reasoned that differences in either the robustness of the response, the targeting of the viral genome, and the pathways involved may

differentially influence mosquito vector competence and viral genetic diversity. We profiled the antiviral small RNA response to WNV in three primary vector species (*Culex sp.*), as well as *Aedes aegypti*, a species which is not believed to contribute to the maintenance or transmission, but which exhibits competence to WNV under laboratory conditions. Our results demonstrate that an anti-WNV small RNA response is largely conserved among WNV vector species, but that one species, *Cx. quinquefasciatus*, demonstrates potentially significant deviation from the stereotypical response that we found in other mosquitoes.

Materials and Methods

Mosquito Field Collections, Rearing and Species Identification

Oviposition traps were baited with an infusion of rabbit food pellets fermented in water for 5-7 days. Traps were checked daily, and *Culex* egg rafts were collected in individual 50 mL conical tubes with water and taken back to the laboratory and allowed to hatch in individual larval rearing bins. *Cx. quinquefasciatus* mosquitoes were collected in two sites in New Mexico separated by ~20 miles: Albuquerque (designated as ABQ) and Bernalillo (BERN). *Cx. tarsalis* egg rafts, which were not found in oviposition traps, likely because *Cx. tarsalis* prefers to oviposit in cleaner water [391], were collected from flooded tire tracks at the Turfmaster Sod Farms located northeast of Fort Collins, CO (designated as FC *Cx. tarsalis*). *Cx. pipiens* egg rafts were collected in Fort Collins, CO (designated as FC *Cx. pipiens*). Larvae were raised on a diet of powdered Tetra fish food or a 1:1 mix of powdered Tetra food and powdered rodent chow. Species identification was done using both L3/L4 larval morphology and a confirmatory PCR-based assay which differentiates multiple possible *Culex* species based on the interspecies

sequence variation in the spacer regions of ribosomal DNA (rDNA) segments [392, 393]. DNA was extracted from L3/L4 larvae using Wizard Genomic DNA Purification Kits (Promega, Madison WI) or DNeasy Blood and Tissue DNA extraction kits (Qiagen, Valencia CA). After confirming the species of larvae from individual egg rafts, larvae were pooled according to species and collection site and allowed to pupate and emerge into ice-cream cartons. Adult mosquitoes were kept at 26-27 °C with a 16:8 light:dark cycle and 70%-80% relative humidity, with water and sucrose provided *ad libitum*. Colonized *Cx. quinquefasciatus* (designated here US-Cxq, a longstanding colony of unknown duration originating from U.S. [394]), *Cx. pipiens* (designated here as PA-2004, established in 2004 from Pennsylvania collections [394]), *Cx. tarsalis* (KR83; established in 1983 from Kern County, CA collections [395]), and *Ae. aegypti* Higgs White Eye (HWE, a white-eye mutant strain of Puerto Rico, Rexville D mosquitoes [18]) and Rockefeller (longstanding strain possibly originating from a Havana, Cuba colony established in 1881 by Carlos Finlay [396]) strain mosquitoes were raised in identical conditions.

Viruses and Experimental Infections

WNV was produced from an infectious clone based on the New York 1999 (WNV_{NY99}) strain of the virus as described previously [397, 283]. Briefly, the plasmid containing the full-length infectious cDNA clone was linearized, and then *in vitro* transcribed into the infectious viral genomic RNA. Purified viral RNA was electroporated into BHK-21 cells, with the electroporation parameters set to 425 V, 1200Ω resistance, 25μF capacitance, and two pulses. Cell supernatant was collected after cells showed obvious signs of cytopathic effect (CPE; usually ~3 days post-electroporation). Cellular debris was removed from the supernatant by

centrifugation at ~3000 g, clarified supernatant was raised to a final concentration of 20% fetal bovine serum (FBS), and aliquots of 0.5 mL were made and stored at -80°C. Virus titer was then quantified by plaque assay on Vero cells. Virus produced in this manner exhibits a high degree of genetic homogeneity [398] and is well characterized phenotypically [399]. Adult female mosquitoes 6-8 days post-eclosion were fed an infectious bloodmeal of defibrinated goose blood or sheep blood mixed 1:1 with $\sim 2 \times 10^8$ PFU/mL of infectious clone derived WNV (WNVicd) and raised to a final concentration of 2mM ATP. Uninfected control mosquitoes were fed a 1:1 mix of defibrinated sheep blood and uninfected BHK-21 cell supernatant raised to a final concentration of 2mM ATP. Engorged mosquitoes were held for 7 or 14 days in a BSL-3 insectary with the same rearing conditions described previously, after which they were cold anesthetized, and midguts dissected and stored in miRvana RNA isolation lysis buffer (Ambion, Austin TX) at -80°C until needed for RNA isolation.

Total RNA Isolation and Small RNA Library Preparations

Total RNA was extracted from homogenized mosquito midguts using the miRvana miRNA isolation kit (Ambion) as per manufacturers suggested protocol for total RNA isolation. Eluted RNA from individual midguts were screened for the presence of WNV genomic RNA by 1-step RT-PCR (Qiagen) using 1971-F (5'-TTGCAAAGTTCCTATCTCGTCAG-3') and 2928c (5'-CCAAATCCAAAATCCTCCACTTCT-3') primers (numbers in primer designation denote genome position). RNA samples positive for WNV RNA were checked for RNA quality on a 2100 Bioanalyzer (Agilent, Santa Clara CA), and then pooled into groups of 5 midgut RNAs. Pooled RNAs were precipitated by adding 3.25 volumes of ice-cold EtOH, 0.1 volume 3M NaOAc (pH

5.5), and 1.5 μ L of linear polyacrylamide (5 mg/mL) as a carrier. After holding overnight at -20°C , the pools were centrifuged at $\sim 20,000$ g, washed twice with 80% EtOH, and re-suspended in nuclease-free water. 1 μ g total RNA was used as the input for small RNA library preparation using either the Illumina v1.5 Small RNA Prep Kit (ABQ, BERN, and Colony WNV 14dpi sRNA libraries) or the TruSeq Small RNA Sample Prep Kit (all others) (Illumina, San Diego CA) as per manufacturer's suggested protocol. Briefly, small RNAs were preferentially 3' and 5' adapter-ligated, reverse transcribed using the Superscript II reverse transcriptase (Invitrogen, Carlsbad CA), and PCR amplified (and in the case of TruSeq libraries, barcoded for multiplexing). Small RNA libraries were size selected on 6% TBE PAGE or 2% TBE-agarose gels, and purified by either overnight elution of the gel slice in nuclease-free water while rocking in the case of PAGE, or with MinElute Gel Extraction kits (Qiagen) in the case of agarose gels. Purified small RNA cDNA libraries were eluted in either water (PAGE gel slices) or Qiagen EB buffer (agarose gel slices) and sequenced on either Illumina GAIIx (*Cx. quinquefasciatus* ABQ, BERN, and US-Cxq WNV 14dpi, *Ae. aegypti* Rockefeller WNV 7dpi libraries) or HiSeq 2000 instruments (all others).

Assembly and Analysis of sRNA Libraries

Sequence FASTQ files were trimmed of the 3' adapter using FASTX Toolkit [400] and aligned to the WNV infectious clone reference genome using Bowtie 0.12.8 [401] and allowing for 0-mismatches. The **-a --best --strata** mode was used, which instructs Bowtie to report only those alignments in the best alignment stratum. SAM output files produced by Bowtie were used as the input for processing through SAMtools [402]. Additional analyses were conducted

using Microsoft Excel, Graphpad Prism 6, and viRome, an R package for the analysis of viral-derived small interfering RNA (viRNA) sequencing data [403].

qRT-PCR

WNV genome equivalents were determined using a Taqman qRT-PCR assay amplifying a 70bp fragment within the WNV E gene (described in [404]). 5 µL of total RNA from individual mosquito midgut samples used to construct our small RNA sequencing libraries or genome equivalent standards were used as the template in duplicate 20 µL reactions using the iScript™ 1-Step RT-PCR Kit for probes (Biorad, Hercules CA) with reagent ratios as per the manufacturer's suggested protocol. The following primer and probe sequences were used for this assay: 1160-F (5'-TCAGCGATCTCTCCACCAAAG-3'), 1229-R (5'-GGGTCAGCACGTTTGTCATTG-3'), and 1207-Probe (5'-TGCCCGACCATGGGAGAAGCTC-3'). Reactions were run on a CFX-96™ real-time system (Biorad). WNV genomic equivalent standards were previously generated by amplifying a 2.4 kb fragment from the WNV E gene using WNV 1031-F (5'-ATTTGGTTCTCGAAGGCGAC-3') and WNV 3430-R (5'-TGGTGGTAAGGTGCAGCTCC-3') primers. The resulting amplicon was then cloned into the pCR2.1-TOPO vector (Invitrogen, Carlsbad CA) downstream of the T7 promoter. The recombinant vector was linearized with KpnI, purified and used as template for *in vitro* transcription using the T7 Megascript kit (Ambion) according the manufacturer's instructions. *In vitro* transcribed RNA was then quantified and aliquoted into serial ten-fold dilutions.

Statistical Analysis

Nucleotide targeting plots of the viral genome were generated using the pileup function of SAMtools. Differences in the relative proportion of viRNAs by size class (i.e 19-23nts and 24-30nts) were determined using Tukey's multiple comparison test. Correlational analysis between separate data sets was conducted using the non-parametric Spearman rank coefficient r_s . Differences in mean r_s values for each species were computed using an unpaired t-test with the Holm-Sidak correction for multiple comparisons.

Results

Field-collected *Cx. spp.* mosquitoes exhibit a stereotypical viRNA response to WNV

Sequencing of small RNAs from field-collected *Cx. quinquefasciatus* mosquito midguts at 14 days post WNV infection revealed that they exhibit a stereotypical distribution of 19-23 nt viRNAs, with the 21 nt population of small RNAs being the most prevalent, as previously reported in colonized *Cx. quinquefasciatus* mosquitoes (**Figure 2.1**) [283]. While there was no significant difference in the relative abundance of 19-23nt viRNAs (consistent in size with products of the DCR-2-dependent siRNA pathway) across the three groups, 24-30nt viRNAs (consistent in size with products of the DCR-2-independent PIWI-interacting [piRNA] pathway) were significantly different across all three groups, with the ABQ group in particular being highly enriched for this population of small RNAs. viRNAs of 19-23nts were asymmetrically distributed along the length of the virus genome, exhibiting both "hot" and "cold" spots of targeting (**Figure 2.2**). Approximately 70% of the 19-23nt viRNAs in all three groups were derived from the positive strand of the virus, in congruence with what has previously been

described for *Cx. quinquefasciatus* mosquitoes infected with WNV [283]. In contrast, in both the ABQ and BERN groups, >90% of viral derived piRNA-like small RNAs (vpiRNAs) from 24-30nts were derived from the positive strand, consistent with the strong strand bias exhibited by piRNAs [282, 316] (**Figure 2.3**). However, this population of small RNAs lacked signatures of ping-pong dependent amplification, which have been observed in alphavirus [282, 313, 316] and bunyavirus [316-318] infected insects or insect cells, but not flaviviruses [281, 315] or reoviruses [318]. In the colonized group, only roughly 70% of 24-30nts viRNAs were derived from the positive strand, and these comprised only slightly greater than 1% of the total 19-30 nt viral-derived small RNA population

We next expanded the study to include additional mosquito species. We collected egg rafts of both *Cx. pipiens* and *Cx. tarsalis* mosquitoes in Fort Collins, CO (FC) and infected emerged adult females with WNV *per os*. Additionally, we infected colonized *Cx. tarsalis*, *Cx. pipiens*, and *Ae. aegypti* mosquitoes in the same manner. Midguts were harvested from mosquitoes at 7 and 14 dpi, and small RNA sequencing libraries were made from pools of 5 infected midguts per timepoint (only the 7 dpi timepoint was sequenced for the *Ae. aegypti* libraries). Distribution of viRNAs by length was similar to that seen in *Cx. quinquefasciatus* mosquitoes, and there was significant variation in the percentage of 24-30nt viRNAs amongst field-collected and colonized groups within the same species (**Figure 2.4A and 2.4B**). Interestingly, small RNA profiles at 7dpi from both FC *Cx. pipiens* and *Cx. tarsalis* failed to show a prominent peak at 21nts though by 14dpi the profiles appeared typical. Rather, these libraries exhibited a more or less even distribution of viRNAs from 19-30nts. Due to this, we compared these libraries to each other, but excluded them from all other intra- and interspecies

comparisons, and found a high degree of correlation ($r_s = 0.85$, data not shown). The percentage of 19-23nt and 24-30nt WNV viRNAs out of the entire 19-30nt population of small RNAs varied greatly amongst all of the libraries, including in the *Cx. tarsalis* KR83 experimental replicates (**Table 2.1**). As seen in *Cx. quinquefasciatus*, WNV viRNAs were asymmetrically distributed along the length of the viral genome in the *Cx. pipiens*, *Cx. tarsalis*, and *Ae. aegypti* data sets. The positive strand/negative strand ratio for 19-23nt products varied within and between species. In *Cx. pipiens*, 19-23nt viRNAs were between 53%-64% derived from the positive strand, while in *Cx. tarsalis* the percentage of 19-23nts derived from the positive strand ranged between 50%-80%, with wide variation seen even among the two KR83 experimental replicates. 19-23nt viRNAs in the *Ae. aegypti* Rockefeller and HWE libraries were 83% and 77% derived from the positive strand, respectively. However, as seen in *Cx. quinquefasciatus*, 24-30nt reads were uniformly between 94%-99% derived from the positive strand of the virus RNA in all of the sequencing libraries (including the FC *Cx. pipiens* WNV 7dpi and FC *Cx. tarsalis* WNV 7dpi libraries, which were predominately positive-strand derived for all 19-30nt reads).

Intra- and interspecies comparisons of midgut anti-WNV small RNA profiles from *Cx. spp.* and *Ae. aegypti* mosquitoes

We next analyzed the correlation in viral genome nucleotide targeting within and between species. Relative intensity of nucleotide targeting (measured as number of times a given nucleotide position was sequenced as part of a read in a given library) of 19-23nt viRNAs was highly correlated between field-collected and colonized mosquitoes of the same species (**Figure 2.5**). The strength of the correlation was considerably decreased when intra-species

comparisons of 24-30nt nucleotide targeting were made (**Figure 2.6**), showing that much of the intra-species conservation of the total RNAi response appears to lie within the siRNA pathway.

Inter-species comparisons were made for all libraries excluding the FC *Cx. pipiens* WNV 7dpi and FC *Cx. tarsalis* WNV 7dpi libraries, and are summarized in **Tables 2.2** and **2.3**. *Cx. quinquefasciatus* mosquitoes had a significantly lower degree of correlation with either *Cx. pipiens* or *Cx. tarsalis* when comparing 19-23nt viRNAs (**Figure 2.7A**). Interestingly, nucleotide targeting intensity was highly similar between multiple comparisons of *Cx. pipiens* and *Cx. tarsalis* libraries, as the two species exhibited similar degrees of correlation between the species as they did within their species. *Aedes aegypti* and *Cx. tarsalis* libraries were also similar to each other, though significance could not be tested due to a lack of replicate correlations from those species. When comparing differences in intensity of nucleotide targeting amongst the 24-30nt size class, there was no significant difference in intensity of nucleotide targeting in 24-30nt vpiRNAs between the three *Cx.* species when compared against *Cx. quinquefasciatus*, with even *Cx. quinquefasciatus* exhibiting low correlations between field-collected and colonized groups. There was a significant difference in the correlations between *Cx. quinquefasciatus* and *Cx. tarsalis* when comparing against *Cx. pipiens* and *Cx. quinquefasciatus* and *Cx. pipiens* when comparing against *Cx. tarsalis* (**Figure 2.7B**). Both *Cx. pipiens* and *Cx. tarsalis* showed much higher degrees of intra-species correlation in 24-30 nt nucleotide targeting than either *Cx. quinquefasciatus* or *Ae. aegypti*.

We next quantified the viral load in the midguts of the individual *Cx. sp.* mosquitoes used to construct the pools as input for small RNA libraries by qRT-PCR. We found no

statistically significant difference in the viral burden in midguts as measured by virus genome equivalent copy numbers (**Figure 2.8**).

Detection of *Culex flavivirus* (CxFV)-derived viRNAs in field-collected *Cx. pipiens* mosquito midguts but not *Cx. quinquefasciatus* or *Cx. tarsalis*

We aligned 19-30nt small RNAs to the *Culex flavivirus* (CxFV, *Flaviviridae*) genome (GenBank Accession # AB262759.2) allowing for 0-mismatches. CxFV-derived viRNAs were found in both the FC *Cx. pipiens* WNV 7dpi and 14dpi libraries, but not FC *Cx. tarsalis* or field-collected *Cx. quinquefasciatus* libraries. In both FC *Cx. pipiens* libraries, CxFV-derived viRNAs fit the stereotypical siRNA distribution pattern with a significant peak at 21nts, even though as previously mentioned this pattern was not observed in WNV-derived viRNAs from the FC *Cx. pipiens* WNV 7dpi library.

Discussion

RNAi is the major innate immune pathway in mosquitoes in response to arbovirus infection, and in the past decade has become a major focus of research in regards to invertebrate innate immunity [383]. However, the degree to which antiviral small RNA pathways vary quantitatively or qualitatively amongst vector species of mosquitoes has not been investigated. Since it is more or less presumed that vector competence is linked to at least some degree with the mosquito innate immune response to virus infection, an understanding of interspecies variation in innate immune responses is therefore critical. Secondly, as far as we are aware, all studies to date have relied on inbred colonized lab strains of mosquitoes or

mosquito cell culture, which may or may not recapitulate what occurs in natural infections. A clear understanding of how well these laboratory systems represent what occurs in nature is therefore critical to extrapolating data from experimental studies to the natural world.

Here we sequenced viral-derived small RNAs from 4 species of mosquitoes, 3 of which encompassed both field collected and colonized populations. We found that all species examined exhibit a stereotypical siRNA response to WNV, with 21nt species being produced in the greatest abundance, as has been described before in mosquitoes [276, 282, 283]. However, between intra-species populations there was significant variation the percentage of viRNAs made up by the 24-30nt size class. These small RNAs were predominately derived from the positive strand, consistent in both size and strand bias with products of the piRNA pathway, which has been shown to be a likely participant in antiviral defense in mosquitoes [315, 282, 281, 316, 317, 313]. Curiously, viRNA profiles from field-collected *Cx. pipiens* and *Cx. tarsalis* at the 7dpi timepoint exhibited atypical size distribution profiles. Additionally, all 19-30nt viRNA reads from these libraries were almost entirely derived from the positive strand of the virus (data not shown). Mosquitoes used to create these two libraries were collected at different times (around one year apart), and infections, dissections, RNA extractions, and preparations of small RNA libraries were conducted separately. Otherwise, both groups were treated the same (rearing conditions, infection protocol, RNA extractions, small RNA library preparation protocol). However, by the 14 dpi timepoint, viRNA size distribution profiles had returned to what is considered stereotypical. It would seem unlikely that both of these libraries would exhibit these signatures due to technical error, since none of the other libraries prepared for this study or subsequent ones discussed later in this dissertation exhibited similar profiles.

Additionally, when compared against one another, 19-23nt small RNA profiles from these two groups were strongly correlated, comparable with the strength of correlation between these groups at 14dpi. Similarly, 24-30nt viRNAs from these libraries were strongly correlated, even more so than at the 14dpi timepoint (7dpi $r_s = 0.87$, 14dpi $r_s = 0.56$). These results confirm that natural populations of vector mosquitoes exhibit a stereotypical viRNA response to virus infection.

We found a high degree of intra-species homogeneity in targeting of the DCR-2 processed 19-23nt siRNA size class in all species. However, the strength of correlation for 24-30nt was generally less, though in *Cx. pipiens* and *Cx. tarsalis*, not markedly. This indicates that much of the conservation in targeting of the viral genome within different populations of the same species is retained within the siRNA pathway. Strikingly, when inter-species 19-23nt viRNA nucleotide targeting profiles were compared, *Cx. pipiens*, *Cx. tarsalis*, and *Ae. aegypti* were more highly correlated with one another than any were with *Cx. quinquefasciatus*. This was a surprising finding, given that *Cx. quinquefasciatus* and *Cx. pipiens* are closely related sister taxa [124]. These differences between *Cx. quinquefasciatus* and *Cx. pipiens* did not relate to viral burden in the midguts as measured by qRT-PCR detection of viral genome equivalents. WNV has been shown to undergo population bottlenecks in *Cx. pipiens* [405], but not *Cx. quinquefasciatus* [406], where viral genetic diversity is maintained. Presumably, RNAi plays a role in defining virus population structure within the mosquito vector, though it is impossible to draw any correlations between this present study and the previously published ones. Still, the finding that *Cx. quinquefasciatus* and *Cx. pipiens* differ in their RNAi targeting of

the WNV genome is provocative given the existing evidence showing differences in how these species interact with WNV.

Evolution of RNAi component genes has been investigated in *Ae. aegypti*, but not *Cx. sp.* mosquitoes. In *Ae. aegypti*, RNAi components including *dcr-2* and *ago-2* have been found to undergo rapid evolution in natural populations [407], and polymorphisms in *dcr-2* have been implicated in influencing vector competence in *Ae. aegypti* to DENV [408]. While not demonstrated in this study, it is plausible that polymorphisms in intra- and inter-specific populations of *Cx. sp.* mosquitoes similarly influence mosquito susceptibility to WNV infection. Such polymorphisms may also account for the variation in RNAi targeting profiles seen between species, particularly between *Cx. quinquefasciatus* and other *Culex* species.

In addition to the above findings, the high degree of intra-specific correlations between small RNA targeting profiles of colonized and field-collected mosquitoes demonstrates that the use of heavily inbred populations, such as those in lab colonies of mosquitoes, can still recapitulate the antiviral RNAi response seen in natural populations. These findings add confidence to reports in previous studies, which have entirely relied on the use of inbred populations of mosquitoes.

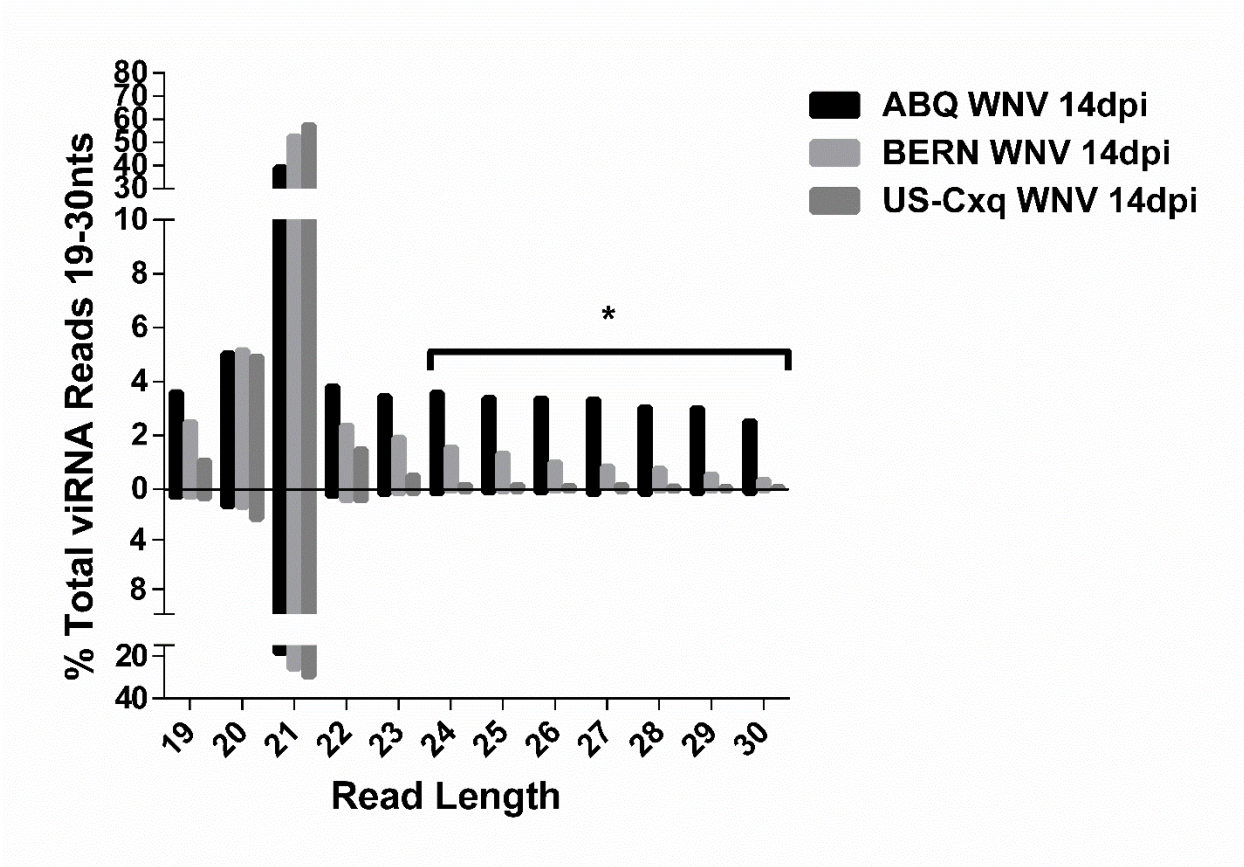


Figure 2.1: Distribution of viRNAs of 19-30nts from Albuquerque, NM, Bernalillo, NM, and colonized *Cx. quinquefasciatus* midguts 14dpi with WNV. Reads mapping to the positive strand are presented on the upper portion of the y-axis and reads mapping to the negative strand on the lower portion of the y-axis. Asterisk denotes significance ($p < 0.05$) by Tukey's multiple comparison test.

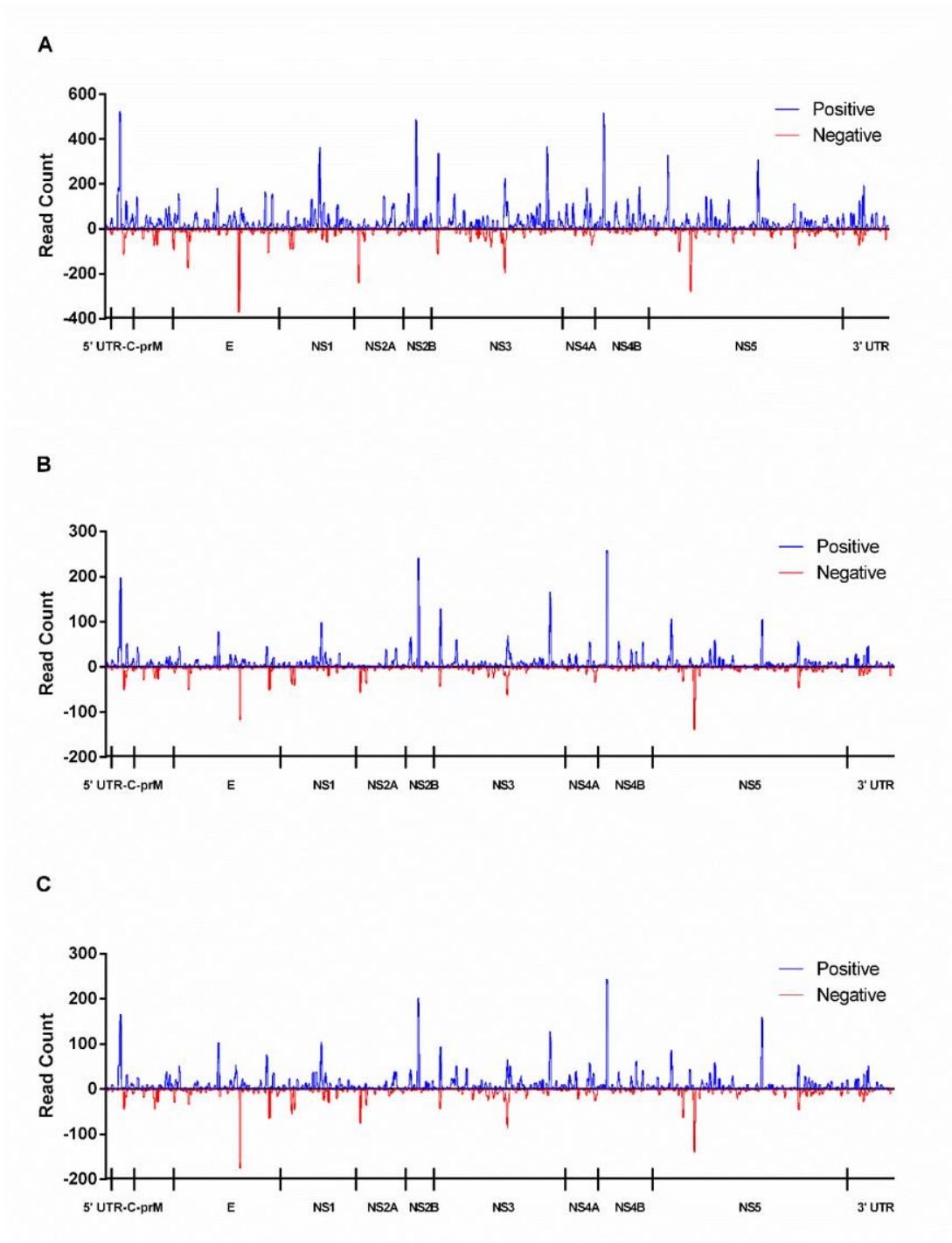


Figure 2.2: Distribution of 19-23nt viRNAs along the length of the viral genome. **A)** Albuquerque, NM (ABQ) **B)** Bernalillo, NM (BERN), **C)** colonized mosquitoes (US-Cxq). Positive strand/negative strand proportions were 0.72/0.27, 0.69/0.31, and 0.66/0.34, respectively.

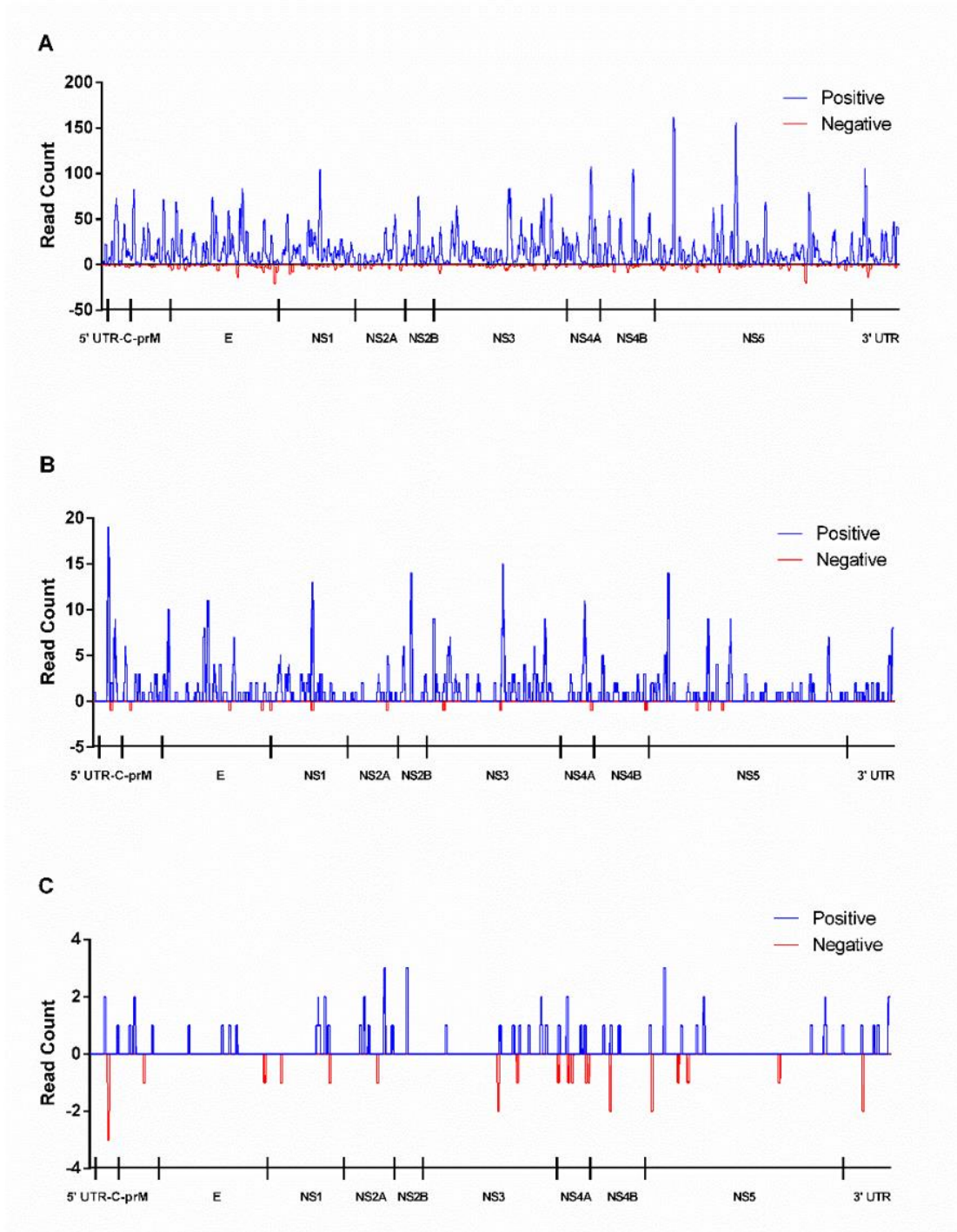


Figure 2.3: Distribution of 24-30nt viRNAs along the length of the viral genome. **A)** Albuquerque, NM, **B)** Bernalillo, NM, **C)** US-Cxq (Colony). Positive strand/negative strand proportions were 0.93/0.07, 0.97/0.03, and 0.71/.29, respectively.

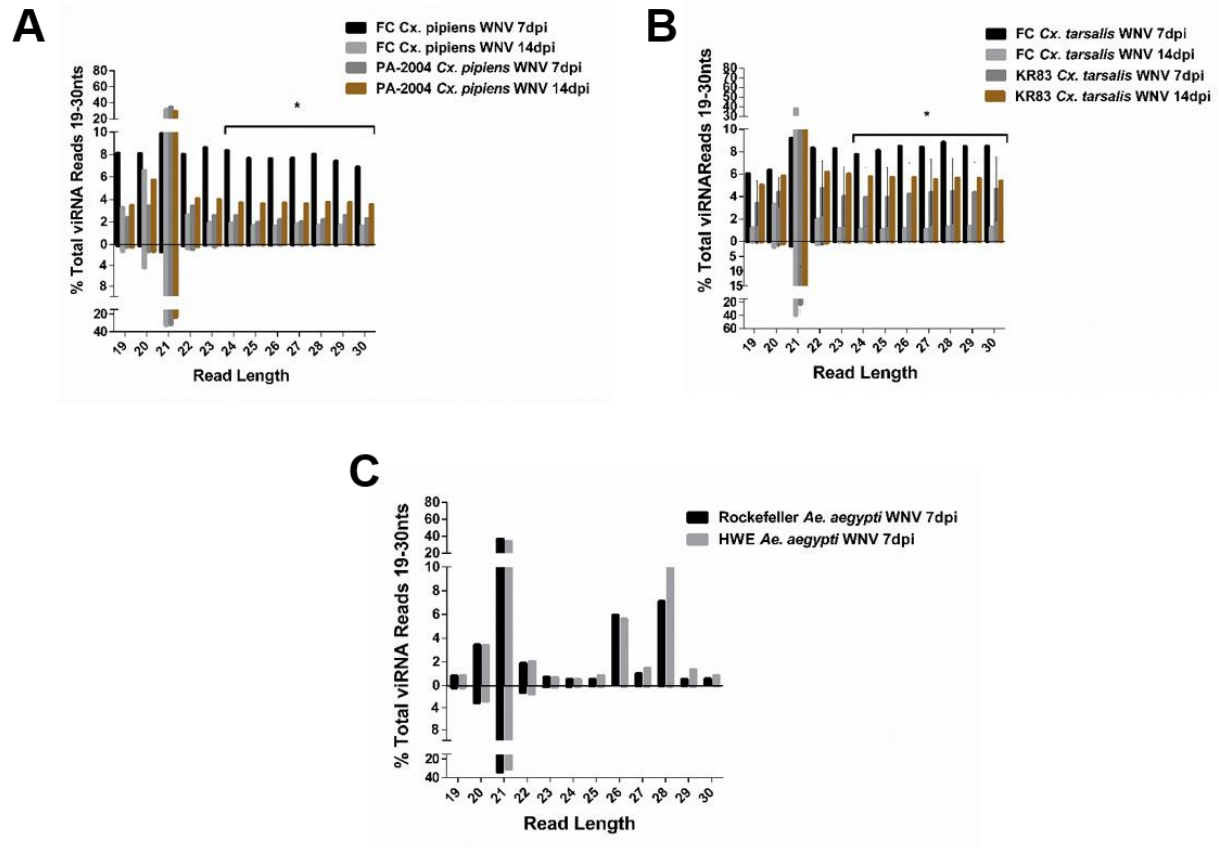


Figure 2.4: Distribution of WNV viRNAs from 19-30nts in length. **A)** Field-collected (FC) and colonized *Cx. pipiens* midguts, **B)** FC and colonized *Cx. tarsalis* midguts. Two separate libraries were made and sequenced for the colony mosquitoes at 7dpi, error bars represent SEM. **C)** Two colonized strains of *Ae. aegypti*. The HWE library was prepared using RNA isolated from whole mosquitoes; the Rockefeller library was prepared from midguts. Comparisons between mean percentages of 19-23nt and 24-30nt populations between populations in *Cx. pipiens* and *Cx. tarsalis* excluded the field-collected 7dpi timepoint for each species since they exhibited atypical viRNA distributions. Asterisks denotes significance ($p < 0.05$) by Tukey’s multiple comparison test.

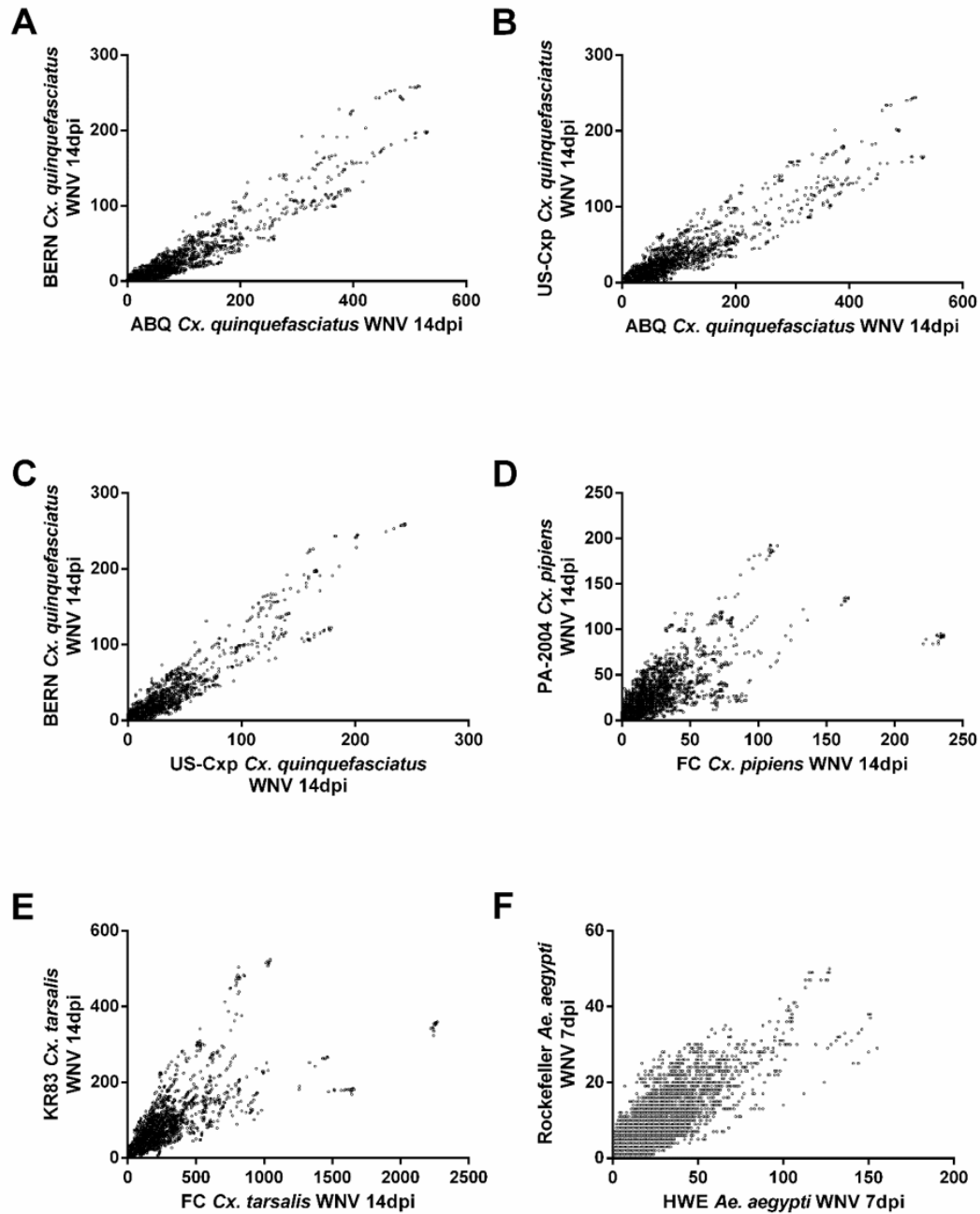


Figure 2.5: Intra-species comparisons of 19-23nt viRNA targeting of the WNV genome. Each point represents a single nucleotide position. All correlations were made using the non-parametric Spearman rank coefficient (r_s). **A)** $r_s = 0.85$, 95% CI= 0.85-0.86, $p < 0.0001$, **B)** $r_s = 0.84$, 95% CI= 0.84-0.85, $p < 0.0001$, **C)** $r_s = 0.80$, 95% CI= 0.79-0.80, $p < 0.0001$, **D)** $r_s = 0.79$, 95% CI= 0.78-0.80, $p < 0.0001$, **E)** $r_s = 0.89$, 95% CI= 0.88-0.89, $p < 0.0001$, **F)** $r_s = 0.76$, 95% CI= 0.76-0.77

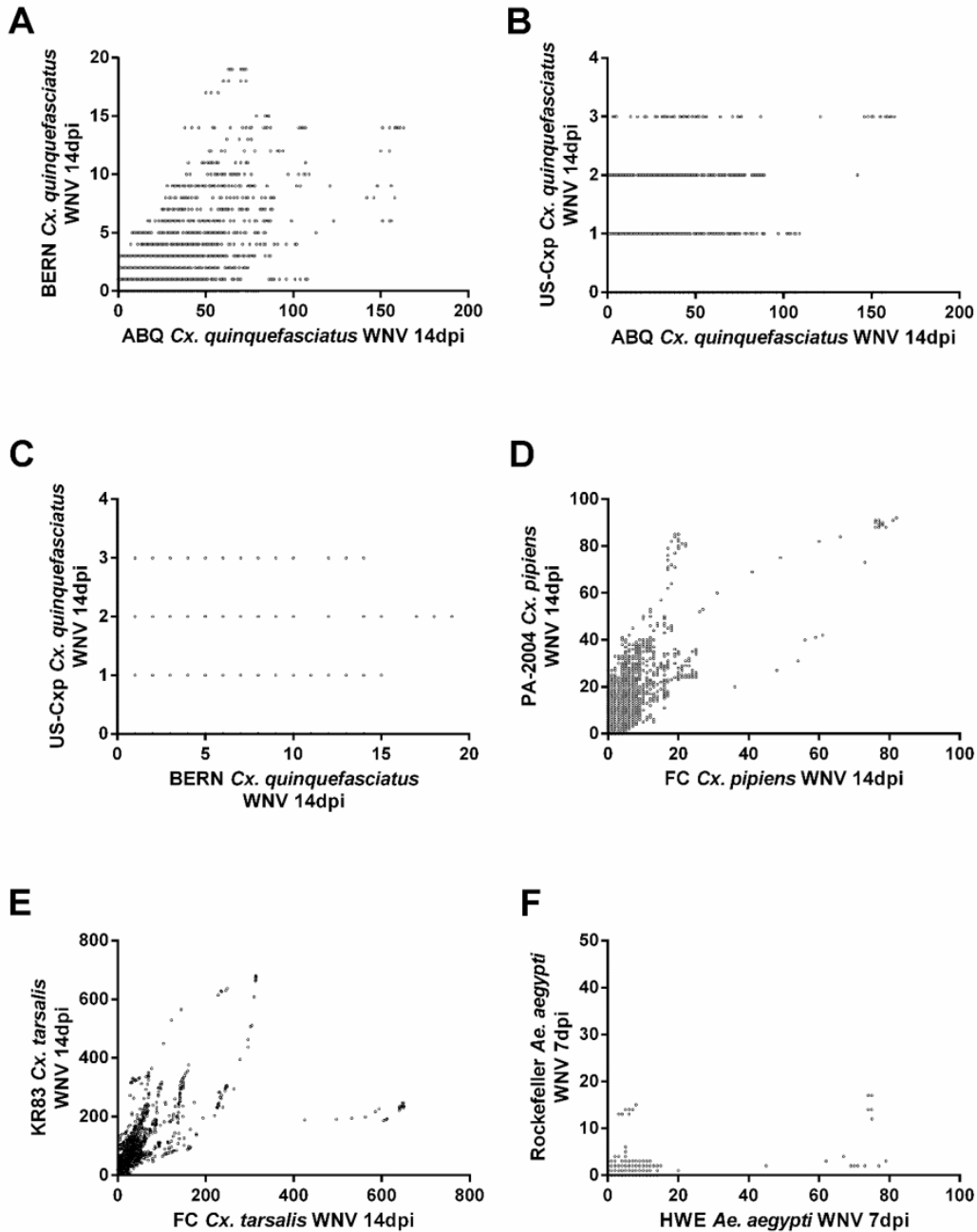


Figure 2.6: Intra-species comparisons of 24-30nt viRNA targeting of the WNV genome. Each point represents a single nucleotide position. All correlations were made using the non-parametric Spearman rank coefficient (r_s). **A)** $r_s = 0.53$, 95% CI= 0.52-0.54, $p < 0.0001$, **B)** $r_s = 0.18$, 95% CI= 0.16-0.20, $p < 0.0001$, **C)** $r_s = 0.17$, 95% CI= 0.16-0.19, $p < 0.0001$, **D)** $r_s = 0.64$, 95% CI= 0.63-0.65, $p < 0.0001$, **E)** $r_s = 0.78$, 95% CI= 0.77-0.79,

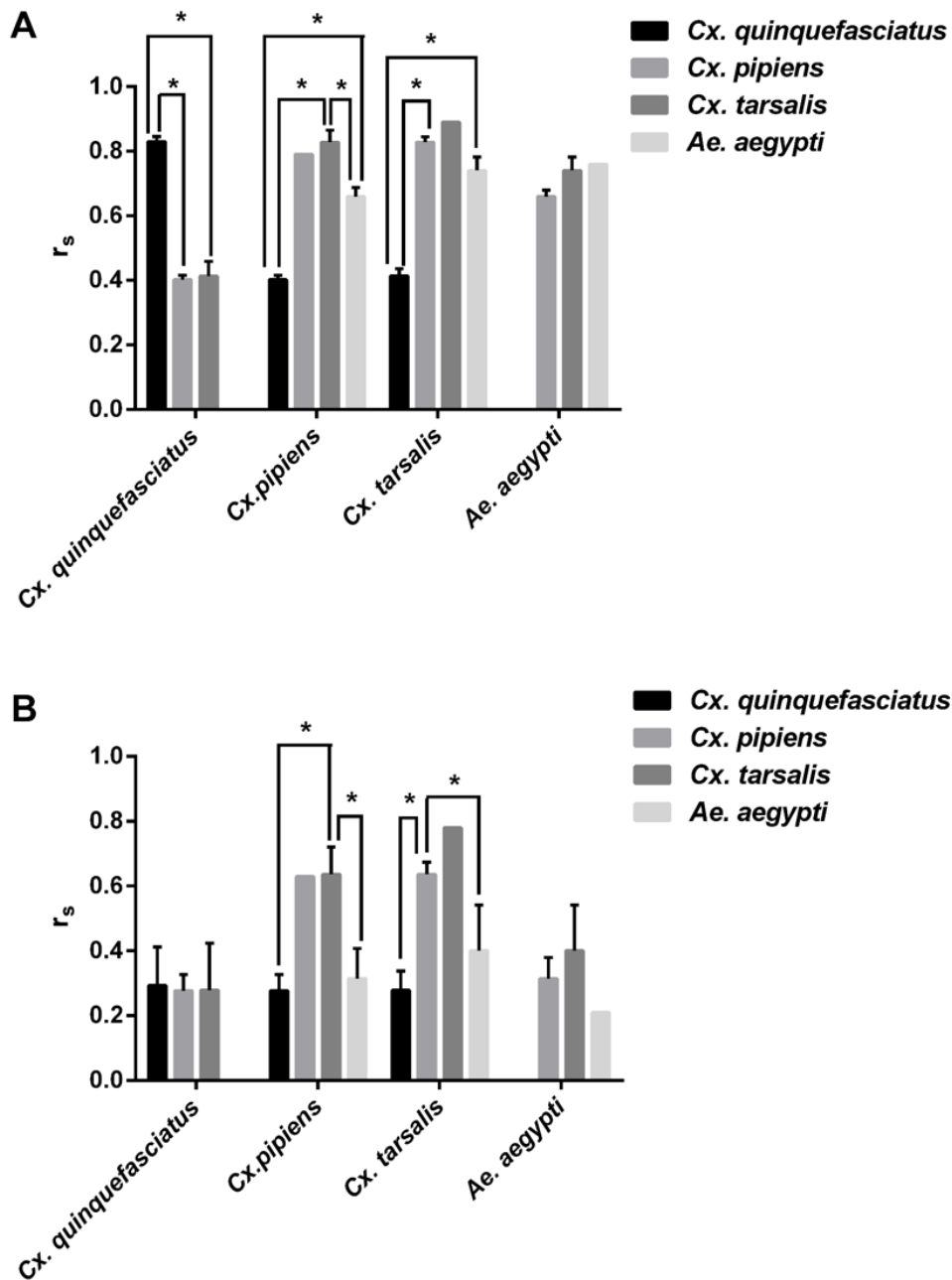


Figure 2.7: Mean r_s values were calculated for both intra-species and inter-species comparison correlations and plotted. Error bars denote SEM. **A)** Mean r_s values for 19-23nt viRNA targeting profiles for all species. **B)** Mean r_s values for 24-30nt targeting profiles for all species. Asterisks denote significance of $p < 0.05$ as measured by independent t-tests using the Holm-Sidak correction for multiple comparisons.

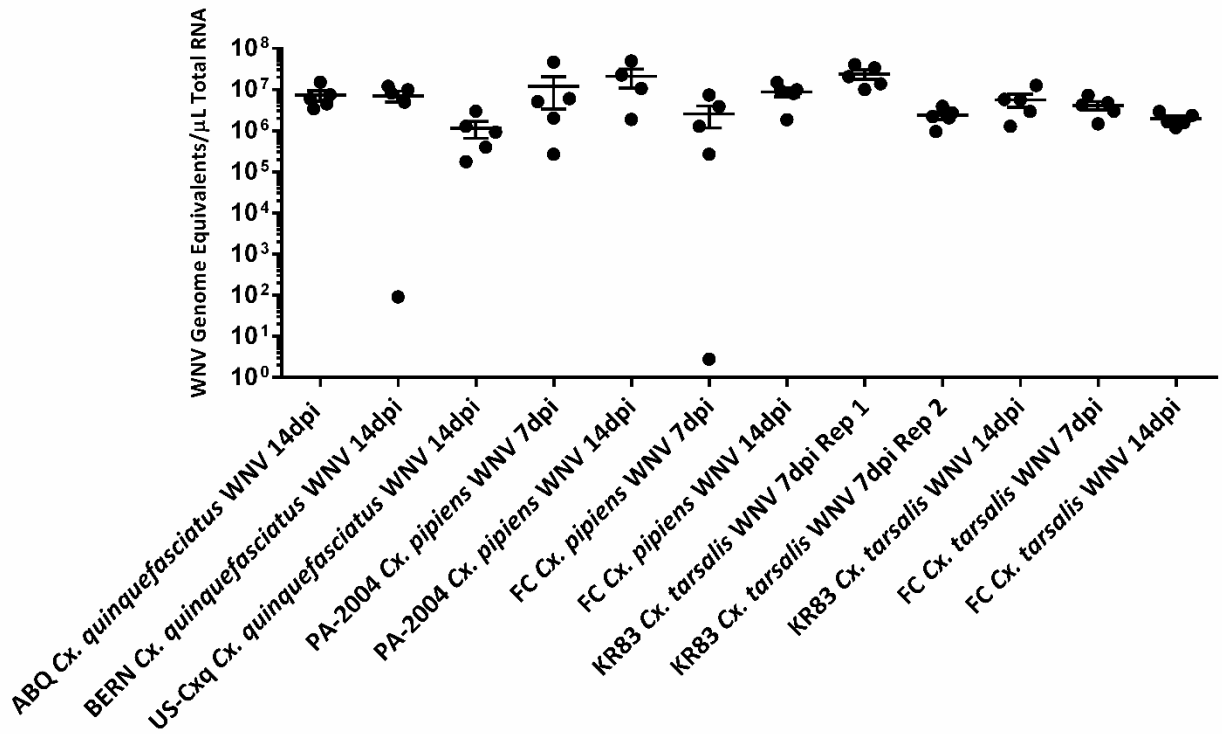


Figure 2.8: WNV genome equivalents in individual *Cx. sp.* mosquito midguts as measured by qRT-PCR. Bars represent mean and SEM.

Table 2.1: Features of sequenced small RNA libraries.

Library Name	Total 19-30 NT Reads w/ Adapters (X10⁶)	Reads Aligning to WNV (%)
ABQ <i>Cx. quinquefasciatus</i> WNV 14dpi	1.9	29291 (1.55)
BERN <i>Cx. quinquefasciatus</i> WNV 14dpi	0.84	7250 (0.86)
US-Cxq <i>Cx. quinquefasciatus</i> WNV 14dpi	1.5	7504 (0.51)
PA-2004 <i>Cx. pipiens</i> WNV 7dpi	2.9	3630 (0.12)
PA-2004 <i>Cx. pipiens</i> WNV 14dpi	2.6	11324 (0.43)
FC <i>Cx. pipiens</i> WNV 7dpi	5.8	22105 (0.38)
FC <i>Cx. pipiens</i> WNV 14dpi	0.58	8014 (1.38)
KR83 <i>Cx. tarsalis</i> WNV 7dpi Rep 1	5.3	157453 (2.99)
KR83 <i>Cx. tarsalis</i> WNV 7dpi Rep 2	7.7	62356 (0.81)
KR83 <i>Cx. tarsalis</i> WNV 14dpi	1.6	37305 (2.34)
FC <i>Cx. tarsalis</i> WNV 7dpi	7.7	92629 (1.2)
FC <i>Cx. tarsalis</i> WNV 14dpi	11.1	73686 (0.66)
HWE <i>Ae. aegypti</i> WNV 7dpi	16.5	12797 (0.08)
Rockefeller <i>Ae. aegypti</i> WNV 7dpi	1.5	4354 (0.29)

Table 2.2: Summary of intra- and interspecies correlations of 19-23nt viRNAs. r_s = Spearman r value. ND= Comparison not determined.

Table 2.2	ABQ Cx. <i>quinquefasciatus</i> WNV 14dpi	BERN Cx. <i>quinquefasciatus</i> WNV 14dpi	US-Cxq Cx. <i>quinquefasciatus</i> WNV 14dpi	FC Cx. <i>pipiens</i> WNV 14dpi	PA-2004 Cx. <i>pipiens</i> WNV 7dpi	PA-2004 Cx. <i>pipiens</i> WNV 14dpi	FC Cx. <i>tarsalis</i> WNV 14dpi	KR83 Cx. <i>tarsalis</i> WNV 7dpi	KR83 Cx. <i>tarsalis</i> WNV 14dpi	HWE Ae. <i>aegypti</i> WNV 7dpi	Rockefeller <i>Ae. aegypti</i> WNV 7dpi
ABQ Cx. <i>quinquefasciatus</i> WNV 14dpi	--	$r_s = 0.85$, 95% CI= 0.85-0.86, $p < 0.0001$	$r_s = 0.84$, 95% CI= 0.84-0.85, $p < 0.0001$	$r_s = 0.43$, 95% CI= 0.42- 0.45, $p < 0.0001$	ND	$r_s = 0.45$, 95% CI= 0.44- 0.47, $p < 0.0001$	$r_s = 0.41$, 95% CI= 0.40- 0.43, $p < 0.0001$	ND	$r_s = 0.49$, 95% CI= 0.47- 0.50, $p < 0.0001$	ND	ND
BERN Cx. <i>quinquefasciatus</i> WNV 14dpi	$r_s = 0.85$, 95% CI= 0.85-0.86, $p < 0.0001$	--	$r_s = 0.80$, 95% CI= 0.79-0.80, $p < 0.0001$	$r_s = 0.39$, 95% CI= 0.37- 0.40, $p < 0.0001$	ND	$r_s = 0.40$, 95% CI= 0.38- 0.41, $p < 0.0001$	$r_s = 0.38$, 95% CI= 0.36- 0.40, $p < 0.0001$	ND	$r_s = 0.43$, 95% CI= 0.41- 0.44, $p < 0.0001$	ND	ND
US-Cxq Cx. <i>quinquefasciatus</i> WNV 14dpi	$r_s = 0.84$, 95% CI= 0.84-0.85, $p < 0.0001$	$r_s = 0.80$, 95% CI= 0.79-0.80, $p < 0.0001$	--	$r_s = 0.36$, 95% CI= 0.34- 0.37, $p < 0.0001$	ND	$r_s = 0.38$, 95% CI= 0.36- 0.39, $p < 0.0001$	$r_s = 0.36$, 95% CI= 0.35- 0.38, $p < 0.0001$	ND	$r_s = 0.41$, 95% CI= 0.39- 0.42, $p < 0.0001$	ND	ND
FC Cx. <i>pipiens</i> WNV 14dpi	$r_s = 0.43$, 95% CI= 0.42-0.45, $p < 0.0001$	$r_s = 0.39$, 95% CI= 0.37-0.40, $p < 0.0001$	$r_s = 0.36$, 95% CI= 0.34-0.37, $p < 0.0001$	--	ND	$r_s = 0.79$, 95% CI= 0.78- 0.80, $p < 0.0001$	$r_s = 0.86$, 95% CI= 0.86- 0.87, $p < 0.0001$	ND	$r_s = 0.85$, 95% CI= 0.85- 0.86, $p < 0.0001$	ND	ND
PA-2004 Cx. <i>pipiens</i> WNV 7dpi	ND	ND	ND	ND	--	ND	ND	$r_s = 0.77$, 95% CI= 0.76- 0.77, $p < 0.0001$	ND	$r_s = 0.68$, 95% CI= 0.67- 0.69, $p < 0.0001$	$r_s = 0.64$, 95% CI= 0.62- 0.65, $p < 0.0001$
PA-2004 Cx. <i>pipiens</i> WNV 14dpi	$r_s = 0.45$, 95% CI= 0.44-0.47, $p < 0.0001$	$r_s = 0.40$, 95% CI= 0.38-0.41, $p < 0.0001$	$r_s = 0.38$, 95% CI= 0.36-0.39, $p < 0.0001$	$r_s = 0.79$, 95% CI= 0.78- 0.80, $p < 0.0001$	ND	--	$r_s = 0.81$, 95% CI= 0.80- 0.82, $p < 0.0001$	ND	$r_s = 0.85$, 95% CI= 0.85- 0.86, $p < 0.0001$	ND	ND
FC Cx. <i>tarsalis</i> WNV 14dpi	$r_s = 0.41$, 95% CI= 0.40-0.43, $p < 0.0001$	$r_s = 0.38$, 95% CI= 0.36-0.40, $p < 0.0001$	$r_s = 0.36$, 95% CI= 0.35-0.38, $p < 0.0001$	$r_s = 0.86$, 95% CI= 0.86- 0.87, $p < 0.0001$	ND	$r_s = 0.81$, 95% CI= 0.80- 0.82, $p < 0.0001$	--	ND	$r_s = 0.89$, 95% CI= 0.88- 0.89, $p < 0.0001$	ND	ND

Table 2.2 (Cont.)	ABQ Cx. <i>quinquefasciatus</i> WNV 14dpi	BERN Cx. <i>quinquefasciatus</i> WNV 14dpi	US-Cxq Cx. <i>quinquefasciatus</i> WNV 14dpi	FC Cx. <i>pipiens</i> WNV 14dpi	PA-2004 Cx. <i>pipiens</i> WNV 7dpi	PA-2004 Cx. <i>pipiens</i> WNV 14dpi	FC Cx. <i>tarsalis</i> WNV 14dpi	KR83 Cx. <i>tarsalis</i> WNV 7dpi	KR83 Cx. <i>tarsalis</i> WNV 14dpi	HWE Ae. <i>aegypti</i> WNV 7dpi	Rockefeller Ae. <i>aegypti</i> WNV 7dpi
KR83 Cx. <i>tarsalis</i> WNV 7dpi	ND	ND	ND	ND	$r_s = 0.77$, 95% CI= 0.76- 0.77, $p < 0.0001$	ND	ND	--	ND	$r_s = 0.77$, 95% CI= 0.76- 0.78, $p < 0.0001$	$r_s = 0.71$, 95% CI= 0.70- 0.72, $p < 0.0001$
KR83 Cx. <i>tarsalis</i> WNV 7dpi	ND	ND	ND	ND	$r_s = 0.77$, 95% CI= 0.76- 0.77, $p < 0.0001$	ND	ND	--	ND	$r_s = 0.77$, 95% CI= 0.76- 0.78, $p < 0.0001$	$r_s = 0.71$, 95% CI= 0.70- 0.72, $p < 0.0001$
KR83 Cx. <i>tarsalis</i> WNV 14dpi	$r_s = 0.49$, 95% CI= 0.47-0.50, $p < 0.0001$	$r_s = 0.43$, 95% CI= 0.41-0.44, $p < 0.0001$	$r_s = 0.41$, 95% CI= 0.39-0.42, $p < 0.0001$	$r_s = 0.85$, 95% CI= 0.85- 0.86, $p < 0.0001$	ND	$r_s = 0.85$, 95% CI= 0.85- 0.86, $p < 0.0001$	$r_s = 0.89$, 95% CI= 0.88- 0.89, $p < 0.0001$	ND	--	ND	ND
HWE Ae. <i>aegypti</i> WNV 7dpi	ND	ND	ND	ND	$r_s = 0.85$, 95% CI= 0.85- 0.86, $p < 0.0001$	ND	ND	$r_s = 0.77$, 95% CI= 0.76- 0.78, $p < 0.0001$	ND	--	$r_s = 0.76$, 95% CI= 0.76- 0.77, $p < 0.0001$
Rockefeller Ae. <i>aegypti</i> WNV 7dpi	ND	ND	ND	ND	$r_s = 0.64$, 95% CI= 0.62- 0.65, $p < 0.0001$	ND	ND	$r_s = 0.71$, 95% CI= 0.70- 0.72, $p < 0.0001$	ND	$r_s = 0.76$, 95% CI= 0.76- 0.77, $p < 0.0001$	--

Table 2.3: Summary of intra- and interspecies correlations of 24-30nt viRNAs. r_s = Spearman r value. ND= Comparison not determined.

Table 2.3	ABQ Cx. <i>quinquefasciatus</i> WNV 14dpi	BERN Cx. <i>quinquefasciatus</i> WNV 14dpi	US-Cxq Cx. <i>quinquefasciatus</i> WNV 14dpi	FC Cx. <i>pipiens</i> WNV 14dpi	PA-2004 Cx. <i>pipiens</i> WNV 7dpi	PA-2004 Cx. <i>pipiens</i> WNV 14dpi	FC Cx. <i>tarsalis</i> WNV 14dpi	KR83 Cx. <i>tarsalis</i> WNV 7dpi	KR83 Cx. <i>tarsalis</i> WNV 14dpi	HWE Ae. <i>aegypti</i> WNV 7dpi	Rockefeller Ae. <i>aegypti</i> WNV 7dpi
ABQ Cx. <i>quinquefasciatus</i> WNV 14dpi	--	$r_s = 0.53$, 95% CI= 0.52-0.55, $p < 0.0001$	$r_s = 0.18$, 95% CI= 0.16-0.20, $p < 0.0001$	$r_s = 0.36$, 95% CI= 0.35-0.38, $p < 0.0001$	ND	$r_s = 0.47$, 95% CI= 0.46-0.49, $p < 0.0001$	$r_s = 0.38$, 95% CI= 0.36-0.39, $p < 0.0001$	ND	$r_s = 0.49$, 95% CI= 0.48-0.51, $p < 0.0001$	ND	ND
BERN Cx. <i>quinquefasciatus</i> WNV 14dpi	$r_s = 0.53$, 95% CI= 0.52-0.55, $p < 0.0001$	--	$r_s = 0.17$, 95% CI= 0.16-0.19, $p < 0.0001$	$r_s = 0.27$, 95% CI= 0.25-0.29, $p < 0.0001$	ND	$r_s = 0.26$, 95% CI= 0.24-0.28, $p < 0.0001$	$r_s = 0.28$, 95% CI= 0.26-0.29, $p < 0.0001$	ND	$r_s = 0.28$, 95% CI= 0.26-0.30, $p < 0.0001$	ND	ND
US-Cxq Cx. <i>quinquefasciatus</i> WNV 14dpi	$r_s = 0.18$, 95% CI= 0.16-0.20, $p < 0.0001$	$r_s = 0.17$, 95% CI= 0.16-0.19, $p < 0.0001$	--	$r_s = 0.14$, 95% CI= 0.12-0.16, $p < 0.0001$	ND	$r_s = 0.16$, 95% CI= 0.14-0.17, $p < 0.0001$	$r_s = 0.12$, 95% CI= 0.10-0.14, $p < 0.0001$	ND	$r_s = 0.12$, 95% CI= 0.10-0.14, $p < 0.0001$	ND	ND
FC Cx. <i>pipiens</i> WNV 14dpi	$r_s = 0.36$, 95% CI= 0.35-0.38, $p < 0.0001$	$r_s = 0.27$, 95% CI= 0.25-0.29, $p < 0.0001$	$r_s = 0.14$, 95% CI= 0.12-0.16, $p < 0.0001$	--	ND	$r_s = 0.64$, 95% CI= 0.63-0.65, $p < 0.0001$	$r_s = 0.56$, 95% CI= 0.55-0.58, $p < 0.0001$	ND	$r_s = 0.65$, 95% CI= 0.63-0.66, $p < 0.0001$	ND	ND
PA-2004 Cx. <i>pipiens</i> WNV 7dpi	ND	ND	ND	ND	--	ND	ND	$r_s = 0.57$, 95% CI= 0.55-0.58, $p < 0.0001$	ND	$r_s = 0.38$, 95% CI= 0.36-0.40, $p < 0.0001$	$r_s = 0.25$, 95% CI= 0.23-0.26, $p < 0.0001$
PA-2004 Cx. <i>pipiens</i> WNV 14dpi	$r_s = 0.47$, 95% CI= 0.46-0.49, $p < 0.0001$	$r_s = 0.26$, 95% CI= 0.24-0.28, $p < 0.0001$	$r_s = 0.16$, 95% CI= 0.14-0.17, $p < 0.0001$	$r_s = 0.64$, 95% CI= 0.63-0.65, $p < 0.0001$	ND	--	$r_s = 0.63$, 95% CI= 0.62-0.64, $p < 0.0001$	ND	$r_s = 0.77$, 95% CI= 0.76-0.78, $p < 0.0001$	ND	ND
FC Cx. <i>tarsalis</i> WNV 14dpi	$r_s = 0.38$, 95% CI= 0.36-0.39, $p < 0.0001$	$r_s = 0.28$, 95% CI= 0.26-0.29, $p < 0.0001$	$r_s = 0.12$, 95% CI= 0.10-0.14, $p < 0.0001$	$r_s = 0.56$, 95% CI= 0.55-0.58, $p < 0.0001$	ND	$r_s = 0.63$, 95% CI= 0.62-0.64, $p < 0.0001$	--	ND	$r_s = 0.78$, 95% CI= 0.77-0.79, $p < 0.0001$	ND	ND
KR83 Cx. <i>tarsalis</i> WNV 7dpi	ND	ND	ND	ND	$r_s = 0.57$, 95% CI= 0.55-0.58, $p < 0.0001$	ND	ND	--	ND	$r_s = 0.50$, 95% CI= 0.48-0.51, $p < 0.0001$	$r_s = 0.30$, 95% CI= 0.28-0.32, $p < 0.0001$

**Table 2.3
(cont.)**

	ABQ <i>Cx. quinquefasciatus</i> WNV 14dpi	BERN <i>Cx. quinquefasciatus</i> WNV 14dpi	US-Cxq <i>Cx. quinquefasciatus</i> WNV 14dpi	FC <i>Cx. pipiens</i> WNV 14dpi	PA-2004 <i>Cx. pipiens</i> WNV 7dpi	PA-2004 <i>Cx. pipiens</i> WNV 14dpi	FC <i>Cx. tarsalis</i> WNV 14dpi	KR83 <i>Cx. tarsalis</i> WNV 7dpi	KR83 <i>Cx. tarsalis</i> WNV 14dpi	HWE <i>Ae. aegypti</i> WNV 7dpi	Rockefeller <i>Ae. aegypti</i> WNV 7dpi
KR83 <i>Cx. tarsalis</i> WNV 14dpi	$r_s = 0.49$, 95% CI= 0.48-0.51, $p < 0.0001$	$r_s = 0.28$, 95% CI= 0.26-0.30, $p < 0.0001$	$r_s = 0.12$, 95% CI= 0.10-0.14, $p < 0.0001$	$r_s = 0.65$, 95% CI= 0.63-0.66, $p < 0.0001$	ND	$r_s = 0.77$, 95% CI= 0.76-0.78, $p < 0.0001$	$r_s = 0.78$, 95% CI= 0.77-0.79, $p < 0.0001$	ND	--	ND	ND
HWE <i>Ae. aegypti</i> WNV 7dpi	ND	ND	ND	ND	$r_s = 0.38$, 95% CI= 0.36-0.40, $p < 0.0001$	ND	ND	$r_s = 0.50$, 95% CI= 0.48-0.51, $p < 0.0001$	ND	--	$r_s = 0.21$, 95% CI= 0.19-0.23, $p < 0.0001$
Rockefeller <i>Ae. aegypti</i> WNV 7dpi	ND	ND	ND	ND	$r_s = 0.25$, 95% CI= 0.23-0.26, $p < 0.0001$	ND	ND	$r_s = 0.30$, 95% CI= 0.28-0.32, $p < 0.0001$	ND	$r_s = 0.21$, 95% CI= 0.19-0.23, $p < 0.0001$	--

Chapter 3: Virus-vector pairings determine the molecular signatures of virus-derived piRNA-like small RNAs in mosquitoes

Introduction

The canonical antiviral RNAi pathway in mosquitoes, the exogenous small-interfering RNA (exo-siRNA) pathway, has been the subject of much investigation in recent years. However, comparatively, very little is known about the role that other small RNA pathways, such as the micro RNA (miRNA) pathway and PIWI-interacting RNA (piRNA) pathway, may play in antiviral defense in mosquitoes. Recently, several studies have provided evidence suggesting that the piRNA pathway or components of the pathway participate in the innate antiviral immune response in insect systems [314, 281, 315, 317, 282, 316, 318, 313]. Like the endogenous siRNA (endo-siRNA) pathway, the piRNA pathway plays a significant role in regulating the expression of endogenous RNA transcripts. piRNAs have been shown to be important repressors of transposable elements (TEs) in the germline cells of a variety of organisms from flies to mice [409-413]. Endogenous piRNAs are believed to originate from two distinct pathways. In the primary piRNA pathway, piRNAs are processed from single-stranded RNA precursors which are transcribed from discrete genomic loci (known as piRNA clusters). Primary piRNAs are typically antisense to TEs, exhibit a strong bias for a 5'-uridine residue (U₁), and in flies, are associated with the PIWI/Aubergine protein complex [310]. Primary piRNAs are then fed into the second pathway, the "ping-pong dependent" amplification cycle. In this pathway, after binding of the target transcript, cleavage occurs ten nucleotides upstream from the 5' end of the primary piRNA, resulting in secondary piRNAs with an adenine residue in the

10 position (A₁₀), and are Argonaute-3 (Ago3) associated [311, 312]. Cleavage of the target transcript presumably occurs via the Slicer activity of Ago-3, as in flies, but not mammals [414]. Secondary piRNAs then bind complementary targets resulting in cleavage at the A-U base-pairing, resulting in piRNAs identical (or very similar) to the initial primary piRNA, exhibiting a 5'-U₁ residue. In fact, this nucleotide bias is a hallmark of endogenous piRNAs in flies and possibly mammals, and is the basis for the ping-pong dependent amplification model [311, 312].

However, examination of our previous small RNA sequence data from *Culex quinquefasciatus*, *Cx. pipiens*, *Cx. tarsalis*, and *Aedes aegypti* mosquito midguts infected by West Nile virus (WNV, *Flaviviridae*) (**Chapter 2**) were not entirely consistent with this model. Although at both 7 and 14 days post infection (dpi) 24-30nt viRNAs from these libraries were predominately derived from the positive strand (>90% in all libraries), consistent with the strong positive-strand bias seen in previous reports of viral-derived piRNA-like small RNAs (vpiRNAs) [314, 317, 282, 316, 318, 313], we failed to observe signatures of ping-pong dependent amplification. Interestingly, this signature has been widely reported in studies of alphavirus [282, 316, 313] and bunyavirus infections [316, 318], but not with flaviviruses (DENV) [281, 315] or reoviruses [318]. Therefore, while a growing body of evidence suggests that the piRNA pathway plays a role in antiviral defense in insects, the biogenesis of the effector molecules remains somewhat obscure. Further, the variety of different virus-vector pairings utilized make comparing the piRNA response across these systems problematic.

Accordingly, we sought to determine whether modes of vpiRNA production and/or processing is virus family-dependent. In particular, we hypothesized that, consistent with the

literature [281, 315], vpiRNAs produced in response to flavivirus infection would lack signatures of ping-pong dependent amplification while piRNAs produced in response to alphavirus infection would exhibit these signatures in a single species of mosquito. *Cx. tarsalis* is a highly competent natural vector for both WNV and Western equine encephalitis virus (WEEV, *Togaviridae*) in North America, and a competent laboratory vector for Sindbis virus (SINV, *Togaviridae*). We therefore infected *Cx. tarsalis* mosquitoes with either a flavivirus (WNV), or alphaviruses (WEEV, SINV) and sequenced small RNAs at 7 and 14dpi. We also investigated tissue-specific small RNA profiles by sequencing both midguts and carcasses sans ovaries to determine whether differences seen in our previous studies and previously published ones may be attributed to compartmental differences in the vpiRNA response. Additionally, we compared 24-30nt small RNA profiles from *Ae. aegypti* mosquitoes infected with WNV to *Ae. aegypti* infected with SINV. Our results demonstrate that vpiRNAs produced in response to alphaviruses, but not flaviviruses, tend to be produced in a ping-pong dependent manner. Moreover, it appears that the mode of vpiRNA biogenesis is a unique property of specific virus-vector pairings.

Materials and Methods

Mosquitoes

Lab-colonized *Cx. tarsalis* mosquito larvae (KR83, described in [395]) were raised on a diet of a 1:1 mix of powdered Tetra food and powdered rodent chow. Pupae were allowed to emerge into containers and adult mosquitoes were kept at 26-27 °C with a 16:8 light:dark cycle and 70%-80% relative humidity, with water and sucrose provided *ad libitum*.

Viruses and Experimental Infections

WNV was produced from an infectious cDNA clone based on the WNV_{NY99} strain of the virus as described elsewhere [397]. WEEV isolate Imperial 181 (WEEV_{Imp181}), an isolate that exhibits low virulence in mice [415] but high infections rates in *Cx. tarsalis* mosquitoes [416, 417], was similarly derived from an infectious cDNA clone (WEEV_{Imp181}icd). Briefly, the plasmid containing the full-length infectious clone was linearized with the NotI-HF restriction enzyme (New England BioLabs, Ipswich MA), and then *in vitro* transcribed into the infectious viral genomic RNA using the T7 Megascript kit (Ambion, Austin TX), and 5'-capped with a m⁷G(5')ppp(5')A cap analog (New England BioLabs, Ipswich MA). Purified viral RNA was electroporated into BHK-21 cells, with the electroporation parameters set to 425 V, 1200Ω resistance, 25μF capacitance, and two pulses. Cell supernatant was collected after cells showed obvious signs of cytopathic effect (CPE; usually ~3 days post-electroporation). Cellular debris was removed from the supernatant by centrifugation at ~3000 g, clarified supernatant was raised to a final concentration of 20% fetal bovine serum (FBS), and aliquots of 0.5 mL were made and stored at -80°C. Virus titer was then quantified by plaque assay on Vero cells. Recombinant infectious-clone derived SINV strain MRE16 with a second introduced subgenomic promoter 5' to the structural genes of the virus (5'dsMRE16icd, described in [418]) was provided as a kind gift by Dr. Brian Foy of Colorado State University. Adult female mosquitoes 6-8 days post-eclosion were fed an infectious bloodmeal of defibrinated sheep blood mixed 1:1 with ~2.5 X 10⁶ PFU/mL of WEEV_{Imp181}icd, ~2 X 10⁸ PFU/mL of WNV_{NY99}icd or ~5 X 10⁷ PFU/mL of infectious clone derived recombinant SINV_{5'dsMRE16}icd and raised to a final concentration of 2mM ATP. Engorged mosquitoes were held for 7 or 14 days in a BSL-3 insectary under the same

conditions described above for larvae, after which they were cold anesthetized, and midguts dissected and stored in miRvana RNA isolation lysis buffer (Ambion) at -80°C until RNA isolation. In separate experiments, mosquitoes infected in the same manner were cold anesthetized at 7 and 14dpi, and both midguts and carcasses sans ovaries separately collected and homogenized in miRvana RNA isolation lysis buffer.

Total RNA Isolation and Small RNA Library Preparations

Total RNA was extracted from homogenized mosquito midguts using the miRvana miRNA isolation kit (Ambion) as per manufacturers suggested protocol for total RNA isolation. Eluted RNA from individual midguts and carcasses from each infection group were screened for the presence of WNV genomic RNA by 1-step RT-PCR (Qiagen, Valencia CA) using 1971-F (5'-TTGCAAAGTTCCTATCTCGTCAG-3') and 2928c (5'-CCAAATCCAAAATCCTCCACTTCT-3') primers, WEEV genomic RNA using 8495-F (5'-GTTCTGCCCGTATTGCAGACACTCA-3') and 8848c (5'-CTCCTGATCTTTCTCTCCACGG -3') primers, or SINV genomic RNA using 9468-F (5'-AAAAGTGACCAGACAAAGTGGGTC-3') and 9901c (5'-GCGGCTACTAGGACCATCAC-3') primers (numbers in primer designation denote genome position). RNA samples positive for viral RNA were checked for RNA quality on a 2100 Bioanalyzer (Agilent, Santa Clara CA), and then pooled into groups of 5 midgut RNAs by virus infection and timepoint. Pooled RNAs were precipitated by adding 3.25 volumes of ice-cold EtOH, 0.1 volume 3M NaOAc (pH 5.5), and 1.5 µL of linear polyacrylamide (5 mg/mL) as a carrier. After holding overnight at -20°C, the pools were centrifuged at ~20,000 g, washed twice with 80% EtOH, and re-suspended in nuclease-free water. 1 µg total RNA was used as the input for small RNA library preparation using the TruSeq

Small RNA Sample Prep Kit (Illumina, San Diego CA) as per manufacturer's suggested protocol. Briefly, small RNAs were preferentially 3' and 5' adapter-ligated, reverse transcribed using the Superscript II reverse transcriptase (Invitrogen, Carlsbad CA), and PCR amplified, during which time a unique oligonucleotide barcode sequence was added to each library for multiplexing. Small RNA libraries were size selected on 2% TBE-agarose gels, and purified with MinElute Gel Extraction kits (Qiagen). Purified small RNA cDNA libraries were eluted in Qiagen EB buffer, validated on the 2100 Bioanalyzer, and sequenced on an Illumina HiSeq 2000 instrument.

Assembly and Analysis of sRNA Libraries

FASTQ files were trimmed of the 3' adapter using FASTX Toolkit [400] and aligned to the WEEV_{Imp181}, WNV_{NY99}, SINV_{5'dsMRE16} infectious clone, or species-specific transposable element reference genomes/sequences using Bowtie 0.12.8 [401] and allowing for 0-mismatches. The **-a --best --strata** mode was used, which instructs Bowtie to report only those alignments in the best alignment stratum. SAM output files produced by Bowtie were used as the input for processing through SAMtools [402]. Nucleotide targeting plots of the viral genome were generated using the pileup function of SAMtools. 5' distance plots and small RNA sequence conservation bar plots were produced using viRome [403], in R [419]. Additional analyses were conducted using Picard [420], Microsoft Excel and Graphpad Prism 6.

RT-PCR screening for PIWI-component transcripts

10 midguts and 10 ovaries were separately dissected from adult female colonized US-Cxq *Cx. quinquefasciatus* mosquitoes, pooled, and homogenized in miRVana lysis buffer

(Ambion). Total RNA was extracted using the miRVana miRNA isolation kit and the total RNA protocol. Midgut and ovary pools were screened for PIWI component transcripts using the primers listed in **Table 3.1**. Reactions without the reverse transcriptase enzyme (-RT) or RNA template (NTC) served as negative controls.

Results

Alphavirus infection of *Cx. tarsalis* results in disparate positive/negative strand targeting ratios in midguts and carcasses

Cx. tarsalis mosquitoes infected with either WNV, WEEV, or SINV all exhibited stereotypical siRNA profiles with a predominant peak at 21 nts (**Figure 1**). 19-23nt viRNAs made up between ~50-90% (\bar{x} = 60.6%, n=5), ~54-88% (\bar{x} = 70.4%, n=6), and ~71-96% (\bar{x} = 85.2%, n=4) of 19-30nt viRNAs derived from WNV, WEEV, and SINV, respectively, across both midgut and carcass libraries for each time point. Similarly, the percentage of 24-30nt vpiRNAs varied across tissue, timepoint and virus, comprising between ~11-50% (\bar{x} = 39.4%, n=5), ~12-46% (\bar{x} = 29.6%, n=6), and ~4-29% (\bar{x} = 14.8, n=4) of 19-30 nt viRNAs derived from WNV, WEEV, and SINV, respectively. Strand bias in 19-23nt viRNAs were consistent with previous studies, averaging between ~57-85% originating from the positive strand across all virus infections, tissues, and timepoints (**Figure 3.2 – 3.4**). vpiRNAs sequenced from both midguts and carcass libraries from mosquitoes infected with WNV exhibited a strong strand bias with between 96% and nearly 100% of these small RNAs being derived from the positive strand of the virus (**Figures 3.5**). However, vpiRNAs sequenced from WEEV- and SINV-infected midguts were only between 51-57% and 64-70% positive-strand derived, respectively (**Figures 3.6A-B and 3.7A-B**). Intriguingly,

vpiRNAs sequenced from the carcasses in these infections were predominantly positive strand-derived (**Figures 3.6C-D** and **3.7C-D**), consistent with ours and others' previous observations [314, 282, 316, 318].

***Cx. sp.* mosquitoes do not produce vpiRNAs with signatures of ping-pong dependent amplification after infection with WNV, WEEV, or SINV.**

We next conducted sequence analysis of 24-30nt vpiRNA populations. As we previously observed with *Cx. quinquefasciatus*, *Cx. pipiens*, and *Ae. aegypti*, vpiRNAs sequenced from *Cx. tarsalis* midguts and carcasses infected with WNV, WEEV, or SINV lacked U₁ or A₁₀ biases expected of products of ping-pong amplification (**Figures 3.8 – 3.13**). We next measured the positional frequency of the 5'-terminus of reads mapping to opposite strands of the virus genome. Products of the ping-pong dependent amplification model would be expected to have 5'-termini separated by 10 nts. As expected from the lack of U₁/A₁₀ bias, we found no such peak at 10 nts in either midguts or carcasses infected with WNV, WEEV, or SINV at either time point. However, there was a high degree of consistency observed in the 5'-distance plots in the same tissues across time points, most obviously in SINV-infected carcasses (**Figure 3.14** and **Figure 3.15**).

To evaluate the possibility that the lack of ping-pong dependent amplification signatures observed in *Culex* midguts was due to the lack of primary components of the piRNA pathway are present in the mosquito midgut, we attempted to amplify these components from tissue mRNAs by RT-PCR. We detected the presence of 6 PIWI-component transcripts (*Ago3*, *Arm1*, *PIWI4*, *PIWI5*, *PIWI6*, *SPNE*) in the midguts of un-infected mature female *Cx. quinquefasciatus*

mosquitoes by RT-PCR (**Figure 3.16**). In *Cx. quinquefasciatus*, *PIWI4*, *PIWI5*, and *PIWI6* are annotated as orthologues to *D. melanogaster Aubergine (Aub)* (*PIWI5*, *PIWI6*, and *PIWI7* are *Aub* orthologues in *Ae. aegypti*) [421]. *Aub* is associated with primary piRNAs being fed into the ping-pong dependent amplification pathway. Thus, we were able to detect the necessary component machinery transcripts within the midguts of *Cx. quinquefasciatus*. Presumably, these transcripts are being translated, and we reason that they are likely similarly expressed in the midguts of *Cx. pipiens* and *Cx. tarsalis*.

***Ae. aegypti* mosquitoes produce ping-pong dependent vpiRNAs in response to SINV infection but not WNV infection**

We previously sequenced small RNAs from midguts from the Rockefeller strain of *Ae. aegypti* as well as whole HWE mosquitoes after experimental infection with WNV. A third *Ae. aegypti* library (Ubi61, a transgenic strain expressing FHV B2, a viral suppressor of RNAi [422]) from orally WNV-infected whole mosquitoes was also made. In all three libraries, infection with WNV failed to produce vpiRNAs exhibiting signatures of ping-pong dependent amplification (**Figure 3.17**), and corresponding 5'-distance plots showed no peak at 10 nts (**Figure 3.15D and 3.15E**). Curiously, a 28 nt RNA sequence (5'-CTGGCTGGGACACCCGCATCACGAGAGGCT-3', underlined nucleotides denote longer/shorter derivations of this sequence that were also present in high abundance) mapping to the positive strand of WNV RNA was found in overwhelming abundance in all three *Ae. aegypti*/WNV libraries. This sequence and its longer/shorter derivations made up 72.7%, 76.0, and 17.6% of the total 24-30nt population in the HWE, Rockefeller, and Ubi61 libraries, respectively. BLAST of this sequence revealed that

there are no known non-WNV sequences that share significant homology with the full 28nt RNA, and that this sequence maps to the NS5 coding region of WNV (positions 9293-9320). To determine whether the striking abundance of this sequence was masking a ping-pong dependent signature in the rest of the 24-30nt population, we reduced all repetitive reads to a single instance using the MarkDuplicates option in Picard [420]. Removing repetitive sequences from these datasets did not reveal latent signatures of ping-pong dependent amplification in the rest of the dataset. Since previous reports have described ping-pong dependent vpiRNAs in *Ae. aegypti* and *Ae. albopictus* mosquitoes [282] and cell culture [317, 316, 313] after infection with alphaviruses and bunyaviruses, we analyzed a previously unpublished *Ae. aegypti* dataset derived from whole mosquitoes 9dpi with a recombinant SINV expressing eGFP (5' dsMRE16-eGFP). 19-23nt viRNAs made up ~53% of the total 19-30nt population, with ~54% of 19-23nt viRNAs being derived from the positive strand (**Figure 3.18**). Similar to WNV infection in *Cx.* mosquitoes, but not alphavirus infection in *Cx. tarsalis* midguts, 92% of 24-30nt vpiRNAs were positive strand derived. Of note, as observed in previous studies of *Ae. spp.* mosquitoes or cells infected with alphaviruses, 24-30nt vpiRNAs show heavy targeting at the 5'-portion of the virus genome and near the subgenomic promoter, with very little targeting in between. Conversely, vpiRNAs from WNV-infected HWE and Rockefeller mosquitoes show a much more even distribution along the length of the viral genome, with the notable exception of a very large peak at NS5 resulting from the aforementioned high abundance read mapping to that gene (data not shown). vpiRNAs from the *Ae. aegypti*/SINV data set exhibited strong biases for a U₁ and A₁₀ on the antisense and sense strand reads, respectively (**Figure 3.19**). As expected, 5'-distance overlap confirmed a peak at 10 nts, suggesting a ping-pong dependent mechanism

(Figure 3.14F). Since we had removed duplicate sequences from the *Ae. aegypti*/WNV libraries, we performed the same treatment to the *Ae. aegypti*/SINV library, to ensure that detection of U₁/A₁₀ biases were not dependent on the abundance of particular sequences. Even after removing duplicate reads, 24-30nt vpiRNAs from the *Ae. aegypti* library still indicated a strong bias for both nucleotides, confirming that the nucleotide bias is due to a preponderance of unique sequences exhibiting the bias as opposed to a relative few in high abundance (data not shown).

Features of endogenous piRNAs in *Cx. quinquefasciatus* and *Ae. aegypti* mosquitoes

We next investigated whether endogenous piRNAs in *Culex* and *Aedes* mosquitoes exhibit signatures of ping-pong dependent amplification. Since TEs are often the targets of endogenous piRNAs, we aligned our *Cx. quinquefasciatus* midgut libraries and *Ae. aegypti* midgut and whole mosquito libraries to published TE sequences from the a recent report describing novel LTR-retrotransposons (LTR-rTEs) in *Cx. quinquefasciatus* [423] and the TEfam database of mosquito transposable element sequences [424]. The *gypsy* family LTR-rTEs selected for alignment against *Cx. quinquefasciatus* small RNA midgut libraries (*CqGypsy-13* and *CqGypsy-47*) universally resulted in alignments mapping antisense to the LTR-rTE, as expected for piRNAs **(Figure 3.20)**. Nucleotide sequence analysis revealed that in all three *Cx. quinquefasciatus* midgut libraries, the predominant base at position 1 was a U **(Figures 3.21 and 3.22)**. However, a lack of sense strand reads made it impossible to confirm ping-pong dependent amplification. We aligned both Rockefeller *Ae. aegypti* midgut libraries and HWE whole mosquito libraries to 3 *Ae. aegypti* *gypsy* LTR-rTEs: *Ty3-Gypsy-121*, *Ty3-Gypsy-122*, and *Ty3-Gypsy-123*. As seen in *Cx.*

quinquefasciatus, midgut library alignments resulted in nearly universally negative strand alignments, with a strong U₁ bias (**Figures 3.23-3.26**). Alignments of the HWE whole mosquito library were predominately antisense, but a sufficient number of reads mapping directly to the LTR-rTE were present that we could perform sequence analysis. In this whole mosquito library, antisense reads exhibited a strong U₁ bias while sense reads exhibited a strong A₁₀ bias, indicative of a ping-pong mechanism (**Figures 3.24-3.26**). However, measuring the distance between 5'-ends of opposite strands did not reveal a peak at 10 nt (data not shown).; this likely resulted from the extremely low abundance of sense strand reads relative to antisense reads. These results suggest that a piRNA pathway is active in both the *Cx. quinquefasciatus* and *Ae. aegypti* midgut epithelium.

Discussion

The piRNA pathway has relatively recently been implicated in participating in the innate antiviral immune response in insects. However, little is known about how this pathway actually functions in response to virus infection. Presumably, vpiRNAs are loaded into a cytoplasmic “piRISC”, which in similar fashion to the siRNA pathway targets viral RNA by sequence complementarity leading to degradation of the viral transcript. Here we present evidence that this pathway can be modulated differentially in different virus/vector pairings, and that the presence or lack of molecular signatures characteristic of the ping-pong dependent model for piRNA biogenesis is neither vector nor virus specific, i.e. certain vectors do not universally produce RNAs with these signatures upon arbovirus infection and certain viruses do not

universally elicit this response in vectors. Rather, there appears to be a complex interplay between the specific virus and vector that determines what types of vpiRNAs are produced.

vpiRNAs generated during alphavirus infection of *Ae. aegypti* mosquitoes and mosquito cells show a strong bias for targeting of both the 5'- and 3'- ends of the viral genome, with very strong positive strand bias [282, 316, 313]. Conversely, in both the midgut and carcass of *Cx. tarsalis* mosquitoes infected with either WEEV or SINV, the distribution of targeting along the length of the virus genome is considerably more even, and no apparent strand bias was observed in midguts infected with WEEV or SINV. However, in the carcasses of these mosquitoes, the expected positive strand bias of vpiRNAs was maintained. This suggests that 24-30nt viRNAs are produced in disparate ways in the midgut and the rest of the soma. It is worth noting that in RVFV-infection of mosquito cells, the lack of strand bias for some (but not all) of the 25-28nt small RNAs sequenced has been observed [317], though this varies depending on which segment of the viral genome is being analyzed, with some segments showing a strong negative strand bias (perhaps expected since RVFV has a negative-sense segmented genome).

We found no evidence of ping-pong dependent signatures from 24-30nt vpiRNAs sequenced from either flavivirus or alphavirus infection of *Cx. tarsalis* mosquitoes, though 24-30nt viRNAs are generally produced in appreciable abundance during these infections. Our previous sequencing of small RNAs from *Cx. spp.* and *Ae. aegypti* mosquitoes infected with WNV similarly showed a lack of these signatures, and this has also been observed in sequencing of small RNAs from DENV-infected *Ae. aegypti* mosquitoes and *Ae. spp.*-derived mosquito cells [281, 315]. However, the finding that alphavirus infection (in particular SINV infection) did not

produce molecular signatures of ping-pong dependent amplification was surprising, given that both the published literature as well as our data described in this manuscript indicate that alphavirus infection in *Ae. aegypti* mosquitoes and mosquito cells does elicit production of ping-pong dependent vpiRNAs [282, 316, 313]. We addressed the issue as to whether the lack of a ping-pong mechanism was unique to the *Cx. tarsalis* midgut by sequencing carcasses sans ovaries; despite this, we found no evidence that this mechanism was functioning in either compartment. We were able to detect piRNA-component protein RNA transcripts in the midguts of *Cx. quinquefasciatus* mosquitoes, and presumably these transcripts are actively being translated. Additionally, our analysis of 24-30nt reads aligning to species-specific LTR-rTE's strongly suggest that a piRNA pathway is active and functional in the midguts of both *Cx. quinquefasciatus* and *Ae. aegypti*. While we did not directly test this for *Cx. tarsalis*, we have extrapolated this data to assume that the piRNA pathway functions in the midgut of these mosquitoes as well. 24-30nt small RNAs aligning to LTR-rTEs from midgut libraries were almost entirely or entirely antisense to the LTR-rTE, and had a predominant U₁ bias. Alignments made with libraries constructed from whole *Ae. aegypti* mosquitoes showed a distinct antisense bias, with a U₁ residue on the antisense strand, and an A₁₀ bias on the positive strand, indicative of a ping-pong dependent mechanism. Given that these libraries were made from whole mosquitoes with ovaries intact, it is possible that some or most of these reads were derived from reproductive tissue, where piRNAs and LTR-rTEs are most abundant. However, production of vpiRNAs with signatures of ping-pong dependent amplification have been reported in the soma of *Ae. aegypti* and *Ae. albopictus* mosquitoes after infection with CHIKV [282].

A perplexing observation in *Ae. aegypti*/WNV libraries was the massive over-representation of a single 28 nt sequence, or slightly shorter/longer derivations of it, which accounted for a substantial proportion of the 24-30 nt reads from those libraries. In Ubi61 mosquitoes, which express Flock house virus (FHV, *Nodaviridae*) B2, a viral suppressor of RNAi, this sequence was still present in great abundance, though as a significantly lower proportion of the total 24-30nt sequence than either of the two RNAi-competent *Ae. aegypti* libraries we sequenced. The sequence, which maps to the NS5 viral replicase gene, was not present in appreciable amounts in any of the numerous *Cx. spp.*/WNV libraries we have sequenced for this and other studies, and is sometimes completely absent from those libraries. Interestingly, we attempted to find this sequence in a previously published C6/36/WNV small RNA dataset and were unable to find it either. It is unlikely that the large proportion of this sequence is due to sequencing bias, since it was replicated in multiple libraries sequenced on different instruments.

One of the more striking observations made in our studies was the disparity between vpiRNAs produced in response to either WNV or SINV-infection in *Ae. aegypti* mosquitoes. We observed no signatures of ping-pong dependent amplification in our sequencing of small RNAs from *Ae. aegypti* midguts or whole mosquitoes infected with WNV, yet a previously unpublished small RNA dataset from *Ae. aegypti* whole mosquitoes infected with a recombinant SINV showed signatures indicative of a ping-pong dependent amplification mechanism. Previous studies with *Ae. aegypti* mosquitoes infected with another flavivirus, DENV-2, showed only a slight bias for an A₁₀ residue, and no bias for a U₁ residue [281, 315]. Similarly, *Ae. aegypti*-derived Aag2 cells infected with DENV fail to produce piRNAs indicative of

a ping-pong mechanism, as do *Ae. albopictus*-derived C6/36 mosquito cells, which have a dysfunctional siRNAi pathway due to a premature stop codon in *dcr-2* [280, 281], but which produce products consistent in size with vpiRNAs [281, 280]. Therefore, it is apparent that the exogenous piRNA response in at least *Ae. aegypti* mosquitoes is differentially modulated upon infection with either flaviviruses or alphaviruses. The reasons for this are unclear. Both flaviviruses and alphaviruses have single-stranded, positive-sense RNA genomes; however alphaviruses produce a smaller 26S subgenomic transcript during replication of the full length 42S genomic RNA [425]. However, these differences in the replication of flaviviruses and alphaviruses do not account for the disparity observed in vpiRNAs produced from *Cx. tarsalis* and *Ae. aegypti* mosquitoes in response to alphavirus infection. Thus, it appears that the products of the exogenous piRNA pathway in mosquitoes during arbovirus infection are dependent on both host and viral determinants. We have summarized our findings and those of previous studies in **Table 3.2**.

Table 3.1: Primer sequences used to screen for PIWI component transcripts in *Cx. quinquefasciatus*. Designation next to gene name denotes Vectorbase ID.

Target Gene	Forward Primer	Reverse Primer
Ago3 (CPIJ005275)	5'-AGTACATCAACCAGCATCGAG-3'	5-TGCAGAATTGTTCCACGTTG-3
Arm1 (CPIJ001245)	5-GTGAATTCCAAGCCCTAATGC-3	5-TCCAGCAACCTACCCAAATC-3
PIWI 4 Txn 1(CPIJ012516)	5-TCAAGGTGCTCATGGAATCG-3	5GACCGTTGAGTAGAATTCCGAG-3
PIWI 5 Txn 1 (CPIJ017382)	5- TGAAGTTGACGCTGATTGGG-3	5- ACGATGGGTAAGTTCTGCAC-3
PIWI 6 (CPIJ017381)	5-CTACATTACCAGCATCCGACAG-3	5-TGCACTTCTCAAACAGGTCG-3
SPNE (CPIJ017541)	5-GAAGGTCTACTCGGTCGTTG-3	5-TCGTGGTCTAGCTTGAAATG-3

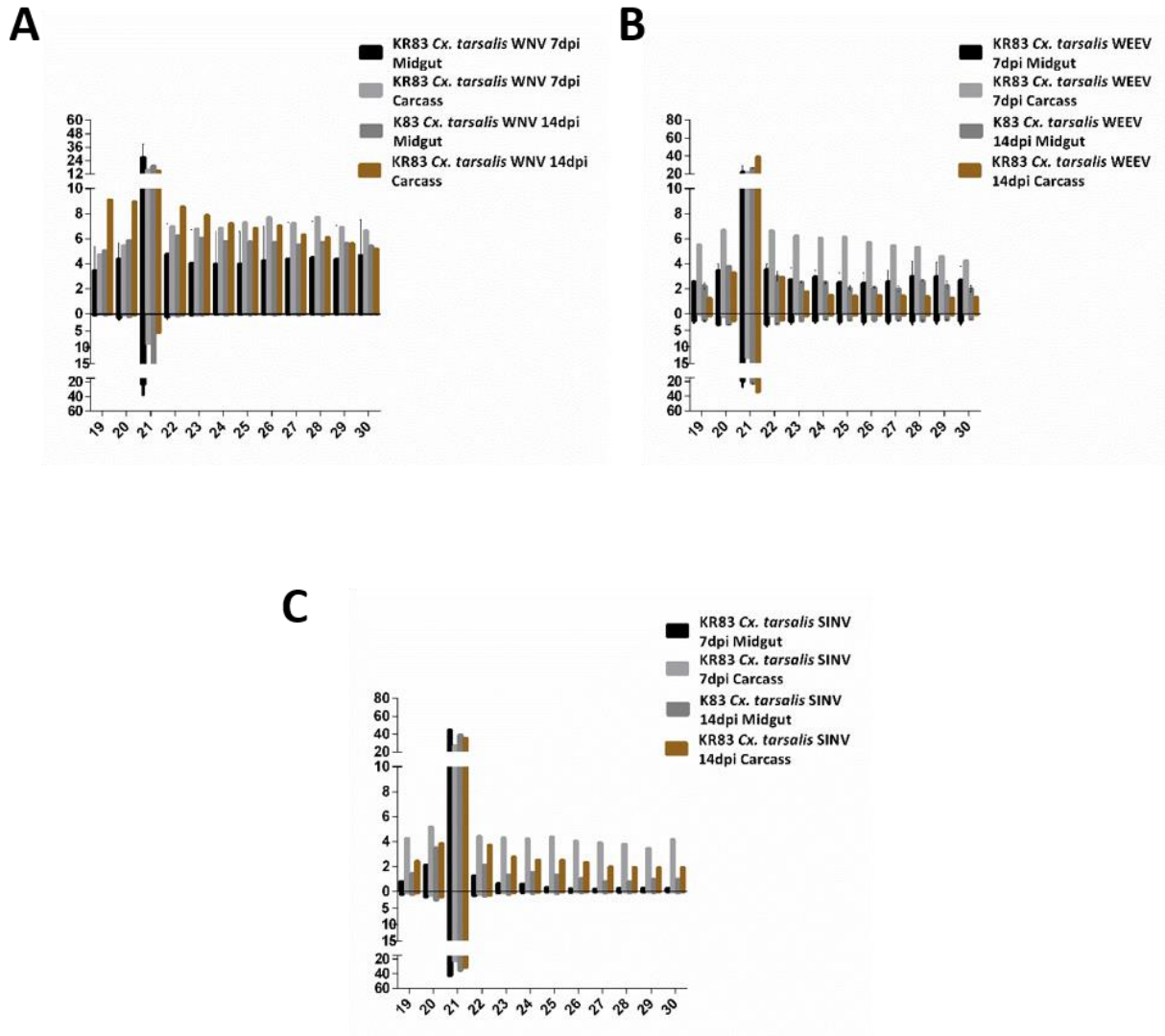


Figure 3.1: Read length distributions for *Cx. tarsalis* small RNA libraries. Reads on the negative portion of the x-axis denote reads mapping to the negative strand of the virus. Error bars represent SEM in libraries with replicates. **A)** *Cx. tarsalis*/WNV_{NY99}, **B)** *Cx. tarsalis*/WEEV_{Imp181}, **C)** *Cx. tarsalis*/SINV_{5'dsMRE16}.

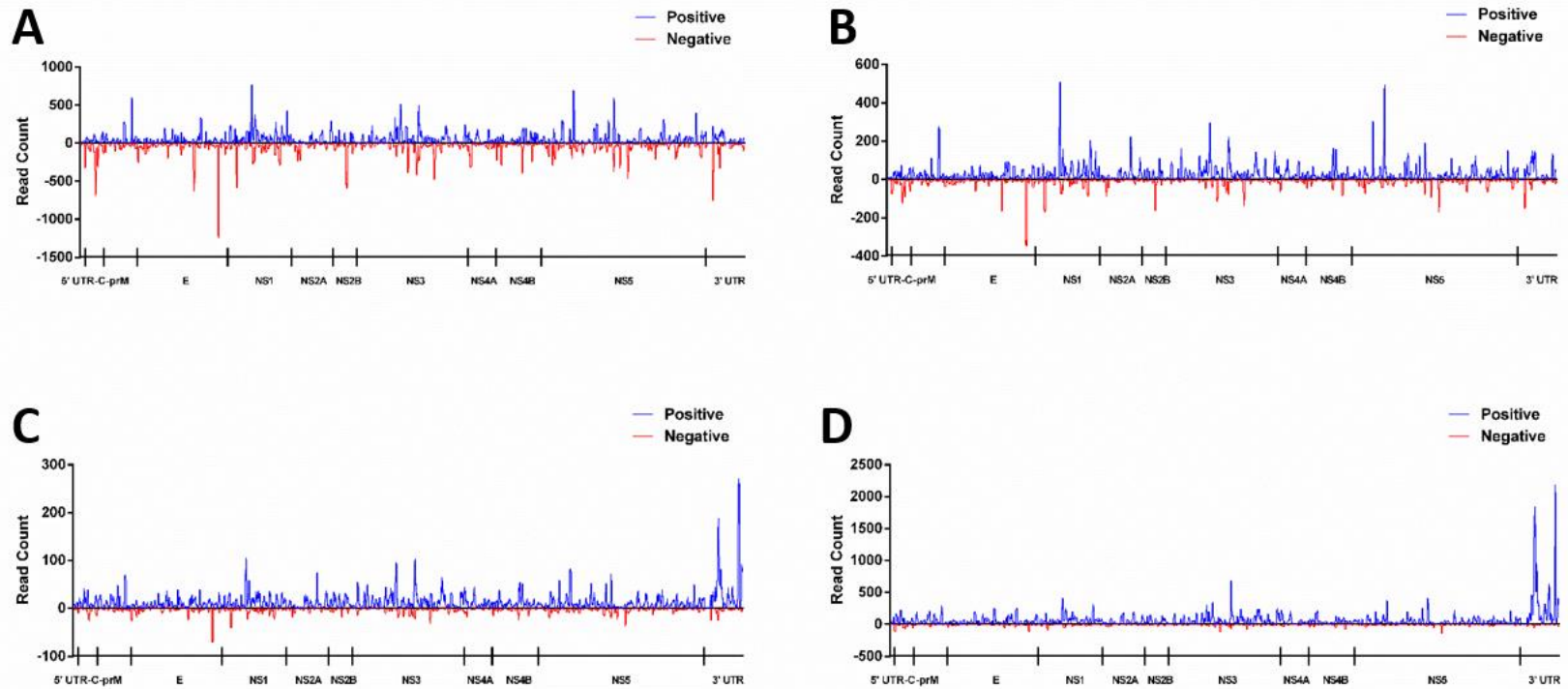


Figure 3.2: Distribution of 19-23 nt reads along the length of the WNV_{NY99} genome. **A)** *Cx. tarsalis* midgut WNV_{NY99} 7dpi. Positive/negative strand ratio is 53.0%/47.0%. This represents one of two experimental replicates; the second had a strand ratio of 80.5%/19.5%. **B)** *Cx. tarsalis* midgut WNV_{NY99} 14dp. Positive/negative strand ratio is 71.4%/28.6%. **C)** *Cx. tarsalis* carcass sans ovaries WNV_{NY99} 7dpi. Positive/negative strand ratio is 80.1%/19.9%. **D)** *Cx. tarsalis* carcass sans ovaries WNV_{NY99} 14dpi. Positive/negative strand ratio is 88.8%/11.2%.

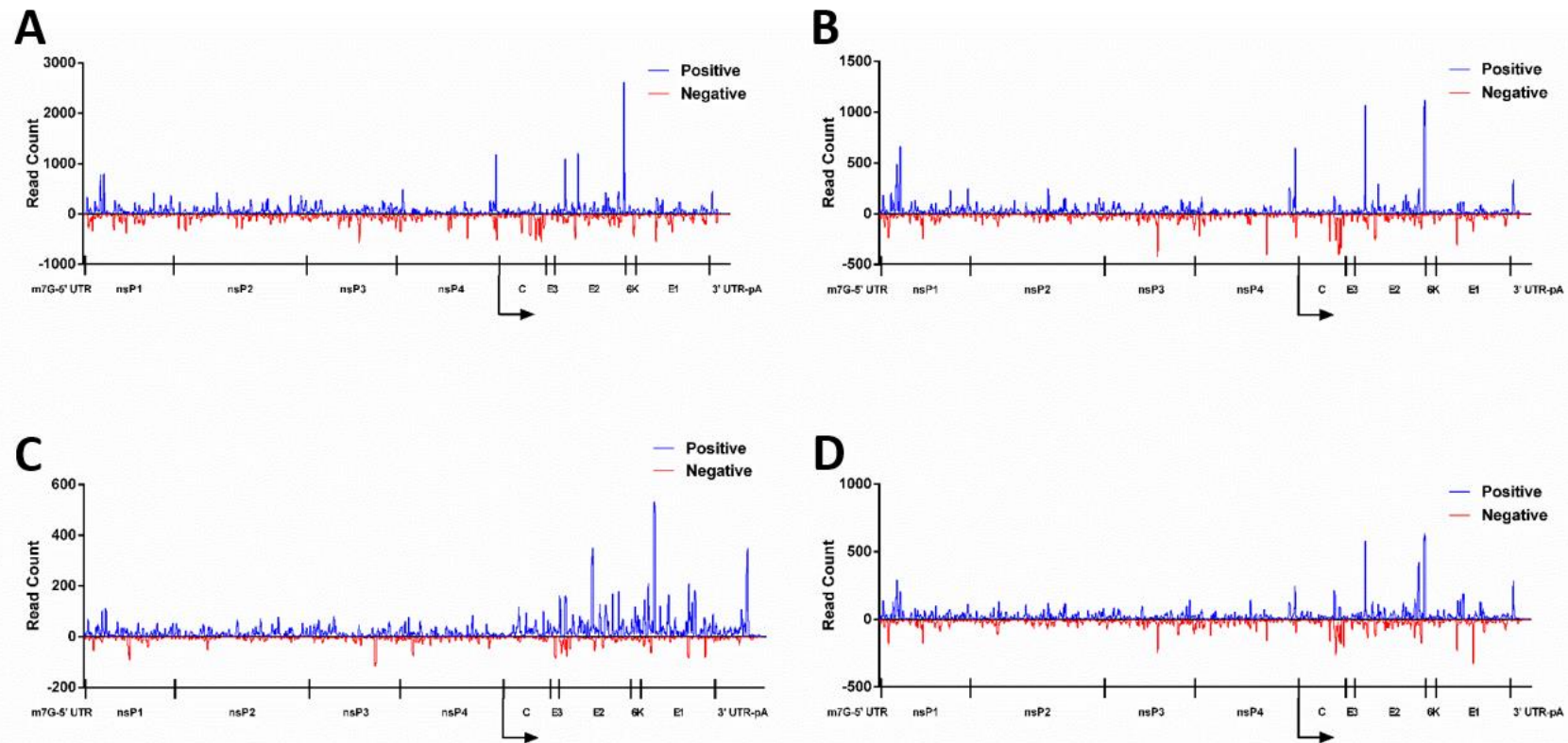


Figure 3.3: Distribution of 19-23 nt reads along the length of the WEEV_{Imp181} genome. **A)** *Cx. tarsalis* midgut WEEV_{Imp181} 7dpi. Positive/negative strand ratio is 55.1%/44.9%. This represents one of two experimental replicates; the second had a strand ratio of 51.4%/48.6%. **B)** *Cx. tarsalis* midgut WEEV_{Imp181} 14dpi. Positive/negative strand ratio is 55.5%/44.5%. This represents one of two experimental replicates; the second had a strand ratio of 51.8%/48.2%. **C)** *Cx. tarsalis* carcass sans ovaries WEEV_{Imp181} 7dpi. Positive/negative strand ratio is 75.5%/24.5%. **D)** *Cx. tarsalis* carcass sans ovaries WEEV_{Imp181} 14dpi. Positive/negative strand ratio is 55.2%/44.8%.

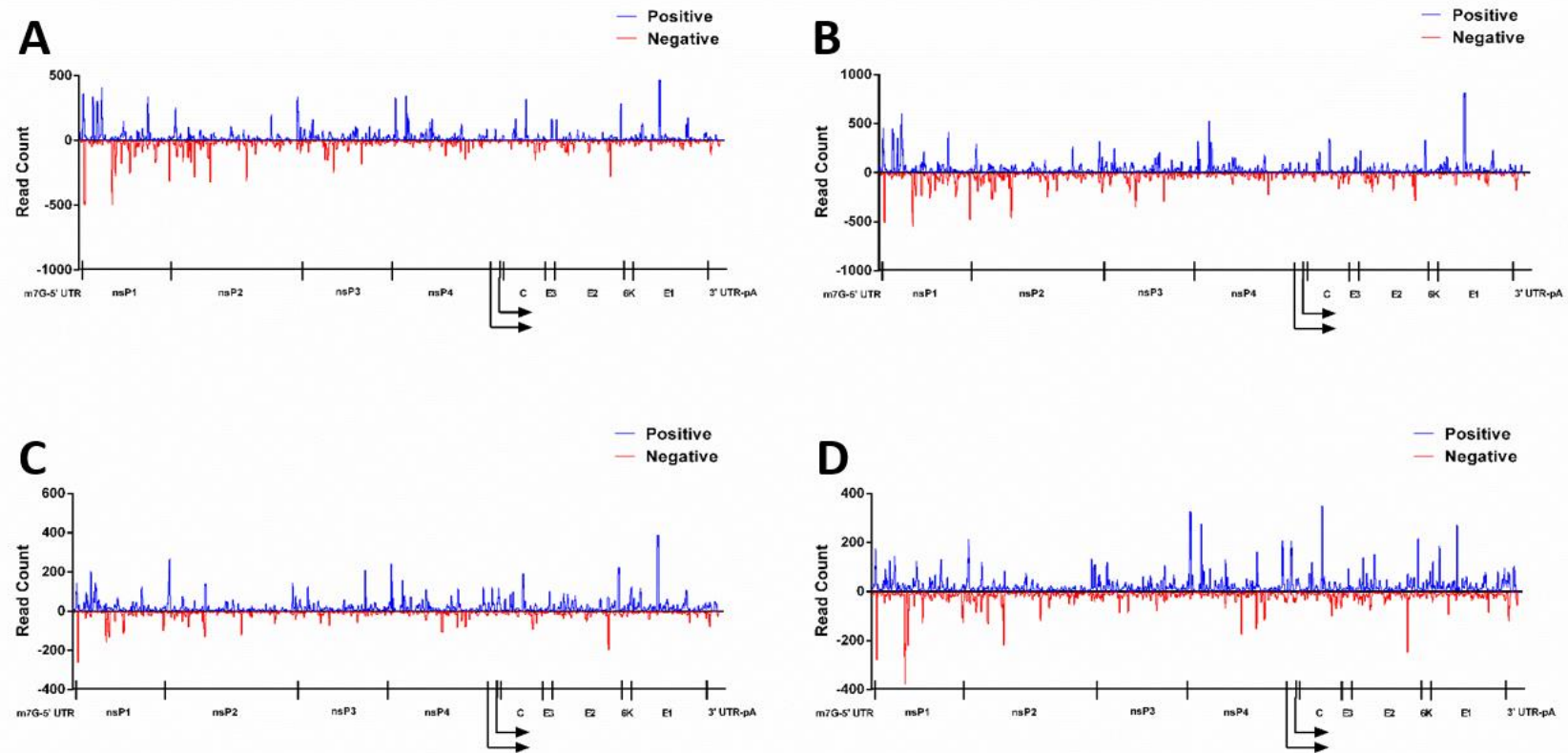


Figure 3.4: Distribution of 19-23 nt reads along the length of the SINV_{5'dsMRE16} genome. **A)** *Cx. tarsalis* midgut SINV_{5'dsMRE16} 7dpi. Positive/negative strand ratio is 51.6%/48.4%. **B)** *Cx. tarsalis* midgut SINV_{5'dsMRE16} 14dpi. Positive/negative strand ratio is 53.5%/46.5%. **C)** *Cx. tarsalis* carcass sans ovaries SINV_{5'dsMRE16} 7dpi. Positive/negative strand ratio is 64.4%/35.6%. **D)** *Cx. tarsalis* carcass sans ovaries SINV_{5'dsMRE16} 14dpi. Positive/negative strand ratio is 57.7%/42.3%.

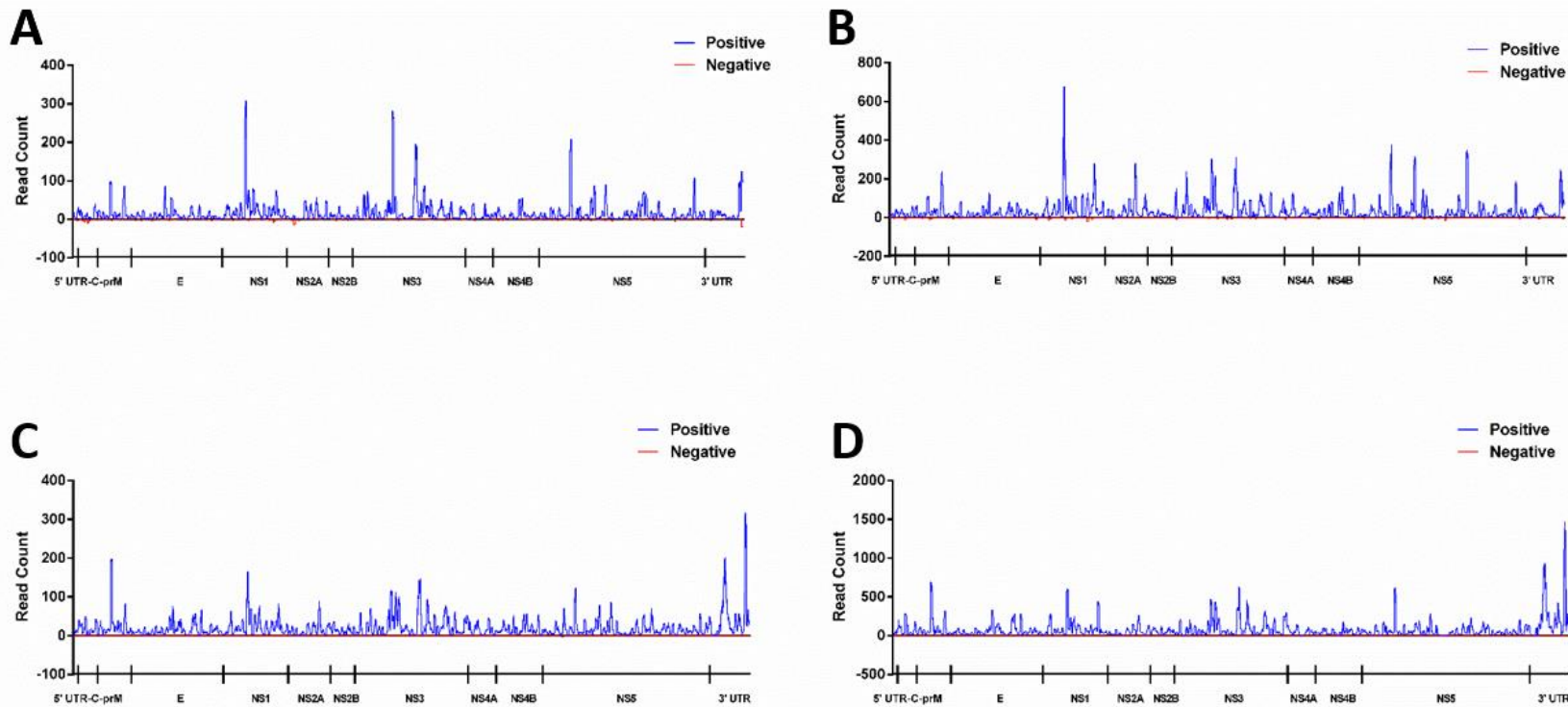


Figure 3.5: Distribution of 24-30 nt reads along the length of the WNV_{NY99} genome. **A)** *Cx. tarsalis* midgut WNV_{NY99} 7dpi. Positive/negative strand ratio is 96.1%/3.9%. This represents one of two experimental replicates; the second had a strand ratio of 98.9%/1.1%. **B)** *Cx. tarsalis* midgut WNV_{NY99} 14dpi. Positive/negative strand ratio is 96.8%/3.2%. **C)** *Cx. tarsalis* carcass sans ovaries WNV_{NY99} 7dpi. Positive/negative strand ratio is 99.4%/0.6%. **D)** *Cx. tarsalis* carcass sans ovaries WNV_{NY99} 14dpi. Positive/negative strand ratio is 99.8%/0.2%.

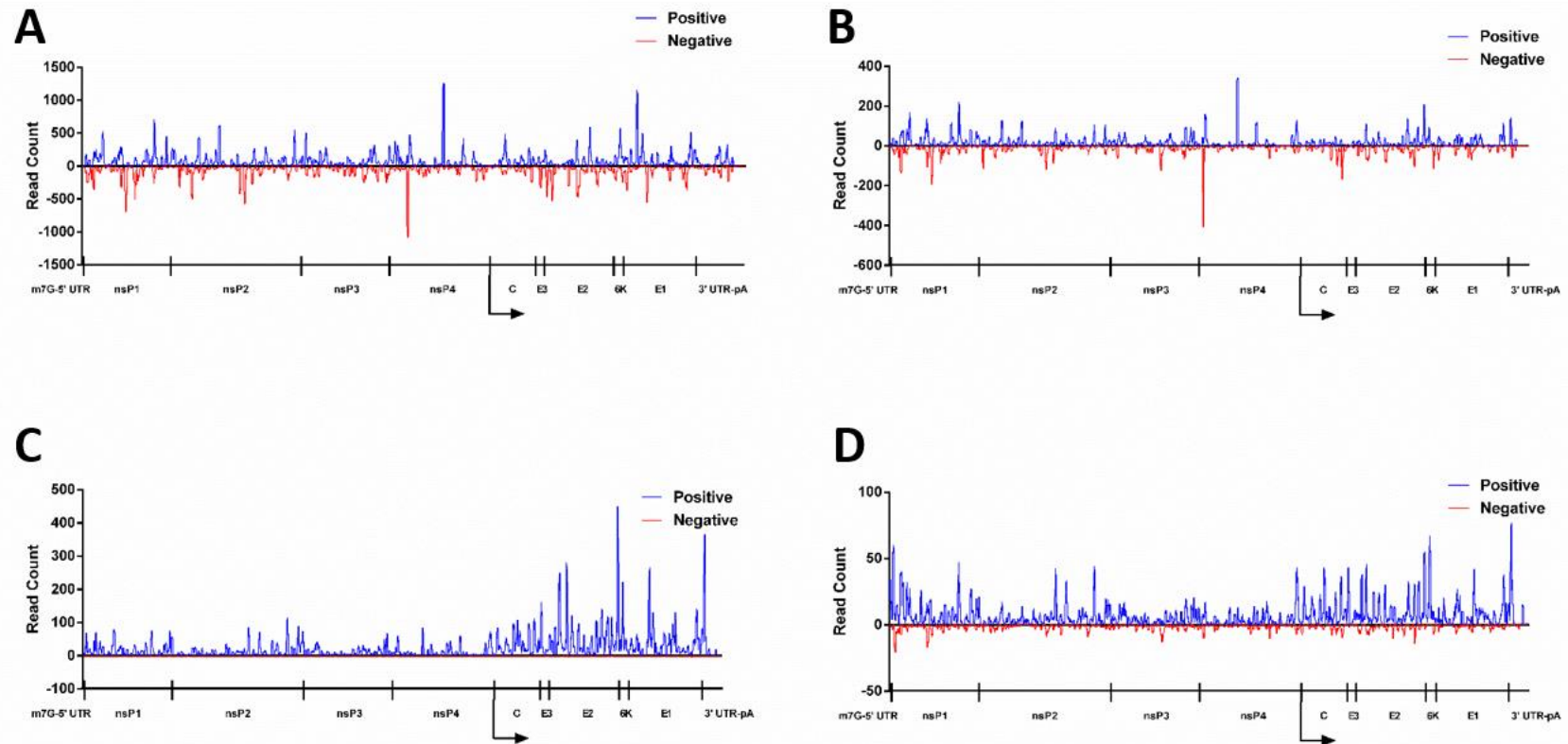


Figure 3.6: Distribution of 24-30 nt reads along the length of the WEEV_{Imp181} genome. **A)** *Cx. tarsalis* midgut WEEV_{Imp181} 7dpi. Positive/negative strand ratio is 55.7%/44.3%. This represents one of two experimental replicates; the second had a strand ratio of 54.2%/45.8%. **B)** *Cx. tarsalis* midgut WEEV_{Imp181} 14dpi. Positive/negative strand ratio is 57.0%/43.0%. This represents one of two experimental replicates; the second had a strand ratio of 51.0%/49.0%. **C)** *Cx. tarsalis* carcass sans ovaries WEEV_{Imp181} 7dpi. Positive/negative strand ratio is 98.2%/1.8%. **D)** *Cx. tarsalis* carcass sans ovaries WEEV_{Imp181} 14dpi. Positive/negative strand ratio is 81.4%/18.6%.

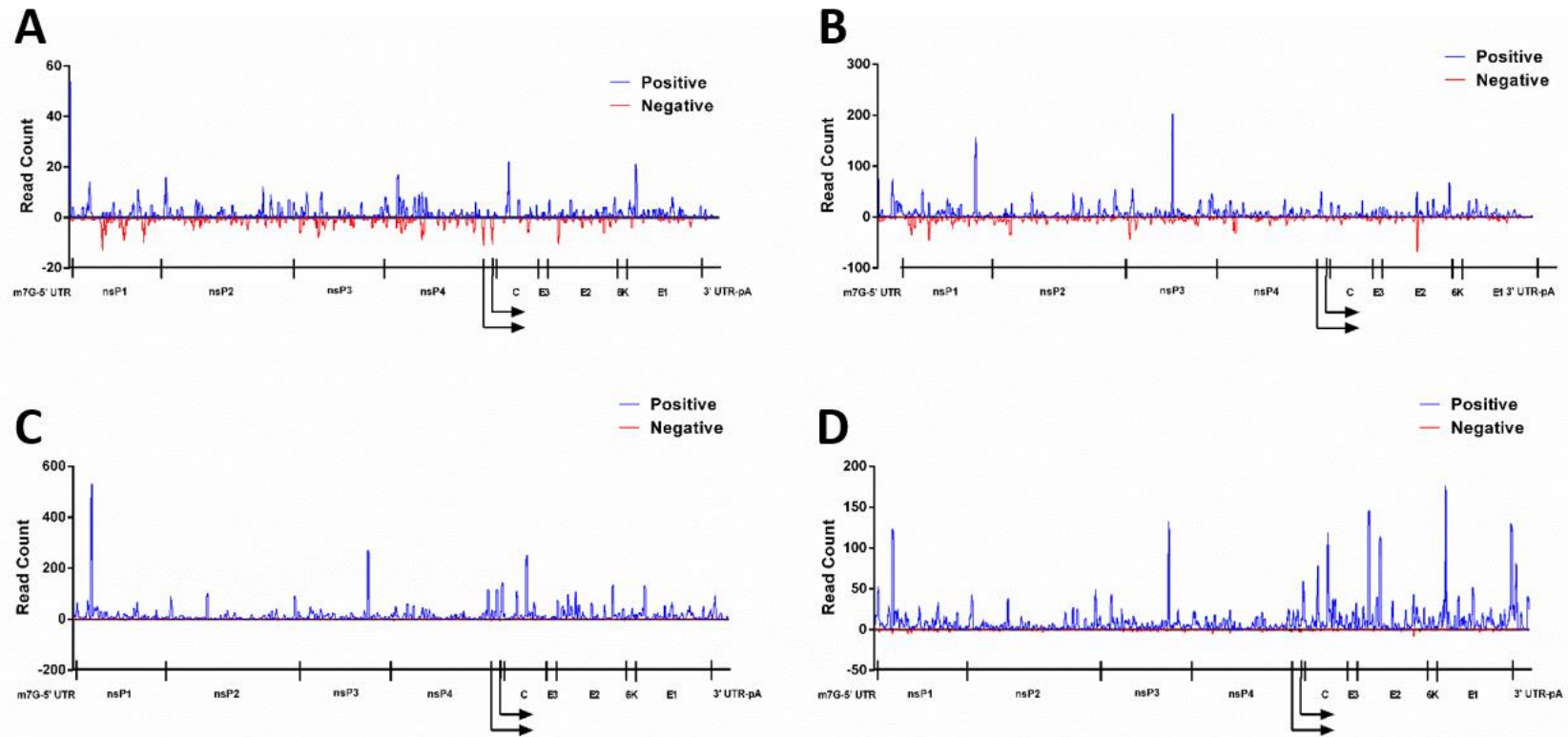


Figure 3.7: Distribution of 24-30 nt reads along the length of the SINV_{5'dsMRE16} genome. **A)** *Cx. tarsalis* midgut SINV_{5'dsMRE16} 7dpi. Positive/negative strand ratio is 63.9%/36.1%. **B)** *Cx. tarsalis* midgut SINV_{5'dsMRE16} 14dpi. Positive/negative strand ratio is 69.7%/30.3%. **C)** *Cx. tarsalis* carcass sans ovaries SINV_{5'dsMRE16} 7dpi. Positive/negative strand ratio is 97.1%/2.9%. **D)** *Cx. tarsalis* carcass sans ovaries SINV_{5'dsMRE16} 14dpi. Positive/negative strand ratio is 95.3%/4.7%.

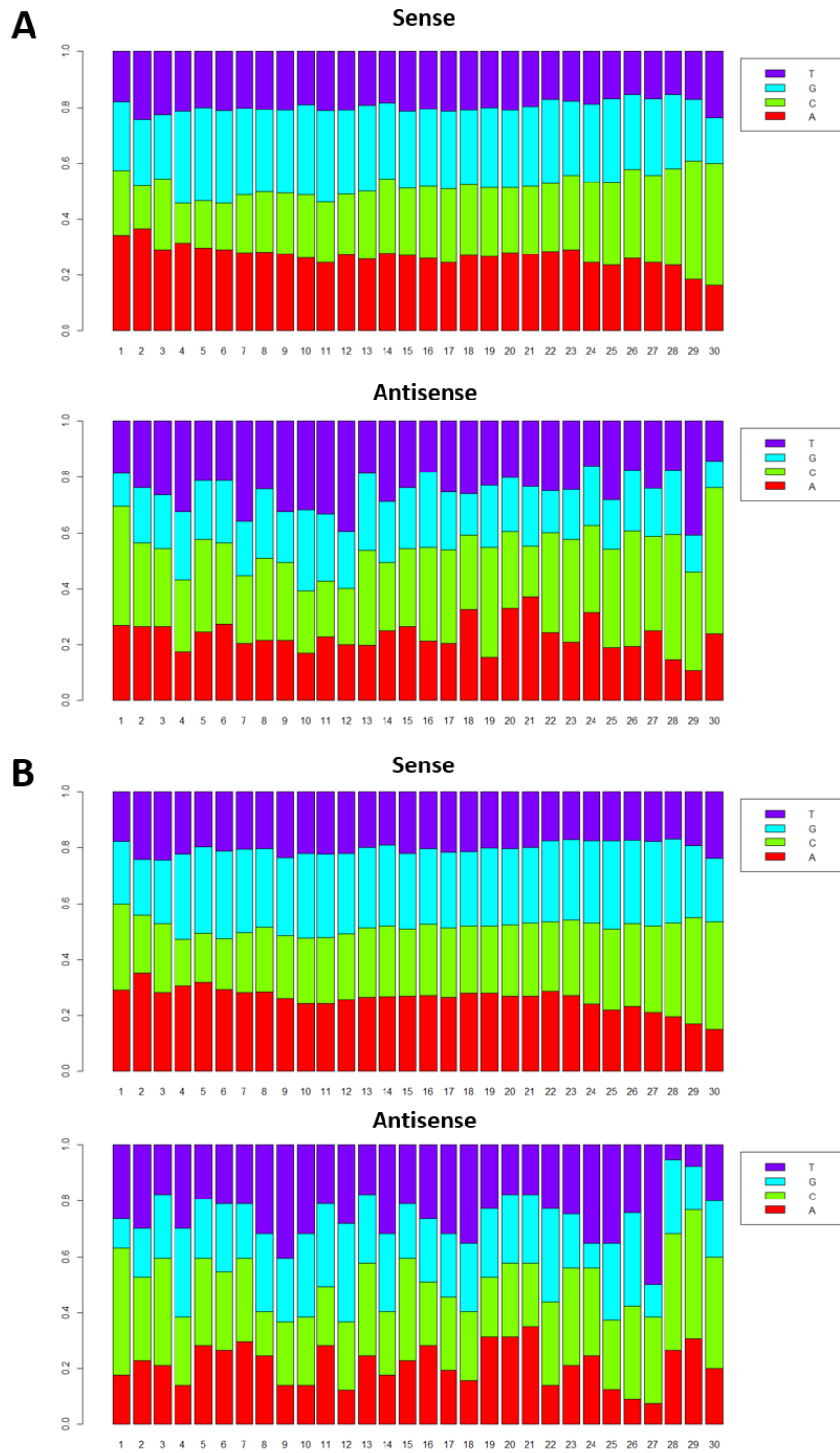


Figure 3.8: Barplot showing the relative frequencies of each nucleotide in the 24-30nt population of small RNAs from *Cx. tarsalis* WNV_{NY99}-infected midguts (A) and carcasses (B) 7dpi.

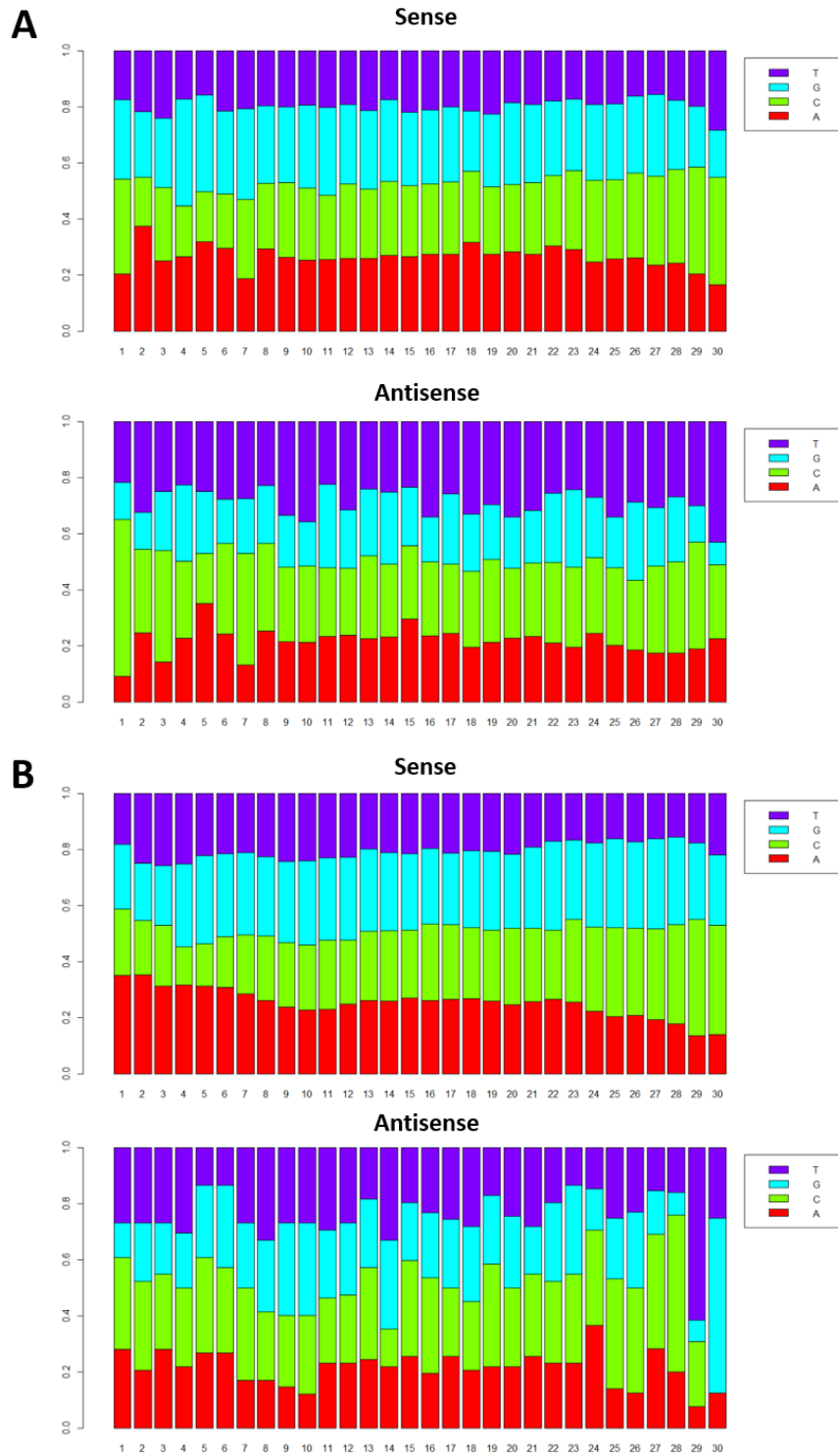


Figure 3.9: Barplot showing the relative frequencies of each nucleotide in the 24-30nt population of small RNAs from *Cx. tarsalis* WNV_{NY99}-infected midguts (A) and carcasses (B) 14dpi.

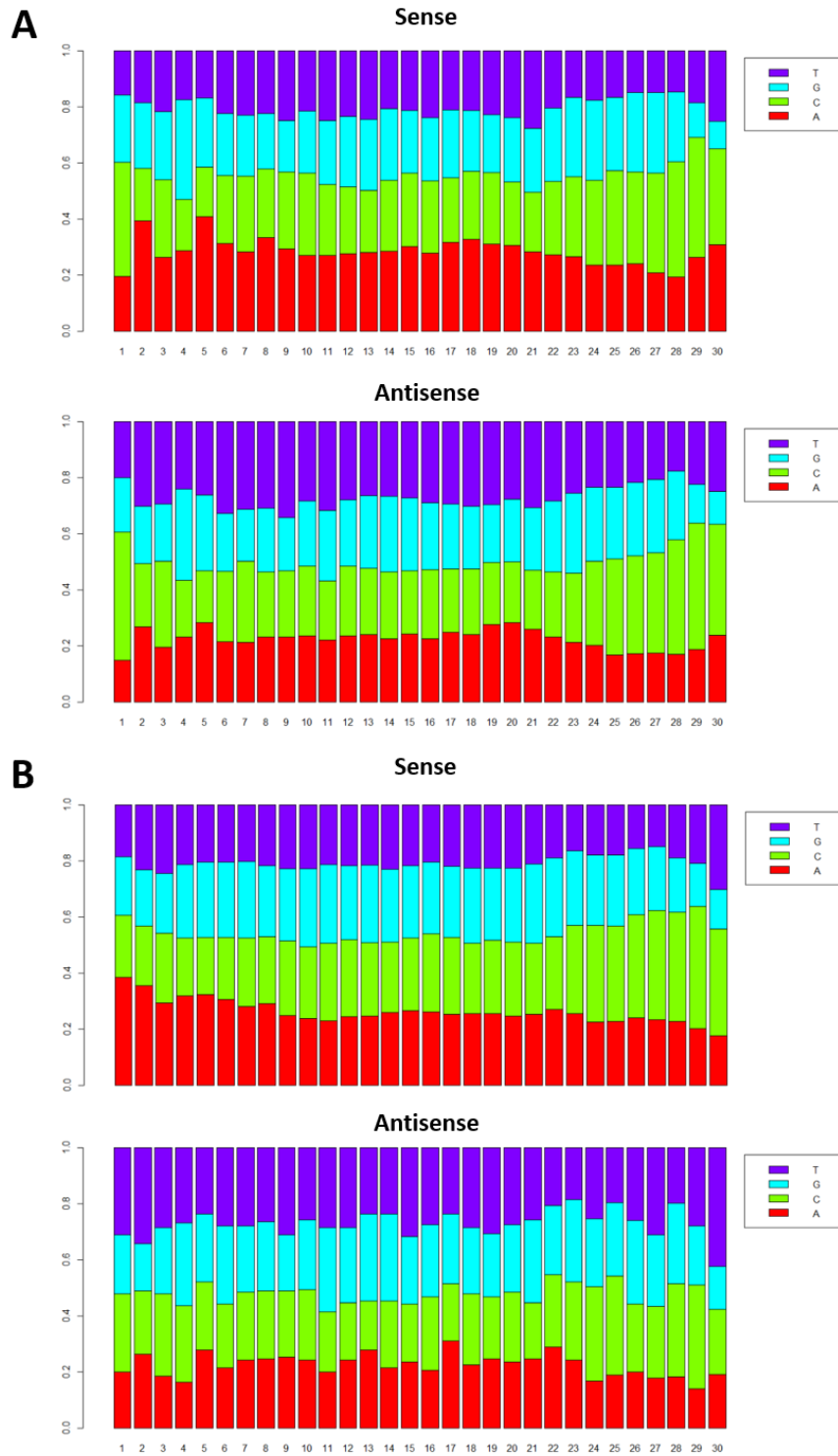


Figure 3.10: Barplot showing the relative frequencies of each nucleotide in the 24-30nt population of small RNAs from *Cx. tarsalis* WEEV₁₈₁-infected midguts (A) and carcasses (B) 7dpi.

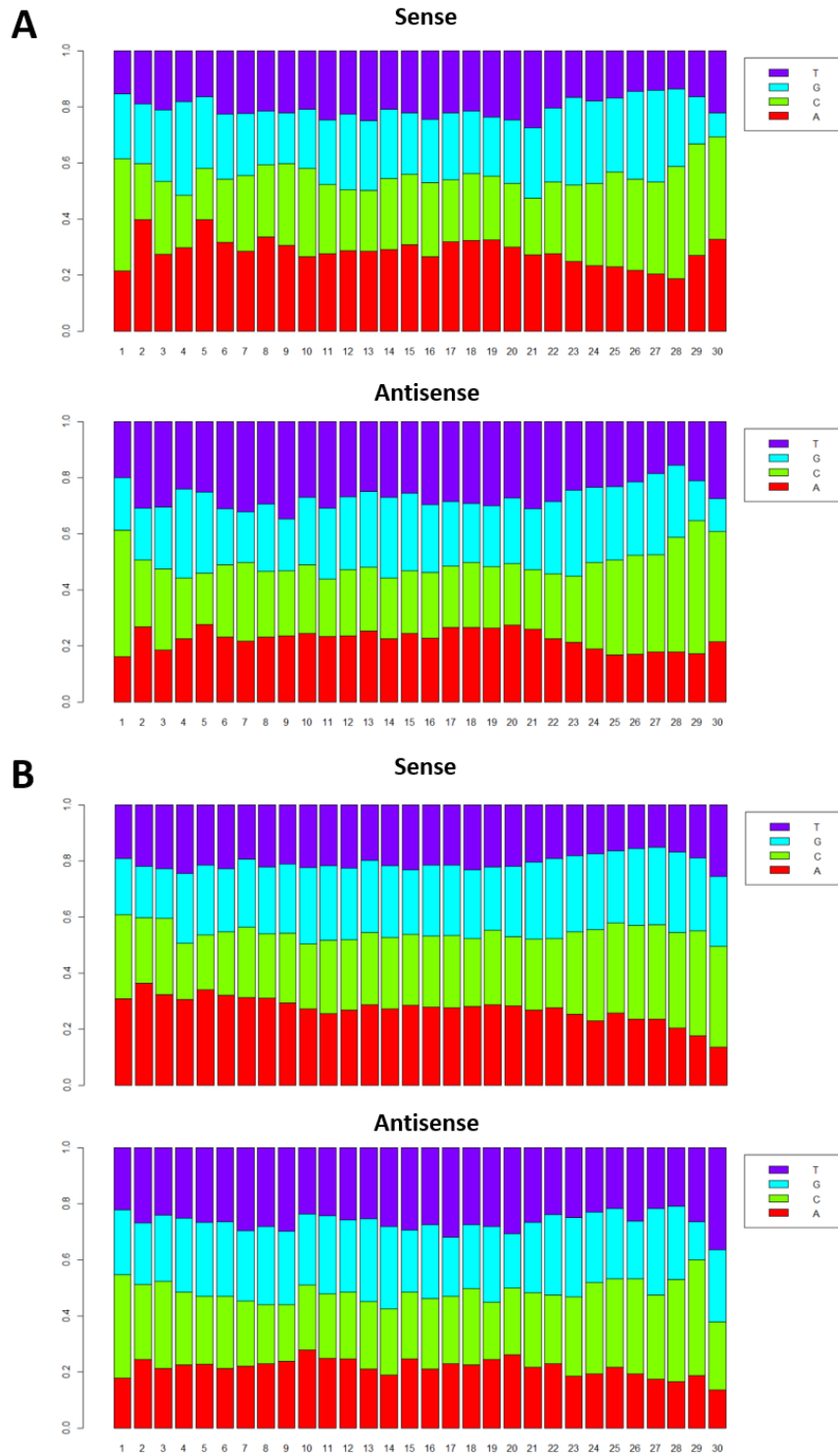


Figure 3.11: Barplot showing the relative frequencies of each nucleotide in the 24-30nt population of small RNAs from *Cx. tarsalis* WEEV_{imp181}-infected midguts (A) and carcasses (B) 7dpi.

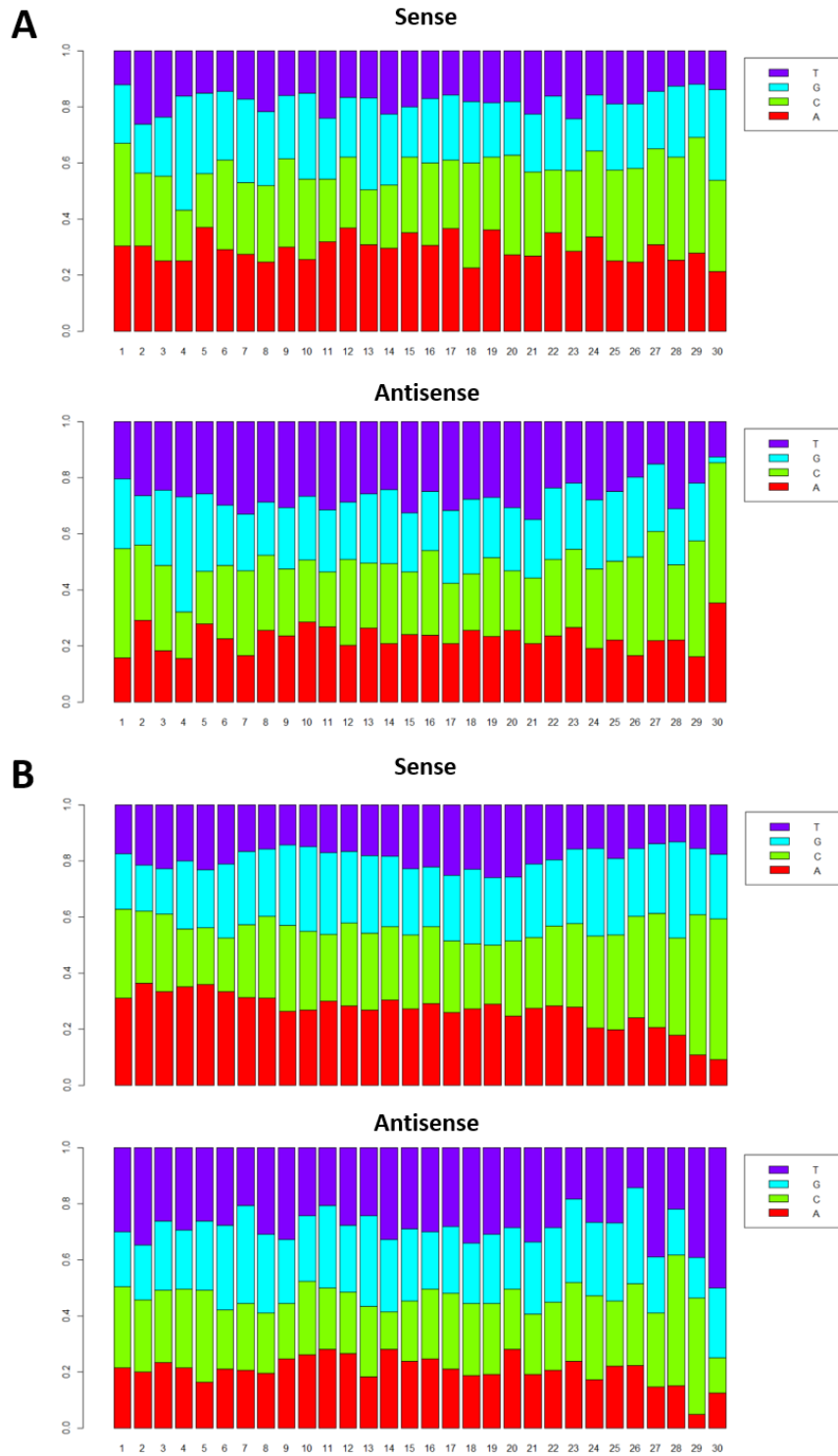


Figure 3.12: Barplot showing the relative frequencies of each nucleotide in the 24-30nt population of small RNAs from *Cx. tarsalis* SINV_{5'}^{dsMRE16}-infected midguts (A) and carcasses (B) 7dpi.

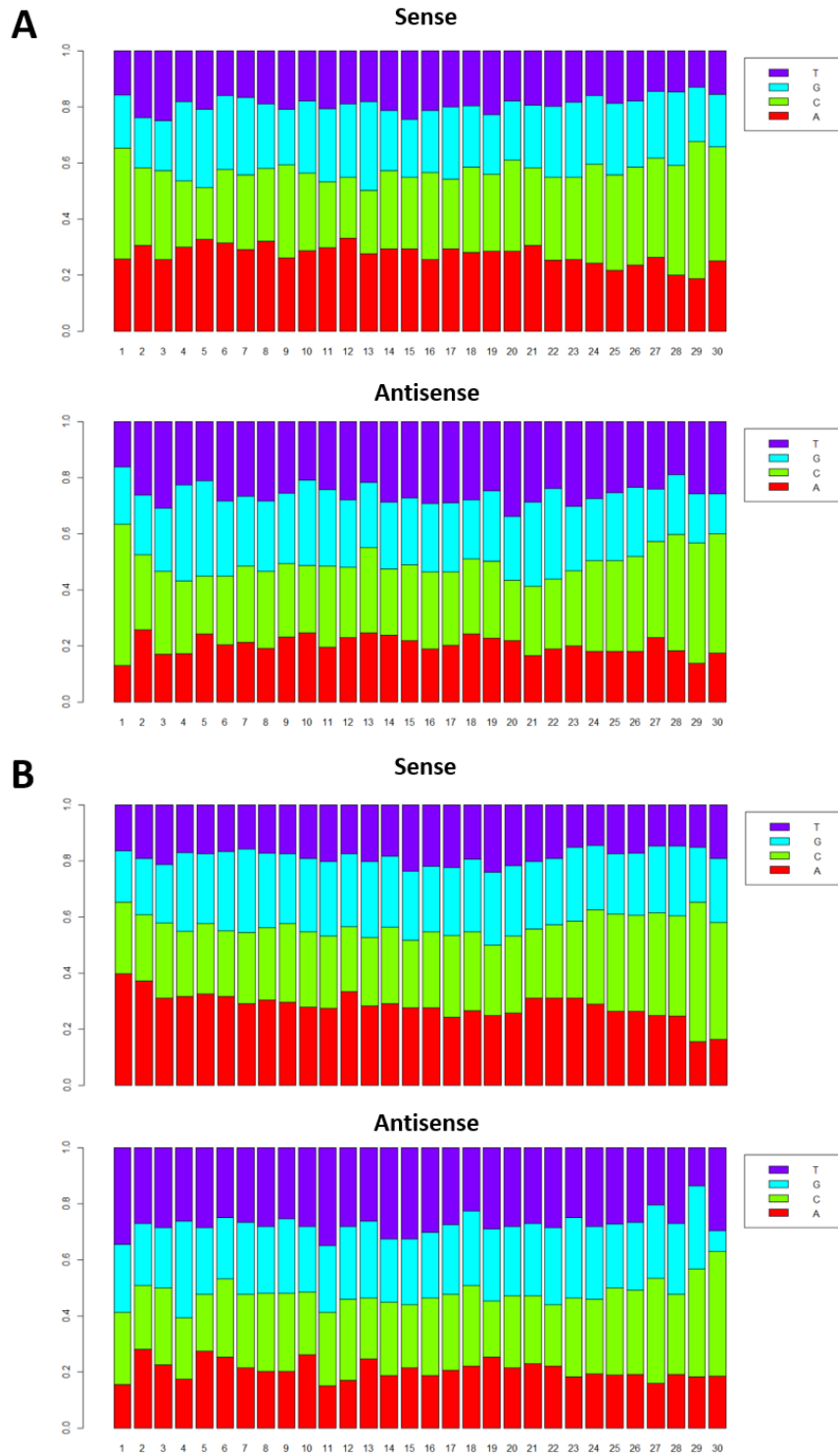


Figure 3.13: Barplot showing the relative frequencies of each nucleotide in the 24-30nt population of small RNAs from *Cx. tarsalis* SINV_{5'}^{dsMRE16}-infected midguts (A) and carcasses (B) 14dpi.

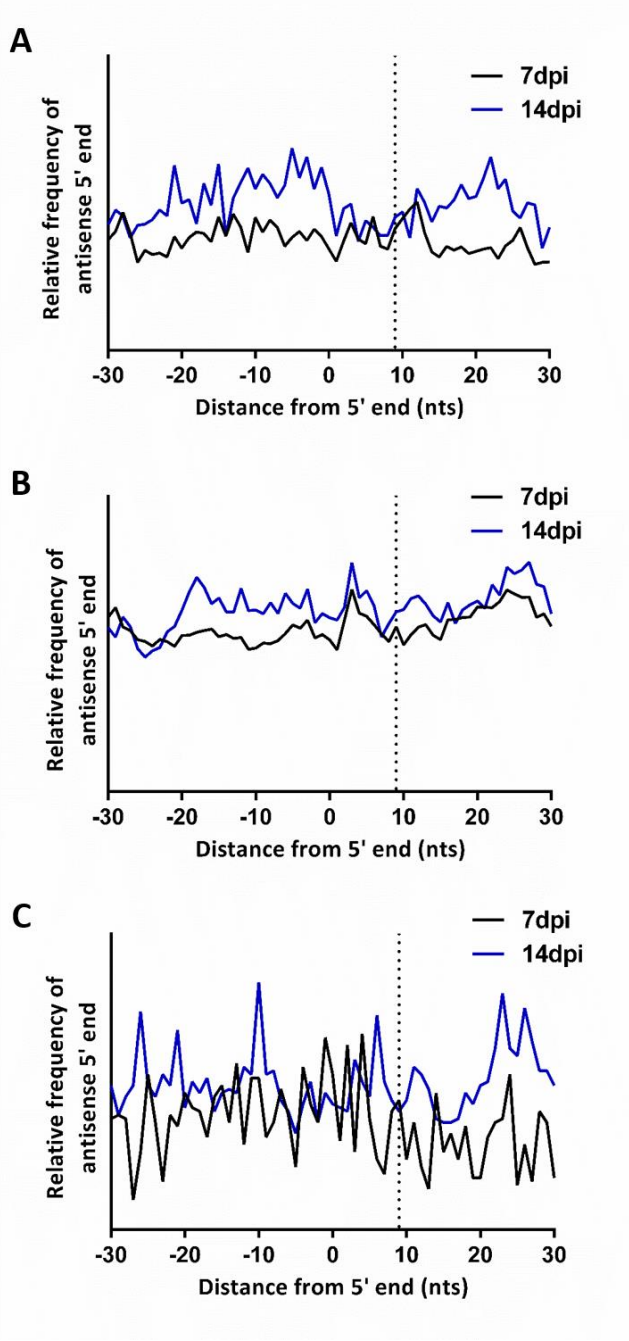


Figure 3.14: 5'-distance plots of 24-30nt reads mapping to opposite strands of the virus genome showing the relative frequency of finding the 5'-end of a complimentary small RNA. The dashed line at 9 nt indicates the position at which a peak would indicate a distance of 10 nt (the first nucleotide is at position 0), indicative of a ping-pong mechanism. **A)** *Cx. tarsalis* WNV_{NY99}-infected midguts, **B)** *Cx. tarsalis* WEEV_{Imp181}-infected midguts, **C)** *Cx. tarsalis* SINV_{5'dsMRE16}-infected midguts

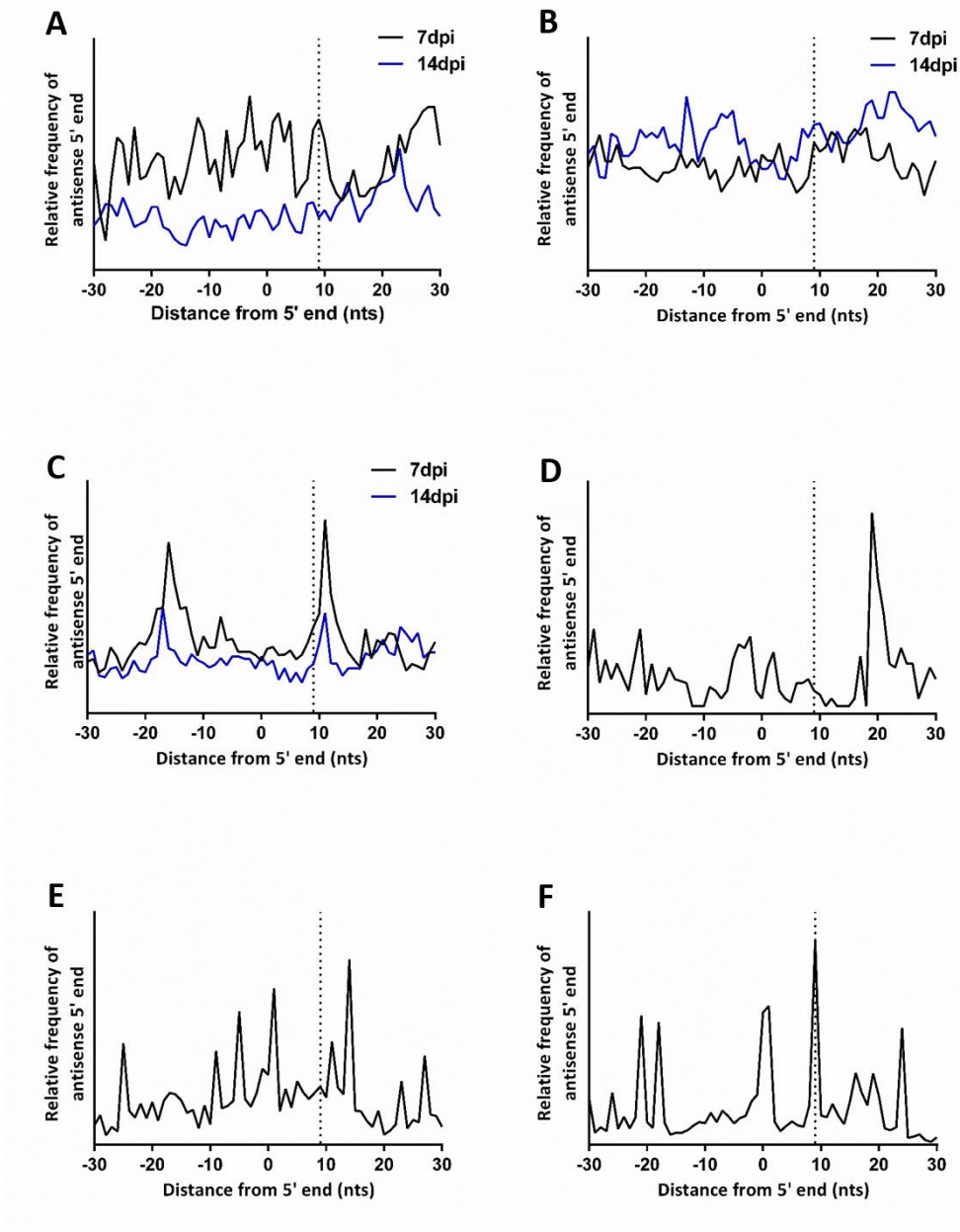


Figure 3.15: 5'-distance plots of 24-30nt reads mapping to opposite strands of the virus genome showing the relative frequency of finding the 5'-end of a complimentary small RNA. The dashed line at 9 nt indicates the position at which a peak would indicate a distance of 10 nt (the first nucleotide is at position 0), indicative of a ping-pong mechanism. **A)** *Cx. tarsalis* WNV_{NY99}-infected carcasses, **B)** *Cx. tarsalis* WEEV_{Imp181}-infected carcasses, **C)** *Cx. tarsalis* SINV_{5'}dsMRE16-infected carcasses, **D)** HWE *Ae. aegypti* WNV_{NY99}-infected whole mosquitoes 7dpi, **E)** Ubi61 *Ae. aegypti* WNV_{NY99}-infected whole mosquitoes 7dpi, **F)** *Ae. aegypti* SINV_{5'}dsMRE16-eGFP-infected whole mosquitoes 9dpi

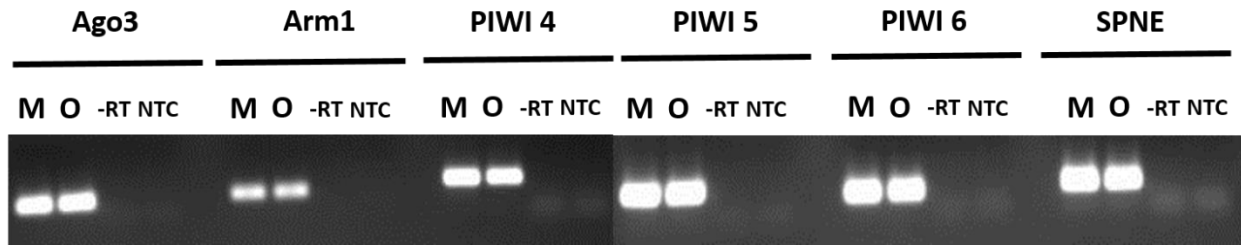


Figure 3.16: RT-PCR detection of 6 PIWI-component protein RNA transcripts in the midgut (M) and ovaries (O) of un-infected adult female *Cx. quinquefasciatus* mosquitoes. Reproductive tissue such as the ovaries are expected to be rich in piRNAs and component proteins, and were used as a positive control to compare against midgut detection. Reactions without reverse transcriptase (-RT) were used to exclude signal being a result of genomic DNA amplification. NTC= no template control.

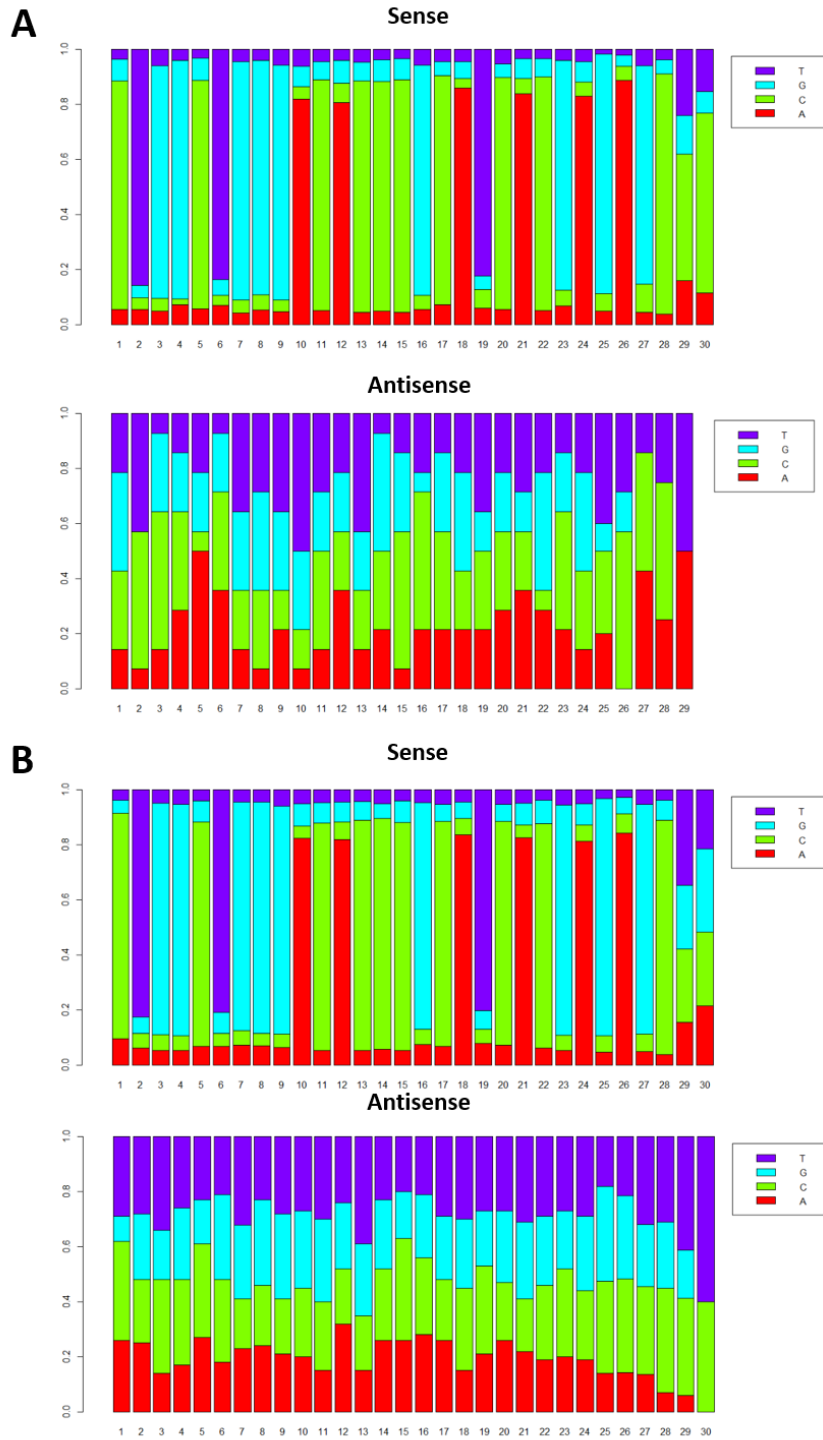


Figure 3.17: Barplot showing the relative frequencies of each nucleotide in the 24-30nt population of small RNAs from WNV_{NY99}-infected *Ae. aegypti* mosquitoes. **(A)** Rockefeller strain midguts 7dpi **(B)** HWE strain whole mosquitoes 7dpi. Data from Ubi61 mosquitoes not shown.

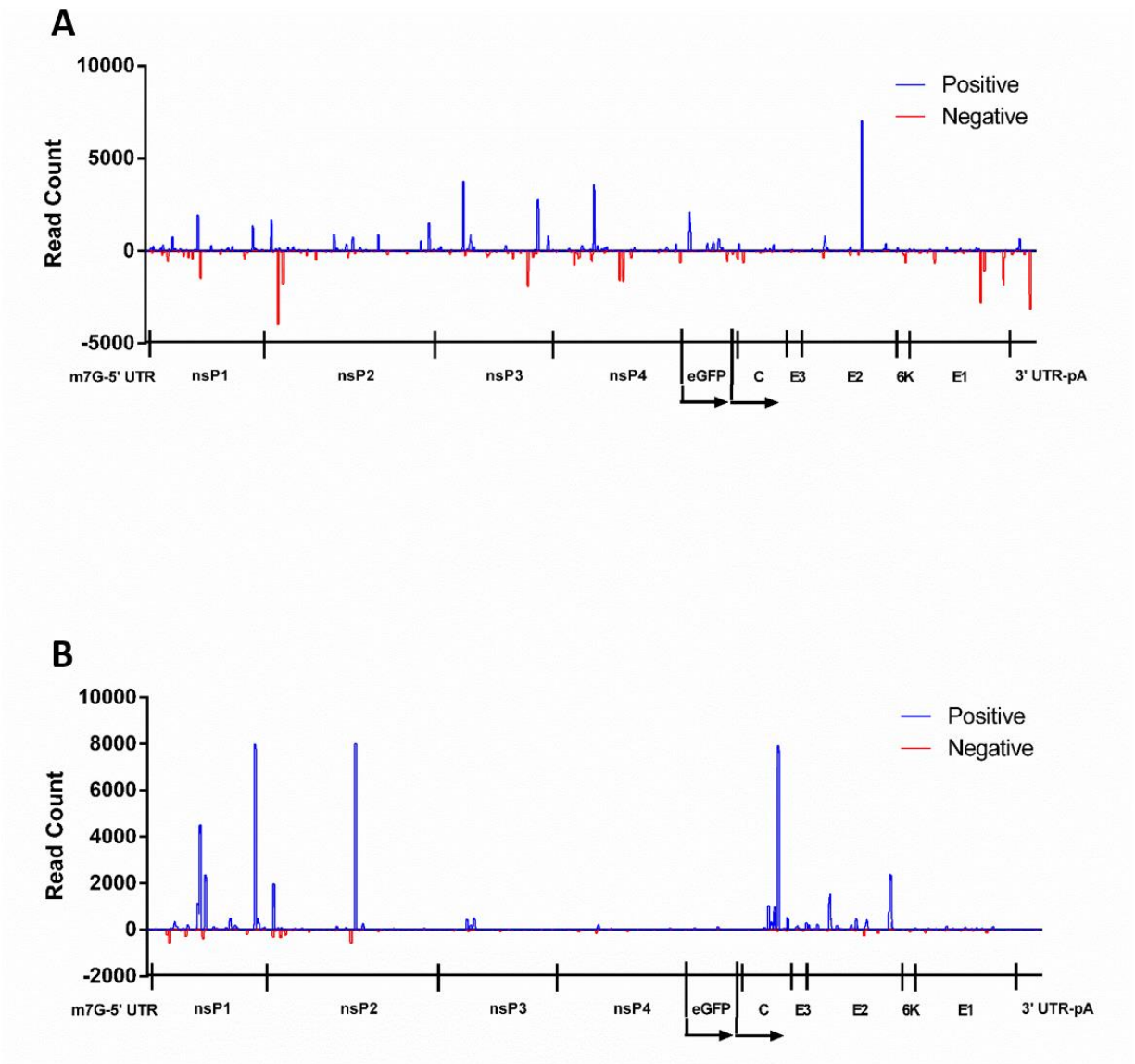


Figure 3.18: Distribution of reads along the length of the SINV_{5'dsMRE16-eGFP} genome. **A)** *Ae. aegypti* whole mosquitoes SINV_{5'dsMRE16} 9dpi 19-23 nt reads. Positive/negative strand ratio is 53.9%/46.1%. **B)** *Ae. aegypti* midgut SINV_{5'dsMRE16-eGFP} 9dpi 24-30 nt reads. Positive/negative strand ratio is 91.8%/8.2

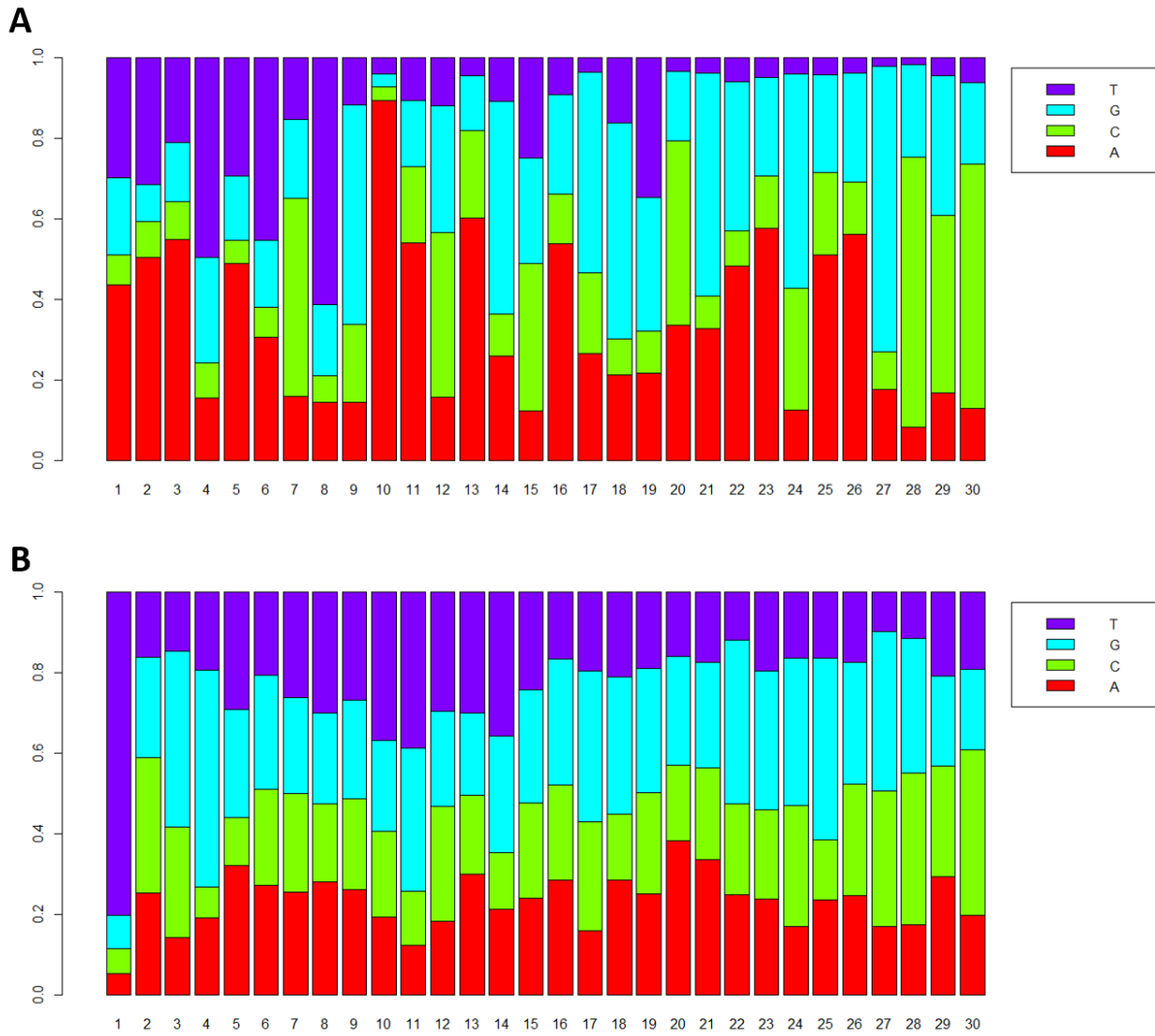


Figure 3.19: Barplot showing the relative frequencies of each nucleotide in the 24-30nt population of small RNAs from SINV_{5'}dsMRE16-eGFP-infected *Ae. aegypti* mosquitoes 9dpi.

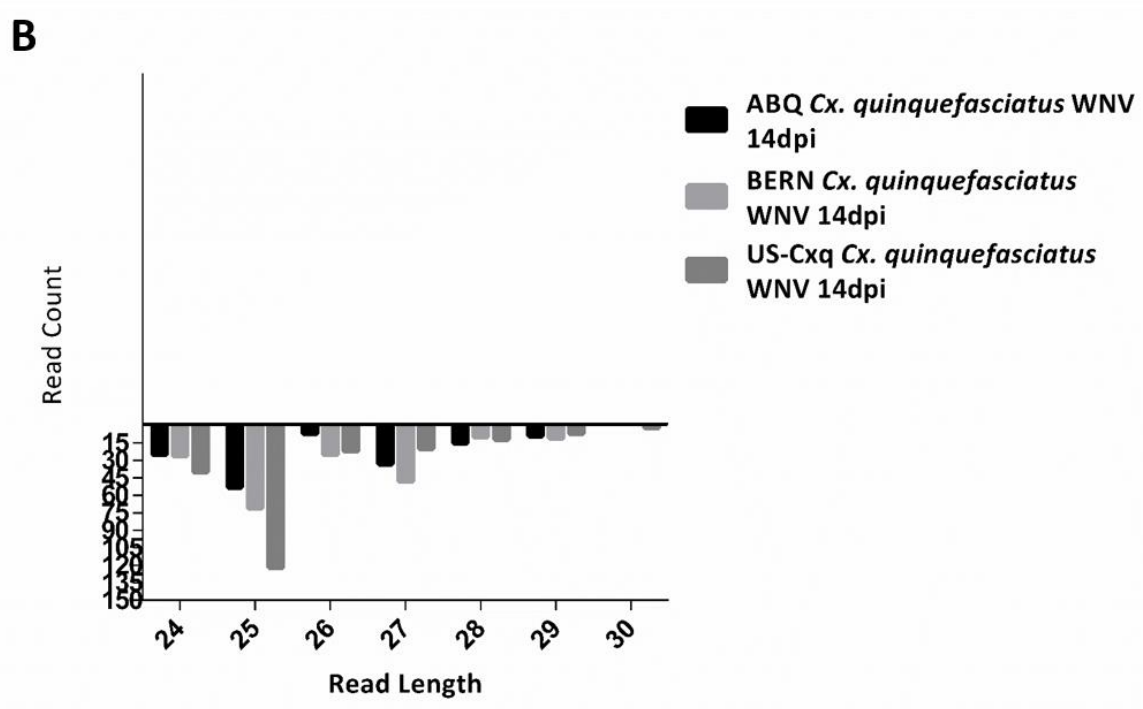
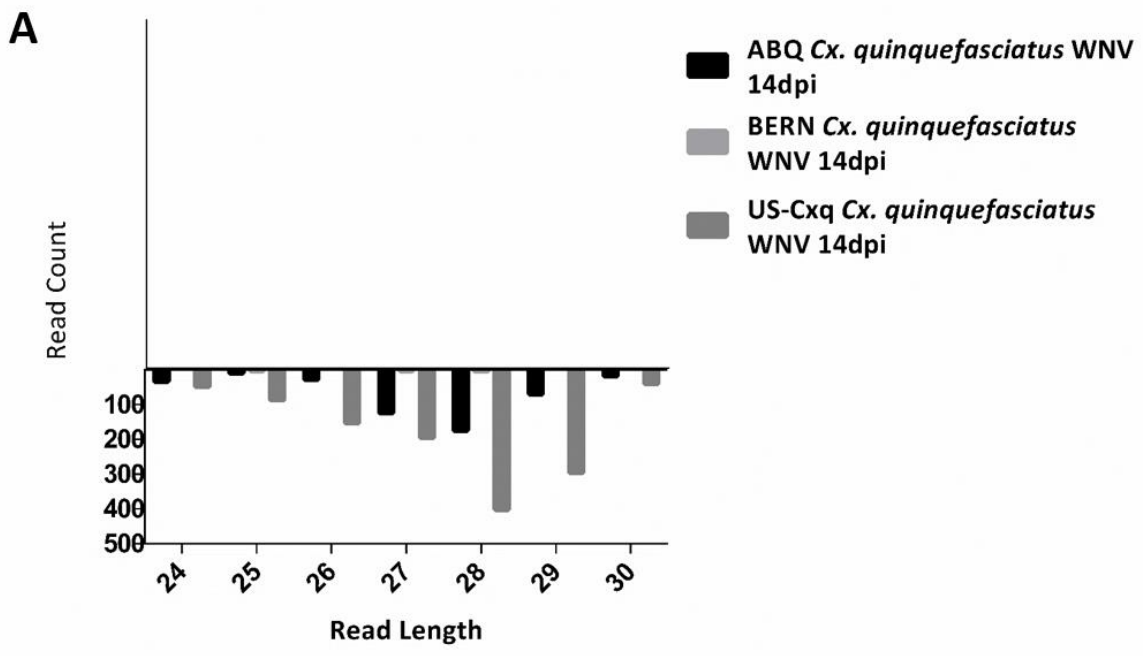


Figure 3.20: Read length distribution of reads aligning to LTR-rTE in *Cx. quinquefasciatus* mosquito midguts. **A)** Reads aligning to *CqGypsy-13*, **B)** Reads aligning to *CqGypsy-47*.

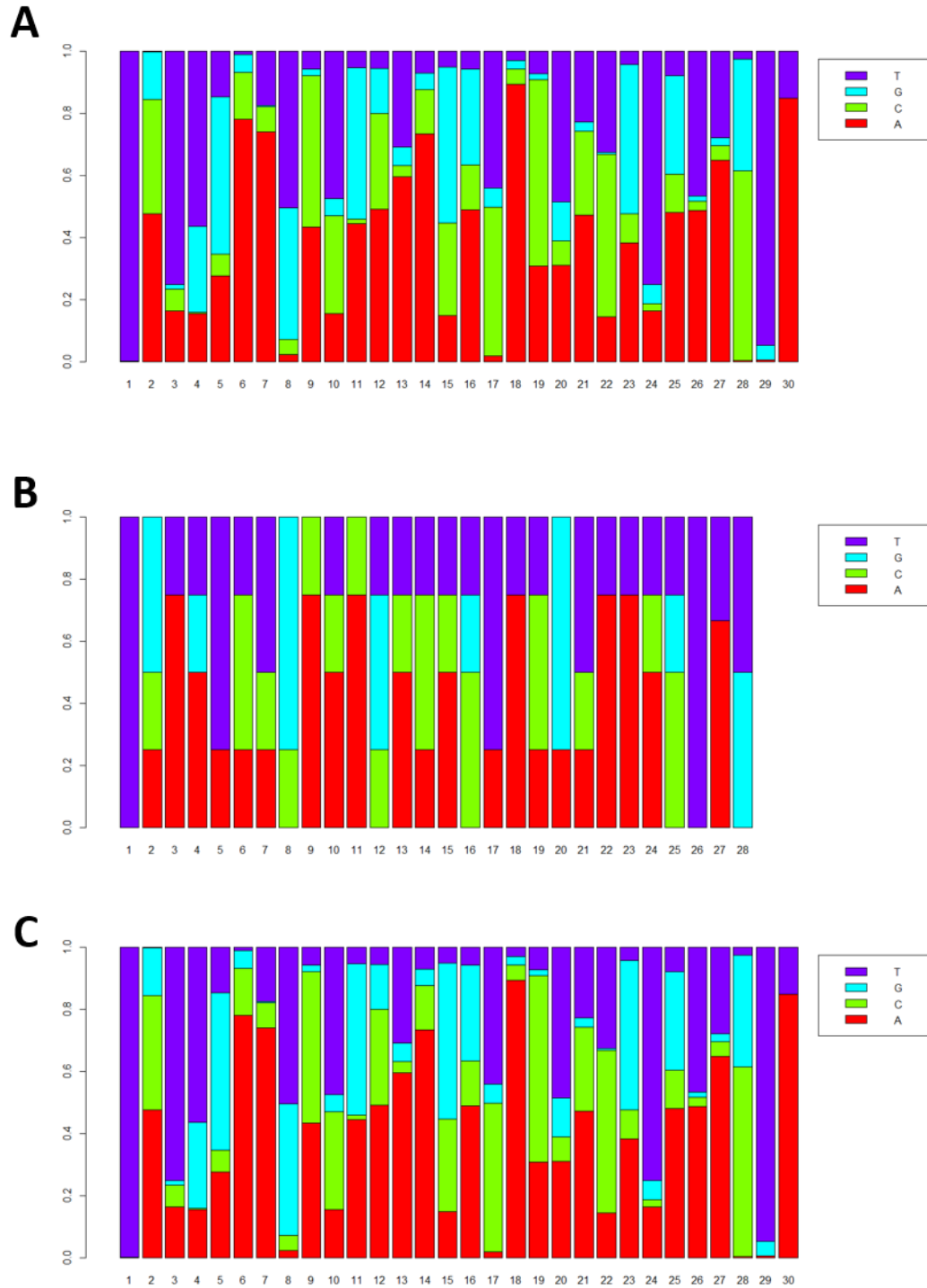


Figure 3.21: Barplot showing the relative frequencies of each nucleotide in 24-30 nt small RNAs mapping to the *CqGypsy-13* LTR-rTE. **A)** ABQ Cx. *quinquefasciatus* WNV 14dpi midgut, **B)** BERN Cx. *quinquefasciatus* WNV 14dpi midgut, **C)** Colonized US-Cxq Cx. *quinquefasciatus* WNV 14dpi midgut

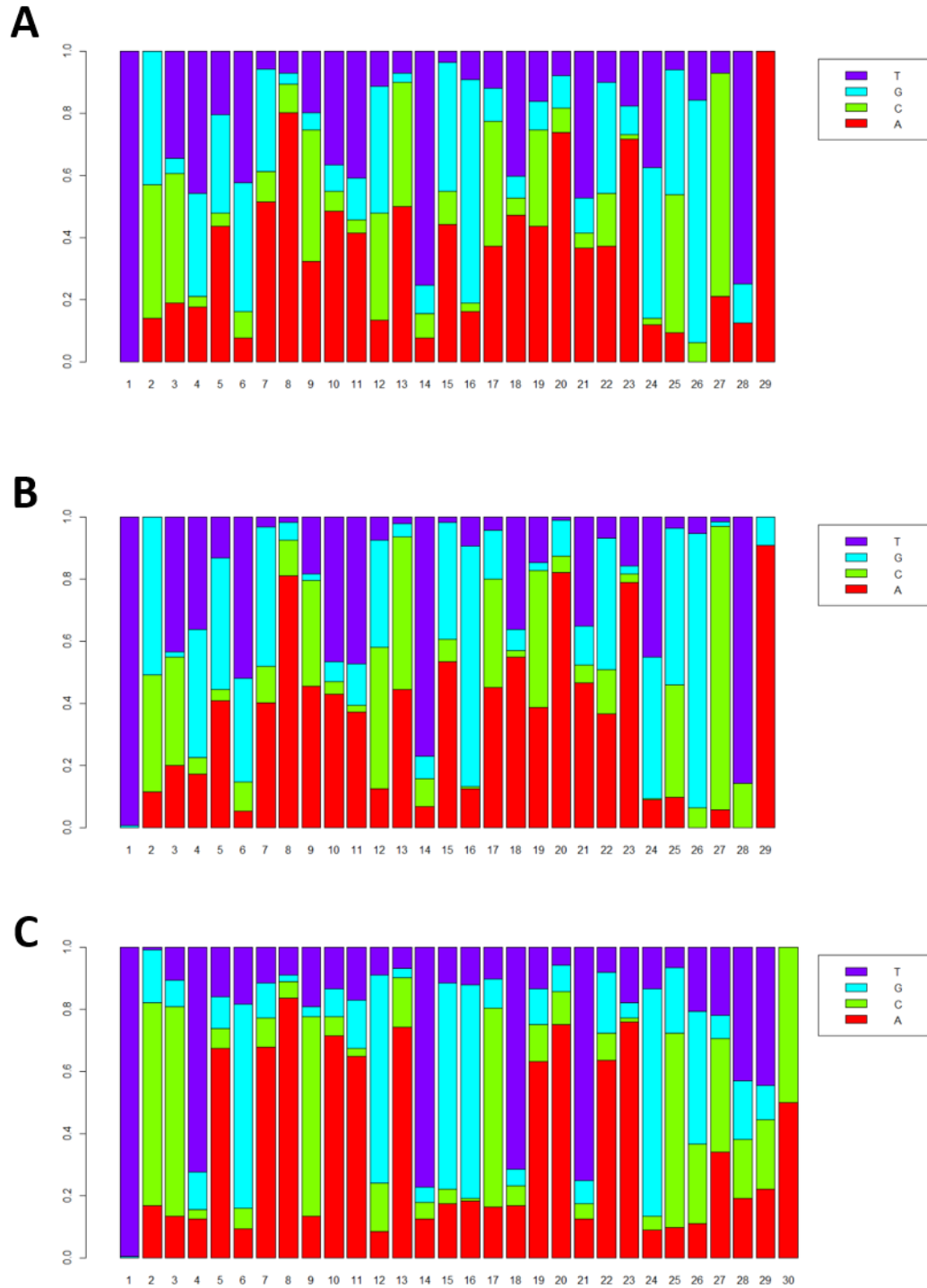


Figure 3.22: Barplot showing the relative frequencies of each nucleotide in 24-30 nt small RNAs mapping to the *CqGypsy-47* LTR-rTE. **A)** ABQ *Cx. quinquefasciatus* WNV 14dpi midgut, **B)** BERN *Cx. quinquefasciatus* WNV 14dpi midgut, **C)** Colonized US-Cxq *Cx. quinquefasciatus* WNV 14dpi midgut

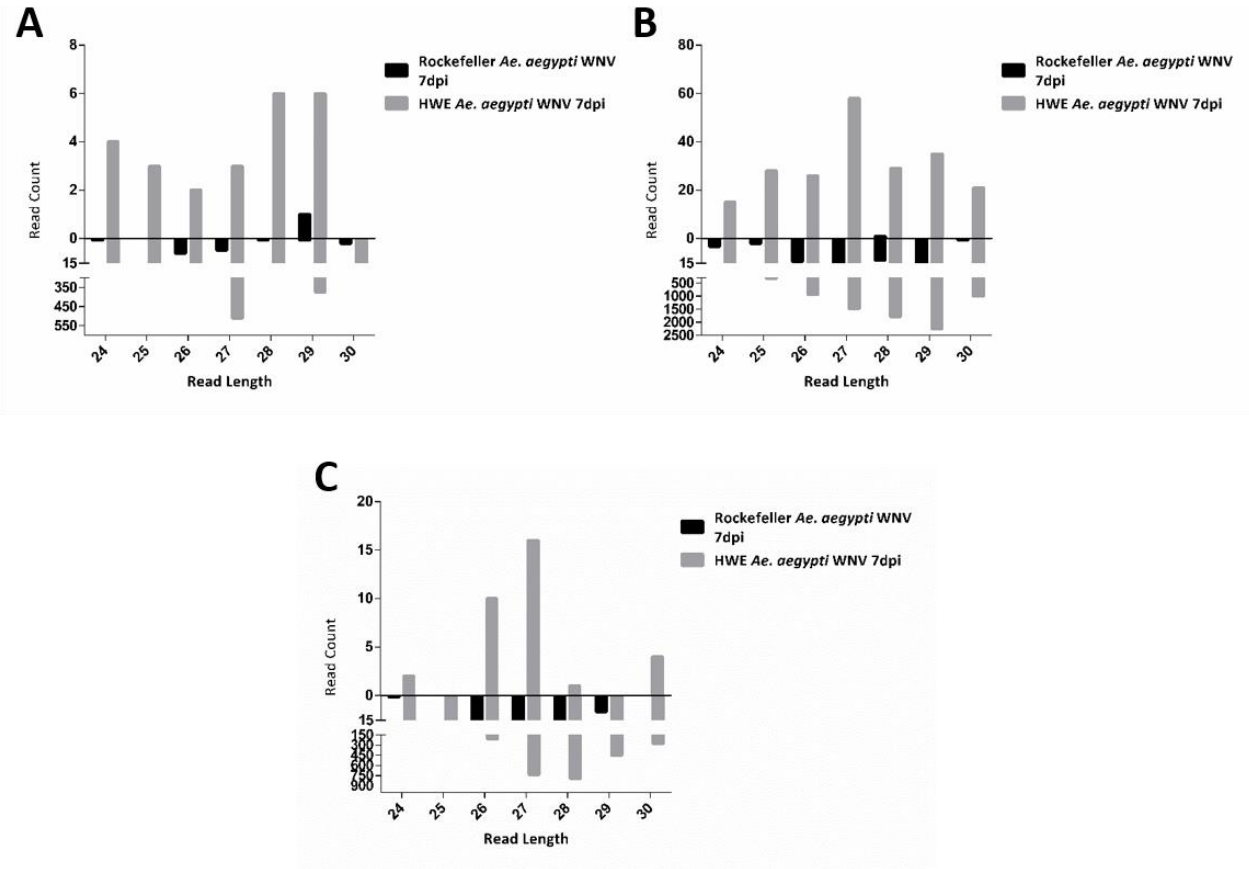


Figure 3.23: Read length distributions of reads aligning to LTR-rTE's in *Ae. aegypti* midguts (Rockefeller) and whole mosquitoes (HWE). **A)** Reads aligning to *Tyr3-Gypsy121*, **B)** Reads aligning to *Tyr3-Gypsy122*, **C)** Reads aligning to *Tyr3-Gypsy123*. Note the change in scale on the positive and negative portions of the y-axis.

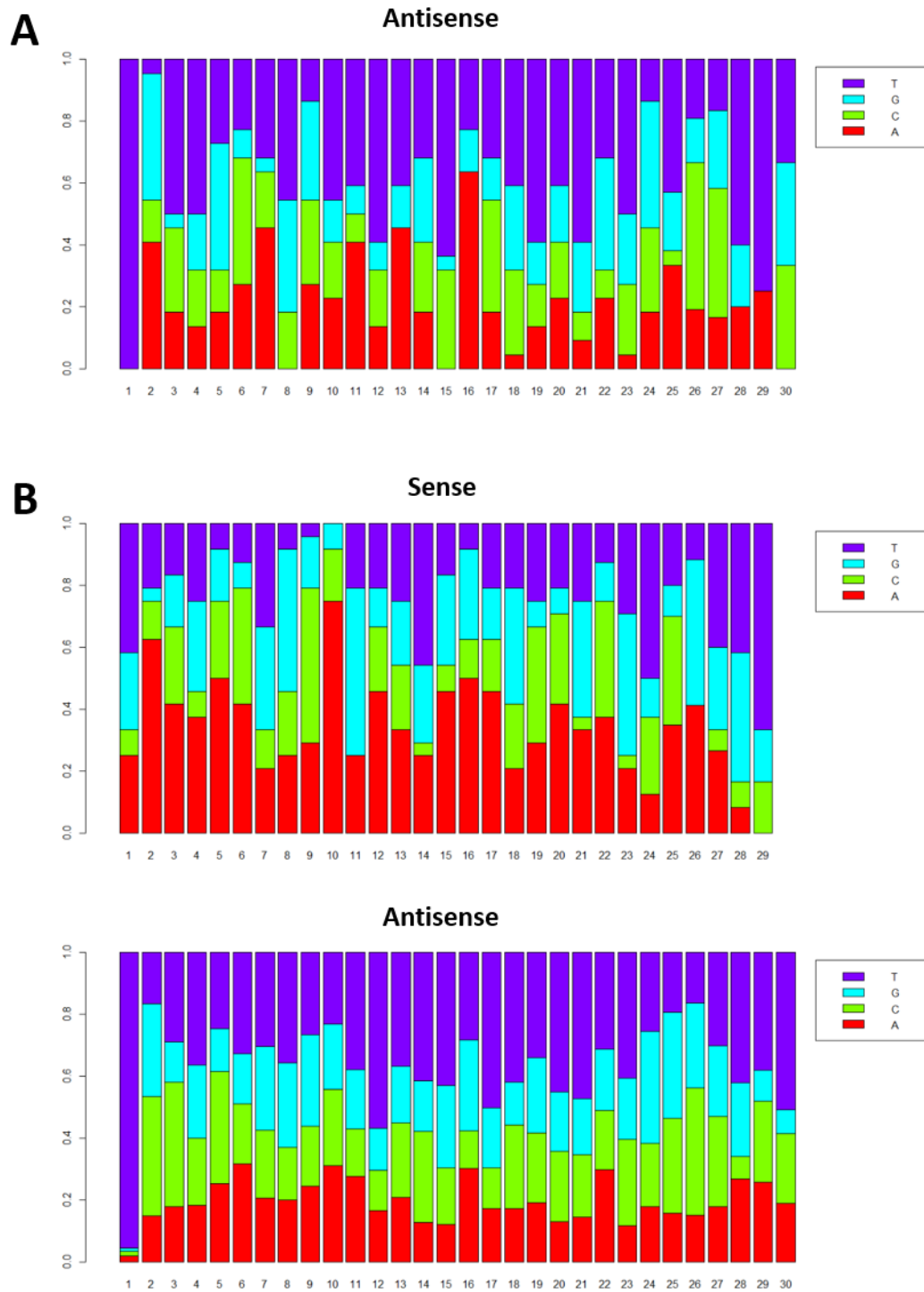


Figure 3.24: Barplot showing the relative frequencies of each nucleotide in 24-30 nt small RNAs mapping to the *Tyr3-Gypsy121* LTR-rTE in *Ae. aegypti*. **A)** Rockefeller *Ae. aegypti* WNV 7dpi midgut reads mapping to antisense strand **B)** HWE *Ae. aegypti* WNV 7dpi whole mosquito reads

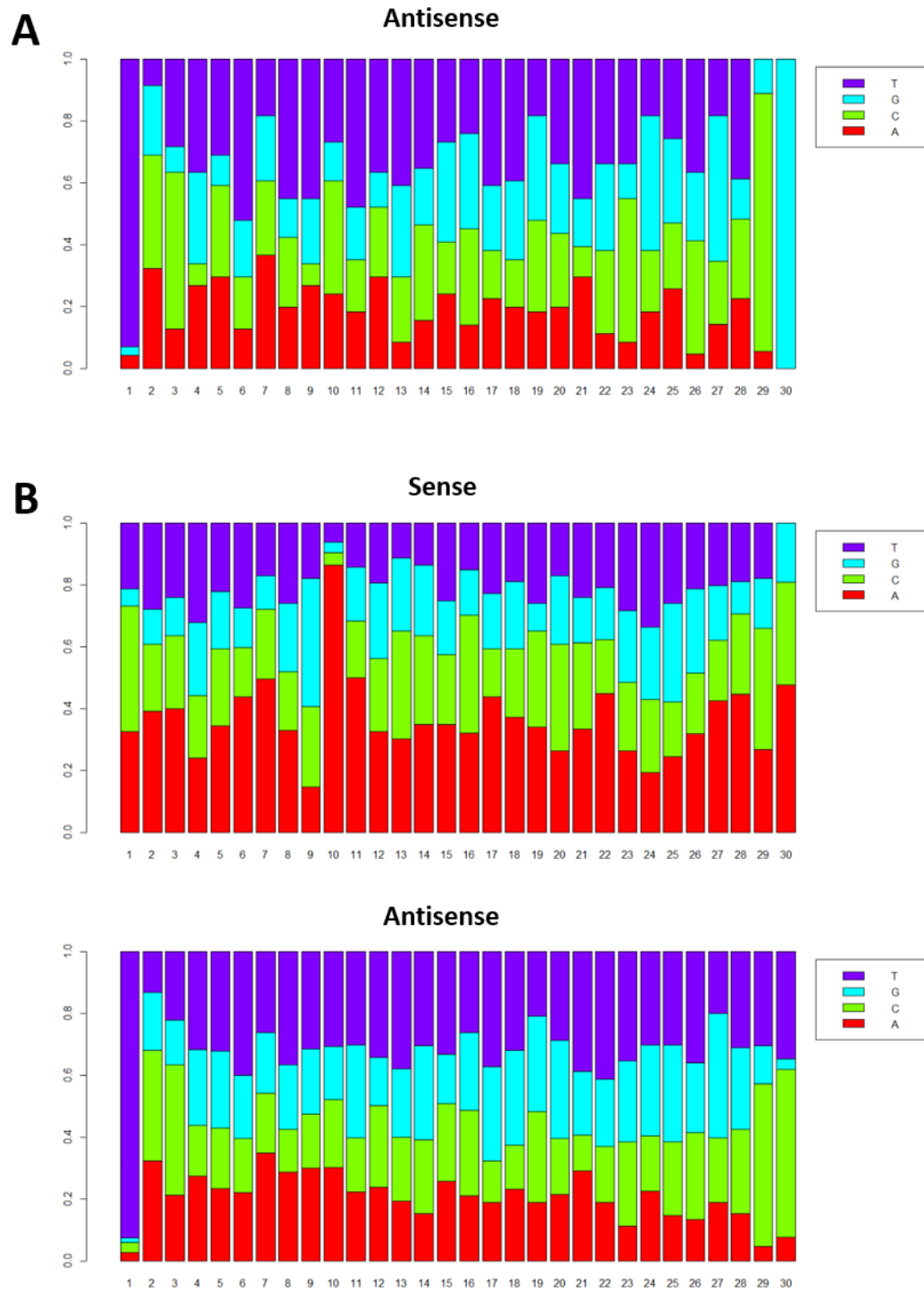


Figure 3.25: Barplot showing the relative frequencies of each nucleotide in 24-30 nt small RNAs mapping to the *Tyr3-Gypsy122* LTR-rTE in *Ae. aegypti*. **A)** Rockefeller *Ae. aegypti* WNV 7dpi midgut reads mapping to antisense strand **B)** HWE *Ae. aeavpti* WNV 7dpi whole mosquito reads

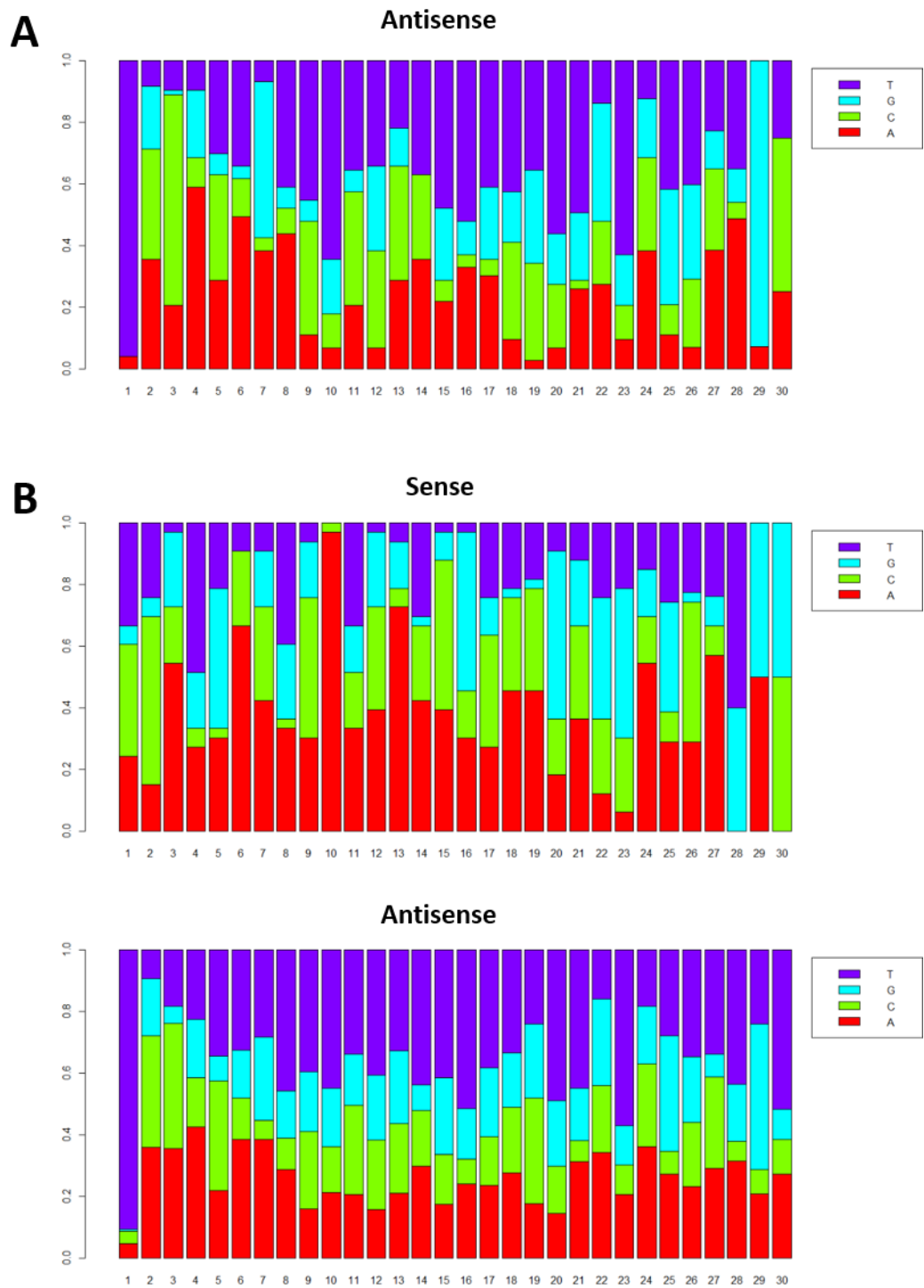


Figure 3.26: Barplot showing the relative frequencies of each nucleotide in 24-30 nt small RNAs mapping to the *Tyr3-Gypsy123* LTR-rTE in *Ae. aegypti*. **A)** Rockefeller *Ae. aegypti* WNV 7dpi midgut reads mapping to antisense strand **B)** HWE *Ae. aegypti* WNV 7dpi whole mosquito reads

Table 3.2: Summary of studies profiling the small RNA response in mosquitoes and mosquito cells to different virus infections. “Yes” indicates a ping-pong dependent piRNA response was found, “No” indicates signatures of a ping-pong dependent mechanism were not found or that incomplete features were found (such as the bias for one nucleotide being present but not the other). ¹This study, ²Brackney et al 2010 *PLoS Neglected Tropical Diseases*, ³Hess et al 2011 *BMC Microbiology*, ⁴Vodovar et al 2012 *PLoS ONE*, ⁵Morazzani et al 2012 *PLoS Pathogens*, ⁶Schnettler et al 2013 *Journal of General Virology*, ⁷Léger et al 2013 *Journal of Virology*, ⁸Scott et al 2010 *PLoS Neglected Tropical Diseases*, ⁹Schnettler et al 2012 *Journal of Virology*. Abbreviations: WNV=West Nile virus, DENV= dengue virus, WEEV= Western equine encephalitis virus, SINV= Sindbis virus, CHIKV= chikungunya virus, SFV= Semliki Forest virus, LACV= La Crosse virus, RVFV= Rift Valley fever virus, SBV= Schmallenberg virus, BTV= blue-tongue virus.

	WNV	DENV	WEEV	SINV	CHIKV	SFV	LACV	RVFV	SBV	BTV
<i>Cx. quinquefasciatus</i>	No ¹	-	-	-	-	-	-	-	-	-
<i>Cx. pipiens</i>	No ¹	-	-	-	-	-	-	-	-	-
<i>Cx. tarsalis</i>	No ¹	-	No ¹	No ¹	-	-	-	-	-	-
<i>Ae. aegypti</i>	No ¹	No ^{3,8}	-	Yes ¹	Yes ⁵	-	-	-	-	-
<i>Ae. albopictus</i>	-	-	-	-	Yes ⁵	-	-	-	-	-
C6/36	No ²	No ⁸	-	Yes ⁴	Yes ⁵	-	Yes ⁴	Yes ⁷	-	-
U4.4	-	-	-	Yes ⁴	Yes ⁵	Yes ⁶	-	Yes ⁷	-	-
Aag2	-	No ⁸	-	-	-	Yes ⁶	-	Yes ⁷	Yes ⁹	No ⁹

**Chapter 4: Small RNA Response of *Culex quinquefasciatus* to West Nile Virus Infection:
Relationship to Vector Competence**

Introduction

Arboviruses perpetuate in nature through alternating replication in two hosts: the invertebrate arthropod host (vector), and the vertebrate host (avian, mammalian, reptilian). Thus, arboviruses must overcome distinct physical and immunological challenges within these disparate hosts or become extinct. It has long been appreciated that different mosquito species, populations within a single species, and individuals within populations vary considerably in their ability to transmit pathogens. The likelihood that a given arthropod is susceptible to infection by a given agent, can support its replication within and dissemination from the midgut (first site of infection) and secondary tissues, and eventually release the agent into saliva is known as “vector competence.” Vector competence is influenced by both intrinsic (e.g. genetics) and extrinsic (diet, temperature) factors [124]. Barriers to infection, dissemination, and transmission, such as the midgut infection barrier (MIB) [200], midgut escape barrier (MEB) [201], salivary gland infection barrier (SIB) [202], and salivary gland escape barrier (SEB) [203] play important roles in defining the infection phenotype and thus the vector competence of the mosquito. Vector competence is a component of vectorial capacity (VC), a calculation of a mosquito population’s capacity to transmit a given pathogen to a naïve population [124].

The impact of RNA interference (RNAi) on arbovirus transmission in nature remains the subject of intensive investigation. The exogenous small-interfering RNA (exo-siRNA) pathway is

the main innate immune pathway responsible for controlling virus infection in mosquitoes [383]. Although it is clear that the exo-siRNA pathway can protect mosquitoes from lethal virus infection [388], and that mosquitoes engineered to express short viral RNA sequences either by transgenesis or co-infection with a heterologous recombinant virus are resistant to infection and/or incapable of transmitting virus [387, 18, 20, 385, 386], the role of RNAi in determining vector competence under natural conditions is unclear. A primary component of the siRNA pathway, *Dcr-2*, has been shown to be undergoing rapid diversifying evolution in *Aedes aegypti* [407], and polymorphisms in this gene correlate with differences in vector competence to DENV among populations of this species [407, 408]. However, it is unknown what phenotypic effect polymorphisms in *Dcr-2* may impart on the activity of the enzyme, nor how this affects the functionality and/or efficacy of the siRNA pathway. In addition, little is known about how the antiviral RNAi response in mosquitoes changes temporally during arbovirus infection, and how early this response is induced after imbibing an infectious bloodmeal. In *Ae. aegypti*, viRNAs derived from DENV-2 have been observed as early as 2 dpi, and the profile of the total viral-derived small RNA population (i.e. genome targeting, strand bias, proportion of small RNA size classes) changes over time from 2 dpi to 9 dpi [315]. Moreover, the impact of RNAi on arbovirus transmission remains obscure.

Accordingly, we sought to define how the exo-siRNA pathway shapes the vector competence phenotype in mosquitoes and to determine whether the exo-siRNA pathway appears to be activated early during arbovirus infection when it may impact mosquito vector competence. Vector competence is a quantitative genetic trait under the control of several genomic loci which collectively account for a relatively small proportion of the observed

variation in vector competence phenotypes [426-428]. Thus, we hypothesized that quantitative and/or qualitative differences in the antiviral RNAi response in mosquitoes influence vector competence. Specifically, we profiled sRNAs in mosquito midguts at multiple time points and across infection phenotypes (midgut-limited infections and infections which had disseminated from the midgut into the hemocoel) in order to (1) track the development of the response and (2) determine whether specific viRNA profiles may be correlated with infection phenotype (midgut limited vs. disseminated). In addition, we also identified viRNA sequences common across multiple replicate libraries and time points and determined their individual efficacy in suppressing WNV replication *in vitro*. Our results suggest that RNAi is ineffective in limiting mosquito susceptibility to WNV infection because it is not activated during the first 24 hours of infection, when virus is entering cells and undergoing replication. Further, we failed to associate a particular profile of viRNA expression with either limitation of WNV to or its escape from mosquito midguts. In sum, these results fail to provide a strong link between RNAi and mosquito vector competence.

Materials and Methods

Mosquitoes

Lab-colonized *Cx. quinquefasciatus* mosquito larvae (designated here as US-Cxq, described in [394]) were raised on a diet of a 1:1 mix of powdered Tetra food and powdered rodent chow. Pupae were allowed to emerge into containers and adult mosquitoes were kept at 26-27 °C with a 16:8 light:dark cycle and 70%-80% relative humidity, with water and sucrose provided *ad libitum*.

Viruses and Experimental Infections

WNV was produced from an infectious cDNA clone based on the WNV_{NY99} strain as previously described [397]. Briefly, purified viral RNA was electroporated into BHK-21 cells, with the electroporation parameters set to 425 V, 1200 Ω resistance, 25 μ F capacitance, and two pulses. Cell supernatant was collected after cells showed obvious signs of cytopathic effect (CPE; usually ~3 days post-electroporation). Cellular debris was removed from the supernatant by centrifugation at ~3000 g, clarified supernatant was raised to a final concentration of 20% fetal bovine serum (FBS), and aliquots of 0.5 mL were made and stored at -80°C. Virus titer was then quantified by plaquing on Vero cells. Adult female mosquitoes 6-8 days post-eclosion were fed an infectious bloodmeal of de-fibrinated sheep blood mixed 1:1 with ~2 X 10⁸ PFU/mL of infectious clone derived WNV (WNV_{icd}). Un-infected control mosquitoes were fed only de-fibrinated sheep blood. Engorged mosquitoes were held for 12 hour, 24 hour, 3 day, 7 day, or 14/16 day extrinsic incubation periods (EIPs) in a BSL-3 insectary with the same rearing conditions described previously, after which they were cold anesthetized, and midguts dissected and stored in MagMax isolation lysis buffer (Ambion) at -80°C until needed for RNA isolation. Legs were also harvested from mosquitoes at 7, 14, and 16 days post infection (dpi) time points in order to assess for disseminated infections.

Total RNA Isolation and Small RNA Library Preparations

Total RNA was extracted from homogenized mosquito midguts and legs using the MagMAX Viral RNA isolation kit (Ambion) as per a modified protocol for enrichment of small RNA isolation in the total RNA fraction [429], using a Kingfisher Flex Magnetic Particle Processor

(Thermo Scientific, Waltham MA). Specifically, the incubation/binding time was increased from 4 minutes to 10 minutes, and the amount of isopropanol added to Wash Buffer #1 was raised from 1:2 to 1:1. Eluted RNA from individual midguts and sets of 6 legs from each mosquito from each infection group and time point were screened for the presence of WNV genomic RNA by 1-step RT-PCR (Qiagen) using 212-F (5'-TTGTGTTGGCTCTCTTGGCGTTCTT-3') and 619-R (5'-CAGCCGACAGCACTGGACATTCATA-3') primers (numbers in primer designation denote genome position). Because accurate determination of infection (as measured by the presence of antisense viral RNA) is problematic at early time points, midguts from 12 and 24 hour time points were not screened for infection and simply designated as "exposed". Since dissemination from the midgut would not be expected to occur by 3 dpi, we only screened midguts from this time point. For the 7, 14, and 16 dpi time points, an infection phenotype of "midgut-limited" was designated if no viral RNA was detectable in legs corresponding to a given midgut, and a "disseminated" phenotype was designated if viral RNA was detectable. Midgut RNA samples positive for viral RNA were checked for RNA quality on a 2100 Bioanalyzer (Agilent), and then pooled into groups of 5 midgut RNAs by infection phenotype and time point. Pooled RNAs were precipitated by adding 3.25 volumes of ice-cold EtOH, 0.1 volume 3M NaOAc (pH 5.5), and 1.5 μ L of linear polyacrylamide (5 mg/mL) as a carrier. After holding overnight at -20°C, the pools were centrifuged at ~20,000 g, washed twice with 80% EtOH, and re-suspended in nuclease-free water. 1 μ g total RNA was used as the input for small RNA library preparation using the TruSeq Small RNA Sample Prep Kit (Illumina) as per manufacturer's suggested protocol. Briefly, small RNAs were preferentially 3' and 5' adapter-ligated, reverse transcribed using the Superscript II reverse transcriptase (Invitrogen), and PCR amplified, during which time a unique

oligonucleotide barcode sequence was added to each library for multiplexing. Three biological replicate libraries were made for each pooled time point/infection phenotype. In addition, we sequenced small RNAs from four separate individual midgut libraries at the 24 hour post-exposure (hpe) time point. Small RNA libraries were size selected on 2% TBE-agarose gels, and purified with MinElute Gel Extraction kits (Qiagen). Purified small RNA cDNA libraries were eluted in Qiagen EB buffer, validated on the 2100 Bioanalyzer, and sequenced on an Illumina HiSeq 2000 instrument.

Assembly and Analysis of sRNA Libraries

Sequence FASTQ files were trimmed of the 3' adapter using FASTX Toolkit [400] and aligned to the WNV_{NY99} infectious clone reference sequence using Bowtie 0.12.8 [401] and allowing for 0-mismatches. The **-a --best --strata** mode was used, which instructs Bowtie to report only those alignments in the best alignment stratum. SAM output files produced by Bowtie were used as the input for processing through SAMtools [402]. Nucleotide targeting plots of the viral genome were generated using the pileup function of SAMtools, and then used for correlational analysis. Additional analyses were conducted using Microsoft Excel, Graphpad Prism 6, and VENNY, an online tool for creating Venn diagrams [430].

Transfection of C6/36 Mosquito Cells with Synthetic siRNAs

Ae. albopictus-derived C6/36 cells were seeded into 6-well plates at a concentration of 1×10^6 cells/well, and transfected one day later with 100 pM concentration of synthetic siRNA duplexes (Dharmacon, Inc., Lafayette CO, siRNA sequences provided in Table 4.1) using

Lipofectamine 2000 transfection reagent (Invitrogen, Carlsbad CA) as per manufacturers suggested protocol. Cells were infected 48 hours post-transfection with infectious clone derived WNV_{NY99} at an MOI of 0.1. 300 μ L of cell supernatant was harvested every 12 hours up to 48 hpi and viral titer quantified by plaque assay on Vero cells.

qRT-PCR

WNV genome equivalents were determined using a Taqman qRT-PCR assay amplifying a 70bp fragment within the WNV E gene (described in [404]). 5 μ L of total RNA from individual mosquito midgut samples used to construct our small RNA sequencing libraries or genome equivalent standards was used as the template in duplicate 20 μ L reactions using the iScriptTM 1-Step RT-PCR Kit for probes (Biorad) with reagent ratios as per the manufacturer's suggested protocol. The following primer and probe sequences were used for this assay: 1160-F (5'-TCAGCGATCTCTCCACCAAAG-3'), 1229-R (5'-GGGTCAGCACGTTTGTTCATTG-3'), and 1207-Probe (5'-TGCCCGACCATGGGAGAAGCTC-3'). Reactions were run on a CFX-96TM real-time system (Biorad). WNV genomic equivalent standards were previously generated by amplifying a 2.4 kb fragment from the WNV E gene using WNV 1031-F (5'-ATTTGGTTCTCGAAGGCGAC-3') and WNV 3430-R (5'-TGGTGGTAAGGTGCAGCTCC-3') primers. The resulting amplicon was then cloned into the pCR2.1-TOPO vector (Invitrogen) downstream of the T7 promoter. The recombinant vector was linearized with KpnI, purified and used as template for *in vitro* transcription using the T7 Megascript kit (Ambion) according the manufacturer's instructions. *In vitro* transcribed RNA was then quantified and aliquoted into serial ten-fold dilutions.

Results

The exogenous siRNA and PIWI-interacting RNA (piRNA) pathways do not appear to be induced at early time points of WNV infection

We sequenced small RNAs from triplicate pools of 5 *Cx. quinquefasciatus* midguts from early (12 hpe, 24 hpe, and 3 dpi) and late (7 dpi, 14 dpi, and 16 dpi) time points after infection with WNV. The percentage of reads mapping to WNV RNA varied considerably between time points, but was relatively consistent between replicates (**Figure 4.1A**). At 12 hpe, few viRNA reads were present, however the percentage of viRNAs relative to total 19-30 nt small RNAs increased considerably by 24 hpe. At 3 dpi, detectable viRNAs had again dropped to proportions comparable to the 12 hpe time point, and gradually increased by 7, 14, and 16 dpi. Analysis of the distribution of sequences by length revealed that 19-30 nt reads mapping to the WNV genome were approximately evenly distributed with no peak at 21 nts, which would be expected from products of Dcr-2 digestion (**Figure 4.1B-C**). Viral replication at these early time points was evident based on the presence of a significant fraction of viRNAs derived from the negative strand of the virus RNA. Bias for reads derived from the positive strand of the virus was elevated at 12 hpe compared to the later time points, with roughly 80% of 19-23 nt reads being generated from this strand (**Figure 4.2A**). In contrast, 19-23 nt viRNAs were more or less equally generated from both the positive and negative strands at all other time points during infection. Strand biases for 24-30 nt sequences, which correspond by size to products of the piRNA pathway, were more skewed toward the positive strand (**Figure 4.2B**). At 12 hpe, roughly 75% of 24-30 nt reads mapping to WNV were derived from the positive strand. At 24 hpe, the ratio of positive:negative strand had decreased to ~60:40, inconsistent with the heavy positive-

strand bias observed in our previous studies as well as the published literature [282, 313, 318, 316, 314]. The expected positive-strand bias began to resolve starting at 3 dpi onward, with ~80-90% of 24-30 nt reads being derived from the positive strand at these time points (**Figure 4.2B**). Interestingly, 24-30 nt small RNAs were significantly enriched in the 14 dpi midgut limited cohort as compared to the 16 dpi disseminated cohort (**Figure 4.1F**). This population of small RNAs represented between 7% and 20% of the total 19-30 nt RNAs across replicates in this cohort. However, 24-30 nt small RNAs in the 7 dpi midgut limited cohort were not significantly enriched over the 7 dpi disseminated group (**Figure 4.1E**). Starting at 3 dpi, the size distribution of 19-23 nts RNAs became approximately normally distributed with a prominent peak at 21 nts (**Figure 4.1C-F**).

Nucleotide targeting of the virus genome by RNAi is highly conserved within and between time points and infection phenotypes

We previously compared intra- and interspecies anti-WNV RNAi profiles across different species and populations of mosquitoes, and found that in particular, the relative intensity of intra-species nucleotide targeting of the virus genome was highly conserved. We compared the 19-23 nt viRNA nucleotide targeting profiles of midgut pools sequenced in triplicate at 3 dpi, 7dpi, 14 dpi, and 16 dpi. The 7 dpi and the 14-16dpi time points were classified into two different infection phenotypes: midgut limited and disseminated, determined by either the lack or presence of detectable viral RNA in the legs, respectively.

To test the hypothesis that qualitative and/or quantitative differences in targeting of the viral genome by the exo-siRNA pathway influences vector competence, we correlated

nucleotide targeting frequencies between individual replicates within a cohort (i.e. 7 dpi midgut limited) and between cohorts (i.e. 7 dpi midgut limited vs. 7dpi disseminated). We focused on the 19-23 nt reads corresponding to products of the siRNA pathway since this population makes up the bulk of the total RNAi response. At 12 hpe, there was a low correlation between replicates as measured by the Spearman r value ($r_s=0.31$) (**Figure 4.3**). In contrast, at 24 hpe, intra-time point replicates were more strongly correlated ($r_s=0.77$). Similar results were observed for intra-time point and intra-infection phenotype correlations for 7, 14, and 16 dpi. Surprisingly, when we made inter-time point and inter-infection phenotype comparisons between individual replicates at 3 dpi, 7 dpi, 14 dpi, and 16 dpi, the strength of the correlation in all cases was statistically equal to the intra-cohort comparisons within replicates. Similarly, the ratio of small 19-23 nt viRNAs derived from either the positive or negative strand across these time points did not change significantly (**Figure 4.2A**). This suggests that once the RNAi pathway is activated, the relative intensity of nucleotide targeting of the virus genome (i.e. the “RNAi profile”) remains constant during the course of infection.

We next measured viral load in individual mosquitoes comprising each replicate pool from 3 dpi to 16 dpi using qRT-PCR. There was no association between viral genome copy number and infection phenotype. When comparing both the 7 dpi midgut limited vs. disseminated libraries and the 14-16 dpi midgut limited and disseminated libraries, titers were higher in the midgut limited libraries when comparing either individual replicate titers or cohort mean titers, though not significantly (**Figure 4.4A-B**).

Abundant viRNAs are inefficient at individually suppressing WNV replication in C6/36 mosquito cells

We next tested whether abundant viRNAs from early (12 hpe, 24 hpe) and later (7 dpi) time points could effectively suppress WNV replication *in vitro*. We identified several highly abundant viRNAs common to both the 12 and 24 hpe libraries, as well as viRNAs common amongst the 7 dpi libraries. We designed synthetic siRNA duplexes to each of these selected viRNA sequences and individually transfected them into *Ae. albopictus*-derived C6/36 cells 48 hours prior to infecting with WNV. With the exception of siRNA 7d at 48 hours post infection (hpi), none of the siRNAs significantly reduced viral titers individually (**Figure 4.5**). The combined effect of these siRNAs was not determined.

Discussion

In this study, we sought to determine the temporal plasticity of the anti-WNV RNAi response in *Cx. quinquefasciatus* mosquitoes, as well as determine the effect of the exo-siRNA pathway in shaping mosquito vector competence to arbovirus infection. At early time points after taking an infectious bloodmeal, small RNAs sequenced from the midguts of WNV-exposed mosquitoes exhibited an atypical size distribution profile, specifically lacking a prominent peak at 21 nts, which is a hallmark of the Dcr-2 mediated siRNA response. Since we lacked the ability to reliably determine prior to sequencing whether these mosquitoes had replicating virus in the midgut, mosquitoes pooled for small RNA libraries at the 12 and 24 hpe time points were deemed as “exposed” as opposed to “infected”. However, small RNA sequencing revealed sequences derived from the negative strand of the virus, indicating active viral replication. A

key question that remains is biogenic origin of the small RNA sequences from these early time points. It is possible that we were observing the early stages of the siRNA response, prior to the development of the stereotypical normal distribution with a peak at 21 nts that has been observed in ours and others' previous studies of invertebrate RNAi responses to RNA viruses [280, 282, 283, 293, 313, 281, 314-318, 431-433]. Conversely, it is also possible that we were sequencing degradation products produced by other cellular non-RNAi RNA decay pathways. The latter scenario seems to be supported by our observations at the 12 hpe time point, since the low correlation of nucleotide frequency within the reads between replicates may be indicative of the "random" production of RNA products, such as through the incomplete exonucleolytic degradation by XRN-1 or the exosome. The Illumina Truseq small RNA protocol we used to make our sequencing libraries is designed to specifically ligate RNAs with a 5'-PO₄ and 3'-OH, which miRNAs, siRNAs, and piRNAs all exhibit, and the size selection step of the protocol ensures a further degree of specificity for small RNA products. However, it is possible that in the absence of appreciable amounts of small RNAs, other RNA products can become preferential targets for adapter ligation and subsequent sequencing. In mammals, Dicer has been shown to cleave targets with high specificity with regards to RNA secondary structure and distance from the 5'-end of the target [434, 435]. It is likely that invertebrate Dicer enzymes similarly recognize signatures in their targets that dictate where cleavage of the target occurs. Indeed, the high degree of intra- and inter-cohort correlation we see between replicates suggests that targeting and subsequent processing of the virus genome by Dcr-2 is not random, but highly specific. Due to the atypical proportions of 24-30 nt RNAs to 19-23 nt RNAs, the apparent lack of consistency in nucleotide targeting between replicates at 12 hpe, and the lack of expected

strand bias at 12 and 24 hpe in the 24-30 nt RNAs, we conclude that neither the siRNA nor piRNA pathways are activated at the earliest, and probably most relevant timepoints during mosquito infection.

By 3 dpi infection, a more stereotypical distribution of viRNAs had appeared, with a prominent peak at 21 nts, indicative of Dcr-2-mediated digestion of the virus genome. There was no statistical difference in the proportions of 19-23 nt viRNAs between replicates or infection phenotypes at any time point; however, at 14 dpi, there was a statistically significant enrichment of 24-30 nt viRNAs in the midgut limited vs. the 16 dpi disseminated group. An enrichment in this size class, which corresponds to products of the piRNA pathway, was not observed between 7 dpi midgut limited and disseminated cohorts. There is a considerable lack of understanding regarding the impact the piRNA pathway has on controlling arbovirus infection, and we hypothesize in the previous chapter that it plays a compensatory or redundant rather than a primary role in RNAi-mediated antiviral defense.

In this study, we hypothesized that qualitative or quantitative differences in the RNAi response may be correlated with vector competence phenotypes in the mosquito midgut; specifically, whether or not the virus is restricted to the midgut epithelium or is allowed to disseminate into distal tissues. Surprisingly, we not only found that once established, the antiviral RNAi profile in mosquito midguts is remarkably constant during the entire course of infection, but that there was little discernable difference in the profiles of midguts from mosquitoes with disparate infection phenotypes. There are several possibilities for this observation. First, these experiments were carried out using highly inbred, colonized mosquitoes with presumably low genetic diversity. While *Dcr-2* has been shown to undergo

rapid evolution in mosquitoes and is correlated with differential vector competencies to virus infection [407, 408], it is unlikely our colonized mosquitoes undergo such selective pressures, since infected mosquitoes are not part of the breeding stock of the colony. Additionally, it is unknown what phenotypic effect on the targeting specificity of Dcr-2 may occur as the result of mutation within that gene. Vector competence is a polygenic trait that is not completely understood, and it is likely that many factors, both internal and external, contribute to the vector competence phenotype in mosquitoes. It is also possible that by limiting our studies to the mosquito midgut, we may have missed important variation in the RNAi response in other tissues; i.e. is a midgut-limited phenotype due to the strict inability of the virus to escape from the midgut, or can a robust RNAi response in the hemolymph (perhaps primed by a hypothetical systemic RNAi response) of the mosquito clear or prevent infection in that compartment. We found no relationship between the viral load in mosquito midguts and the infection phenotype; in fact, mosquitoes with disseminated infections had slightly lower virus genomic copy numbers than mosquitoes with midgut limited infections, though this difference was not statistically significant. Thus, we conclude that not only does the antiviral RNAi response fail to limit viral load in midgut limited versus disseminated infection phenotypes, but that it is not associated with either the restriction or dissemination of the virus from the midgut.

We also investigated the individual efficacy of highly abundant viRNAs from our sequencing data in limiting WNV replication *in vitro*. In congruence with previous unpublished data from our lab, we found that at best, there was modest suppression of WNV replication in C6/36 cells infected with WNV 48 hours post transfection with synthetic siRNAs. A single siRNA

at 48 hpi showed statistically significant suppression of WNV as measured by Dunnett's multiple comparisons test. A relatively recent paper demonstrated that low abundance Semliki Forest virus (SFV, *Togaviridae*)-derived viRNAs were more effective at suppressing virus replication than highly abundant viRNAs in *Ae. albopictus*-derived U4.4 and *Ae. aegypti*-derived Aag2 cells [433]. However, previous unpublished work from our lab has shown that synthetic siRNAs designed from low abundance WNV-derived viRNAs were no more effective at suppressing viral replication than highly abundant viRNAs. Thus, susceptibility to replicative inhibition by individual virus-specific siRNAs may be a feature of some arboviruses but not others.

Table 4.1: Sequences for synthetic siRNAs transfected into C6/36 mosquito cells prior to WNV infection. The number designation in the name denotes the libraries these sequences were identified from, i.e. 1224 indicates that these sequences were abundant in both 12 and 24 hpe libraries, 7 means that these sequences were abundant amongst the 7 dpi libraries. The two terminal U's at the 3' end of each sequence (underlined) are artificial 3'-overhangs inserted to mimic the 2 nt 3' overhangs present on siRNA duplexes, and were not derived from the actual viRNA sequences.

siRNA Name	Sense Sequence	Antisense Sequence
1224a	5'-GGCACCAGAGCCCGAGUCA <u>UU</u> -3'	5'-UGACUCGGGCUCUGGUGCC <u>UU</u> -3'
1224b	5'-ACUUCCCGGCCUGACUUUC <u>UU</u> -3'	5'-GAAAGUCAGGCCGGGAAGU <u>UU</u> -3'
1224c	5'-CUUCCCGGCCUGACUUUC <u>UU</u> -3'	5'-AGAAAGUCAGGCCGGGAAGU <u>UU</u> -3'
1224d	5'-CUCCUCCAACUGCGAGAAACGUG <u>UU</u> -3'	5'-AGAAAGUCAGGCCGGGAAGU <u>UU</u> -3'
1224e	5'-GCUCUAAUUCUGGGACGUCCG <u>UU</u> -3'	5'-CGGACGUCCAGAAUUAGAGC <u>UU</u> -3'
7a	5'-GGUGCGAGUGGCAGGUCCACG <u>UU</u> -3'	5'-CGUGGACCUGCCACUCGCAC <u>UU</u> -3'
7b	5'-CAGCGAACUGGCGGAGCCUGU <u>UU</u> -3'	5'-ACAGGCUCCGCCAGUUCGCUG <u>UU</u> -3'
7c	5'-GACUUACAGACUGAGAUCCCG <u>UU</u> -3'	5'-CGGGAUCUCAGUCUGUAAGUC <u>UU</u> -3'
7d	5'-GACAGUACGAGAAGCCGGAU <u>UU</u> -3'	5'-AUCCGGCUUCUCGUACUGUC <u>UU</u> -3'
7e	5'-GGCAGUCCUCUCAGUGCUUCA <u>UU</u> -3'	5'-UGAAGCACUGAGAGGACUGCC <u>UU</u> -3'

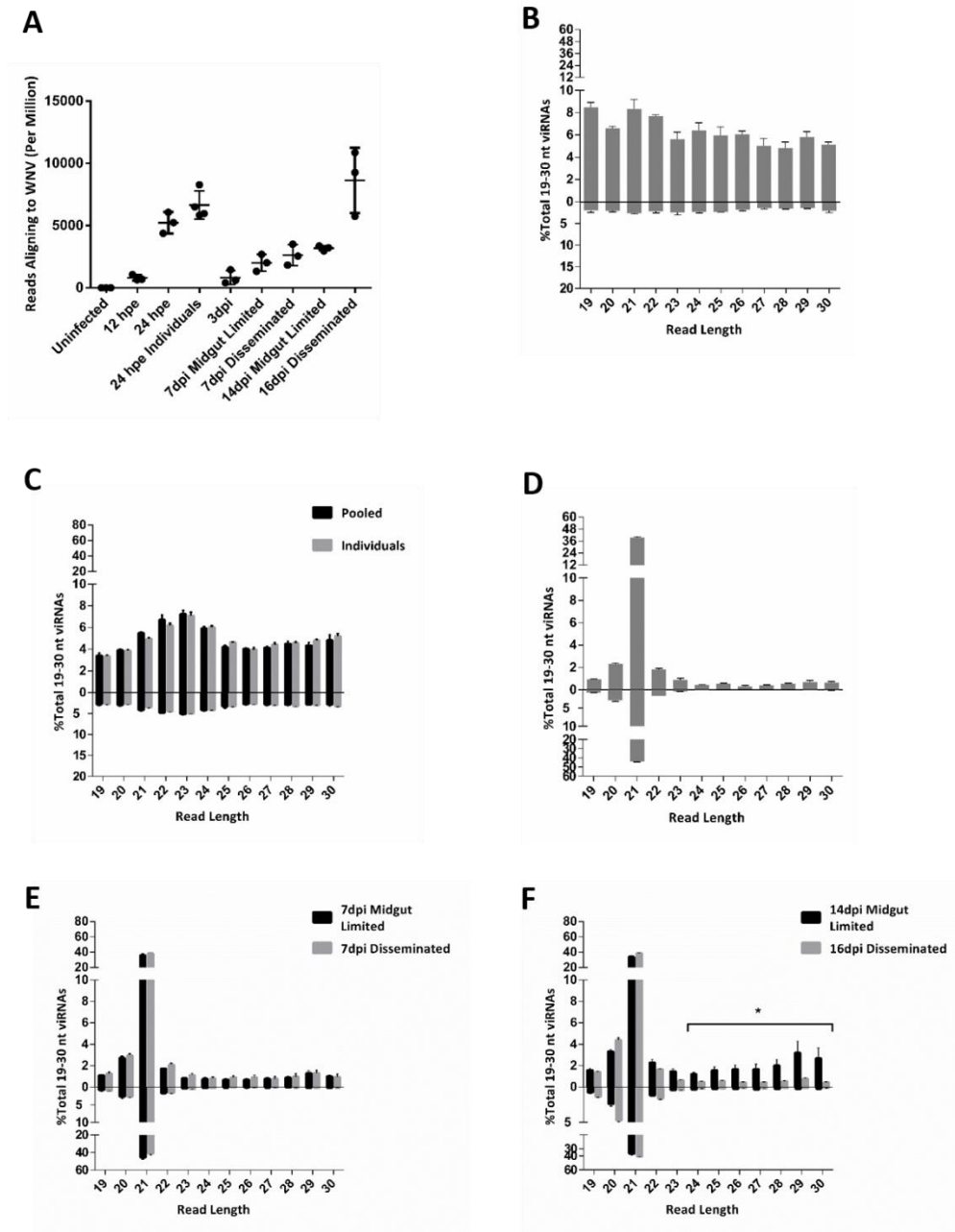


Figure 4.1: Features of small RNA libraries. A) Relative abundance of small RNA reads mapping to the WNV genome normalized per million. Error bars represent mean and SEM. **B-F)** Distribution of viRNA sequences by size at 12 hpe (**B**), 24 hpe (**C**), 3 dpi (**D**), 7 dpi (**E**), and 14/16 dpi (**F**). Mean values of 3 replicates are plotted, error bars represent SEM. Asterisk in (**F**) denotes significant difference in 24-30 nt abundance by an unpaired t-test with Welch's correction ($p=0.007$).

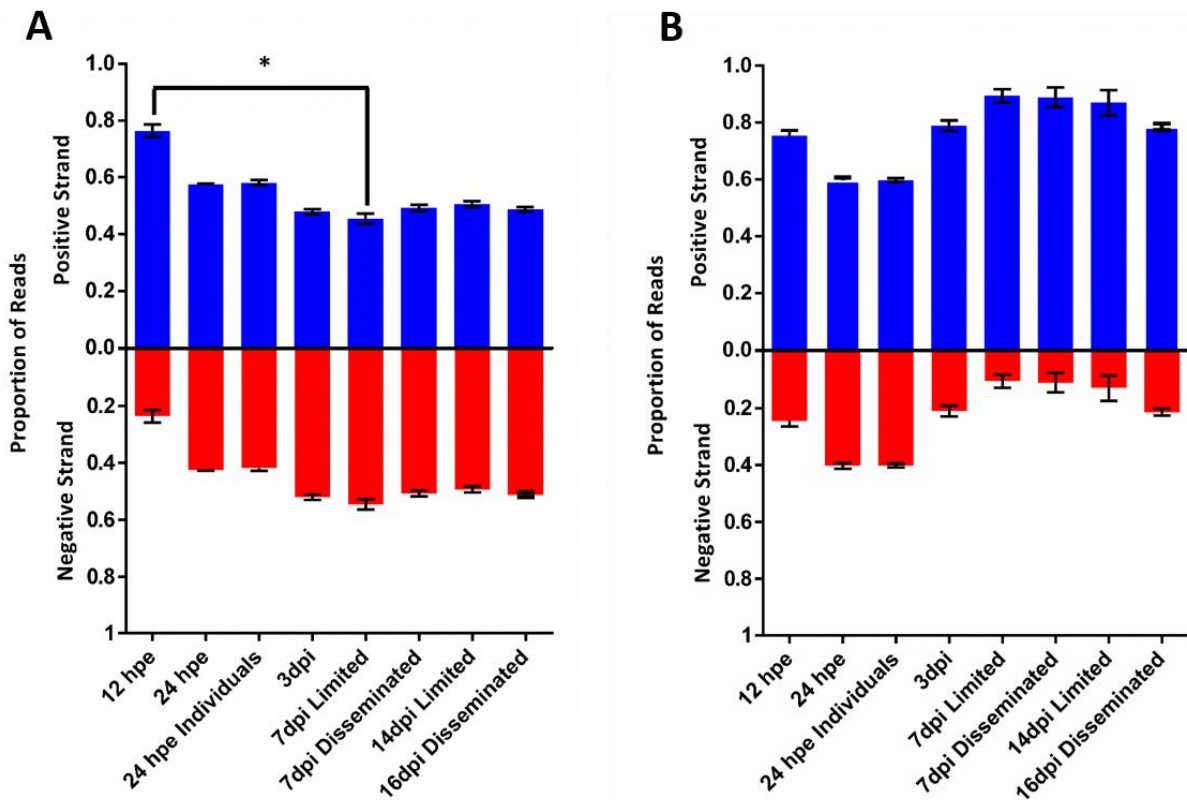


Figure 4.2: Positive/negative strand ratios for small RNA libraries. A) 19-23 nt reads, B) 24-30 nt reads. Mean values for three replicates from each cohort are plotted. Error bars represent SEM. Asterisk denotes significance ($p \leq 0.05$) as tested by Dunn's multiple comparisons test.

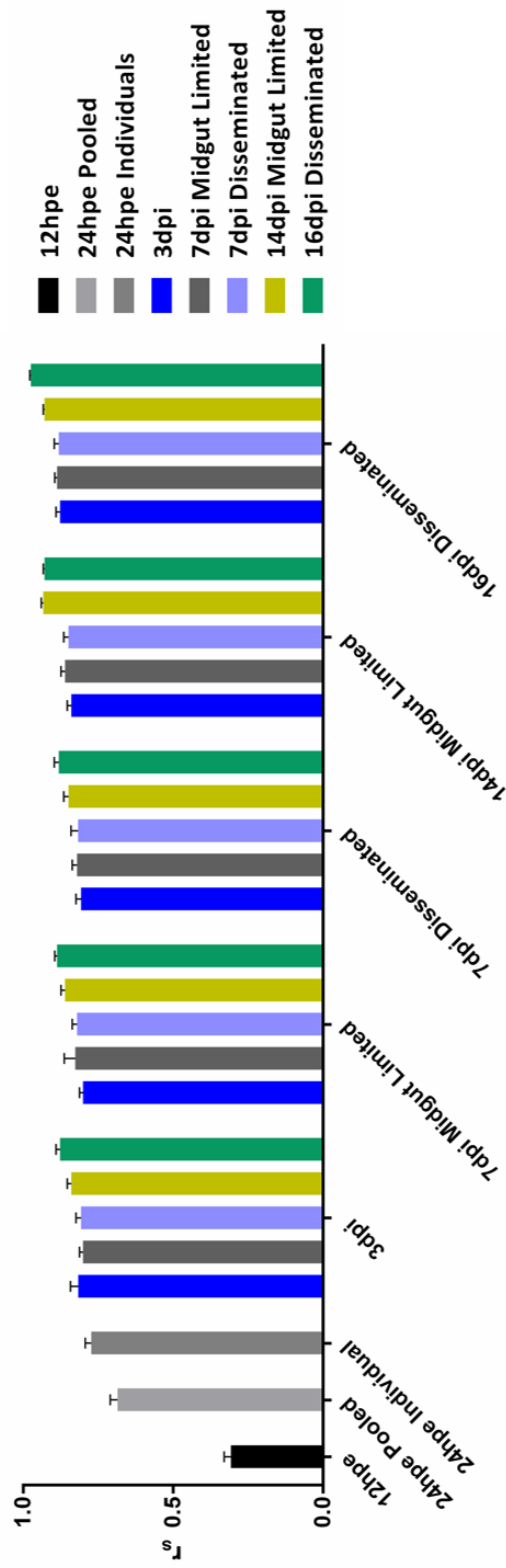


Figure 4.3: Intra- and inter-cohort comparisons of replicate mean r_s values. Intra-cohort correlations were performed by comparing each of the three replicates from each cohort against one another using the non-parametric Spearman rank coefficient (r_s). Inter-cohort comparison were made for each individual replicate from one cohort against each individual replicate from another cohort (only performed for 3 dpi, 7 dpi, 14 dpi, and 16 dpi cohorts). Mean r_s values for each comparison are plotted. Error bars represent SEM.

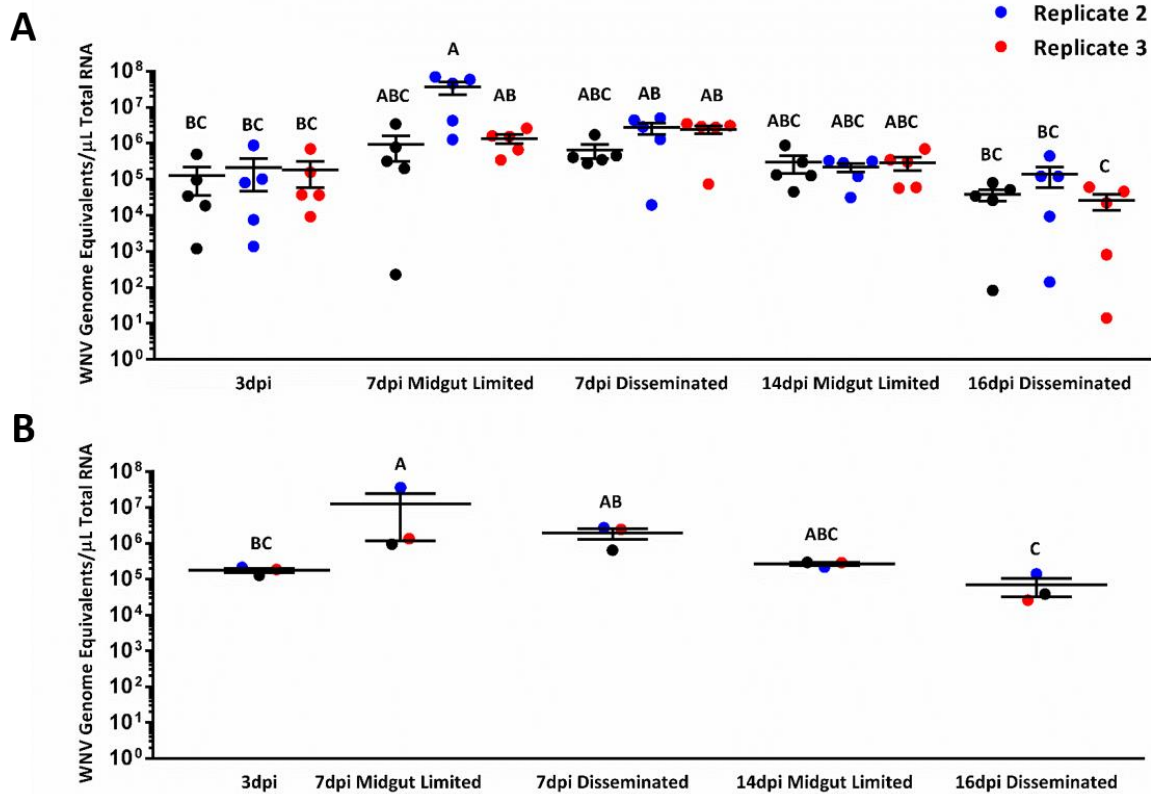


Figure 4.4: WNV genome equivalents from library pools as measured by qRT-PCR. Taqman qRT-PCR was performed on individual mosquito midguts used to create small RNA library pools. **A)** WNV genome equivalents/ μ L total RNA for individual mosquitoes from each replicate within the 3 dpi, 7 dpi, 14 dpi, and 16 dpi cohorts. Bars represent mean and SEM. **B)** Mean genome equivalent titers for each replicate. Bars represent mean and SEM. For both graphs, statistically homogeneous data sets share common letters. Statistical significance ($p \leq 0.05$) was determined by \log_{10} transforming the data and then performing Tukey's multiple comparison test on the means.

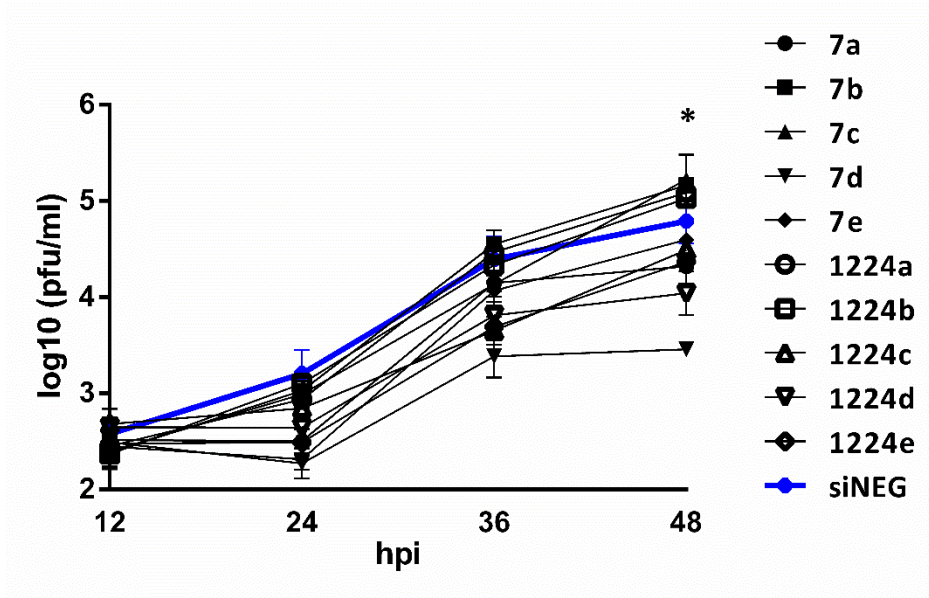


Figure 4.5: Synthetic siRNA transfection of C6/36 cells. C6/36 cells were transfected with synthetic siRNA duplexes 48 hours prior to infection with WNV. Cell supernatant was harvested every 12 hours up to 48 hpi and viral titers quantified by plaque assay. Mean titers of three replicates are plotted, error bars represent SEM. Asterisk denotes WNV titer from the 7d siRNA treatment group at 48 hours which was significantly less than the negative siRNA control (siNEG) as determined by Dunnett's multiple comparisons test ($p \leq 0.05$).

Chapter 5: Concluding Remarks

Arboviruses constitute both emerging and re-emerging threats to human and livestock health worldwide. In particular, mosquito-borne arboviruses cause the majority of severe disease outbreaks. It is therefore critical that we develop a complete understanding of mosquito-virus interactions, both from macro (i.e. natural history, ecology, etc.) and molecular (i.e. virus evolution, vector innate immunity) perspectives. Additionally, a detailed understanding of these factors is important in order to ascertain how they influence differences in susceptibility to arbovirus infection and likelihood of transmission in natural populations of mosquitoes, i.e. vector competence.

RNAi is the major innate immune response to arbovirus infection in mosquitoes [383]. Over a decade of research has been invested into investigating the role small RNA pathways play in controlling arbovirus infection in mosquitoes. What has become clear is that RNAi, specifically the exo-siRNA pathway, protects mosquitoes from lethal infection [388], and data from other infection models suggest that an equilibrium between the antiviral-RNAi response and viral replication allows for the establishment of a persistent, non-pathogenic infection [297]. Insights into the importance of the antiviral function of small RNA pathways have inspired research into the development of novel arbovirus control strategies which seek to exploit these immune pathways [385, 18, 20, 387, 386]. However, there is still a considerable lack of understanding regarding the degree to which the antiviral RNAi response varies amongst mosquito species and populations, as well as how it influences mosquito vector competence.

Additionally, it has only been recently that the role of another small RNA pathway, the piRNA pathway, has been implicated in participating in antiviral defense in mosquitoes.

The work contained in this dissertation sought to resolve these questions and increase our understanding of small RNA pathways in the context of innate immunity to arboviruses in mosquitoes. We first began by profiling virus-derived small RNAs in the midguts of *Culex* sp. mosquitoes in response to WNV infection using the Illumina next-generation sequencing technology. The midgut is the first site of infection after imbibing an infectious bloodmeal, and a failure to infect/replicate sufficiently/disseminate from this tissue results in a dead-end infection for the virus. Since there is a lack of studies that have investigated innate immune mechanisms in natural populations of mosquitoes to arbovirus infection, we collected egg rafts from three species of WNV vector mosquitoes from the field: *Cx. quinquefasciatus*, *Cx. pipiens*, and *Cx. tarsalis*. We reared larvae to adulthood in the laboratory, and experimentally infected adult female mosquitoes *per os* with an infectious clone derived virus based on the NY99 strain of WNV. We then compared viral-derived small RNA populations of 19-30 nts sequenced from midgut pools of infected mosquitoes. In addition, we sequenced midgut pools from colonized *Cx. quinquefasciatus*, *Cx. tarsalis*, *Cx. pipiens*, and *Ae. aegypti* mosquitoes reared and infected in the same manner. We found that there was a high degree of intra-species correlation between the 19-23 nt viRNAs (consistent in size with products of the Dcr-2 dependent exo-siRNA pathway) in all of the species studied. We also made interspecies comparisons between WNV-derived viRNAs and found a striking level of correlation between species; with the notable exception of *Cx. quinquefasciatus*, which significantly differed in the targeting of the virus genome when compared to *Cx. tarsalis*, *Ae. aegypti*, and even the closely related sister taxa *Cx.*

pipiens. Previous work has shown that WNV undergoes population bottlenecks in *Cx. pipiens* [405], but not *Cx. quinquefasciatus* [406]. It is therefore possible that qualitative differences in the total RNAi response may differentially influence virus diversification and population structure. As we did not analyze virus genetic diversity from our sequenced mosquitoes, it is impossible to draw a correlate; however, future studies should address this point.

While profiling 19-30 nt viral-derived small RNAs from both field-collected and colonized *Cx. quinquefasciatus* mosquitoes, we found that while the relative proportion of 19-23 nt did not differ statistically between the groups, the proportion of 24-30 nt small RNAs, corresponding in size to products of the piRNA pathway, did differ significantly across the three groups. The piRNA pathway is a relatively recently described small RNA pathway that plays important roles in spermatogenesis [301] in flies, and is an important suppressor of transposable elements in gametic tissue [301]. Endogenous piRNAs typically exhibit strong strand biases, being primarily antisense to TE's [305], and exhibit preferences for a 5'-uracil residue on primary piRNAs and an adenosine at position 10 of secondary piRNAs [311, 312]. The ping-pong dependent amplification model has been proposed to explain these nucleotide biases. Recently, the piRNA pathway has been implicated in participating in antiviral defense in flies and mosquitoes [282, 313, 281, 314-318] Moreover, when we analyzed the strand bias and nucleotide bias for these small RNAs in all of our *Culex* and *Ae. aegypti* libraries, we found a very strong bias for reads derived from the positive strand of the virus; however, no preference for a U₁ residue on the primary (negative) strand or a A₁₀ on the secondary strand (positive) was observed in these putative viral-derived piRNA-like small RNAs (vpiRNAs). This is partially consistent with what has been observed for DENV-2 in both mosquitoes and mosquito cells

[315, 281], for which only a slight bias for an A₁₀ was observed, but contrary to what has been observed in alphavirus and bunyavirus infected mosquitoes or mosquito cells, where viral-derived piRNAs (vpiRNAs) consistent with the model for ping-pong dependent amplification have been sequenced [317, 282, 313, 318, 316]. Therefore, we hypothesized that infection with either alphaviruses or flaviviruses results in the disparate biogenesis and/or processing of small RNAs through the piRNA pathway.

We chose *Cx. tarsalis*, an important natural vector for both WNV and WEEV, and a competent laboratory vector for SINV, as our single-species infection model, and sequenced both midguts and carcasses sans ovaries from mosquitoes experimentally infected with these viruses. Remarkably, we found that infection with none of these viruses resulted in production of 24-30 nt small RNAs with signatures of ping-pong dependent amplification. Additionally, we found that while a strong bias for reads being derived from the positive strand of the virus was maintained in both midguts and carcasses of mosquitoes infected with WNV, only the carcasses of mosquitoes infected with either WEEV or SINV exhibited a strong positive strand bias. This observation challenged our hypothesis that production of 24-30 nt small RNAs that either exhibited signatures of ping-pong dependent amplification or did not was virus dependent. When we analyzed a previously made library from *Ae. aegypti* infected with SINV, we found that a strong positive strand bias was maintained, along with the expected nucleotide biases observed for other alphavirus infections in *Ae. spp.* mosquitoes and cells. However, *Ae. aegypti* does not produce piRNA-like small RNAs with these molecular signatures to WNV. Therefore, we concluded that the specific products of the piRNA pathway in mosquitoes are dependent on both host *and* virus, and that specific viruses do not universally elicit production of ping-pong

dependent piRNA-like small RNAs, nor do specific vectors universally produce ping-pong dependent piRNA-like small RNAs to arbovirus infection.

We were able to confirm the presence of transcripts for required machinery for the ping-pong dependent pathway in *Cx. quinquefasciatus* midguts, providing evidence that it is likely this pathway is functional in this tissue. Secondly, we aligned small RNA reads to several selected TE sequences from *Cx. quinquefasciatus*, finding not only that they exhibited strong strand bias (antisense to the TE), but also the expected nucleotide bias. This implies that the pathway is intact in *Cx. quinquefasciatus* (and presumably *Cx. pipiens* and *Cx. tarsalis*), but for currently unknown reasons, is not triggered by arbovirus infection.

The role of RNAi in influencing the vector competence phenotype in mosquitoes is poorly understood. We do know that vector competence is a quantitative genetic trait, under the control of several loci [426-428] ; however, collectively, these loci account for little of the wide variation in observed vector competence phenotype amongst species and populations within species. Therefore, we hypothesized that since RNAi is the major innate immune pathway responsible for controlling arbovirus infection in mosquitoes, it also plays a role in shaping the vector competence of the insect. Using multiple biological replicates, we profiled the midgut small RNA response to WNV infection in our colonized *Cx. quinquefasciatus* mosquitoes at both early (12 hpe, 24 hpe, 3 dpi) and late (7 dpi, 14/16 dpi) time points as well as different infection phenotypes (midgut limited and disseminated). Remarkably, we found little evidence for activity of the siRNA or piRNA pathways at 12 hpe and 24 hpe, though by 3 dpi, products of Dcr-2 dependent digestion of the virus genome were evident. Additionally, we found no correlation between a particular viRNA profile and either limitation to or escape from

the midguts of infected mosquitoes. Moreover, neither infection phenotype nor RNAi profile was correlated with virus load in the midgut. Based on these lines of evidence, we conclude that RNAi fails to control virus replication at key time points during infection, specifically, when the virus is first entering cells and undergoing replication.

Taken together, these investigations into the antiviral RNAi pathways in mosquitoes to arbovirus infection add to the continually growing body of evidence highlighting the importance of small RNA pathways in controlling arbovirus infection. However, there are numerous unanswered questions that remain ripe for exploration. For example, little is known about the effect persistent viral infection has on altering the RNAi response in natural populations, where vertical (transovarial) transmission of arboviruses, in particular bunyaviruses, is possible [436, 186, 437]. *Bombyx mori* larvae are frequently persistently infected with *Bombyx mori* cytoplasmic polyhedrosis virus (BmCPV, *Reoviridae*) [438], and have been found to have frameshift mutations in *r2d2*, a core component of the siRNA pathway [439]. Similarly, virus infection has been correlated with deficiencies in RNAi in *C. elegans* [440]. This has led to the hypothesis that persistent infection leads to the alterations in the RNAi response in insects [438]. Whether the RNAi response is similarly altered by arboviruses in mosquitoes is undetermined. Another interesting avenue of future research would be the existence of a mechanism for systemic RNAi in mosquitoes, such as that described in *Drosophila* [292]. Future studies should address these and related points.

References

1. Gubler, D.J. The global emergence/resurgence of arboviral diseases as public health problems. *Arch. Med. Res.* **2002**, *33*, 330-342.
2. Ciota, A.T.; Kramer, L.D. Insights into arbovirus evolution and adaptation from experimental studies. *Viruses* **2010**, *2*, 2594-2617.
3. Michaud, V.; Randriamparany, T.; Albina, E. Comprehensive phylogenetic reconstructions of African swine fever virus: proposal for a new classification and molecular dating of the virus. *PLoS ONE* **2013**, *8*, e69662.
4. Control, U.S.C.f.D. Arbovirus Catalog Available online: <https://wwwn.cdc.gov/arbocat/default.aspx>
5. Bhatt, S.; Gething, P.W.; Brady, O.J.; Messina, J.P.; Farlow, A.W., et al. The global distribution and burden of dengue. *Nature* **2013**, *496*, 504-507.
6. Vega-Rua, A.; Zouache, K.; Girod, R.; Failloux, A.B.; Lourenco-de-Oliveira, R. High vector competence of *Aedes aegypti* and *Aedes albopictus* from ten American countries as a crucial factor of the spread of Chikungunya. *J. Virol.* **2014**.
7. Fischer, D.; Thomas, S.M.; Neteler, M.; Tjaden, N.B.; Beierkuhnlein, C. Climatic suitability of *Aedes albopictus* in Europe referring to climate change projections: comparison of mechanistic and correlative niche modelling approaches. *Euro Surveillance* **2014**, *19*.
8. Harrigan, R.J.; Thomassen, H.A.; Buermann, W.; Smith, T.B. A continental risk assessment of West Nile virus under climate change. *Glob Chang Biol* **2014**.
9. Kilpatrick, A.M.; Meola, M.A.; Moudy, R.M.; Kramer, L.D. Temperature, viral genetics, and the transmission of West Nile virus by *Culex pipiens* mosquitoes. *PLoS Pathog* **2008**, *4*, e1000092.
10. Durand, B.; Lecollinet, S.; Beck, C.; Martinez-Lopez, B.; Balenghien, T., et al. Identification of hotspots in the European union for the introduction of four zoonotic arboviroses by live animal trade. *PLoS ONE* **2013**, *8*, e70000.
11. Gubler, D.J. Resurgent vector-borne diseases as a global health problem. *Emerging Infect. Dis.* **1998**, *4*, 442-450.
12. Alphey, L.; Nimmo, D.; O'Connell, S.; Alphey, N. Insect population suppression using engineered insects. *Adv. Exp. Med. Biol.* **2008**, *627*, 93-103.
13. Alphey, L.; Benedict, M.; Bellini, R.; Clark, G.G.; Dame, D.A., et al. Sterile-insect methods for control of mosquito-borne diseases: an analysis. *Vector Borne Zoonotic Dis.* **2010**, *10*, 295-311.
14. Catteruccia, F.; Crisanti, A.; Wimmer, E.A. Transgenic technologies to induce sterility. *Malar J* **2009**, *8 Suppl 2*, S7.
15. Gemmell, N.J.; Jalilzadeh, A.; Didham, R.K.; Soboleva, T.; Tompkins, D.M. The Trojan female technique: a novel, effective and humane approach for pest population control. *Proc Biol Sci* **2013**, *280*, 20132549.
16. Adelman, Z.N.; Jasinskiene, N.; James, A.A. Development and applications of transgenesis in the yellow fever mosquito, *Aedes aegypti*. *Mol. Biochem. Parasitol.* **2002**, *121*, 1-10.

17. Facchinelli, L.; Valerio, L.; Ramsey, J.M.; Gould, F.; Walsh, R.K., et al. Field cage studies and progressive evaluation of genetically-engineered mosquitoes. *PLoS Negl Trop Dis* **2013**, *7*, e2001.
18. Franz, A.W.; Sanchez-Vargas, I.; Adelman, Z.N.; Blair, C.D.; Beaty, B.J., et al. Engineering RNA interference-based resistance to dengue virus type 2 in genetically modified *Aedes aegypti*. *Proc Natl Acad Sci U S A* **2006**, *103*, 4198-4203.
19. Travanty, E.A.; Adelman, Z.N.; Franz, A.W.; Keene, K.M.; Beaty, B.J., et al. Using RNA interference to develop dengue virus resistance in genetically modified *Aedes aegypti*. *Insect Biochem Mol Biol* **2004**, *34*, 607-613.
20. Olson, K.E.; Adelman, Z.N.; Travanty, E.A.; Sanchez-Vargas, I.; Beaty, B.J., et al. Developing arbovirus resistance in mosquitoes. *Insect Biochem. Mol. Biol.* **2002**, *32*, 1333-1343.
21. Degennaro, M.; McBride, C.S.; Seeholzer, L.; Nakagawa, T.; Dennis, E.J., et al. orco mutant mosquitoes lose strong preference for humans and are not repelled by volatile DEET. *Nature* **2013**.
22. Wise de Valdez, M.R.; Nimmo, D.; Betz, J.; Gong, H.F.; James, A.A., et al. Genetic elimination of dengue vector mosquitoes. *Proc Natl Acad Sci U S A* **2011**, *108*, 4772-4775.
23. Bian, G.; Zhou, G.; Lu, P.; Xi, Z. Replacing a native *Wolbachia* with a novel strain results in an increase in endosymbiont load and resistance to dengue virus in a mosquito vector. *PLoS Negl Trop Dis* **2013**, *7*, e2250.
24. Blagrove, M.S.; Arias-Goeta, C.; Failloux, A.B.; Sinkins, S.P. *Wolbachia* strain wMel induces cytoplasmic incompatibility and blocks dengue transmission in *Aedes albopictus*. *Proc Natl Acad Sci U S A* **2012**, *109*, 255-260.
25. Hoffmann, A.A.; Montgomery, B.L.; Popovici, J.; Iturbe-Ormaetxe, I.; Johnson, P.H., et al. Successful establishment of *Wolbachia* in *Aedes* populations to suppress dengue transmission. *Nature* **2011**, *476*, 454-457.
26. McMeniman, C.J.; Lane, R.V.; Cass, B.N.; Fong, A.W.; Sidhu, M., et al. Stable introduction of a life-shortening *Wolbachia* infection into the mosquito *Aedes aegypti*. *Science* **2009**, *323*, 141-144.
27. Moreira, L.A.; Iturbe-Ormaetxe, I.; Jeffery, J.A.; Lu, G.; Pyke, A.T., et al. A *Wolbachia* symbiont in *Aedes aegypti* limits infection with dengue, Chikungunya, and Plasmodium. *Cell* **2009**, *139*, 1268-1278.
28. Pan, X.; Zhou, G.; Wu, J.; Bian, G.; Lu, P., et al. *Wolbachia* induces reactive oxygen species (ROS)-dependent activation of the Toll pathway to control dengue virus in the mosquito *Aedes aegypti*. *Proc Natl Acad Sci U S A* **2012**, *109*, E23-31.
29. Walker, T.; Johnson, P.H.; Moreira, L.A.; Iturbe-Ormaetxe, I.; Frentiu, F.D., et al. The wMel *Wolbachia* strain blocks dengue and invades caged *Aedes aegypti* populations. *Nature* **2011**, *476*, 450-453.
30. Nene, V.; Wortman, J.R.; Lawson, D.; Haas, B.; Kodira, C., et al. Genome sequence of *Aedes aegypti*, a major arbovirus vector. *Science* **2007**, *316*, 1718-1723.
31. Arensburger, P.; Megy, K.; Waterhouse, R.M.; Abrudan, J.; Amedeo, P., et al. Sequencing of *Culex quinquefasciatus* establishes a platform for mosquito comparative genomics. *Science* **2010**, *330*, 86-88.

32. Holt, R.A.; Subramanian, G.M.; Halpern, A.; Sutton, G.G.; Charlab, R., et al. The genome sequence of the malaria mosquito *Anopheles gambiae*. *Science* **2002**, *298*, 129-149.
33. Adams, M.J.; King, A.M.; Carstens, E.B. Ratification vote on taxonomic proposals to the International Committee on Taxonomy of Viruses (2013). *Arch. Virol.* **2013**, *158*, 2023-2030.
34. Stapleton, J.T.; Fong, S.; Muerhoff, A.S.; Bukh, J.; Simmonds, P. The GB viruses: a review and proposed classification of GBV-A, GBV-C (HGV), and GBV-D in genus *Pegivirus* within the family *Flaviviridae*. *J. Gen. Virol.* **2011**, *92*, 233-246.
35. Fields, B.N.; Knipe, D.M.; Howley, P.M. *Fields Virology*; 5th ed.; Wolters Kluwer Health/Lippincott Williams & Wilkins: Philadelphia, 2007; p.^pp.
36. Peleg, J. Behaviour of infectious RNA from four different viruses in continuously subcultured *Aedes aegypti* mosquito embryo cells. *Nature* **1969**, *221*, 193-194.
37. Cleaves, G.R.; Dubin, D.T. Methylation status of intracellular dengue type 2 40 S RNA. *Virology* **1979**, *96*, 159-165.
38. Wengler, G.; Wengler, G.; Gross, H.J. Studies on virus-specific nucleic acids synthesized in vertebrate and mosquito cells infected with flaviviruses. *Virology* **1978**, *89*, 423-437.
39. Mukhopadhyay, S.; Kuhn, R.J.; Rossmann, M.G. A structural perspective of the flavivirus life cycle. *Nat. Rev. Microbiol.* **2005**, *3*, 13-22.
40. Staples, J.E.; Monath, T.P. Yellow fever: 100 years of discovery. *JAMA* **2008**, *300*, 960-962.
41. Murphy, F.A. Togavirus morphology and morphogenesis. In *The Togaviruses: Biology, Structure, Replication*; Schlesinger, R. W., Ed. Academic Press: New York, 1980; pp. 241-316.
42. Gollins, S.W.; Porterfield, J.S. Flavivirus infection enhancement in macrophages: an electron microscopic study of viral cellular entry. *J. Gen. Virol.* **1985**, *66* (Pt 9), 1969-1982.
43. Ishak, R.; Tovey, D.G.; Howard, C.R. Morphogenesis of yellow fever virus 17D in infected cell cultures. *J. Gen. Virol.* **1988**, *69* (Pt 2), 325-335.
44. Gollins, S.W.; Porterfield, J.S. The uncoating and infectivity of the flavivirus West Nile on interaction with cells: effects of pH and ammonium chloride. *J. Gen. Virol.* **1986**, *67* (Pt 9), 1941-1950.
45. Allison, S.L.; Schalich, J.; Stiasny, K.; Mandl, C.W.; Kunz, C., et al. Oligomeric rearrangement of tick-borne encephalitis virus envelope proteins induced by an acidic pH. *J. Virol.* **1995**, *69*, 695-700.
46. Gollins, S.W.; Porterfield, J.S. pH-dependent fusion between the flavivirus West Nile and liposomal model membranes. *J. Gen. Virol.* **1986**, *67* (Pt 1), 157-166.
47. Brinton, M.A. The molecular biology of West Nile Virus: a new invader of the western hemisphere. *Annu. Rev. Microbiol.* **2002**, *56*, 371-402.
48. Lindenbach, B.D.; Rice, C.M. Molecular biology of flaviviruses. *Adv. Virus Res.* **2003**, *59*, 23-61.
49. Kaufusi, P.H.; Kelley, J.F.; Yanagihara, R.; Nerurkar, V.R. Induction of endoplasmic reticulum-derived replication-competent membrane structures by West Nile virus non-structural protein 4B. *PLoS ONE* **2014**, *9*, e84040.

50. Ackermann, M.; Padmanabhan, R. De novo synthesis of RNA by the dengue virus RNA-dependent RNA polymerase exhibits temperature dependence at the initiation but not elongation phase. *J. Biol. Chem.* **2001**, *276*, 39926-39937.
51. Guyatt, K.J.; Westaway, E.G.; Khromykh, A.A. Expression and purification of enzymatically active recombinant RNA-dependent RNA polymerase (NS5) of the flavivirus Kunjin. *J. Virol. Methods* **2001**, *92*, 37-44.
52. Egloff, M.P.; Benarroch, D.; Selisko, B.; Romette, J.L.; Canard, B. An RNA cap (nucleoside-2'-O-)-methyltransferase in the flavivirus RNA polymerase NS5: crystal structure and functional characterization. *EMBO J.* **2002**, *21*, 2757-2768.
53. Gillespie, L.K.; Hoenen, A.; Morgan, G.; Mackenzie, J.M. The endoplasmic reticulum provides the membrane platform for biogenesis of the flavivirus replication complex. *J. Virol.* **2010**, *84*, 10438-10447.
54. Yu, L.; Takeda, K.; Markoff, L. Protein-protein interactions among West Nile non-structural proteins and transmembrane complex formation in mammalian cells. *Virology* **2013**, *446*, 365-377.
55. Mackenzie, J.M.; Westaway, E.G. Assembly and maturation of the flavivirus Kunjin virus appear to occur in the rough endoplasmic reticulum and along the secretory pathway, respectively. *J. Virol.* **2001**, *75*, 10787-10799.
56. Plevka, P.; Battisti, A.J.; Junjhon, J.; Winkler, D.C.; Holdaway, H.A., et al. Maturation of flaviviruses starts from one or more icosahedrally independent nucleation centres. *EMBO Rep* **2011**, *12*, 602-606.
57. Elshuber, S.; Allison, S.L.; Heinz, F.X.; Mandl, C.W. Cleavage of protein prM is necessary for infection of BHK-21 cells by tick-borne encephalitis virus. *J. Gen. Virol.* **2003**, *84*, 183-191.
58. Stadler, K.; Allison, S.L.; Schlich, J.; Heinz, F.X. Proteolytic activation of tick-borne encephalitis virus by furin. *J. Virol.* **1997**, *71*, 8475-8481.
59. Gubler, D.J.; Kuno, G.; Markoff, L. Flaviviruses. In *Fields Virology*; 5th ed.; Knipe, D. M.; Howley, P. M., Eds.; Lippincott Williams & Wilkins: Philadelphia, PA, 2007; Vol. 1, pp. 1153-1252.
60. Gould, E.A.; de Lamballerie, X.; Zanotto, P.M.; Holmes, E.C. Origins, evolution, and vector/host coadaptations within the genus Flavivirus. *Adv. Virus Res.* **2003**, *59*, 277-314.
61. Kuno, G.; Chang, G.J.; Tsuchiya, K.R.; Karabatsos, N.; Cropp, C.B. Phylogeny of the genus Flavivirus. *J. Virol.* **1998**, *72*, 73-83.
62. Billoir, F.; de Chesse, R.; Tolou, H.; de Micco, P.; Gould, E.A., et al. Phylogeny of the genus flavivirus using complete coding sequences of arthropod-borne viruses and viruses with no known vector. *J. Gen. Virol.* **2000**, *81 Pt 9*, 2339.
63. Calisher, C.H.; Karabatsos, N.; Dalrymple, J.M.; Shope, R.E.; Porterfield, J.S., et al. Antigenic relationships between flaviviruses as determined by cross-neutralization tests with polyclonal antisera. *J. Gen. Virol.* **1989**, *70 (Pt 1)*, 37-43.
64. Gaunt, M.W.; Sall, A.A.; de Lamballerie, X.; Falconar, A.K.; Dzhivanian, T.I., et al. Phylogenetic relationships of flaviviruses correlate with their epidemiology, disease association and biogeography. *J. Gen. Virol.* **2001**, *82*, 1867-1876.
65. Labuda, M.; Nuttall, P.A. Tick-borne viruses. *Parasitology* **2004**, *129 Suppl*, S221-245.

66. Fall, G.; Diallo, M.; Loucoubar, C.; Faye, O.; Sall, A.A. Vector Competence of *Culex neavei* and *Culex quinquefasciatus* (Diptera: Culicidae) from Senegal for Lineages 1, 2, Koutango and a Putative New Lineage of West Nile Virus. *Am. J. Trop. Med. Hyg.* **2014**, *90*, 747-754.
67. Ebel, G.D.; Kramer, L.D. West Nile Virus: Molecular Epidemiology and Diversity. In *West Nile Encephalitis Virus Infection*; Diamond, M. S., Ed. Springer: 2009.
68. Lanciotti, R.S.; Roehrig, J.T.; Deubel, V.; Smith, J.; Parker, M., et al. Origin of the West Nile virus responsible for an outbreak of encephalitis in the northeastern United States. *Science* **1999**, *286*, 2333-2337.
69. May, F.J.; Davis, C.T.; Tesh, R.B.; Barrett, A.D. Phylogeography of West Nile virus: from the cradle of evolution in Africa to Eurasia, Australia, and the Americas. *J. Virol.* **2011**, *85*, 2964-2974.
70. Hall, R.A.; Scherret, J.H.; Mackenzie, J.S. Kunjin virus: an Australian variant of West Nile? *Ann. N. Y. Acad. Sci.* **2001**, *951*, 153-160.
71. Lanciotti, R.S.; Ebel, G.D.; Deubel, V.; Kerst, A.J.; Murri, S., et al. Complete genome sequences and phylogenetic analysis of West Nile virus strains isolated from the United States, Europe, and the Middle East. *Virology* **2002**, *298*, 96-105.
72. Bakonyi, T.; Ivanics, E.; Erdelyi, K.; Ursu, K.; Ferenczi, E., et al. Lineage 1 and 2 strains of encephalitic West Nile virus, central Europe. *Emerging Infect. Dis.* **2006**, *12*, 618-623.
73. Bagnarelli, P.; Marinelli, K.; Trotta, D.; Monachetti, A.; Tavio, M., et al. Human case of autochthonous West Nile virus lineage 2 infection in Italy, September 2011. *Euro Surveill* **2011**, *16*.
74. Papa, A.; Xanthopoulou, K.; Gewehr, S.; Mourelatos, S. Detection of West Nile virus lineage 2 in mosquitoes during a human outbreak in Greece. *Clin. Microbiol. Infect.* **2011**, *17*, 1176-1180.
75. Chaintoutis, S.C.; Chaskopoulou, A.; Chassalevris, T.; Koehler, P.G.; Papanastassopoulou, M., et al. West Nile virus lineage 2 strain in Greece, 2012. *Emerging Infect. Dis.* **2013**, *19*, 827-829.
76. Pesko, K.N.; Ebel, G.D. West Nile virus population genetics and evolution. *Infect Genet Evol* **2011**.
77. *Virus Taxonomy: Ninth Report of the International Committee on Taxonomy of Viruses*; 1 ed.; Elsevier: 2012; p.^pp.
- 1327.
78. Charrel, R.N.; Brault, A.C.; Gallian, P.; Lemasson, J.J.; Murgue, B., et al. Evolutionary relationship between Old World West Nile virus strains. Evidence for viral gene flow between Africa, the Middle East, and Europe. *Virology* **2003**, *315*, 381-388.
79. Domingo, E.; Holland, J.J. RNA virus mutations and fitness for survival. *Annu. Rev. Microbiol.* **1997**, *51*, 151-178.
80. Holland, J.J.; De La Torre, J.C.; Steinhauer, D.A. RNA virus populations as quasispecies. *Curr. Top. Microbiol. Immunol.* **1992**, *176*, 1-20.
81. Lauring, A.S.; Frydman, J.; Andino, R. The role of mutational robustness in RNA virus evolution. *Nat. Rev. Microbiol.* **2013**, *11*, 327-336.

82. Sanjuan, R.; Nebot, M.R.; Chirico, N.; Mansky, L.M.; Belshaw, R. Viral mutation rates. *J. Virol.* **2010**, *84*, 9733-9748.
83. Eckerle, L.D.; Becker, M.M.; Halpin, R.A.; Li, K.; Venter, E., et al. Infidelity of SARS-CoV Nsp14-exonuclease mutant virus replication is revealed by complete genome sequencing. *PLoS Pathog* **2010**, *6*, e1000896.
84. Gnadig, N.F.; Beaucourt, S.; Campagnola, G.; Borderia, A.V.; Sanz-Ramos, M., et al. Coxsackievirus B3 mutator strains are attenuated in vivo. *Proc Natl Acad Sci U S A* **2012**, *109*, E2294-2303.
85. Graham, R.L.; Becker, M.M.; Eckerle, L.D.; Bolles, M.; Denison, M.R., et al. A live, impaired-fidelity coronavirus vaccine protects in an aged, immunocompromised mouse model of lethal disease. *Nat. Med.* **2012**, *18*, 1820-1826.
86. Sanjuan, R.; Moya, A.; Elena, S.F. The distribution of fitness effects caused by single-nucleotide substitutions in an RNA virus. *Proc Natl Acad Sci U S A* **2004**, *101*, 8396-8401.
87. Elena, S.F. RNA virus genetic robustness: possible causes and some consequences. *Curr Opin Virol* **2012**, *2*, 525-530.
88. Coffey, L.L.; Beeharry, Y.; Borderia, A.V.; Blanc, H.; Vignuzzi, M. Arbovirus high fidelity variant loses fitness in mosquitoes and mice. *Proc Natl Acad Sci U S A* **2011**, *108*, 16038-16043.
89. Tsetsarkin, K.A.; McGee, C.E.; Volk, S.M.; Vanlandingham, D.L.; Weaver, S.C., et al. Epistatic roles of E2 glycoprotein mutations in adaptation of chikungunya virus to *Aedes albopictus* and *Ae. aegypti* mosquitoes. *PLoS ONE* **2009**, *4*, e6835.
90. Gubler, D.J. The changing epidemiology of yellow fever and dengue, 1900 to 2003: full circle? *Comp. Immunol., Microbiol. Infect. Dis.* **2004**, *27*, 319-330.
91. Romano, A.P.; Costa, Z.G.; Ramos, D.G.; Andrade, M.A.; Jayme Vde, S., et al. Yellow Fever outbreaks in unvaccinated populations, Brazil, 2008-2009. *PLoS Negl Trop Dis* **2014**, *8*, e2740.
92. Soghaier, M.A.; Hagar, A.; Abbas, M.A.; Elmangory, M.M.; Eltahir, K.M., et al. Yellow Fever outbreak in Darfur, Sudan in October 2012; the initial outbreak investigation report. *J Infect Public Health* **2013**, *6*, 370-376.
93. Hu, Q.; Chen, B.; Zhu, Z.; Tian, J.; Zhou, Y., et al. Recurrence of Japanese encephalitis epidemic in Wuhan, China, 2009-2010. *PLoS ONE* **2013**, *8*, e52687.
94. Sarkar, A.; Taraphdar, D.; Mukhopadhyay, S.K.; Chakrabarti, S.; Chatterjee, S. Molecular evidence for the occurrence of Japanese encephalitis virus genotype I and III infection associated with acute encephalitis in patients of West Bengal, India, 2010. *Virol J* **2012**, *9*, 271.
95. Petersen, L.R.; Brault, A.C.; Nasci, R.S. West Nile virus: review of the literature. *JAMA* **2013**, *310*, 308-315.
96. Smithburn, K.C.; Hughes, T.P.; Burke, A.W.; Paul, J.H. A neurotropic virus isolated from the blood of a native of Uganda. *Am. J. Trop. Med. Hyg.* **1940**, *20*, 471-492.
97. Campbell, G.L.; Marfin, A.A.; Lanciotti, R.S.; Gubler, D.J. West Nile virus. *Lancet Infect. Dis.* **2002**, *2*, 519-529.
98. Murgue, B.; Murri, S.; Triki, H.; Deubel, V.; Zeller, H.G. West Nile in the Mediterranean basin: 1950-2000. *Ann. N. Y. Acad. Sci.* **2001**, *951*, 117-126.

99. Tsai, T.F.; Popovici, F.; Cernescu, C.; Campbell, G.L.; Nedelcu, N.I. West Nile encephalitis epidemic in southeastern Romania. *Lancet* **1998**, *352*, 767-771.
100. Centers for Disease, C.; Prevention Outbreak of West Nile-like viral encephalitis--New York, 1999. *MMWR. Morb. Mortal. Wkly. Rep.* **1999**, *48*, 845-849.
101. Briese, T.; Jia, X.Y.; Huang, C.; Grady, L.J.; Lipkin, W.I. Identification of a Kunjin/West Nile-like flavivirus in brains of patients with New York encephalitis. *Lancet* **1999**, *354*, 1261-1262.
102. Davis, C.T.; Ebel, G.D.; Lanciotti, R.S.; Brault, A.C.; Guzman, H., et al. Phylogenetic analysis of North American West Nile virus isolates, 2001-2004: evidence for the emergence of a dominant genotype. *Virology* **2005**, *342*, 252-265.
103. Snapinn, K.W.; Holmes, E.C.; Young, D.S.; Bernard, K.A.; Kramer, L.D., et al. Declining growth rate of West Nile virus in North America. *J. Virol.* **2007**, *81*, 2531-2534.
104. Moudy, R.M.; Meola, M.A.; Morin, L.L.; Ebel, G.D.; Kramer, L.D. A newly emergent genotype of West Nile virus is transmitted earlier and more efficiently by *Culex* mosquitoes. *Am J Trop Med Hyg* **2007**, *77*, 365-370.
105. Anderson, J.F.; Main, A.J.; Cheng, G.; Ferrandino, F.J.; Fikrig, E. Horizontal and vertical transmission of West Nile virus genotype NY99 by *Culex salinarius* and genotypes NY99 and WN02 by *Culex tarsalis*. *Am. J. Trop. Med. Hyg.* **2012**, *86*, 134-139.
106. Ebel, G.D.; Carricaburu, J.; Young, D.; Bernard, K.A.; Kramer, L.D. Genetic and phenotypic variation of West Nile virus in New York, 2000-2003. *Am J Trop Med Hyg* **2004**, *71*, 493-500.
107. Bessaud, M.; Peyrefitte, C.N.; Pastorino, B.A.; Tock, F.; Merle, O., et al. Chikungunya virus strains, Reunion Island outbreak. *Emerging Infect. Dis.* **2006**, *12*, 1604-1606.
108. Schuffenecker, I.; Itean, I.; Michault, A.; Murri, S.; Frangeul, L., et al. Genome microevolution of chikungunya viruses causing the Indian Ocean outbreak. *PLoS Med* **2006**, *3*, e263.
109. Tsetsarkin, K.A.; Vanlandingham, D.L.; McGee, C.E.; Higgs, S. A single mutation in chikungunya virus affects vector specificity and epidemic potential. *PLoS Path.* **2007**, *3*, e201.
110. Tsetsarkin, K.A.; Weaver, S.C. Sequential adaptive mutations enhance efficient vector switching by Chikungunya virus and its epidemic emergence. *PLoS Pathog* **2011**, *7*, e1002412.
111. Vazeille, M.; Moutailler, S.; Coudrier, D.; Rousseaux, C.; Khun, H., et al. Two Chikungunya isolates from the outbreak of La Reunion (Indian Ocean) exhibit different patterns of infection in the mosquito, *Aedes albopictus*. *PLoS ONE* **2007**, *2*, e1168.
112. Gilotra, S.K.; Rozeboom, L.E.; Bhattacharya, N.C. Observations on possible competitive displacement between populations of *Aedes aegypti* Linnaeus and *Aedes albopictus* Skuse in Calcutta. *Bull. W.H.O.* **1967**, *37*, 437-446.
113. Duncombe, J.; Espino, F.; Marollano, K.; Velazco, A.; Ritchie, S.A., et al. Characterising the spatial dynamics of sympatric *Aedes aegypti* and *Aedes albopictus* populations in the Philippines. *Geospat Health* **2013**, *8*, 255-265.
114. Kamgang, B.; Ngoagouni, C.; Manirakiza, A.; Nakoune, E.; Paupy, C., et al. Temporal patterns of abundance of *Aedes aegypti* and *Aedes albopictus* (Diptera: Culicidae) and

- mitochondrial DNA analysis of *Ae. albopictus* in the Central African Republic. *PLoS Negl Trop Dis* **2013**, *7*, e2590.
115. Paupy, C.; Ollomo, B.; Kamgang, B.; Moutailler, S.; Rousset, D., et al. Comparative role of *Aedes albopictus* and *Aedes aegypti* in the emergence of Dengue and Chikungunya in central Africa. *Vector Borne Zoonotic Dis.* **2010**, *10*, 259-266.
 116. Raharimalala, F.N.; Ravaomanarivo, L.H.; Ravelonandro, P.; Rafaraso, L.S.; Zouache, K., et al. Biogeography of the two major arbovirus mosquito vectors, *Aedes aegypti* and *Aedes albopictus* (Diptera, Culicidae), in Madagascar. *Parasit Vectors* **2012**, *5*, 56.
 117. Vazeille, M.; Jeannin, C.; Martin, E.; Schaffner, F.; Failloux, A.B. Chikungunya: a risk for Mediterranean countries? *Acta Trop.* **2008**, *105*, 200-202.
 118. Vazeille, M.; Moutailler, S.; Pages, F.; Jarjaval, F.; Failloux, A.B. Introduction of *Aedes albopictus* in Gabon: what consequences for dengue and chikungunya transmission? *Trop Med Int Health* **2008**, *13*, 1176-1179.
 119. Calisher, C.H. West Nile virus in the New World: appearance, persistence, and adaptation to a new niche--an opportunity taken. *Viral Immunol.* **2000**, *13*, 411-414.
 120. Jupp, P.G.; McIntosh, B.M.; Blackburn, N.K. Experimental assessment of the vector competence of *Culex (Culex) neavei* Theobald with West Nile and Sindbis viruses in South Africa. *Trans. R. Soc. Trop. Med. Hyg.* **1986**, *80*, 226-230.
 121. Sardelis, M.R.; Turell, M.J.; Dohm, D.J.; O'Guinn, M.L. Vector competence of selected North American *Culex* and *Coquillettidia* mosquitoes for West Nile virus. *Emerging Infect. Dis.* **2001**, *7*, 1018-1022.
 122. Turell, M.J.; O'Guinn, M.L.; Dohm, D.J.; Webb, J.P., Jr.; Sardelis, M.R. Vector competence of *Culex tarsalis* from Orange County, California, for West Nile virus. *Vector Borne Zoonotic Dis.* **2002**, *2*, 193-196.
 123. Turell, M.J.; Sardelis, M.R.; Dohm, D.J.; O'Guinn, M.L. Potential North American vectors of West Nile virus. *Ann. N. Y. Acad. Sci.* **2001**, *951*, 317-324.
 124. Ciota, A.T.; Kramer, L.D. Vector-virus interactions and transmission dynamics of west nile virus. *Viruses* **2013**, *5*, 3021-3047.
 125. Ebel, G.D.; Rochlin, I.; Longacker, J.; Kramer, L.D. *Culex restuans* (Diptera: Culicidae) relative abundance and vector competence for West Nile Virus. *J Med Entomol* **2005**, *42*, 838-843.
 126. Goddard, L.B.; Roth, A.E.; Reisen, W.K.; Scott, T.W. Vector competence of California mosquitoes for West Nile virus. *Emerging Infect. Dis.* **2002**, *8*, 1385-1391.
 127. Turell, M.J.; Dohm, D.J.; Sardelis, M.R.; Oguinn, M.L.; Andreadis, T.G., et al. An update on the potential of north American mosquitoes (Diptera: Culicidae) to transmit West Nile Virus. *J. Med. Entomol.* **2005**, *42*, 57-62.
 128. Turell, M.J.; O'Guinn, M.; Oliver, J. Potential for New York mosquitoes to transmit West Nile virus. *Am. J. Trop. Med. Hyg.* **2000**, *62*, 413-414.
 129. Kilpatrick, A.M.; Fonseca, D.M.; Ebel, G.D.; Reddy, M.R.; Kramer, L.D. Spatial and temporal variation in vector competence of *Culex pipiens* and *Cx. restuans* mosquitoes for West Nile virus. *Am. J. Trop. Med. Hyg.* **2010**, *83*, 607-613.
 130. Hubalek, Z.; Halouzka, J. West Nile fever--a reemerging mosquito-borne viral disease in Europe. *Emerging Infect. Dis.* **1999**, *5*, 643-650.

131. Moskvitina, N.S.; Romanenko, V.N.; Ternovoi, V.A.; Ivanova, N.V.; Protopopova, E.V., et al. [Detection of the West Nile Virus and its genetic typing in ixodid ticks (Parasitiformes: Ixodidae) in Tomsk City and its suburbs]. *Parazitologija* **2008**, *42*, 210-225.
132. Mumcuoglu, K.Y.; Banet-Noach, C.; Malkinson, M.; Shalom, U.; Galun, R. Argasid ticks as possible vectors of West Nile virus in Israel. *Vector Borne Zoonotic Dis.* **2005**, *5*, 65-71.
133. Reiter, P. West Nile virus in Europe: understanding the present to gauge the future. *Euro Surveill* **2010**, *15*, 19508.
134. Hagman, K.; Barboutis, C.; Ehrenborg, C.; Fransson, T.; Jaenson, T.G., et al. On the potential roles of ticks and migrating birds in the ecology of West Nile virus. *Infect Ecol Epidemiol* **2014**, *4*.
135. Abbassy, M.M.; Osman, M.; Marzouk, A.S. West Nile virus (Flaviviridae:Flavivirus) in experimentally infected Argas ticks (Acari:Argasidae). *Am. J. Trop. Med. Hyg.* **1993**, *48*, 726-737.
136. Hutcheson, H.J.; Gorham, C.H.; Machain-Williams, C.; Lorono-Pino, M.A.; James, A.M., et al. Experimental transmission of West Nile virus (Flaviviridae: Flavivirus) by *Carios capensis* ticks from North America. *Vector Borne Zoonotic Dis.* **2005**, *5*, 293-295.
137. Komar, N.; Langevin, S.; Hinten, S.; Nemeth, N.; Edwards, E., et al. Experimental infection of North American birds with the New York 1999 strain of West Nile virus. *Emerging Infect. Dis.* **2003**, *9*, 311-322.
138. Work, T.H.; Hurlbut, H.S.; Taylor, R.M. Indigenous wild birds of the Nile Delta as potential West Nile virus circulating reservoirs. *Am. J. Trop. Med. Hyg.* **1955**, *4*, 872-888.
139. Austin, R.J.; Whiting, T.L.; Anderson, R.A.; Drebot, M.A. An outbreak of West Nile virus-associated disease in domestic geese (*Anser anser domesticus*) upon initial introduction to a geographic region, with evidence of bird to bird transmission. *Can. Vet. J.* **2004**, *45*, 117-123.
140. Banet-Noach, C.; Simanov, L.; Malkinson, M. Direct (non-vector) transmission of West Nile virus in geese. *Avian Pathol* **2003**, *32*, 489-494.
141. Kipp, A.M.; Lehman, J.A.; Bowen, R.A.; Fox, P.E.; Stephens, M.R., et al. West Nile virus quantification in feces of experimentally infected American and fish crows. *Am. J. Trop. Med. Hyg.* **2006**, *75*, 688-690.
142. Nemeth, N.M.; Thomsen, B.V.; Spraker, T.R.; Benson, J.M.; Bosco-Lauth, A.M., et al. Clinical and pathologic responses of American crows (*Corvus brachyrhynchos*) and fish crows (*C. ossifragus*) to experimental West Nile virus infection. *Vet. Pathol.* **2011**, *48*, 1061-1074.
143. Shirafuji, H.; Kanehira, K.; Kubo, M.; Shibahara, T.; Kamio, T. Experimental West Nile virus infection in jungle crows (*Corvus macrorhynchos*). *Am. J. Trop. Med. Hyg.* **2008**, *78*, 838-842.
144. Grubaugh, N.D., personal communication. In 2014.
145. Kramer, L.D.; Bernard, K.A. West Nile virus in the western hemisphere. *Curr. Opin. Infect. Dis.* **2001**, *14*, 519-525.
146. Brault, A.C.; Huang, C.Y.; Langevin, S.A.; Kinney, R.M.; Bowen, R.A., et al. A single positively selected West Nile viral mutation confers increased virogenesis in American crows. *Nat. Genet.* **2007**, *39*, 1162-1166.

147. van der Meulen, K.M.; Pensaert, M.B.; Nauwynck, H.J. West Nile virus in the vertebrate world. *Arch. Virol.* **2005**, *150*, 637-657.
148. Jacobson, E.R.; Ginn, P.E.; Troutman, J.M.; Farina, L.; Stark, L., et al. West Nile virus infection in farmed American alligators (*Alligator mississippiensis*) in Florida. *J. Wildl. Dis.* **2005**, *41*, 96-106.
149. Klenk, K.; Snow, J.; Morgan, K.; Bowen, R.; Stephens, M., et al. Alligators as West Nile virus amplifiers. *Emerging Infect. Dis.* **2004**, *10*, 2150-2155.
150. Miller, D.L.; Mauel, M.J.; Baldwin, C.; Burtle, G.; Ingram, D., et al. West Nile virus in farmed alligators. *Emerging Infect. Dis.* **2003**, *9*, 794-799.
151. Nevarez, J.G.; Mitchell, M.A.; Morgan, T.; Roy, A.; Johnson, A. Association of West Nile virus with lymphohistiocytic proliferative cutaneous lesions in American alligators (*Alligator mississippiensis*) detected by RT-PCR. *J Zoo Wildl Med* **2008**, *39*, 562-566.
152. Unlu, I.; Kramer, W.L.; Roy, A.F.; Foil, L.D. Detection of West Nile virus RNA in mosquitoes and identification of mosquito blood meals collected at alligator farms in Louisiana. *J. Med. Entomol.* **2010**, *47*, 625-633.
153. Machain-Williams, C.; Padilla-Paz, S.E.; Weber, M.; Cetina-Trejo, R.; Juarez-Ordaz, J.A., et al. Antibodies to West Nile virus in wild and farmed crocodiles in southeastern Mexico. *J. Wildl. Dis.* **2013**, *49*, 690-693.
154. Steinman, A.; Banet-Noach, C.; Tal, S.; Levi, O.; Simanov, L., et al. West Nile virus infection in crocodiles. *Emerging Infect. Dis.* **2003**, *9*, 887-889.
155. Steinman, A.; Banet-Noach, C.; Simanov, L.; Grinfeld, N.; Aizenberg, Z., et al. Experimental infection of common garter snakes (*Thamnophis sirtalis*) with West Nile virus. *Vector Borne Zoonotic Dis.* **2006**, *6*, 361-368.
156. Shortridge, K.F.; Ng, M.H.; Oya, A.; Kobayashi, M.; Munro, R., et al. Arbovirus infections in reptiles: immunological evidence for a high incidence of Japanese encephalitis virus in the cobra *Naja naja*. *Trans. R. Soc. Trop. Med. Hyg.* **1974**, *68*, 454-460.
157. Graham, S.P.; Hassan, H.K.; Chapman, T.; White, G.; Guyer, C., et al. Serosurveillance of eastern equine encephalitis virus in amphibians and reptiles from Alabama, USA. *Am. J. Trop. Med. Hyg.* **2012**, *86*, 540-544.
158. Bowen, G.S. Prolonged western equine encephalitis viremia in the Texas tortoise (*Gopherus berlandieri*). *Am. J. Trop. Med. Hyg.* **1977**, *26*, 171-175.
159. Prior, M.G.; Agnew, R.M. Antibody against Western equine encephalitis virus occurring in the serum of garter snakes (Colubridae: *Thamnophis*) in Saskatchewan. *Can. J. Comp. Med.* **1971**, *35*, 40-43.
160. Gebhardt, L.P.; Stanton, G.J.; Hill, D.W.; Collett, G.C. Natural Overwintering Hosts of the Virus of Western Equine Encephalitis. *New Engl. J. Med.* **1964**, *271*, 172-177.
161. Gebhardt, L.P.; Hill, D.W. Overwintering of Western equine encephalitis virus. *Proc. Soc. Exp. Biol. Med.* **1960**, *104*, 695-698.
162. Bowen, R.A.; Nemeth, N.M. Experimental infections with West Nile virus. *Curr. Opin. Infect. Dis.* **2007**, *20*, 293-297.
163. Bernard, K.A.; Maffei, J.G.; Jones, S.A.; Kauffman, E.B.; Ebel, G., et al. West Nile virus infection in birds and mosquitoes, New York State, 2000. *Emerging Infect. Dis.* **2001**, *7*, 679-685.

164. Kilpatrick, A.M.; Kramer, L.D.; Campbell, S.R.; Alleyne, E.O.; Dobson, A.P., et al. West Nile virus risk assessment and the bridge vector paradigm. *Emerging Infect. Dis.* **2005**, *11*, 425-429.
165. Bell, J.A.; Brewer, C.M.; Mickelson, N.J.; Garman, G.W.; Vaughan, J.A. West Nile virus epizootiology, central Red River Valley, North Dakota and Minnesota, 2002-2005. *Emerging Infect. Dis.* **2006**, *12*, 1245-1247.
166. Goldberg, T.L.; Anderson, T.K.; Hamer, G.L. West Nile virus may have hitched a ride across the Western United States on *Culex tarsalis* mosquitoes. *Mol. Ecol.* **2010**, *19*, 1518-1519.
167. Molaei, G.; Cummings, R.F.; Su, T.; Armstrong, P.M.; Williams, G.A., et al. Vector-host interactions governing epidemiology of West Nile virus in Southern California. *Am. J. Trop. Med. Hyg.* **2010**, *83*, 1269-1282.
168. Vitek, C.J.; Richards, S.L.; Mores, C.N.; Day, J.F.; Lord, C.C. Arbovirus transmission by *Culex nigripalpus* in Florida, 2005. *J. Med. Entomol.* **2008**, *45*, 483-493.
169. Barrera, R.; MacKay, A.; Amador, M.; Vasquez, J.; Smith, J., et al. Mosquito vectors of West Nile virus during an epizootic outbreak in Puerto Rico. *J. Med. Entomol.* **2010**, *47*, 1185-1195.
170. Karpf, A.R.; Brown, D.T. Comparison of Sindbis virus-induced pathology in mosquito and vertebrate cell cultures. *Virology* **1998**, *240*, 193-201.
171. Li, Y.G.; Siripanyaphinyo, U.; Tumkosit, U.; Noranate, N.; A, A.n., et al. Chikungunya virus induces a more moderate cytopathic effect in mosquito cells than in mammalian cells. *Intervirology* **2013**, *56*, 6-12.
172. Bowers, D.F.; Coleman, C.G.; Brown, D.T. Sindbis virus-associated pathology in *Aedes albopictus* (Diptera: Culicidae). *J Med Entomol* **2003**, *40*, 698-705.
173. Girard, Y.A.; Popov, V.; Wen, J.; Han, V.; Higgs, S. Ultrastructural study of West Nile virus pathogenesis in *Culex pipiens quinquefasciatus* (Diptera: Culicidae). *J Med Entomol* **2005**, *42*, 429-444.
174. Girard, Y.A.; Schneider, B.S.; McGee, C.E.; Wen, J.; Han, V.C., et al. Salivary gland morphology and virus transmission during long-term cytopathologic West Nile virus infection in *Culex* mosquitoes. *Am J Trop Med Hyg* **2007**, *76*, 118-128.
175. Kelly, E.M.; Moon, D.C.; Bowers, D.F. Apoptosis in mosquito salivary glands: Sindbis virus-associated and tissue homeostasis. *J Gen Virol* **2012**, *93*, 2419-2424.
176. Mims, C.A.; Day, M.F.; Marshall, I.D. Cytopathic effect of Semliki Forest virus in the mosquito *Aedes aegypti*. *Am J Trop Med Hyg* **1966**, *15*, 775-784.
177. Vaidyanathan, R.; Scott, T.W. Apoptosis in mosquito midgut epithelia associated with West Nile virus infection. *Apoptosis* **2006**, *11*, 1643-1651.
178. Weaver, S.C.; Lorenz, L.H.; Scott, T.W. Pathologic changes in the midgut of *Culex tarsalis* following infection with Western equine encephalomyelitis virus. *Am J Trop Med Hyg* **1992**, *47*, 691-701.
179. Weaver, S.C.; Scott, T.W.; Lorenz, L.H.; Lerdthusnee, K.; Romoser, W.S. Togavirus-associated pathologic changes in the midgut of a natural mosquito vector. *J. Virol.* **1988**, *62*, 2083-2090.

180. Ciota, A.T.; Styer, L.M.; Meola, M.A.; Kramer, L.D. The costs of infection and resistance as determinants of West Nile virus susceptibility in *Culex* mosquitoes. *BMC Ecol.* **2011**, *11*, 23.
181. Dohm, D.J.; Romoser, W.S.; Turell, M.J.; Linthicum, K.J. Impact of stressful conditions on the survival of *Culex pipiens* exposed to Rift Valley fever virus. *J. Am. Mosq. Control Assoc.* **1991**, *7*, 621-623.
182. Patrican, L.A.; DeFoliart, G.R. Lack of adverse effect of transovarially acquired La Crosse virus infection on the reproductive capacity of *Aedes triseriatus* (Diptera: Culicidae). *J. Med. Entomol.* **1985**, *22*, 604-611.
183. Putnam, J.L.; Scott, T.W. Blood-feeding behavior of dengue-2 virus-infected *Aedes aegypti*. *Am. J. Trop. Med. Hyg.* **1995**, *52*, 225-227.
184. Styer, L.M.; Meola, M.A.; Kramer, L.D. West Nile virus infection decreases fecundity of *Culex tarsalis* females. *J. Med. Entomol.* **2007**, *44*, 1074-1085.
185. Jackson, B.T.; Brewster, C.C.; Paulson, S.L. La Crosse virus infection alters blood feeding behavior in *Aedes triseriatus* and *Aedes albopictus* (Diptera: Culicidae). *J. Med. Entomol.* **2012**, *49*, 1424-1429.
186. Lambrechts, L.; Scott, T.W. Mode of transmission and the evolution of arbovirus virulence in mosquito vectors. *Proc Biol Sci* **2009**, *276*, 1369-1378.
187. Whitfield, S.G.; Murphy, F.A.; Sudia, W.D. St. Louis encephalitis virus: an ultrastructural study of infection in a mosquito vector. *Virology* **1973**, *56*, 70-87.
188. Marsh, M.; Matlin, K.; Simons, K.; Reggio, H.; White, J., et al. Are lysosomes a site of enveloped-virus penetration? *Cold Spring Harbor Symp. Quant. Biol.* **1982**, *46 Pt 2*, 835-843.
189. Salazar, M.I.; Richardson, J.H.; Sanchez-Vargas, I.; Olson, K.E.; Beaty, B.J. Dengue virus type 2: replication and tropisms in orally infected *Aedes aegypti* mosquitoes. *BMC Microbiol.* **2007**, *7*, 9.
190. Smith, D.R.; Adams, A.P.; Kenney, J.L.; Wang, E.; Weaver, S.C. Venezuelan equine encephalitis virus in the mosquito vector *Aedes taeniorhynchus*: infection initiated by a small number of susceptible epithelial cells and a population bottleneck. *Virology* **2008**, *372*, 176-186.
191. Scholle, F.; Girard, Y.A.; Zhao, Q.; Higgs, S.; Mason, P.W. trans-Packaged West Nile virus-like particles: infectious properties in vitro and in infected mosquito vectors. *J. Virol.* **2004**, *78*, 11605-11614.
192. Cheng, G.; Cox, J.; Wang, P.; Krishnan, M.N.; Dai, J., et al. A C-type lectin collaborates with a CD45 phosphatase homolog to facilitate West Nile virus infection of mosquitoes. *Cell* **2010**, *142*, 714-725.
193. Perera-Lecoin, M.; Meertens, L.; Carnec, X.; Amara, A. Flavivirus entry receptors: an update. *Viruses* **2014**, *6*, 69-88.
194. Liu, Y.; Zhang, F.; Liu, J.; Xiao, X.; Zhang, S., et al. Transmission-blocking antibodies against mosquito C-type lectins for dengue prevention. *PLoS Pathog* **2014**, *10*, e1003931.
195. Salas-Benito, J.; Reyes-Del Valle, J.; Salas-Benito, M.; Ceballos-Olvera, I.; Mosso, C., et al. Evidence that the 45-kD glycoprotein, part of a putative dengue virus receptor complex

- in the mosquito cell line C6/36, is a heat-shock related protein. *Am. J. Trop. Med. Hyg.* **2007**, *77*, 283-290.
196. Vega-Almeida, T.O.; Salas-Benito, M.; De Nova-Ocampo, M.A.; Del Angel, R.M.; Salas-Benito, J.S. Surface proteins of C6/36 cells involved in dengue virus 4 binding and entry. *Arch. Virol.* **2013**, *158*, 1189-1207.
 197. Sakoonwatanyoo, P.; Boonsanay, V.; Smith, D.R. Growth and production of the dengue virus in C6/36 cells and identification of a laminin-binding protein as a candidate serotype 3 and 4 receptor protein. *Intervirology* **2006**, *49*, 161-172.
 198. Kuadkitkan, A.; Wikan, N.; Fongsaran, C.; Smith, D.R. Identification and characterization of prohibitin as a receptor protein mediating DENV-2 entry into insect cells. *Virology* **2010**, *406*, 149-161.
 199. Khoo, C.C.; Piper, J.; Sanchez-Vargas, I.; Olson, K.E.; Franz, A.W. The RNA interference pathway affects midgut infection- and escape barriers for Sindbis virus in *Aedes aegypti*. *BMC Microbiol.* **2010**, *10*, 130.
 200. Chamberlain, R.W.; Sudia, W.D. Mechanism of transmission of viruses by mosquitoes. *Annu. Rev. Entomol.* **1961**, *6*, 371-390.
 201. Kramer, L.D.; Hardy, J.L.; Presser, S.B.; Houk, E.J. Dissemination barriers for western equine encephalomyelitis virus in *Culex tarsalis* infected after ingestion of low viral doses. *Am. J. Trop. Med. Hyg.* **1981**, *30*, 190-197.
 202. Hardy, J.L.; Houk, E.J.; Kramer, L.D.; Reeves, W.C. Intrinsic factors affecting vector competence of mosquitoes for arboviruses. *Annu. Rev. Entomol.* **1983**, *28*, 229-262.
 203. Grimstad, P.R.; Paulson, S.L.; Craig, G.B., Jr. Vector competence of *Aedes hendersoni* (Diptera: Culicidae) for La Crosse virus and evidence of a salivary-gland escape barrier. *J. Med. Entomol.* **1985**, *22*, 447-453.
 204. Chen, Y.; Maguire, T.; Hileman, R.E.; Fromm, J.R.; Esko, J.D., et al. Dengue virus infectivity depends on envelope protein binding to target cell heparan sulfate. *Nat. Med.* **1997**, *3*, 866-871.
 205. Germe, R.; Crance, J.M.; Garin, D.; Guimet, J.; Lortat-Jacob, H., et al. Heparan sulfate-mediated binding of infectious dengue virus type 2 and yellow fever virus. *Virology* **2002**, *292*, 162-168.
 206. Hilgard, P.; Stockert, R. Heparan sulfate proteoglycans initiate dengue virus infection of hepatocytes. *Hepatology* **2000**, *32*, 1069-1077.
 207. Kroschewski, H.; Allison, S.L.; Heinz, F.X.; Mandl, C.W. Role of heparan sulfate for attachment and entry of tick-borne encephalitis virus. *Virology* **2003**, *308*, 92-100.
 208. Lee, E.; Pavy, M.; Young, N.; Freeman, C.; Lobigs, M. Antiviral effect of the heparan sulfate mimetic, PI-88, against dengue and encephalitic flaviviruses. *Antiviral Res.* **2006**, *69*, 31-38.
 209. Okamoto, K.; Kinoshita, H.; Parquet Mdel, C.; Raekiansyah, M.; Kimura, D., et al. Dengue virus strain DEN2 16681 utilizes a specific glycochain of syndecan-2 proteoglycan as a receptor. *J. Gen. Virol.* **2012**, *93*, 761-770.
 210. Das, S.; Laxminarayana, S.V.; Chandra, N.; Ravi, V.; Desai, A. Heat shock protein 70 on Neuro2a cells is a putative receptor for Japanese encephalitis virus. *Virology* **2009**, *385*, 47-57.

211. Zhu, Y.Z.; Cao, M.M.; Wang, W.B.; Wang, W.; Ren, H., et al. Association of heat-shock protein 70 with lipid rafts is required for Japanese encephalitis virus infection in Huh7 cells. *J. Gen. Virol.* **2012**, *93*, 61-71.
212. Thongtan, T.; Wikan, N.; Wintachai, P.; Rattanasungsan, C.; Srisomsap, C., et al. Characterization of putative Japanese encephalitis virus receptor molecules on microglial cells. *J. Med. Virol.* **2012**, *84*, 615-623.
213. Reyes-Del Valle, J.; Chavez-Salinas, S.; Medina, F.; Del Angel, R.M. Heat shock protein 90 and heat shock protein 70 are components of dengue virus receptor complex in human cells. *J. Virol.* **2005**, *79*, 4557-4567.
214. Cabrera-Hernandez, A.; Thepparit, C.; Suksanpaisan, L.; Smith, D.R. Dengue virus entry into liver (HepG2) cells is independent of hsp90 and hsp70. *J. Med. Virol.* **2007**, *79*, 386-392.
215. Jindadamrongwech, S.; Thepparit, C.; Smith, D.R. Identification of GRP 78 (BiP) as a liver cell expressed receptor element for dengue virus serotype 2. *Arch. Virol.* **2004**, *149*, 915-927.
216. Davis, C.W.; Nguyen, H.Y.; Hanna, S.L.; Sanchez, M.D.; Doms, R.W., et al. West Nile virus discriminates between DC-SIGN and DC-SIGNR for cellular attachment and infection. *J. Virol.* **2006**, *80*, 1290-1301.
217. Tassaneetrithep, B.; Burgess, T.H.; Granelli-Piperno, A.; Trumfheller, C.; Finke, J., et al. DC-SIGN (CD209) mediates dengue virus infection of human dendritic cells. *J. Exp. Med.* **2003**, *197*, 823-829.
218. Navarro-Sanchez, E.; Altmeyer, R.; Amara, A.; Schwartz, O.; Fieschi, F., et al. Dendritic-cell-specific ICAM3-grabbing non-integrin is essential for the productive infection of human dendritic cells by mosquito-cell-derived dengue viruses. *EMBO Rep* **2003**, *4*, 723-728.
219. Mondotte, J.A.; Lozach, P.Y.; Amara, A.; Gamarnik, A.V. Essential role of dengue virus envelope protein N glycosylation at asparagine-67 during viral propagation. *J. Virol.* **2007**, *81*, 7136-7148.
220. Davis, C.W.; Mattei, L.M.; Nguyen, H.Y.; Ansarah-Sobrinho, C.; Doms, R.W., et al. The location of asparagine-linked glycans on West Nile virions controls their interactions with CD209 (dendritic cell-specific ICAM-3 grabbing nonintegrin). *J. Biol. Chem.* **2006**, *281*, 37183-37194.
221. Dejnirattisai, W.; Webb, A.I.; Chan, V.; Jumnainsong, A.; Davidson, A., et al. Lectin switching during dengue virus infection. *J. Infect. Dis.* **2011**, *203*, 1775-1783.
222. Miller, J.L.; de Wet, B.J.; Martinez-Pomares, L.; Radcliffe, C.M.; Dwek, R.A., et al. The mannose receptor mediates dengue virus infection of macrophages. *PLoS Pathog* **2008**, *4*, e17.
223. Chen, S.T.; Lin, Y.L.; Huang, M.T.; Wu, M.F.; Cheng, S.C., et al. CLEC5A is critical for dengue-virus-induced lethal disease. *Nature* **2008**, *453*, 672-676.
224. Thepparit, C.; Smith, D.R. Serotype-specific entry of dengue virus into liver cells: identification of the 37-kilodalton/67-kilodalton high-affinity laminin receptor as a dengue virus serotype 1 receptor. *J. Virol.* **2004**, *78*, 12647-12656.

225. Meertens, L.; Carnec, X.; Lecoin, M.P.; Ramdasi, R.; Guivel-Benhassine, F., et al. The TIM and TAM families of phosphatidylserine receptors mediate dengue virus entry. *Cell Host Microbe* **2012**, *12*, 544-557.
226. Jemielity, S.; Wang, J.J.; Chan, Y.K.; Ahmed, A.A.; Li, W., et al. TIM-family proteins promote infection of multiple enveloped viruses through virion-associated phosphatidylserine. *PLoS Pathog* **2013**, *9*, e1003232.
227. Chu, J.J.; Ng, M.L. Interaction of West Nile virus with alpha v beta 3 integrin mediates virus entry into cells. *J. Biol. Chem.* **2004**, *279*, 54533-54541.
228. Chu, J.J.; Ng, M.L. Characterization of a 105-kDa plasma membrane associated glycoprotein that is involved in West Nile virus binding and infection. *Virology* **2003**, *312*, 458-469.
229. Li, Y.; Kakinami, C.; Li, Q.; Yang, B.; Li, H. Human apolipoprotein A-I is associated with dengue virus and enhances virus infection through SR-BI. *PLoS ONE* **2013**, *8*, e70390.
230. Che, P.; Tang, H.; Li, Q. The interaction between claudin-1 and dengue viral prM/M protein for its entry. *Virology* **2013**, *446*, 303-313.
231. Gao, F.; Duan, X.; Lu, X.; Liu, Y.; Zheng, L., et al. Novel binding between pre-membrane protein and claudin-1 is required for efficient dengue virus entry. *Biochem. Biophys. Res. Commun.* **2010**, *391*, 952-957.
232. Hershkovitz, O.; Rosental, B.; Rosenberg, L.A.; Navarro-Sanchez, M.E.; Jivov, S., et al. NKp44 receptor mediates interaction of the envelope glycoproteins from the West Nile and dengue viruses with NK cells. *J. Immunol.* **2009**, *183*, 2610-2621.
233. Lim, P.Y.; Behr, M.J.; Chadwick, C.M.; Shi, P.Y.; Bernard, K.A. Keratinocytes are cell targets of West Nile virus in vivo. *J. Virol.* **2011**, *85*, 5197-5201.
234. Cho, H.; Diamond, M.S. Immune responses to West Nile virus infection in the central nervous system. *Viruses* **2012**, *4*, 3812-3830.
235. Petersen, L.R.; Carson, P.J.; Biggerstaff, B.J.; Custer, B.; Borchardt, S.M., et al. Estimated cumulative incidence of West Nile virus infection in US adults, 1999-2010. *Epidemiol. Infect.* **2013**, *141*, 591-595.
236. Lindsey, N.P.; Staples, J.E.; Lehman, J.A.; Fischer, M.; Centers for Disease, C., et al. Surveillance for human West Nile virus disease - United States, 1999-2008. *MMWR. Surveill. Summ.* **2010**, *59*, 1-17.
237. Carson, P.J.; Borchardt, S.M.; Custer, B.; Prince, H.E.; Dunn-Williams, J., et al. Neuroinvasive disease and West Nile virus infection, North Dakota, USA, 1999-2008. *Emerging Infect. Dis.* **2012**, *18*, 684-686.
238. Bode, A.V.; Sejvar, J.J.; Pape, W.J.; Campbell, G.L.; Marfin, A.A. West Nile virus disease: a descriptive study of 228 patients hospitalized in a 4-county region of Colorado in 2003. *Clin. Infect. Dis.* **2006**, *42*, 1234-1240.
239. Lindsey, N.P.; Staples, J.E.; Lehman, J.A.; Fischer, M. Medical risk factors for severe West Nile Virus disease, United States, 2008-2010. *Am. J. Trop. Med. Hyg.* **2012**, *87*, 179-184.
240. Murray, K.; Baraniuk, S.; Resnick, M.; Arafat, R.; Kilborn, C., et al. Risk factors for encephalitis and death from West Nile virus infection. *Epidemiol. Infect.* **2006**, *134*, 1325-1332.
241. Zimmerman, P.A.; Buckler-White, A.; Alkhatib, G.; Spalding, T.; Kubofcik, J., et al. Inherited resistance to HIV-1 conferred by an inactivating mutation in CC chemokine

- receptor 5: studies in populations with contrasting clinical phenotypes, defined racial background, and quantified risk. *Mol. Med.* **1997**, *3*, 23-36.
242. Hill, A.V. The immunogenetics of human infectious diseases. *Annu. Rev. Immunol.* **1998**, *16*, 593-617.
243. Glass, W.G.; McDermott, D.H.; Lim, J.K.; Lekhong, S.; Yu, S.F., et al. CCR5 deficiency increases risk of symptomatic West Nile virus infection. *J. Exp. Med.* **2006**, *203*, 35-40.
244. Ishikawa, T.; Yamanaka, A.; Konishi, E. A review of successful flavivirus vaccines and the problems with those flaviviruses for which vaccines are not yet available. *Vaccine* **2014**, *32*, 1326-1337.
245. Petrovsky, N.; Larena, M.; Siddharthan, V.; Prow, N.A.; Hall, R.A., et al. An inactivated cell culture Japanese encephalitis vaccine (JE-ADVAX) formulated with delta inulin adjuvant provides robust heterologous protection against West Nile encephalitis via cross-protective memory B cells and neutralizing antibody. *J. Virol.* **2013**, *87*, 10324-10333.
246. Brandler, S.; Tangy, F. Vaccines in development against West Nile virus. *Viruses* **2013**, *5*, 2384-2409.
247. Heinz, F.X.; Stiasny, K. Flaviviruses and flavivirus vaccines. *Vaccine* **2012**, *30*, 4301-4306.
248. Dayan, G.H.; Pugachev, K.; Bevilacqua, J.; Lang, J.; Monath, T.P. Preclinical and clinical development of a YFV 17 D-based chimeric vaccine against West Nile virus. *Viruses* **2013**, *5*, 3048-3070.
249. Biedenbender, R.; Bevilacqua, J.; Gregg, A.M.; Watson, M.; Dayan, G. Phase II, randomized, double-blind, placebo-controlled, multicenter study to investigate the immunogenicity and safety of a West Nile virus vaccine in healthy adults. *J. Infect. Dis.* **2011**, *203*, 75-84.
250. Dayan, G.H.; Bevilacqua, J.; Coleman, D.; Buldo, A.; Risi, G. Phase II, dose ranging study of the safety and immunogenicity of single dose West Nile vaccine in healthy adults \geq 50 years of age. *Vaccine* **2012**, *30*, 6656-6664.
251. Tang, F.; Zhang, J.S.; Liu, W.; Zhao, Q.M.; Zhang, F., et al. Failure of Japanese encephalitis vaccine and infection in inducing neutralizing antibodies against West Nile virus, People's Republic of China. *Am. J. Trop. Med. Hyg.* **2008**, *78*, 999-1001.
252. Yamshchikov, G.; Borisevich, V.; Kwok, C.W.; Nistler, R.; Kohlmeier, J., et al. The suitability of yellow fever and Japanese encephalitis vaccines for immunization against West Nile virus. *Vaccine* **2005**, *23*, 4785-4792.
253. Lobigs, M.; Pavy, M.; Hall, R.A.; Lobigs, P.; Cooper, P., et al. An inactivated Vero cell-grown Japanese encephalitis vaccine formulated with Advax, a novel inulin-based adjuvant, induces protective neutralizing antibody against homologous and heterologous flaviviruses. *J. Gen. Virol.* **2010**, *91*, 1407-1417.
254. Goverdhan, M.K.; Kulkarni, A.B.; Gupta, A.K.; Tupe, C.D.; Rodrigues, J.J. Two-way cross-protection between West Nile and Japanese encephalitis viruses in bonnet macaques. *Acta Virol.* **1992**, *36*, 277-283.
255. Tesh, R.B.; Travassos da Rosa, A.P.; Guzman, H.; Araujo, T.P.; Xiao, S.Y. Immunization with heterologous flaviviruses protective against fatal West Nile encephalitis. *Emerging Infect. Dis.* **2002**, *8*, 245-251.

256. Takasaki, T.; Yabe, S.; Nerome, R.; Ito, M.; Yamada, K., et al. Partial protective effect of inactivated Japanese encephalitis vaccine on lethal West Nile virus infection in mice. *Vaccine* **2003**, *21*, 4514-4518.
257. Larena, M.; Prow, N.A.; Hall, R.A.; Petrovsky, N.; Lobigs, M. JE-ADVAX vaccine protection against Japanese encephalitis virus mediated by memory B cells in the absence of CD8(+) T cells and pre-exposure neutralizing antibody. *J. Virol.* **2013**, *87*, 4395-4402.
258. Honda-Okubo, Y.; Saade, F.; Petrovsky, N. Advax, a polysaccharide adjuvant derived from delta inulin, provides improved influenza vaccine protection through broad-based enhancement of adaptive immune responses. *Vaccine* **2012**, *30*, 5373-5381.
259. Kanesa-Thanan, N.; Putnak, J.R.; Mangiafico, J.A.; Saluzzo, J.E.; Ludwig, G.V. Short report: absence of protective neutralizing antibodies to West Nile virus in subjects following vaccination with Japanese encephalitis or dengue vaccines. *Am. J. Trop. Med. Hyg.* **2002**, *66*, 115-116.
260. Zohrabian, A.; Hayes, E.B.; Petersen, L.R. Cost-effectiveness of West Nile virus vaccination. *Emerging Infect. Dis.* **2006**, *12*, 375-380.
261. Prasad, A.N.; Brackney, D.E.; Ebel, G.D. The role of innate immunity in conditioning mosquito susceptibility to west nile virus. *Viruses* **2013**, *5*, 3142-3170.
262. Lindbo, J.A.; Silva-Rosales, L.; Proebsting, W.M.; Dougherty, W.G. Induction of a Highly Specific Antiviral State in Transgenic Plants: Implications for Regulation of Gene Expression and Virus Resistance. *Plant Cell* **1993**, *5*, 1749-1759.
263. Ratcliff, F.; Harrison, B.D.; Baulcombe, D.C. A similarity between viral defense and gene silencing in plants. *Science* **1997**, *276*, 1558-1560.
264. Fire, A.; Xu, S.; Montgomery, M.K.; Kostas, S.A.; Driver, S.E., et al. Potent and specific genetic interference by double-stranded RNA in *Caenorhabditis elegans*. *Nature* **1998**, *391*, 806-811.
265. Kennerdell, J.R.; Carthew, R.W. Use of dsRNA-mediated genetic interference to demonstrate that *frizzled* and *frizzled 2* act in the wingless pathway. *Cell* **1998**, *95*, 1017-1026.
266. Liu, Q.; Rand, T.A.; Kalidas, S.; Du, F.; Kim, H.E., et al. R2D2, a bridge between the initiation and effector steps of the *Drosophila* RNAi pathway. *Science* **2003**, *301*, 1921-1925.
267. Yang, Z.; Ebright, Y.W.; Yu, B.; Chen, X. HEN1 recognizes 21-24 nt small RNA duplexes and deposits a methyl group onto the 2' OH of the 3' terminal nucleotide. *Nucleic Acids Res* **2006**, *34*, 667-675.
268. Horwich, M.D.; Li, C.; Matranga, C.; Vagin, V.; Farley, G., et al. The *Drosophila* RNA methyltransferase, DmHen1, modifies germline piRNAs and single-stranded siRNAs in RISC. *Curr Biol* **2007**, *17*, 1265-1272.
269. Rand, T.A.; Ginalski, K.; Grishin, N.V.; Wang, X. Biochemical identification of Argonaute 2 as the sole protein required for RNA-induced silencing complex activity. *Proc Natl Acad Sci U S A* **2004**, *101*, 14385-14389.
270. Pusch, O.; Boden, D.; Silbermann, R.; Lee, F.; Tucker, L., et al. Nucleotide sequence homology requirements of HIV-1-specific short hairpin RNA. *Nucleic Acids Res* **2003**, *31*, 6444-6449.

271. Westerhout, E.M.; Ooms, M.; Vink, M.; Das, A.T.; Berkhout, B. HIV-1 can escape from RNA interference by evolving an alternative structure in its RNA genome. *Nucleic Acids Res* **2005**, *33*, 796-804.
272. Aliyari, R.; Wu, Q.; Li, H.W.; Wang, X.H.; Li, F., et al. Mechanism of induction and suppression of antiviral immunity directed by virus-derived small RNAs in *Drosophila*. *Cell Host Microbe* **2008**, *4*, 387-397.
273. Galiana-Arnoux, D.; Dostert, C.; Schneemann, A.; Hoffmann, J.A.; Imler, J.L. Essential function in vivo for Dicer-2 in host defense against RNA viruses in *drosophila*. *Nat. Immunol.* **2006**, *7*, 590-597.
274. van Rij, R.P.; Saleh, M.C.; Berry, B.; Foo, C.; Houk, A., et al. The RNA silencing endonuclease Argonaute 2 mediates specific antiviral immunity in *Drosophila melanogaster*. *Genes Dev* **2006**, *20*, 2985-2995.
275. Keene, K.M.; Foy, B.D.; Sanchez-Vargas, I.; Beaty, B.J.; Blair, C.D., et al. RNA interference acts as a natural antiviral response to O'nyong-nyong virus (Alphavirus; Togaviridae) infection of *Anopheles gambiae*. *Proc Natl Acad Sci U S A* **2004**, *101*, 17240-17245.
276. Myles, K.M.; Wiley, M.R.; Morazzani, E.M.; Adelman, Z.N. Alphavirus-derived small RNAs modulate pathogenesis in disease vector mosquitoes. *Proc Natl Acad Sci U S A* **2008**, *105*, 19938-19943.
277. Campbell, C.L.; Keene, K.M.; Brackney, D.E.; Olson, K.E.; Blair, C.D., et al. *Aedes aegypti* uses RNA interference in defense against Sindbis virus infection. *BMC Microbiol.* **2008**, *8*, 47.
278. Sanchez-Vargas, I.; Scott, J.C.; Poole-Smith, B.K.; Franz, A.W.; Barbosa-Solomieu, V., et al. Dengue virus type 2 infections of *Aedes aegypti* are modulated by the mosquito's RNA interference pathway. *PLoS Pathog* **2009**, *5*, e1000299.
279. Chotkowski, H.L.; Ciota, A.T.; Jia, Y.; Puig-Basagoiti, F.; Kramer, L.D., et al. West Nile virus infection of *Drosophila melanogaster* induces a protective RNAi response. *Virology* **2008**, *377*, 197-206.
280. Brackney, D.E.; Scott, J.C.; Sagawa, F.; Woodward, J.E.; Miller, N.A., et al. C6/36 *Aedes albopictus* cells have a dysfunctional antiviral RNA interference response. *PLoS Negl Trop Dis* **2010**, *4*, e856.
281. Scott, J.C.; Brackney, D.E.; Campbell, C.L.; Bondu-Hawkins, V.; Hjelle, B., et al. Comparison of dengue virus type 2-specific small RNAs from RNA interference-competent and -incompetent mosquito cells. *PLoS Negl Trop Dis* **2010**, *4*, e848.
282. Morazzani, E.M.; Wiley, M.R.; Murreddu, M.G.; Adelman, Z.N.; Myles, K.M. Production of Virus-Derived Ping-Pong-Dependent piRNA-like Small RNAs in the Mosquito Soma. *PLoS Pathog* **2012**, *8*, e1002470.
283. Brackney, D.E.; Beane, J.E.; Ebel, G.D. RNAi targeting of West Nile virus in mosquito midguts promotes virus diversification. *PLoS Pathog* **2009**, *5*, e1000502.
284. Konishi, M.; Wu, C.H.; Kaito, M.; Hayashi, K.; Watanabe, S., et al. siRNA-resistance in treated HCV replicon cells is correlated with the development of specific HCV mutations. *J. Viral Hepat.* **2006**, *13*, 756-761.
285. Martínez, F.; Lafforgue, G.; Morelli, M.J.; González-Candelas, F.; Chua, N.-H., et al. Ultradeep Sequencing Analysis of Population Dynamics of Virus Escape Mutants in RNAi-Mediated Resistant Plants. *Mol Biol Evol* **2012**, *29*, 3297-3307.

286. Gitlin, L.; Stone, J.K.; Andino, R. Poliovirus escape from RNA interference: short interfering RNA-target recognition and implications for therapeutic approaches. *J. Virol.* **2005**, *79*, 1027-1035.
287. Jerzak, G.; Bernard, K.A.; Kramer, L.D.; Ebel, G.D. Genetic variation in West Nile virus from naturally infected mosquitoes and birds suggests quasispecies structure and strong purifying selection. *J Gen Virol* **2005**, *86*, 2175-2183.
288. Voinnet, O. Non-cell autonomous RNA silencing. *FEBS Lett.* **2005**, *579*, 5858-5871.
289. Feinberg, E.H.; Hunter, C.P. Transport of dsRNA into cells by the transmembrane protein SID-1. *Science* **2003**, *301*, 1545-1547.
290. Winston, W.M.; Molodowitch, C.; Hunter, C.P. Systemic RNAi in *C. elegans* requires the putative transmembrane protein SID-1. *Science* **2002**, *295*, 2456-2459.
291. Saleh, M.C.; van Rij, R.P.; Hekele, A.; Gillis, A.; Foley, E., et al. The endocytic pathway mediates cell entry of dsRNA to induce RNAi silencing. *Nat Cell Biol* **2006**, *8*, 793-802.
292. Saleh, M.C.; Tassetto, M.; van Rij, R.P.; Goic, B.; Gausson, V., et al. Antiviral immunity in *Drosophila* requires systemic RNA interference spread. *Nature* **2009**, *458*, 346-350.
293. Attarzadeh-Yazdi, G.; Fragkoudis, R.; Chi, Y.; Siu, R.W.; Ulper, L., et al. Cell-to-cell spread of the RNA interference response suppresses Semliki Forest virus (SFV) infection of mosquito cell cultures and cannot be antagonized by SFV. *J. Virol.* **2009**, *83*, 5735-5748.
294. Sijen, T.; Fleenor, J.; Simmer, F.; Thijssen, K.L.; Parrish, S., et al. On the role of RNA amplification in dsRNA-triggered gene silencing. *Cell* **2001**, *107*, 465-476.
295. Pak, J.; Fire, A. Distinct populations of primary and secondary effectors during RNAi in *C. elegans*. *Science* **2007**, *315*, 241-244.
296. Sijen, T.; Steiner, F.A.; Thijssen, K.L.; Plasterk, R.H. Secondary siRNAs result from unprimed RNA synthesis and form a distinct class. *Science* **2007**, *315*, 244-247.
297. Goic, B.; Vodovar, N.; Mondotte, J.A.; Monot, C.; Frangeul, L., et al. RNA-mediated interference and reverse transcription control the persistence of RNA viruses in the insect model *Drosophila*. *Nat. Immunol.* **2013**, *14*, 396-403.
298. Rechavi, O.; Minevich, G.; Hobert, O. Transgenerational inheritance of an acquired small RNA-based antiviral response in *C. elegans*. *Cell* **2011**, *147*, 1248-1256.
299. Deddouche, S.; Matt, N.; Budd, A.; Mueller, S.; Kemp, C., et al. The DExD/H-box helicase Dicer-2 mediates the induction of antiviral activity in *drosophila*. *Nat. Immunol.* **2008**, *9*, 1425-1432.
300. Paradkar, P.N.; Trinidad, L.; Voysey, R.; Duchemin, J.B.; Walker, P.J. Secreted Vago restricts West Nile virus infection in *Culex* mosquito cells by activating the Jak-STAT pathway. *Proc Natl Acad Sci U S A* **2012**, *109*, 18915-18920.
301. Lin, H.; Spradling, A.C. A novel group of pumilio mutations affects the asymmetric division of germline stem cells in the *Drosophila* ovary. *Development* **1997**, *124*, 2463-2476.
302. Aravin, A.; Gaidatzis, D.; Pfeffer, S.; Lagos-Quintana, M.; Landgraf, P., et al. A novel class of small RNAs bind to MILI protein in mouse testes. *Nature* **2006**, *442*, 203-207.
303. Girard, A.; Sachidanandam, R.; Hannon, G.J.; Carmell, M.A. A germline-specific class of small RNAs binds mammalian Piwi proteins. *Nature* **2006**, *442*, 199-202.
304. Grivna, S.T.; Beyret, E.; Wang, Z.; Lin, H. A novel class of small RNAs in mouse spermatogenic cells. *Genes Dev* **2006**, *20*, 1709-1714.

305. Saito, K.; Nishida, K.M.; Mori, T.; Kawamura, Y.; Miyoshi, K., et al. Specific association of Piwi with rasiRNAs derived from retrotransposon and heterochromatic regions in the *Drosophila* genome. *Genes Dev* **2006**, *20*, 2214-2222.
306. Watanabe, T.; Takeda, A.; Tsukiyama, T.; Mise, K.; Okuno, T., et al. Identification and characterization of two novel classes of small RNAs in the mouse germline: retrotransposon-derived siRNAs in oocytes and germline small RNAs in testes. *Genes Dev* **2006**, *20*, 1732-1743.
307. Saito, K.; Sakaguchi, Y.; Suzuki, T.; Siomi, H.; Siomi, M.C. Pimet, the *Drosophila* homolog of HEN1, mediates 2'-O-methylation of Piwi- interacting RNAs at their 3' ends. *Genes Dev* **2007**, *21*, 1603-1608.
308. Lee, E.J.; Banerjee, S.; Zhou, H.; Jammalamadaka, A.; Arcila, M., et al. Identification of piRNAs in the central nervous system. *RNA* **2011**, *17*, 1090-1099.
309. Yan, Z.; Hu, H.Y.; Jiang, X.; Maierhofer, V.; Neb, E., et al. Widespread expression of piRNA-like molecules in somatic tissues. *Nucleic Acids Res* **2011**, *39*, 6596-6607.
310. Nishida, K.M.; Saito, K.; Mori, T.; Kawamura, Y.; Nagami-Okada, T., et al. Gene silencing mechanisms mediated by Aubergine piRNA complexes in *Drosophila* male gonad. *RNA* **2007**, *13*, 1911-1922.
311. Brennecke, J.; Aravin, A.A.; Stark, A.; Dus, M.; Kellis, M., et al. Discrete small RNA-generating loci as master regulators of transposon activity in *Drosophila*. *Cell* **2007**, *128*, 1089-1103.
312. Gunawardane, L.S.; Saito, K.; Nishida, K.M.; Miyoshi, K.; Kawamura, Y., et al. A slicer-mediated mechanism for repeat-associated siRNA 5' end formation in *Drosophila*. *Science* **2007**, *315*, 1587-1590.
313. Schnettler, E.; Donald, C.L.; Human, S.; Watson, M.; Siu, R.W., et al. Knockdown of piRNA pathway proteins results in enhanced Semliki Forest virus production in mosquito cells. *J. Gen. Virol.* **2013**, *94*, 1680-1689.
314. Wu, Q.; Luo, Y.; Lu, R.; Lau, N.; Lai, E.C., et al. Virus discovery by deep sequencing and assembly of virus-derived small silencing RNAs. *Proc Natl Acad Sci U S A* **2010**, *107*, 1606-1611.
315. Hess, A.M.; Prasad, A.N.; Ptitsyn, A.; Ebel, G.D.; Olson, K.E., et al. Small RNA profiling of Dengue virus-mosquito interactions implicates the PIWI RNA pathway in anti-viral defense. *BMC Microbiol.* **2011**, *11*, 45.
316. Vodovar, N.; Bronkhorst, A.W.; van Cleef, K.W.; Miesen, P.; Blanc, H., et al. Arbovirus-Derived piRNAs Exhibit a Ping-Pong Signature in Mosquito Cells. *PLoS ONE* **2012**, *7*, e30861.
317. Leger, P.; Lara, E.; Jagla, B.; Sismeiro, O.; Mansuroglu, Z., et al. Dicer-2 and Piwi Mediated Rna Interference in Rift Valley Fever Virus Infected Mosquito Cells. *J. Virol.* **2012**.
318. Schnettler, E.; Ratinier, M.; Watson, M.; Shaw, A.E.; McFarlane, M., et al. RNA interference targets arbovirus replication in *Culicoides* cells. *J. Virol.* **2012**.
319. Li, H.; Li, W.X.; Ding, S.W. Induction and suppression of RNA silencing by an animal virus. *Science* **2002**, *296*, 1319-1321.

320. Blakqori, G.; Delhay, S.; Habjan, M.; Blair, C.D.; Sanchez-Vargas, I., et al. La Crosse bunyavirus nonstructural protein NSs serves to suppress the type I interferon system of mammalian hosts. *J. Virol.* **2007**, *81*, 4991-4999.
321. Soldan, S.S.; Plassmeyer, M.L.; Matukonis, M.K.; Gonzalez-Scarano, F. La Crosse virus nonstructural protein NSs counteracts the effects of short interfering RNA. *J. Virol.* **2005**, *79*, 234-244.
322. Kakumani, P.K.; Ponia, S.S.; S, R.K.; Sood, V.; Chinnappan, M., et al. Role of RNA interference (RNAi) in dengue virus replication and identification of NS4B as an RNAi suppressor. *J. Virol.* **2013**, *87*, 8870-8883.
323. Pijlman, G.P.; Funk, A.; Kondratieva, N.; Leung, J.; Torres, S., et al. A highly structured, nuclease-resistant, noncoding RNA produced by flaviviruses is required for pathogenicity. *Cell Host Microbe* **2008**, *4*, 579-591.
324. Funk, A.; Truong, K.; Nagasaki, T.; Torres, S.; Floden, N., et al. RNA structures required for production of subgenomic flavivirus RNA. *J. Virol.* **2010**, *84*, 11407-11417.
325. Silva, P.A.; Pereira, C.F.; Dalebout, T.J.; Spaan, W.J.; Bredenbeek, P.J. An RNA pseudoknot is required for production of yellow fever virus subgenomic RNA by the host nuclease XRN1. *J. Virol.* **2010**, *84*, 11395-11406.
326. Schnettler, E.; Sterken, M.G.; Leung, J.Y.; Metz, S.W.; Geertsema, C., et al. Noncoding flavivirus RNA displays RNA interference suppressor activity in insect and Mammalian cells. *J. Virol.* **2012**, *86*, 13486-13500.
327. Ding, S.W.; Voinnet, O. Antiviral immunity directed by small RNAs. *Cell* **2007**, *130*, 413-426.
328. Moon, S.L.; Anderson, J.R.; Kumagai, Y.; Wilusz, C.J.; Akira, S., et al. A noncoding RNA produced by arthropod-borne flaviviruses inhibits the cellular exoribonuclease XRN1 and alters host mRNA stability. *RNA* **2012**, *18*, 2029-2040.
329. Christensen, B.M.; Li, J.; Chen, C.C.; Nappi, A.J. Melanization immune responses in mosquito vectors. *Trends Parasitol* **2005**, *21*, 192-199.
330. Lemaitre, B.; Hoffmann, J. The host defense of *Drosophila melanogaster*. *Annu. Rev. Immunol.* **2007**, *25*, 697-743.
331. Anderson, K.V.; Bokla, L.; Nusslein-Volhard, C. Establishment of dorsal-ventral polarity in the *Drosophila* embryo: the induction of polarity by the Toll gene product. *Cell* **1985**, *42*, 791-798.
332. Lemaitre, B.; Meister, M.; Govind, S.; Georgel, P.; Steward, R., et al. Functional analysis and regulation of nuclear import of dorsal during the immune response in *Drosophila*. *EMBO J* **1995**, *14*, 536-545.
333. Lemaitre, B.; Reichhart, J.M.; Hoffmann, J.A. *Drosophila* host defense: differential induction of antimicrobial peptide genes after infection by various classes of microorganisms. *Proc Natl Acad Sci U S A* **1997**, *94*, 14614-14619.
334. Zambon, R.A.; Nandakumar, M.; Vakharia, V.N.; Wu, L.P. The Toll pathway is important for an antiviral response in *Drosophila*. *Proc Natl Acad Sci U S A* **2005**, *102*, 7257-7262.
335. Xi, Z.; Ramirez, J.L.; Dimopoulos, G. The *Aedes aegypti* toll pathway controls dengue virus infection. *PLoS Pathog* **2008**, *4*, e1000098.

336. Ramirez, J.L.; Dimopoulos, G. The Toll immune signaling pathway control conserved anti-dengue defenses across diverse *Ae. aegypti* strains and against multiple dengue virus serotypes. *Dev Comp Immunol* **2010**, *34*, 625-629.
337. Luplertlop, N.; Surasombatpattana, P.; Patramool, S.; Dumas, E.; Wasinpiyamongkol, L., et al. Induction of a peptide with activity against a broad spectrum of pathogens in the *Aedes aegypti* salivary gland, following Infection with Dengue Virus. *PLoS Pathog* **2011**, *7*, e1001252.
338. Sanders, H.R.; Foy, B.D.; Evans, A.M.; Ross, L.S.; Beaty, B.J., et al. Sindbis virus induces transport processes and alters expression of innate immunity pathway genes in the midgut of the disease vector, *Aedes aegypti*. *Insect Biochem Mol Biol* **2005**, *35*, 1293-1307.
339. Colpitts, T.M.; Cox, J.; Vanlandingham, D.L.; Feitosa, F.M.; Cheng, G., et al. Alterations in the *Aedes aegypti* transcriptome during infection with West Nile, dengue and yellow fever viruses. *PLoS Pathog* **2011**, *7*, e1002189.
340. Fragkoudis, R.; Chi, Y.; Siu, R.W.; Barry, G.; Attarzadeh-Yazdi, G., et al. Semliki Forest virus strongly reduces mosquito host defence signaling. *Insect Mol Biol* **2008**, *17*, 647-656.
341. Bartholomay, L.C.; Waterhouse, R.M.; Mayhew, G.F.; Campbell, C.L.; Michel, K., et al. Pathogenomics of *Culex quinquefasciatus* and meta-analysis of infection responses to diverse pathogens. *Science* **2010**, *330*, 88-90.
342. Corbo, J.C.; Levine, M. Characterization of an immunodeficiency mutant in *Drosophila*. *Mech Dev* **1996**, *55*, 211-220.
343. Levashina, E.A.; Ohresser, S.; Lemaitre, B.; Imler, J.L. Two distinct pathways can control expression of the gene encoding the *Drosophila* antimicrobial peptide metchnikowin. *J Mol Biol* **1998**, *278*, 515-527.
344. Costa, A.; Jan, E.; Sarnow, P.; Schneider, D. The Imd pathway is involved in antiviral immune responses in *Drosophila*. *PLoS ONE* **2009**, *4*, e7436.
345. De Gregorio, E.; Spellman, P.T.; Tzou, P.; Rubin, G.M.; Lemaitre, B. The Toll and Imd pathways are the major regulators of the immune response in *Drosophila*. *EMBO J* **2002**, *21*, 2568-2579.
346. Avadhanula, V.; Weasner, B.P.; Hardy, G.G.; Kumar, J.P.; Hardy, R.W. A novel system for the launch of alphavirus RNA synthesis reveals a role for the Imd pathway in arthropod antiviral response. *PLoS Pathog* **2009**, *5*, e1000582.
347. Huang, Z.; Kingsolver, M.B.; Avadhanula, V.; Hardy, R.W. An antiviral role for antimicrobial peptides during the arthropod response to alphavirus replication. *J. Virol.* **2013**, *87*, 4272-4280.
348. Tsai, C.W.; McGraw, E.A.; Ammar, E.D.; Dietzgen, R.G.; Hogenhout, S.A. *Drosophila melanogaster* mounts a unique immune response to the Rhabdovirus sigma virus. *Appl Environ Microbiol* **2008**, *74*, 3251-3256.
349. Dostert, C.; Jouanguy, E.; Irving, P.; Troxler, L.; Galiana-Arnoux, D., et al. The Jak-STAT signaling pathway is required but not sufficient for the antiviral response of *drosophila*. *Nat. Immunol.* **2005**, *6*, 946-953.
350. Waldock, J.; Olson, K.E.; Christophides, G.K. *Anopheles gambiae* antiviral immune response to systemic O'nyong-nyong infection. *PLoS Negl Trop Dis* **2012**, *6*, e1565.

351. Yan, R.; Small, S.; Desplan, C.; Dearolf, C.R.; Darnell, J.E., Jr. Identification of a Stat gene that functions in Drosophila development. *Cell* **1996**, *84*, 421-430.
352. Brown, S.; Hu, N.; Hombria, J.C. Identification of the first invertebrate interleukin JAK/STAT receptor, the Drosophila gene domeless. *Curr Biol* **2001**, *11*, 1700-1705.
353. Binari, R.; Perrimon, N. Stripe-specific regulation of pair-rule genes by hopscotch, a putative Jak family tyrosine kinase in Drosophila. *Genes Dev* **1994**, *8*, 300-312.
354. Kemp, C.; Mueller, S.; Goto, A.; Barbier, V.; Paro, S., et al. Broad RNA interference-mediated antiviral immunity and virus-specific inducible responses in Drosophila. *J Immunol* **2013**, *190*, 650-658.
355. Souza-Neto, J.A.; Sim, S.; Dimopoulos, G. An evolutionary conserved function of the JAK-STAT pathway in anti-dengue defense. *Proc Natl Acad Sci U S A* **2009**, *106*, 17841-17846.
356. Popham, H.J.; Shelby, K.S.; Brandt, S.L.; Coudron, T.A. Potent virucidal activity in larval *Heliothis virescens* plasma against *Helicoverpa zea* single capsid nucleopolyhedrovirus. *J Gen Virol* **2004**, *85*, 2255-2261.
357. Shelby, K.S.; Popham, H.J. Plasma phenoloxidase of the larval tobacco budworm, *Heliothis virescens*, is virucidal. *J Insect Sci* **2006**, *6*, 1-12.
358. Zhao, P.; Lu, Z.; Strand, M.R.; Jiang, H. Antiviral, anti-parasitic, and cytotoxic effects of 5,6-dihydroxyindole (DHI), a reactive compound generated by phenoloxidase during insect immune response. *Insect Biochem Mol Biol* **2011**, *41*, 645-652.
359. Tamang, D.; Tseng, S.M.; Huang, C.Y.; Tsao, I.Y.; Chou, S.Z., et al. The use of a double subgenomic Sindbis virus expression system to study mosquito gene function: effects of antisense nucleotide number and duration of viral infection on gene silencing efficiency. *Insect Mol Biol* **2004**, *13*, 595-602.
360. Rodriguez-Andres, J.; Rani, S.; Varjak, M.; Chase-Topping, M.E.; Beck, M.H., et al. Phenoloxidase activity acts as a mosquito innate immune response against infection with Semliki Forest virus. *PLoS Pathog* **2012**, *8*, e1002977.
361. Gutierrez, M.G.; Master, S.S.; Singh, S.B.; Taylor, G.A.; Colombo, M.I., et al. Autophagy is a defense mechanism inhibiting BCG and *Mycobacterium tuberculosis* survival in infected macrophages. *Cell* **2004**, *119*, 753-766.
362. Ling, Y.M.; Shaw, M.H.; Ayala, C.; Coppens, I.; Taylor, G.A., et al. Vacuolar and plasma membrane stripping and autophagic elimination of *Toxoplasma gondii* in primed effector macrophages. *J Exp Med* **2006**, *203*, 2063-2071.
363. Kudchodkar, S.B.; Levine, B. Viruses and autophagy. *Rev Med Virol* **2009**, *19*, 359-378.
364. Elmore, S. Apoptosis: a review of programmed cell death. *Toxicol Pathol* **2007**, *35*, 495-516.
365. Best, S.M. Viral subversion of apoptotic enzymes: escape from death row. *Annu Rev Microbiol* **2008**, *62*, 171-192.
366. Levine, B.; Mizushima, N.; Virgin, H.W. Autophagy in immunity and inflammation. *Nature* **2011**, *469*, 323-335.
367. Tanida, I. Autophagy basics. *Microbiol. Immunol.* **2011**, *55*, 1-11.
368. Shelly, S.; Lukinova, N.; Bambina, S.; Berman, A.; Cherry, S. Autophagy is an essential component of Drosophila immunity against vesicular stomatitis virus. *Immunity* **2009**, *30*, 588-598.

369. Nakamoto, M.; Moy, R.H.; Xu, J.; Bambina, S.; Yasunaga, A., et al. Virus recognition by Toll-7 activates antiviral autophagy in *Drosophila*. *Immunity* **2012**, *36*, 658-667.
370. Kerr, J.F.; Wyllie, A.H.; Currie, A.R. Apoptosis: a basic biological phenomenon with wide-ranging implications in tissue kinetics. *Br. J. Cancer* **1972**, *26*, 239-257.
371. Fulda, S.; Debatin, K.M. Extrinsic versus intrinsic apoptosis pathways in anticancer chemotherapy. *Oncogene* **2006**, *25*, 4798-4811.
372. Courtiade, J.; Pauchet, Y.; Vogel, H.; Heckel, D.G. A comprehensive characterization of the caspase gene family in insects from the order Lepidoptera. *BMC Genomics* **2011**, *12*, 357.
373. Settles, E.W.; Friesen, P.D. Flock house virus induces apoptosis by depletion of *Drosophila* inhibitor-of-apoptosis protein DIAP1. *J. Virol.* **2008**, *82*, 1378-1388.
374. Vandergaast, R.; Schultz, K.L.; Cerio, R.J.; Friesen, P.D. Active depletion of host cell inhibitor-of-apoptosis proteins triggers apoptosis upon baculovirus DNA replication. *J. Virol.* **2011**, *85*, 8348-8358.
375. Hershberger, P.A.; Dickson, J.A.; Friesen, P.D. Site-specific mutagenesis of the 35-kilodalton protein gene encoded by *Autographa californica* nuclear polyhedrosis virus: cell line-specific effects on virus replication. *J. Virol.* **1992**, *66*, 5525-5533.
376. Clem, R.J.; Miller, L.K. Apoptosis reduces both the in vitro replication and the in vivo infectivity of a baculovirus. *J. Virol.* **1993**, *67*, 3730-3738.
377. Liu, B.; Behura, S.K.; Clem, R.J.; Schneemann, A.; Becnel, J., et al. P53-mediated rapid induction of apoptosis conveys resistance to viral infection in *Drosophila melanogaster*. *PLoS Pathog* **2013**, *9*, e1003137.
378. Wang, H.; Blair, C.D.; Olson, K.E.; Clem, R.J. Effects of inducing or inhibiting apoptosis on Sindbis virus replication in mosquito cells. *J Gen Virol* **2008**, *89*, 2651-2661.
379. Blitvich, B.J.; Blair, C.D.; Kempf, B.J.; Hughes, M.T.; Black, W.C., et al. Developmental- and tissue-specific expression of an inhibitor of apoptosis protein 1 homologue from *Aedes triseriatus* mosquitoes. *Insect Mol Biol* **2002**, *11*, 431-442.
380. Ocampo, C.B.; Caicedo, P.A.; Jaramillo, G.; Ursic Bedoya, R.; Baron, O., et al. Differential Expression of Apoptosis Related Genes in Selected Strains of *Aedes aegypti* with Different Susceptibilities to Dengue Virus. *PLoS ONE* **2013**, *8*, e61187.
381. Baron, O.L.; Ursic-Bedoya, R.J.; Lowenberger, C.A.; Ocampo, C.B. Differential gene expression from midguts of refractory and susceptible lines of the mosquito, *Aedes aegypti*, infected with Dengue-2 virus. *J Insect Sci* **2010**, *10*, 41.
382. Wang, H.; Gort, T.; Boyle, D.L.; Clem, R.J. Effects of manipulating apoptosis on Sindbis virus infection of *Aedes aegypti* mosquitoes. *J. Virol.* **2012**, *86*, 6546-6554.
383. Blair, C.D. Mosquito RNAi is the major innate immune pathway controlling arbovirus infection and transmission. *Future Microbiol* **2011**, *6*, 265-277.
384. Sanchez-Vargas, I.; Travanty, E.A.; Keene, K.M.; Franz, A.W.; Beaty, B.J., et al. RNA interference, arthropod-borne viruses, and mosquitoes. *Virus Res.* **2004**, *102*, 65-74.
385. Adelman, Z.N.; Blair, C.D.; Carlson, J.O.; Beaty, B.J.; Olson, K.E. Sindbis virus-induced silencing of dengue viruses in mosquitoes. *Insect Mol. Biol.* **2001**, *10*, 265-273.
386. Higgs, S.; Rayner, J.O.; Olson, K.E.; Davis, B.S.; Beaty, B.J., et al. Engineered resistance in *Aedes aegypti* to a West African and a South American strain of yellow fever virus. *Am. J. Trop. Med. Hyg.* **1998**, *58*, 663-670.

387. Olson, K.E.; Higgs, S.; Gaines, P.J.; Powers, A.M.; Davis, B.S., et al. Genetically engineered resistance to dengue-2 virus transmission in mosquitoes. *Science* **1996**, *272*, 884-886.
388. Cirimotich, C.M.; Scott, J.C.; Phillips, A.T.; Geiss, B.J.; Olson, K.E. Suppression of RNA interference increases alphavirus replication and virus-associated mortality in *Aedes aegypti* mosquitoes. *BMC Microbiol.* **2009**, *9*, 49.
389. Nayak, A.; Berry, B.; Tassetto, M.; Kunitomi, M.; Acevedo, A., et al. Cricket paralysis virus antagonizes Argonaute 2 to modulate antiviral defense in *Drosophila*. *Nat. Struct. Mol. Biol.* **2010**, *17*, 547-554.
390. Mukherjee, S.; Hanley, K.A. RNA interference modulates replication of dengue virus in *Drosophila melanogaster* cells. *BMC Microbiol.* **2010**, *10*, 127.
391. Brust, R.A. Oviposition behavior of natural populations of *Culex tarsalis* and *Culex restuans* (Diptera: Culicidae) in artificial pools. *J. Med. Entomol.* **1990**, *27*, 248-255.
392. Crabtree, M.B.; Savage, H.M.; Miller, B.R. Development of a species-diagnostic polymerase chain reaction assay for the identification of *Culex* vectors of St. Louis encephalitis virus based on interspecies sequence variation in ribosomal DNA spacers. *Am J Trop Med Hyg* **1995**, *53*, 105-109.
393. Iranpour, M.; Lindsay, L.R.; Dibernardo, A. Development of three additional *Culex* species-specific polymerase chain reaction primers and their application in West Nile virus surveillance in Canada. *J Am Mosq Control Assoc* **2010**, *26*, 37-42.
394. Ciota, A.T.; Chin, P.A.; Kramer, L.D. The effect of hybridization of *Culex pipiens* complex mosquitoes on transmission of West Nile virus. *Parasit Vectors* **2013**, *6*, 305.
395. Eberle, M.W.; Reisen, W.K. Studies on autogeny in *Culex tarsalis*: 1. Selection and genetic experiments. *J. Am. Mosq. Control Assoc.* **1986**, *2*, 38-43.
396. Kuno, G. Early history of laboratory breeding of *Aedes aegypti* (Diptera: Culicidae) focusing on the origins and use of selected strains. *J. Med. Entomol.* **2010**, *47*, 957-971.
397. Shi, P.Y.; Tilgner, M.; Lo, M.K.; Kent, K.A.; Bernard, K.A. Infectious cDNA clone of the epidemic west nile virus from New York City. *J. Virol.* **2002**, *76*, 5847-5856.
398. Jerzak, G.; Bernard, K.A.; Kramer, L.D.; Ebel, G.D. Genetic variation in West Nile virus from naturally infected mosquitoes and birds suggests quasispecies structure and strong purifying selection. *J. Gen. Virol.* **2005**, *86*, 2175-2183.
399. Jerzak, G.V.; Bernard, K.; Kramer, L.D.; Shi, P.Y.; Ebel, G.D. The West Nile virus mutant spectrum is host-dependant and a determinant of mortality in mice. *Virology* **2007**, *360*, 469-476.
400. FASTX-Toolkit. Available online: http://hannonlab.cshl.edu/fastx_toolkit/
401. Langmead, B.; Trapnell, C.; Pop, M.; Salzberg, S.L. Ultrafast and memory-efficient alignment of short DNA sequences to the human genome. *Genome Biol* **2009**, *10*, R25.
402. Li, H.; Handsaker, B.; Wysoker, A.; Fennell, T.; Ruan, J., et al. The Sequence Alignment/Map format and SAMtools. *Bioinformatics* **2009**, *25*, 2078-2079.
403. Watson, M.; Schnettler, E.; Kohl, A. viRome: an R package for the visualization and analysis of viral small RNA sequence datasets. *Bioinformatics* **2013**, *29*, 1902-1903.
404. Lanciotti, R.S.; Kerst, A.J.; Nasci, R.S.; Godsey, M.S.; Mitchell, C.J., et al. Rapid detection of west nile virus from human clinical specimens, field-collected mosquitoes, and avian samples by a TaqMan reverse transcriptase-PCR assay. *J. Clin. Microbiol.* **2000**, *38*, 4066-4071.

405. Ciota, A.T.; Ehrbar, D.J.; Van Slyke, G.A.; Payne, A.F.; Willsey, G.G., et al. Quantification of intrahost bottlenecks of West Nile virus in *Culex pipiens* mosquitoes using an artificial mutant swarm. *Infect Genet Evol* **2012**, *12*, 557-564.
406. Brackney, D.E.; Pesko, K.N.; Brown, I.K.; Deardorff, E.R.; Kawatachi, J., et al. West Nile virus genetic diversity is maintained during transmission by *Culex pipiens quinquefasciatus* mosquitoes. *PLoS ONE* **2011**, *6*, e24466.
407. Bernhardt, S.A.; Simmons, M.P.; Olson, K.E.; Beaty, B.J.; Blair, C.D., et al. Rapid intraspecific evolution of miRNA and siRNA genes in the mosquito *Aedes aegypti*. *PLoS ONE* **2012**, *7*, e44198.
408. Lambrechts, L.; Quillery, E.; Noel, V.; Richardson, J.H.; Jarman, R.G., et al. Specificity of resistance to dengue virus isolates is associated with genotypes of the mosquito antiviral gene Dicer-2. *Proc Biol Sci* **2013**, *280*, 20122437.
409. Saito, K.; Siomi, M.C. Small RNA-mediated quiescence of transposable elements in animals. *Dev. Cell* **2010**, *19*, 687-697.
410. Senti, K.A.; Brennecke, J. The piRNA pathway: a fly's perspective on the guardian of the genome. *Trends Genet.* **2010**, *26*, 499-509.
411. Siomi, M.C.; Miyoshi, T.; Siomi, H. piRNA-mediated silencing in *Drosophila* germlines. *Semin. Cell Dev. Biol.* **2010**, *21*, 754-759.
412. van Rij, R.P.; Berezikov, E. Small RNAs and the control of transposons and viruses in *Drosophila*. *Trends Microbiol.* **2009**, *17*, 163-171.
413. Siomi, M.C.; Sato, K.; Pezic, D.; Aravin, A.A. PIWI-interacting small RNAs: the vanguard of genome defence. *Nat. Rev. Mol. Cell Biol.* **2011**, *12*, 246-258.
414. Kim, V.N.; Han, J.; Siomi, M.C. Biogenesis of small RNAs in animals. *Nat. Rev. Mol. Cell Biol.* **2009**, *10*, 126-139.
415. Logue, C.H.; Bosio, C.F.; Welte, T.; Keene, K.M.; Ledermann, J.P., et al. Virulence variation among isolates of western equine encephalitis virus in an outbred mouse model. *J. Gen. Virol.* **2009**, *90*, 1848-1858.
416. Mossel, E.C.; Ledermann, J.P.; Phillips, A.T.; Borland, E.M.; Powers, A.M., et al. Molecular determinants of mouse neurovirulence and mosquito infection for Western equine encephalitis virus. *PLoS ONE* **2013**, *8*, e60427.
417. Reisen, W.K.; Fang, Y.; Brault, A.C. Limited interdecadal variation in mosquito (Diptera: Culicidae) and avian host competence for Western equine encephalomyelitis virus (Togaviridae: Alphavirus). *Am. J. Trop. Med. Hyg.* **2008**, *78*, 681-686.
418. Foy, B.D.; Myles, K.M.; Pierro, D.J.; Sanchez-Vargas, I.; Uhlirova, M., et al. Development of a new Sindbis virus transducing system and its characterization in three Culicine mosquitoes and two Lepidopteran species. *Insect Mol. Biol.* **2004**, *13*, 89-100.
419. Team, R.C. R: A language and environment for statistical computing. Available online: <http://www.R-project.org/>
420. Picard. Available online: <http://picard.sourceforge.net/> (05/14/2014),
421. Campbell, C.L.; Black, W.C.t.; Hess, A.M.; Foy, B.D. Comparative genomics of small RNA regulatory pathway components in vector mosquitoes. *BMC Genomics* **2008**, *9*, 425.
422. Khoo, C.C.; Doty, J.B.; Heersink, M.S.; Olson, K.E.; Franz, A.W. Transgene-mediated suppression of the RNA interference pathway in *Aedes aegypti* interferes with gene

- silencing and enhances Sindbis virus and dengue virus type 2 replication. *Insect Mol Biol* **2013**, *22*, 104-114.
423. Marsano, R.M.; Leronna, D.; D'Addabbo, P.; Viggiano, L.; Tarasco, E., et al. Mosquitoes LTR retrotransposons: a deeper view into the genomic sequence of *Culex quinquefasciatus*. *PLoS ONE* **2012**, *7*, e30770.
424. TEfam. Available online: <http://tefam.biochem.vt.edu/tefam/index.php> (05/15/14),
425. Strauss, J.H.; Strauss, E.G. The alphaviruses: gene expression, replication, and evolution. *Microbiol Rev* **1994**, *58*, 491-562.
426. Bennett, K.E.; Flick, D.; Fleming, K.H.; Jochim, R.; Beaty, B.J., et al. Quantitative trait loci that control dengue-2 virus dissemination in the mosquito *Aedes aegypti*. *Genetics* **2005**, *170*, 185-194.
427. Bosio, C.F.; Fulton, R.E.; Salasek, M.L.; Beaty, B.J.; Black, W.C.t. Quantitative trait loci that control vector competence for dengue-2 virus in the mosquito *Aedes aegypti*. *Genetics* **2000**, *156*, 687-698.
428. Richards, S.L.; Anderson, S.L.; Lord, C.C.; Smartt, C.T.; Tabachnick, W.J. Relationships between infection, dissemination, and transmission of West Nile virus RNA in *Culex pipiens quinquefasciatus* (Diptera: Culicidae). *J Med Entomol* **2012**, *49*, 132-142.
429. Zhu, W.; Qin, W.; Atasoy, U.; Sauter, E.R. Circulating microRNAs in breast cancer and healthy subjects. *BMC Res Notes* **2009**, *2*, 89.
430. Oliveros, J.C. VENNY. An interactive tool for comparing lists with Venn Diagrams. Available online: <http://bioinfogp.cnb.csic.es/tools/venny/index.html>.
431. Parameswaran, P.; Sklan, E.; Wilkins, C.; Burgon, T.; Samuel, M.A., et al. Six RNA viruses and forty-one hosts: viral small RNAs and modulation of small RNA repertoires in vertebrate and invertebrate systems. *PLoS Pathog* **2010**, *6*, e1000764.
432. Sabin, L.R.; Zheng, Q.; Thekkat, P.; Yang, J.; Hannon, G.J., et al. Dicer-2 processes diverse viral RNA species. *PLoS ONE* **2013**, *8*, e55458.
433. Siu, R.W.; Fragkoudis, R.; Simmonds, P.; Donald, C.L.; Chase-Topping, M.E., et al. Antiviral RNA interference responses induced by Semliki Forest virus infection of mosquito cells: characterization, origin, and frequency-dependent functions of virus-derived small interfering RNAs. *J. Virol.* **2011**, *85*, 2907-2917.
434. Vermeulen, A.; Behlen, L.; Reynolds, A.; Wolfson, A.; Marshall, W.S., et al. The contributions of dsRNA structure to Dicer specificity and efficiency. *RNA* **2005**, *11*, 674-682.
435. Park, J.E.; Heo, I.; Tian, Y.; Simanshu, D.K.; Chang, H., et al. Dicer recognizes the 5' end of RNA for efficient and accurate processing. *Nature* **2011**, *475*, 201-205.
436. Rosen, L. Overwintering mechanisms of mosquito-borne arboviruses in temperate climates. *Am. J. Trop. Med. Hyg.* **1987**, *37*, 69S-76S.
437. Hughes, M.T.; Gonzalez, J.A.; Reagan, K.L.; Blair, C.D.; Beaty, B.J. Comparative potential of *Aedes triseriatus*, *Aedes albopictus*, and *Aedes aegypti* (Diptera: Culicidae) to transovarially transmit La Crosse virus. *J Med Entomol* **2006**, *43*, 757-761.
438. Swevers, L.; Vanden Broeck, J.; Smaghe, G. The possible impact of persistent virus infection on the function of the RNAi machinery in insects: a hypothesis. *Front Physiol* **2013**, *4*, 319.

439. Swevers, L.; Liu, J.; Huvenne, H.; Smagghe, G. Search for limiting factors in the RNAi pathway in silkworm tissues and the Bm5 cell line: the RNA-binding proteins R2D2 and Translin. *PLoS ONE* **2011**, *6*, e20250.
440. Felix, M.A.; Ashe, A.; Piffaretti, J.; Wu, G.; Nuez, I., et al. Natural and experimental infection of *Caenorhabditis* nematodes by novel viruses related to nodaviruses. *PLoS Biol.* **2011**, *9*, e1000586.